ANNÉE 2013

THÈSE / UNIVERSITÉ DE RENNES 1
sous le sceau de l'Université Européenne de Bretagne

pour le grade de

DOCTEUR DE L'UNIVERSITÉ DE RENNES 1

Mention : Sciences de la Terre

Ecole doctorale Sciences de la Matière, Rennes

présentée par

Alain Zanella

Préparée à l'unité de recherche UMR 6118
Géosciences Rennes
Université de Rennes 1

Surpression de fluides et fracturation de roches mères en différents contextes tectoniques : modélisation analogique et exemples de terrain

Thèse soutenue à Rennes le 29.11.2013

devant le jury composé de :

Régis MOURGUES
Professeur, Université du Mans / *rapporteur*

François ROURE
Directeur expert, IFP -Energies Nouvelles / *rapporteur*

John COSGROVE
Professeur, Imperial College of London / *examinateur*

Denis GAPAIS
Professeur, Université de Rennes 1 / *examinateur*

Peter R. COBBOLD
D.R. Emérite CNRS, Université de Rennes 1 / *directeur de thèse*

à Gaby et Michel

Préface

Ce travail de thèse a été financé, pour la partie recherche, par la société pétrolière norvégienne Statoil. Ce manuscrit de thèse est rédigé sous la forme d'articles scientifiques en anglais. Trois d'entre eux sont acceptés dans la revue *Marine and Petroleum Geology* et deux autres sont soumis, l'un dans la revue *American Association of Petroleum Geologists Bulletin* et le dernier dans la revue *Journal of the Geological Society of London*. Pour chacun de ces articles une introduction ainsi qu'un résumé en français est disponible en début de chaque chapitre. Je tiens à remercier tous mes co-auteurs pour leur contribution.

Remerciements

La thèse est une aventure unique au cours de laquelle nous avons souvent des moments de solitude et de doute que je n'aurais pas pu surmonter sans toutes les personnes qui m'ont entourées. Famille, amis, collègues, tous ont répondu présent et ont participé, à leur manière, à cette période importante de ma vie. Aussi, c'est un réel plaisir que de leurs écrire ces quelques lignes.

Tout d'abord Merci à mon directeur de thèse, Peter ! Merci de m'avoir donné une chance en Master tout d'abord, puis en thèse bien sûr. Merci de m'avoir transmis ton savoir et ton expérience et de m'avoir remotivé dans les moments de doute. J'ai énormément appris notamment lors des ces nombreuses missions de terrain. Je me souviendrai longtemps de toutes nos discussions, notamment autour des petites pauses café, qui m'ont toujours fait beaucoup réfléchir. Et bien sûr, s'il y a bien une phrase que je retiendrai à l'avenir c'est : « On ne sait jamais ! ».

Merci aux membres du jury d'avoir pris le temps de relire et de juger ce travail. Merci Denis d'avoir pris part à ce jury et de nous avoir fortement soutenu pour que cette thèse voie le jour, je ne l'oublierai pas. Merci à John Cosgrove pour ses commentaires et ses conseils judicieux. Merci à François Roure et à Régis Mourgues pour leurs rapports très encourageants et leurs critiques constructives. Un grand Merci à Helge Løseth (Statoil) pour avoir suivi cette thèse durant ces trois années et avoir pris part également au jury en temps qu'invité.

Au cours de la thèse de nombreuses collaborations ont vu le jour. Tout d'abord au sein même de Géosciences, mais également avec des personnes d'autres laboratoires en France et même à l'étranger. Tous m'ont apporté une aide précieuse qui a largement contribué à l'aboutissement de ce travail de trois ans. Pour le travail de modélisation, je tiens donc à remercier Jean-Jacques, Pascal et Bruno de Géosciences. Pour la construction du nouvel appareillage je tiens particulièrement à remercier Patrick Weber ainsi que toute son équipe à l'INSA de Rennes. Grâce à leur savoir-faire ils m'ont permis de concrétiser ce projet de modélisation. Merci également à toutes les personnes qui ont été présente dans ce labo de modélisation durant ces quelques années.

Je tiens également à remercier tous mes collaborateurs de thèse. Merci Olivier pour avoir participé, de part ton stage de M2, à l'aventure. Je garde un très bon souvenir de ton stage et de ton travail. Merci Philippe pour la géochimie, Christian pour ton aide dans la 3D goCad. Et bien sûr Merci Gilles pour avoir été très patient pour m'apprendre les manips de datation Ar-Ar et pour ces missions de terrain en Amérique du sud. Merci Dominique pour ton expertise de pointe dans l'électronique ! Je te dis un grand Merci et "Biiiiiip" ! Merci à toute l'équipe sédim pour les nombreuses discussions, les moments croissants, et votre enthousiasme. Un Merci spécial à Marie-Paule et Chantal que j'ai peut être fait un peu souffrir avec toutes ces missions. Je n'oublie pas également David, Jean B., Yann, Jean P., Aline, Marie-Anne, Maïwenn, Annick, Catherine, Isabelle et Eddie qui sont des personnes importantes dans la vie du labo et qui font leur possible pour que tout roule dans cette maison ; Merci à vous. Heureusement, vous êtes trop fortes ! Merci Jacques pour nous avoir ouvert les portes de Nancy pour ces analyses sur les veines de calcite. Merci Tony pour toutes ces séances de microscope à Trondheim. Merci à toute l'équipe de Statoil pour m'avoir accueillie plusieurs fois dans le centre de recherche en Norvège. Merci donc à Marita, Helge, Nuno, Lars, Tony et tous les autres que j'ai pu rencontrer sur le terrain à Neuquén ou en congrès.

Bien sûr je pense à toi Xavier que j'ai un peu torturé avec les lames minces de calcite fibreuse. Pourtant c'était facile sur le papier, non ? Merci pour ces belles lames.

Ah Géosciences, une belle équipe ! Un immense Merci à tous les camarades thésards, ingénieurs, post-docs et stagiaires qui ont toujours assuré une ambiance de folie, parfois même jusqu'au bout de la nuit ! Je me souviendrai longtemps de notre équipe internationale de tarot. Ave Mélo et Justine pour les grand-chelems !!! Nous resterons les maîtres ! Merci à mes très chers collègues de bureau 211 « le bureau de l'élite !!! », Éline et Gwen. Éline, trop top la mission en Ecosse. Et Gwen je crois que tu seras toujours le plus fort à TLMVPSP ! Vous avez largement participé à la réussite de ce travail de par vos conseils et votre amitié. Et Merci encore à tous : Cloclo et Gillou (vive Call of…), Mélo (mon maître du tarot) et Hervé (les visiteurs déchirent !), Justine (J^2) (la meilleure des partenaires de tarot), Romain T., Pipo, Thibault (maintenant je dis Merci !), Céline, Yannick, Hugo, Fabou, Anne-Claire, Christoff, Étienne, Morgane, Pietro, Loïc, Paul, Camille, Brendan, Fernando (mon guide patagonien…), Guillaume, Marie, Justine, Roman (le chef cuisto), Youss, Lena, Sam, Émilie, Benoît, Carlos, Christophe, Gloria, Sylvia, Lorie, Charlotte, Maya , Wei, Mélanie, Thomas, Sarah, Gemma, Antoine, Jérôme, Sandra, Sébastien, JL, JC, Jo, Flo, Laeti, Lucie, Jamay.

Enfin, je tiens à remercier mes proches. Ils ont toujours été présents et ont toujours cru en moi. Merci Pôpa et Môman !!! Sans vous je ne serais pas là du tout… C'est grâce à vous que je suis arrivé jusqu'ici et je ne l'oublierai jamais. Merci à ma grande sœur (enfin petite par la taille mais grande par l'esprit…). Je ne te l'ai peut-être jamais dit mais tu as toujours été un exemple pour moi. Tu m'as montré que dans la vie il fallait persévérer pour construire son avenir, un grand Merci pour ça ! Merci Loïc et Merci Pou ! Vous aussi vous avez joué un rôle important dans tout ça. Merci d'avoir aussi été là Lolo pour ces petites parties de détente sur la console. Et Pou, Merci pour tous ces moments de rigolade, notamment au ski. Belle-Môman et beau-Pôpa, Merci. Vous aussi vous avez cru en moi sans jamais douter. Gaby, Michel, Annick et Georgette, mes chers grands-parents, à vous aussi je tiens à vous dire Merci car vous avez toujours été présents quand il le fallait et même plus. Enfin je tiens à terminer ces remerciements par la personne qui compte le plus pour moi. Celle qui a vraiment tout suivi et parfois subi aussi à certains moments : Marie. Merci d'avoir été présente dans tous les moments, les bons comme les moins bons... Tu as souvent su trouver les mots pour me rassurer. Peu le savent mais c'est toi qui as dû me supporter dans les moments de stress intense, car oui j'ai stressé (le mythe tombe !), et je dois dire que tu as fait preuve de beaucoup de patience et de compréhension. Sans toi je suis certain que je n'y serais jamais arriver. Je t'aime, Merci !

Table des Matières

Introduction générale

Introduction

Les évidences de surpression de fluides et de fracturation hydraulique sont des phénomènes géologiques très répandus. Leurs expressions peuvent prendre différentes formes, à différentes échelles, et s'observent parfois facilement à travers les paysages. Il existe ainsi plusieurs exemples de ces phénomènes tel que le volcanisme, les geysers, et les volcans de boue. D'autres en revanche restent plus discrets et méconnus, mais sont parfois d'intérêts économiques majeurs. C'est le cas par exemple lorsque les surpressions de fluides s'expriment au cœur des bassins sédimentaires, lieux de génération des hydrocarbures.

Le monde pétrolier s'est intéressé très rapidement aux phénomènes de surpression de fluides et à la fracturation hydraulique. La raison principale est que ces phénomènes sont au cœur des questions énergétiques actuelles. Néanmoins, il existe des intérêts scientifiques majeurs qui résident dans l'étude de ces phénomènes. En effet, l'étude des surpressions de fluides et de la fracturation hydraulique peut apporter énormément de réponses pour comprendre leurs origines, mais aussi leurs évolutions dans le temps. Comprendre les systèmes en surpression de fluides dans les bassins sédimentaires, c'est comprendre comment un fluide peut être généré, puis peut migrer (latéralement et verticalement) et se retrouver piégé dans les sédiments. Enfin, ce même fluide peut aussi être à l'origine de la fracturation hydraulique d'une roche. Ainsi, tenter de répondre aux questions relatives à ces processus c'est étudier un système fluide/roche, de la génération d'un fluide jusqu'à la fracturation de la roche. Pour le monde industriel, les enjeux sont considérables. La compréhension des surpressions de fluides au sein même des systèmes pétroliers est primordiale. Ainsi lors des forages, et notamment ceux qui utilisent la fracturation hydraulique, une bonne connaissance de l'état de fracturation naturel de la roche peut être déterminant pour l'exploitation d'un gisement.

Dans ce travail de thèse, nous nous intéresserons ainsi aux surpressions de fluides et à la fracturation hydraulique dans les bassins sédimentaires, en donnant un accent particulier à l'expression de ces processus au sein même des roches mères d'hydrocarbures.

Indépendamment du contexte géologique, les bassins sédimentaires sont souvent affectés par des fluides en surpression. Les roches de nature imperméable, comme les roches mères, sont particulièrement sujettes à ces phénomènes. La raison réside bien entendu dans le fait qu'elles sont imperméables et qu'elles s'opposent naturellement à la migration d'un fluide et favorisent donc l'apparition de pressions de fluide anormalement élevées. Mais ces roches sont également à l'origine des fluides, comme les huiles ou les gaz qui constituent les hydrocarbures. On doit alors considérer qu'à l'intérieur même des roches mères une partie solide de la roche, la matière organique, va devenir un fluide au moment de la maturation.

Depuis la description des mécanismes de fracturation hydraulique faite par Hubbert et Willis (1957) jusqu'à aujourd'hui, les surpressions de fluides et la fracturation hydraulique ont déjà fait l'objet de plusieurs études. Celles-ci se sont notamment multipliées durant ces quinze dernières années, probablement en réponse à l'intérêt pétrolier qu'elles peuvent susciter. En conséquence, de nombreuses avancées ont été faites, tant sur le plan théorique que sur le plan expérimental. Ainsi, Mourgues et Cobbold (2003) ont montré que lorsqu'une surpression de fluides était présente au sein des pores d'une roche, des forces appelées « forces de courant » étaient alors générées. Ces forces s'appliquent directement aux roches, indépendamment de la vitesse d'écoulement, et peuvent changer l'orientation des contraintes principales effectives appliquées au système. La fracturation hydraulique est alors caractérisée par la formation d'une fracture sous l'effet d'une forte pression de fluides. Elle peut donc théoriquement se former en l'absence totale de contraintes tectoniques. Par la suite, les travaux de Cobbold et Rodrigues (2007) ont montré que les fractures hydrauliques horizontales étaient la conséquence d'un gradient de pression de fluide élevé et des forces de courant. Ces découvertes vont changer la conception de certains objets géologiques, comme les veines de calcites fibreuses parallèles à la stratification de la roche : le beef.

De nos jours, nous ne regardons plus de la même manière les veines fibreuses parallèles à la stratification d'une roche. Elles sont nommées 'beef' du fait de leur grande ressemblance avec les fibres d'un muscle (Buckland & De la Bèche 1835). Cependant, ces travaux sont restés assez largement méconnus. Aussi, le lien entre ces objets géologiques et les surpressions de fluides n'a été fait que très récemment. En effet, lors de leur étude Rodrigues et al. (2009) ont montré que le beef était formé par des veines antitaxiales qui étaient la conséquence des surpressions de fluides et de la fracturation hydraulique des roches. Dans cette étude, les auteurs mentionnent qu'il semble exister un lien entre le beef et la génération d'hydrocarbures, sans que celui-ci ne soit clairement démontré.

Sur le plan expérimental, les surpressions de fluides et la fracturation hydraulique ont déjà été étudiées. Cependant, il a fallut attendre la fin des années 90 pour voir apparaître les premiers modèles analogiques assistés par des fluides (Cobbold & Castro 1999). En seulement quinze ans, la modélisation analogique s'est hissée à la première place des outils utilisés par les géologues pour comprendre ces phénomènes. Ainsi, des modèles analogiques capables de réaliser des expériences sous l'effet des surpressions de fluides ont été réalisés (Cobbold et al. 2001 ; Mourgues & Cobbold 2003 ; Cobbold & Rodrigues 2007 ; Rodrigues et al. 2009). Dans tous ces modèles, les surpressions de fluides ont été obtenues par des injections de fluides (eau ou air) à la base. Ces modèles s'attachent donc plus particulièrement aux conséquences des surpressions de fluides qu'à leur origine. À travers toutes ces modélisations, nous avons pu comprendre que les surpressions de fluides avaient un très grand impact sur la déformation des sédiments (Cobbold et al. 2004 ; Rodrigues et al. 2009).

Objectifs et travail de thèse

Précédemment, nous avons vu que les conséquences des surpressions de fluides étaient relativement bien connues. Néanmoins, pour les mécanismes qui en sont à l'origine il n'y a pas de consensus. Ce travail de thèse vise donc à mieux comprendre ces mécanismes qui semblent liés à la génération d'hydrocarbures. Pour cela, nous avons développé une étude en deux axes majeurs. D'un coté nous avons étudié directement sur le terrain les évidences de surpression de fluides, comme le beef. Mais nous avons également porté notre attention sur les veines d'hydrocarbures solides, ou bitumes, qui sont également le résultat de la fracturation hydraulique des roches sous l'effet de surpression de fluides. Puis, d'un autre coté, nous avons choisi de nous intéresser aux origines des surpressions de fluides à l'aide de la modélisation analogique. Pour ceci, nous avons développé un nouvel appareillage, capable de générer son propre fluide dans un système fermé.

Ce manuscrit de thèse est composé de cinq chapitres, chacun rédigé sous forme d'article scientifique. Certains sont publiés, tandis que d'autres sont soumis.

Le Chapitre 1 traite de la grande étendue des phénomènes de surpression de fluides à l'échelle du globe. Il illustre le contexte de cette thèse tout en nous permettant d'apporter des conclusions supplémentaires sur les surpressions de fluides. Par une synthèse bibliographique, nous montrons que le beef est largement répandu mondialement. Nous en tirons ainsi la conclusion que les surpressions de fluides, qui en sont à l'origine, le sont également.

Dans les trois chapitres suivants (Chapitres 2, 3 et 4), nous détaillons les études que nous avons réalisées sur trois bassins sédimentaires différents, ces derniers étant au cœur de systèmes pétroliers.

Ainsi, dans le Chapitre 2 nous présentons notre étude sur le bassin du Wessex en Angleterre du sud. Nous avons choisi ce bassin pour sa relation historique avec le beef. En effet, c'est dans ce dernier que le beef trouve son origine. Mais au delà de l'aspect historique, le bassin du Wessex constitue un cadre très intéressant pour l'étude des circulations et des surpressions de fluides à l'échelle d'un bassin. Nous avons donc cherché à mieux caractériser les origines des fluides responsables de la formation du beef.

La partie nord du bassin de Neuquén, Argentine, constitue l'objet d'étude du Chapitre 3. Cette zone, fortement affectée par le volcanisme et la déformation, nous a fourni des informations primordiales qui mettent en relation la déformation, la génération d'hydrocarbures et le volcanisme. Dans ce bassin, le beef et le bitume caractérisent les évidences de surpressions de fluides. La présence de grandes provinces volcaniques pose la question de la relation entre le volcanisme et la maturation et la migration des hydrocarbures.

Pour conclure sur des cas naturels, nous avons étudié le bassin de Magellan à l'extrême sud de l'Amérique du sud. Cette étude est abordée dans le Chapitre 4. Notre étude de terrain, couplée aux données auxquelles nous avons pu avoir accès, nous permet de conclure sur le rôle des surpressions de fluides sur la déformation dans un bassin d'avant-pays.

Enfin, dans un dernier chapitre (le Chapitre 5), nous mettons en avant la modélisation analogique. Nous montrons comment, après avoir développé un nouveau dispositif expérimental, nous pouvons approcher les mécanismes à l'origine des surpressions de fluides et de la fracturation hydraulique dans les roches mères.

Chapitre 1

Surpression de fluides, fracturation hydraulique et ‘beef’

1.1 Introduction

Les surpressions de fluides sont très répandues à l’échelle de la planète. Elles sont notamment présentes des les bassins sédimentaires et sont souvent au cœur même des systèmes pétroliers. Dans certains cas, les surpressions de fluides sont tellement importantes qu’elles sont capables de générer des fractures hydrauliques dans les roches. Ces mécanismes de fracturation hydraulique sont connus depuis longtemps de la communauté scientifique (Hubbert et Willis 1957). Pourtant, aujourd’hui il n’existe pas de consensus quant à l’origine des surpressions de fluides. Plusieurs auteurs ont néanmoins déjà mentioné des causes possibles, comme la compaction mécanique (e.g. Von Terzaghi 1923), les variations de volume des fluides ou les transformations minéralogiques (e.g. Osborne & Swarbrick 1997), ou encore la génération d’hydrocarbures (Swarbrick et al. 2002). Ces dernières années, beaucoup de travaux se sont succédés et ont amené à une meilleure compréhension de la fracturation hydraulique issue des surpressions de fluides (e.g. Cobbold & Castro 1999 ; Mourgues & Cobbold 2003 ; Cobbold & Rodrigues 2007). Rodrigues et al. (2009) montrent alors récemment que les veines fibreuses parallèles à la stratification de la roche sont le résultat de la fracturation hydraulique des roches sous l’effet des surppressions de fluides. Ces veines appellées ‘beef’ sont alors le témoin que la fracturation hydraulique naturelle est possible et est associée aux mécanismes des surpressions de fluides.

Pour appréhender l’étendue de ces processus, nous avons recherché les indices de beef à travers le monde. Dans ce premier chapitre, nous faisons donc un bilan, principalement basé sur une étude bibliographique, des occurrences de beef. Nous abordons également les mécanismes à l’origine de ces derniers en reprenant la littérature. Ce travail constituera notre contexte pour la suite du manuscrit.

1.2 Article#1: Bedding-parallel fibrous veins (beef and cone-in-cone): Worlwide occurrence and possible significance in terms of fluid overpressure, hydrocarbon generation and mineralization.

Les recherches effectuées sur l’étendue des phénomènes ‘beef’ et ‘cone-in-cone’ ont amenées à la rédaction d’un article scientifique publié dans la revue *Marine and Petroleum Geology*. Cet article se veut un article de synthèse sur les différentes formes de veines parallèles à la stratification de la roche à travers le monde. Il évoque également les mécanismes de génération de ces objets géologiques.

1.2.1 Résumé de l’article#1

Les veines parallèles à la stratification de la roche sont très répandues dans les bassins sédimentaires à travers le monde, spécialement dans les niveaux de basse perméabilité. Le terme ‘beef’ réfère aux veines parallèles à la stratification d’une roche, constituées de minéraux fibreux, parallèles entre eux et ayant cristallisés quasi-verticallement. D’autres structures comme les ‘cone-in-cone’, plus complexes encore mais tout aussi communes, sont présentes dans ces veines. Devant l’importance de ce phénomène, nous avons compilé un catalogue mondial (157 localités) pour ces deux structures, le ‘beef’ et le ‘cone-in-cone’. Typiquement, les veines se constituent de minéraux blancs, comme de la calcite, du gypse ou du quartz. Cependant, dans certains cas elles peuvent contenir des minéraux accessoires d’intérêt économique, comme du bitume, des sulfures, de l’émeraude, de la pechblende ou encore de l’or. Dans ces même veines, il arrive même que les inclusions de fluides contiennent des hydrocarbures (huile ou gaz).

Le beef de calcite (110 localités) est commun dans les argiles riches en matière organique d’origine marine carbonatée, spécialement celles (1) du Cambrien-Ordovicien, (2) du Devonien-Carbonifère, (3) du Jurassique inférieur, ou (4) du Crétacé inférieur au Paléogène. Le beef de gypse (30 localités) est commun dans les niveaux stratigraphiques évaporitiques ou lacustres d’origine continentale, spécialement ceux d’âge triassic ou néogène. Enfin, le beef de quartz (17 localités) est répendu dans les séquences turbiditiques, notamment celles de l’Ordovicien ou du Protérozoïque. La répartition du beef en fonction de sa composition semble refléter le contrôle climatique sur l’enregistrement de la sédimentation. À partir de ce point, nous en déduisons que les espèces minérales, qui constituent les fibres des veines, n'ont pas beaucoup migré verticalement.

Les températures typiques de formation des différents minéraux sont (1) moins de 60°C pour le beef de gypse, (2) entre 70°C et 120°C pour le beef de calcite, et de 200°C à 350°C pour le beef de quartz. Ainsi, le beef de calcite contenant des hydrocarbures pourrait être un bon indicateur pour un système pétrolier dans lequel de l'huile ou du gaz a migré en même temps qu'un fluide de phase aqueuse. Nous pensons que le beef et le cone-in-cone sont les résultats d'une fracturation en tension et d'une dilatation verticale contemporaine de la croissance des fibres minérales. Les causes possibles peuvent ainsi être (1) la force de cristallisation, ou (2) les forces d'écoulement dues à la surpression de fluides. Pour les veines formées à plusieurs kilomètres de profondeur, les surpressions de fluides sont la cause la plus probable.

1.2.2 Article#1

Marine and Petroleum Geology 43 (2013) 1–20

Contents lists available at SciVerse ScienceDirect

Marine and Petroleum Geology

journal homepage: www.elsevier.com/locate/marpetgeo

Review article

Bedding-parallel fibrous veins (beef and cone-in-cone): Worldwide occurrence and possible significance in terms of fluid overpressure, hydrocarbon generation and mineralization

Peter R. Cobbold [a,*], Alain Zanella [a], Nuno Rodrigues [a,b], Helge Løseth [b]

[a] Geosciences (UMR6118), CNRS and Université de Rennes 1, 35042 Rennes, France
[b] Statoil Research Centre, 7005 Trondheim, Norway

ARTICLE INFO

Article history:
Received 21 September 2012
Accepted 31 January 2013
Available online 22 February 2013

Keywords:
Veins
Beef
Cone-in-cone
Calcite
Gypsum
Quartz
Petroleum
Hydraulic fracturing
Overpressure
Seepage forces

ABSTRACT

Bedding-parallel fibrous veins are common worldwide in sedimentary basins, especially within strata of low permeability. The term "beef" refers to bedding-parallel veins of fibrous minerals, where the fibres are mutually parallel and have formed quasi-vertically. More complex on a smaller scale are "cone-in-cone" structures, yet these are also common within bedding-parallel veins. For both beef and cone-in-cone we have compiled a worldwide catalogue (157 localities). Typically, the veins consist mainly of white gangue minerals (for example, calcite, gypsum, or quartz), but may also contain accessory minerals of economic interest (for example, bitumen, sulphides, emerald, pitchblende or gold). Fluid inclusions may contain oil or gas.

Calcite beef (110 localities) is common in organic-rich shale of marine-carbonate origin, especially of (1) Cambrian–Ordovician, (2) Devonian–Carboniferous, (3) early Jurassic, or (4) Cretaceous to Palaeogene ages. Gypsum beef (30 localities) is common in evaporitic or lacustrine strata of continental origin, especially of Triassic or Neogene ages. Quartz beef (17 localities) is common within meta-turbidite sequences, especially of Ordovician or Proterozoic ages. Because these modal ages seem to reflect climatic controls, we infer that the fibre-forming mineral species have not travelled far, vertically. The same conclusion holds for accessory minerals.

Typical temperatures of formation are (1) up to 60 °C for gypsum beef, (2) 70 °C to 120 °C for calcite beef, and (3) 200 °C to 350 °C for quartz beef. Hydrocarbon-bearing calcite beef may be a good indicator of a petroleum system, in which oil or gas migrate, together with aqueous solutions. We argue that beef and cone-in-cone layers result from tensile fracturing and vertical dilation, coeval with fibre growth. Possible causes are either (1) force of crystallization, or (2) seepage forces, due to fluid overpressure. For layers that form at depths of several km, fluid overpressure is the more likely cause.

1. Historical introduction

In this section we review the early literature on "beef" and "cone-in-cone", explaining what these terms have meant to successive geologists. In the past, the use of different languages and terms has probably led to some confusion, which we hope to settle, while exploring useful sources of information.

1.1. Beef

The term "beef" has appeared in geological publications for the last two hundred years or so, especially in the United Kingdom. It refers to fibrous minerals in bedding-parallel veins, where the fibres are approximately perpendicular to the margins. On the coast of SW England, where outcrops are of good quality, veins of fibrous calcite or of gypsum (satin spar) are relatively common in flat-lying Mesozoic strata, especially shale (Fig. 1). They therefore caught the attention of early geologists. Thus Webster (1826) described "layers of fibrous carbonate of lime and also of fibrous sulphate of lime". More specifically, Buckland and De la Beche (1835) stated, "the fibres of this limestone, like those of satin spar, are at right angles to the planes of the beds which they compose, and which vary from two to six inches in thickness. From the resemblance of its small and parallel fibres to the fibres of animal muscle, this limestone is known among the workmen by the name of "Beef". Later authors, who referred to "beef" in Mesozoic strata of SW England, were Brodie (1854), Judd (1871), Andrews (1881), Woodward (1893),

* Corresponding author. Tel.: +33 (0)223236096; fax: +33 (0)223236100.
E-mail address: peter.cobbold@univ-rennes1.fr (P.R. Cobbold).

0264-8172/$ – see front matter © 2013 Elsevier Ltd. All rights reserved.
http://dx.doi.org/10.1016/j.marpetgeo.2013.01.010

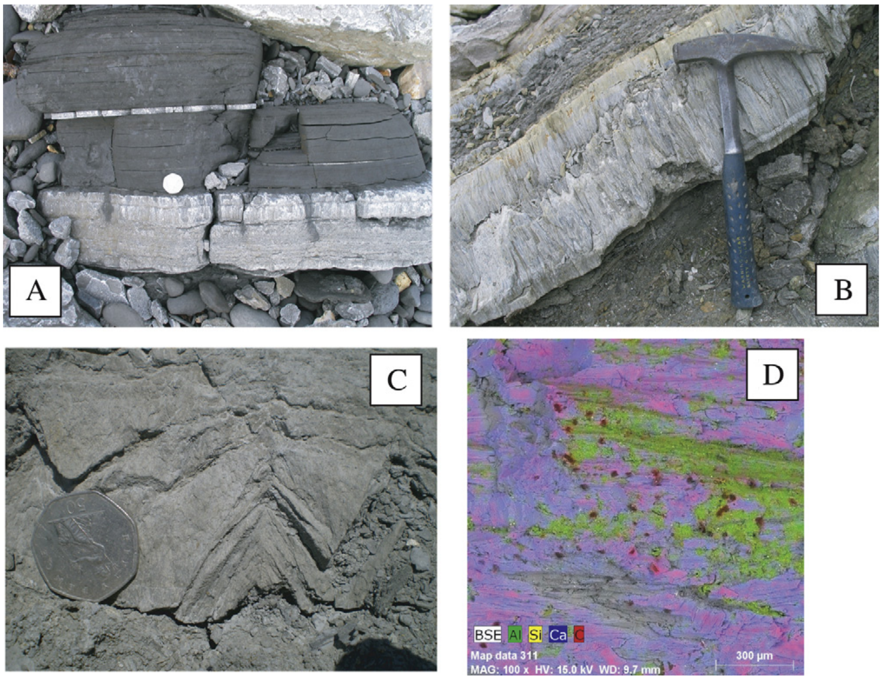

Figure 1. Calcite beef and cone-in-cone from Dorset, SW England. A. Bedding-parallel layers of calcite beef (white) of various thicknesses within fissile shale (black) of Shales-with-Beef member, Charmouth Mudstone Fm, Charmouth. Calcite fibres are perpendicular to bedding, or nearly so. B. Calcite beef within tilted bedding, Lulworth Cove. Calcite fibres are somewhat oblique to the pole to bedding, indicating component of bedding-parallel slip, top to East (right). C. Cone-in-cone structures in Shales-with-Beef member at foot of cliffs between Lyme Regis and Charmouth. Conical shapes are due to thin layers of mudstone. Notice smooth lower surfaces of layers, contrasting with typical corrugations (steps) on upper surfaces. D. Hydrocarbons in beef, Lyme Regis. Image is from Environmental Scanning Electron Microscope (ESEM). Calcite fibres (violet) appear nearly horizontal. Hydrocarbons (red) are within fluid inclusions. Large solid inclusions (yellow-green) are of shale.

Andrews and Jukes-Brown (1894), Geikie (1902) and Reid (1903). As a result, Lang (1914) and Lang et al. (1923) went on to give the name "Shales-with-Beef" to an early Jurassic sequence (a Member of the Charmouth Mudstone Formation), in which calcite beef is abundant (Fig. 1). In the meantime, geologists had identified calcite beef in other parts of the United Kingdom, for example, the Inner Hebrides Islands of NW Scotland (Judd, 1878; Harker, 1908; Lee, 1920), Ayrshire, SW Scotland (Young, 1885), the Midlands of England (Woodward, 1893; Thompson, 1902), Somerset (Short, 1904; Reynolds and Vaughan, 1904; Richardson, 1911) and South Wales (Richardson, 1905). By analogy, Davies (1915) noted the resemblance of beef to fibrous crystals of ice, which form flat-lying layers ("needle ice") in soil and may be responsible for "frost heave".

1.2. Cone-in-cone structures

The term "cone-in-cone" refers to conical structures, which individually are of cm-scale, but may form aggregates. The term has been in use widely and for a longer time than beef. We distinguish five periods in the geological literature.

1. In the early German literature, the term "tutenmergel" (literally, "cornet marl") refers to an aggregate of mineral fibres (generally of calcite), in which (1) layers of fibres lie between nesting conical surfaces, which have a common axis, (2) the fibres are parallel or somewhat oblique to this axis, (3) thin films of clay or shale line the conical surfaces and (4) parallel nests of coaxial cones form an aggregate, such as the rim of a concretion, a lens or even a layer, lying within a sequence of marl or shale (Hausmann, 1812; Leonhard, 1823; Linck and Noll, 1928). The term "tutenmergel" may have come from the mineralogist Abraham Gottlob Werner in the 18th Century. Hausmann (1812) described it from shale at exposure in Görarp, southern Sweden. Linck (1931) and earlier authors also used the term "nagelkalk" (literally "nail calc") to describe layers, from which cones protrude, resembling nailheads on a wooden board.
2. In the early literature from the United Kingdom, "cone-in-cone" came to acquire the same meaning as "tutenmergel". Ure (1793) described such structures in Carboniferous strata of SW Scotland, thinking that they were fossils. Yates (1821) described fibrous conical structures in limestone beds from Staffordshire, using the original miners' term for them, which was "curl". Lonsdale (1832) may have been the first to use the term "cone-in-cone" for fibrous aggregates of calcite in Mesozoic strata near Bath. Sorby (1860) also referred to cone-in-cone and noted that the "cones often occur in bands, parallel to the stratification of the rock". For such reasons, Richardson (1923, page 91) referred to "The Cone-in-Cone Structure in the Beef" (e.g. Fig. 1C). Both Sorby and Richardson attributed cone-in-cone and beef to a process of crystal growth. Meanwhile, their colleagues were discovering fibrous cone-in-cone in outlying parts of the former British Empire, such as New Zealand (Mantell, 1850), Canada (Hector, 1861; Dawson, 1862), Australia (Daintree, 1872), South Africa (Stow, 1874), Egypt (Beadnell, 1905) and Northern Rhodesia, now Zambia (Molyneux, 1909). Newton and Teall (1897) described cone-in-cone from Franz Josef Land, now part of Russia. When Young (1885) suggested that decomposition of organic matter and flow of gas were important factors in the genesis of cone-in-

cone, this led to considerable debate, especially in the Geological Magazine (Newberry, 1885; Gresley, 1887, 1892; Cameron, 1892; Garwood, 1892; Harker, 1892; Sach, 1892; Young, 1886, 1892a, 1892b, 1892c), but also elsewhere (Cole, 1893; Bonney, 1897; Gresley, 1898; Haselhurst, 1915).

3. On moving from Britain to the United States of America, Gresley (1894) described cone-in-cone from Kansas and this led to numerous descriptions of such structures from elsewhere in the country (Keyes, 1896; Harnly, 1898; Broadhead, 1907; Tarr, 1922; Twenhofel and Tester, 1926; Shaub, 1937). In Latin America, explorers from the U.S.A. found cone-in-cone in petroleum source rocks, for example in Brazil (Stauffer, 1911), Peru (Iddings and Olsson, 1928) and Venezuela (Hedberg et al., 1947). Stauffer (1911) mentioned "well laminated almost slaty black shale, with concretionary beds containing the cone-in-cone structure and having a strong odour of petroleum".
4. During World War II and shortly before or after it, descriptions appeared in the French literature of cone-in-cone and beef from localities in France, Belgium, and their respective colonies in Africa (Morocco, Algeria, Madagascar and the Belgian Congo) and this triggered another debate as to mechanisms of formation (Cayeux, 1935; Denaeyer, 1938, 1939a, 1939b, 1939c, 1940a, 1940b, 1940c, 1940d, 1942, 1943a, 1943b, 1944a, 1944b, 1945, 1946, 1947a, 1947b, 1947c, 1952; Bonte, 1942, 1945a, 1945b, 1952; Bonte et al., 1947; Gay, 1942; Thoral, 1942; Maubeuge, 1945; David, 1952; Durand-Delga, 1952). Denaeyer (1947b) compared the cone-in-cone or nagelkalk of France with the cone-in-cone or beef of the United Kingdom.
5. Since then, there have been many reports of cone-in-cone in veins worldwide (Table 1; Fig. 2). There have also been some very detailed descriptions, both macroscopic and microscopic, and further discussions on possible mechanisms of formation (Brown, 1954; Franks, 1969; Woodland, 1964; Gilman and Metzger, 1967; Marshall, 1982; Selles-Martinez, 1994; Kolokol'tsev, 2002).

In our worldwide catalogue, we have included localities, for which authors have referred to "cone-in-cone", but only where it has been clear to us that the structures occur within bedding-parallel layers.

1.3. Fibrous veinlets

Some early authors described bedding-parallel fibrous veins, without using the terms beef or cone-in-cone. A good example was Taber (1918), who described "veinlets" from New York State, U.S.A. More generally, he developed ideas on the mechanisms of growth of fibrous mineral veins (Taber, 1916) and of fibrous ice (Taber, 1930).

2. Calcite beef worldwide

We have compiled a catalogue of worldwide localities, where beef or cone-in-cone occur in bedding-parallel layers (Cobbold et al., 2012). Where the fibres consist dominantly of calcite, we have recorded 110 localities (Table 1; Fig. 2A). Typically, a fibre of calcite is less than 1 mm wide and has grown parallel (or at a small angle) to its crystallographic c-axis (Bradshaw and Phillips, 1967).

The 110 localities of calcite beef are widespread, yet they concentrate in some areas, especially around the Atlantic Ocean. We have recorded the lithological compositions and stratigraphic ages of the host rocks (Table 1). The most frequent rock type is marine shale. Our histogram of ages (Fig. 2A) has modal highs for the following 4 periods: (1) Cambrian–Ordovician, (2) Devonian–Carboniferous, (3) Early Jurassic and (4) Cretaceous–Palaeogene. In contrast, we have found no record of early Triassic host rocks for calcite beef. We notice that our age distribution closely follows that of Markello et al. (2007), who compiled a global atlas of 8369 carbonate reservoirs in oil fields. We therefore suspect that controls on carbonate abundance have been climatic; in other words, that the modal highs reflect periods of abundant carbonate production on Earth, as a result of a warm climate or abundant carbon dioxide in the atmosphere. Because Jurassic to Palaeogene rifting preceded opening of the Atlantic Ocean, it is not surprising that calcite beef should be common on its margins.

The Neuquén Basin of western Argentina is one area where we have studied calcite beef in detail (Fig. 3). It is especially common in black mudstones of the upper Jurassic Vaca Muerta Fm (Parnell et al., 2000; Rodrigues et al., 2009), which happens to be the main source rock for petroleum in the Neuquén Basin. In some areas, the beef accounts for as much as 10% by volume of the rock (Fig. 3A). The veins are typically several cm wide and tens (or hundreds) of metres long. Commonly, each vein is symmetric about a central suture, which is dark, due to the presence of hydrocarbons (Fig. 3B) In many (but not all) of the beef veins from the Neuquén Basin, calcite fibres have formed in two generations (Rodrigues et al., 2009). Fibres of the first generation occupy the inner parts of the veins (Fig. 3C). They are steep to vertical, contain hydrocarbons, and formed in the Cretaceous, when the source rocks were maturing. Fibres of the second generation occupy the outer parts of the veins. They are whiter and oblique to the margins. In most (if not all) of the veins, each calcite fibre has grown in optical continuity (Fig. 3D and E). From the overall orthorhombic symmetry of the outer parts, Rodrigues et al. (2009) inferred they formed by differential shear, between more resistant veins and less resistant matrix, during bulk horizontal shortening of the rock. If so, the fibres grew from a central suture towards the outer edges of the veins, in other words, antitaxially. It is common for an original shell (for example, an ammonite) to be visible along the central suture of a beef vein, whereas corresponding moulds are visible at the outer edges of the vein (Fig. 3F). Because the calcite fibres link the shell to its moulds, we infer that the growing fibres have tracked the displacements of the walls. Some of the veins contain conical layers of shale (Fig. 3G). Where the layers are at high angles to the vein walls, they are not continuous but form chains of fragments (Fig. 3F). By imparting rigid displacements and rotations to these fragments, it is possible to obtain continuous and horizontal layers, which we infer to have been original thin sedimentary strata. This is good evidence that the fragments have resulted from vertical extension, while the calcite fibres were growing.

By analysis of both carbon and oxygen isotopes, Rodrigues (2008) was able to show that the calcite in the beef fibres formed late in the diagenetic alteration of the host rock. For aqueous inclusions, he measured homogenization temperatures in the range of 92°–113 °C (in other words, in the oil window). Independently, using Raman spectroscopy, he determined the compositions of oil inclusions and from these he estimated high overpressures (about half way between hydrostatic and lithostatic). The results provide good evidence for overpressure during oil migration in the Neuquén Basin and they help to explain the formation of horizontal fractures. During more recent fieldwork in the Neuquen Basin, we have found that calcite beef occurs, not only in the Vaca Muerta Fm, but also, more locally, in the underlying Los Molles Fm (early Jurassic) and the overlying Agrio Fm (early Cretaceous), which are also source rocks for petroleum.

The Wessex Basin of southern England is another oil-producing area, where we have studied beef and cone-in-cone in some detail (Fig. 1; Zanella and Cobbold, 2011, 2012; work in progress). On reading early descriptions of this basin (see Historical Introduction), as well as the informative website of West (2012), it became

Table 1
Worldwide localities of beef or cone-in-cone layers (mainly from publications). Locality numbers (first column) appear on corresponding maps (Fig. 2). In last column, number 1 (or 0) indicates whether any authors of this compilation have visited corresponding locality (or not).

No.	Calcite "beef"							
	Country	Area	Host rock name	Host rock age	Host rock type	Composition of fibres	References	Visit
1	United Kingdom	Somerset	Westbury Fm	Late Triassic	Mudstone, limestone	Calcite	Short (1904), Richardson (1911), Warrington et al. (1986), Gallois (2009)	0
2	United Kingdom	South Wales	Westbury Fm	Late Triassic	Mudstone, limestone	Calcite	Richardson (1905), Kelling and Moshrif (1977)	0
3	United Kingdom	South Wales	Carboniferous Lst.	Carboniferous	Mudstone, limestone	Calcite	George (1954)	0
4	United Kingdom	Wales	Welsh Basin	Ordovician	Marine shale	Calcite, dolomite, quartz	Fitches (1987)	0
5	United Kingdom	Wessex Basin, Isle of Purbeck	Purbeck Gp	Early Cretaceous	Marine shale	Calcite	Webster (1826), Buckland & De la Beche (1835)	1
6	United Kingdom	Wessex Basin, Lyme Regis	Shales-with-Beef Mbr	Early Jurassic	Marine shale	Calcite	Sorby (1860), Lang (1914), Lang et al. (1923), Marshall (1982), Gallois (2008)	1
7	United Kingdom	Wessex Basin, Kimmeridge Bay	Kimmeridge Clay Fm	Middle Jurassic	Marine shale	Calcite	Morgans-Bell et al. (2001)	1
8	United Kingdom	Wessex Basin, Vale of Wardour	Purbeck Gp	Late Jurassic	Limestone	Calcite	Andrews and Jukes-Brown (1894), Reid (1903)	0
9	United Kingdom	Wessex Basin, Isle of Wight	Vectis Fm	Early Cretaceous	Marine shale	Calcite	Judd (1871)	1
10	United Kingdom	Weald Basin, Sussex	Purbeck Gp	Early Cretaceous	Marine shale	Calcite	Howitt (1964)	0
11	United Kingdom	Weald Basin, Kent	Wealden Gp, Hastings Beds	Early Cretaceous	Marine shale	Calcite	Lamplugh and Kitchin (1911)	0
12	United Kingdom	Larne Basin, N. Ireland	(No name)	Early Jurassic	Marine shale	Calcite	Shelton (1997)	0
13	United Kingdom	N. Ireland	(No name)	Carboniferous	Marine shale	Calcite	Evans et al. (1998)	0
14	United Kingdom	Inner Hebrides, Scotland	Great Estuarine Gp	Late Jurassic	Marine shale	Calcite	Judd (1878), Harker (1908), Lee (1920), Marshall (1982)	1
15	United Kingdom	Eathie, Cromarty, Scotland	Kimmeridge Clay Fm	Middle Jurassic	Marine shale	Calcite	Wignall and Pickering (1993)	1
16	United Kingdom	Balintore, Cromarty, Scotland	Balintore Fm	Early Jurassic	Marine shale	Calcite	Authors' own observations	1
17	United Kingdom	Ayrshire, SW Scotland	Carboniferous Limestone	Carboniferous	Marine shale	Calcite, hydrocarbons	Young (1885), Denaeyer (1947c)	0
18	United Kingdom	Staffordshire, England	Milldale Limestone	Carboniferous	Marine shale	Calcite	Cossey et al. (1995)	0
19	United Kingdom	Northampton, England	Estuarine Series	Middle Jurassic	Marine shale	Calcite	Woodward (1893), Thompson (1902)	0
20	United Kingdom	Midlands, England	Blisworth Fm	Middle Jurassic	Marine shale	Calcite	Hendry (2002), Hudson and Clements (2007)	0
21	United Kingdom	North Yorkshire coast, England	Whitby Mudstone Fm	Early Jurassic	Marine shale	Calcite	Fox-Strangways and Barrow (1882), Denaeyer (1947c)	0
22	United Kingdom	Eastern England shelf	Kimmeridge Clay Fm	Middle Jurassic	Marine shale	Calcite	Lott (1985), Penn et al. (1986)	0
23	United Kingdom	North Sea, Outer Moray Firth	Alba Sandstones	Eocene	Marine claystone	Calcite	Hillier and Cosgrove (2002)	0
24	Netherlands	North Sea, Dutch Central Graben	Posidonia Fm (Toarcian)	Early Jurassic	Marine shale	Calcite	Trabucho-Alexandre et al. (2012)	0
25	Belgium	Saint-Mard, Prov. Luxembourg	Marnes de Grandcourt Fm	Early Jurassic	Marine shale	Calcite	Denaeyer (1943a)	0
26	France	Paris Basin, Foug, Lorraine	Argiles de la Woëvre	Middle Jurassic	Marine shale	Calcite	Denaeyer (1943b)	1
27	France	Paris Basin, Nancy area, Lorraine	Schistes Carton Fm (Toarcian)	Early Jurassic	Marine shale	Calcite	Guibal (1841), Denaeyer (1943b, 1944b), Maubeuge (1945)	0
28	France	Paris Basin, Blainville, Lorraine	Upper Muschelkalk Fm	Middle Triassic	Limestone and marl	Calcite	Denaeyer (1943b, 1944b), Maubeuge (1945)	1
29	France	Montagne Noire	(No name)	Ordovician	Marine shale	Calcite	Denaeyer (1943b), Bonte (1945b), Becq-Giraudon (1990)	0
30	Germany	Hils Syncline, Hanover	Posidonia Fm	Early Jurassic	Marine shale	Calcite, bitumen, oil	Jochum et al. (1995)	0
31	Poland	Silesia	Gogolin Fm	Middle Triassic	Limestone	Calcite	Kowal-Linka (2010)	0
32	Poland	Silesia	Kupferschiefer	Permian	Marine shale	Calcite, sulphides, gypsum	Jowett (1987)	0
33	Czech Republic	Prague Basin	Liten Fm	Silurian	Marine shale	Calcite, bitumen	Dobes et al. (1999), Volk et al. (2002), Suchy et al. (2002)	0
34	Italy	Rimini	Upper variegated clay	Oligocene	Claystone	Calcite	Perrone et al. (1998)	0
35	Norway	Svalbard	Wilhelmoya Fm	Early Jurassic	Marine shale	Calcite	Dypvik et al. (1985)	0
36	Denmark	Bornholm	Alum Shale	Cambrian	Marine shale	Calcite	Pedersen (1989)	0
37	Sweden	SE Sweden	Alum Shale	Cambrian	Marine shale	Calcite	Thickpenny (1984), Israelson et al. (1996), Egenhoff et al. (2012)	0
38	Sweden	Höganäs Basin, Skane	Rya Fm, Doshult Mbr	Early Jurassic	Marine shale	Calcite	Hausmann (1812), Frandsen and Surlyk (2003)	0
39	Greenland	Kuhn 0, NE Greenland		Aptian	Marine shale	Calcite	Donovan (1957)	0
40	Russia	Franz Josef Land, Northbrook Is.		Middle Jurassic	Marine shale	Calcite	Newton and Teall (1897), Pompeckj (1900)	0
41	Russia	Siberia		Silurian	Marine shale	Calcite	Kokolol'tsev (2002)	0

42	China	Junggar Basin	Loucaogou Fm	Permian	Marine shale	Calcite	Jiao et al. (2007)	0
43	China	Junggar Basin	Xiaoquangou Gp	Late Triassic	Marine shale	Calcite	Vincent and Allen (2001)	0
44	China	Junggar Basin	Sangonghe Fm	Early Jurassic	Marine shale	Calcite	Vincent and Allen (2001), Shao et al. (2003)	0
45	Algeria	NE Constantinois		Late Cretaceous	Marine shale	Calcite	David (1952), Durand-Delga (1952)	0
46	Morocco	Erfoud	Merdani Fm	Carboniferous	Shale	Calcite	Lugli et al. (2005)	0
47	Morocco	Rif		Late Cretaceous	Slate	Calcite	Frizon de Lamotte and Leikine (1985)	0
48	Oman	Oman Mountains		Late Proterozoic	Shale	Calcite	Schwarz and Koehn (2011)	0
49	Iran	Kopet Dagh Basin, NE Iran	Sanganeh Fm	Late Cretaceous	Marine shale	Calcite	Raisossadat (2004), Mahboubi et al. (2010)	0
50	Canada	Liard Basin, B. Columbia	Lepine Fm	Late Cretaceous	Marine shale	Calcite	Jowett and Schröder-Adams (2005)	0
51	Canada	Western Canada	Nordegg Mbr	Late Jurassic	Marine shale	Calcite	Riediger and Coniglio (1992)	0
52	Canada	British Columbia	Pardonet Fm	Late Triassic	Marine shale	Calcite	Orchard et al. (2001)	0
53	Canada	Northwest Terr.	Hare Indian Fm	Devonian	Marine shale	Calcite	MacKenzie (1972), Al-Aasm et al. (1993, 1996)	0
54	Canada	Baffin Island	Arctic Bay Fm	Middle Proterozoic	Marine shale	Calcite	Turner and Kamber (2012)	0
55	Canada	Quebec	Escuminac Fm	Devonian	Marine shale	Calcite	Woodland (1964), El Albani et al. (2002)	0
56	Canada	Quebec	Beekmantown -Trenton	Ordovician	Marine limestone	Calcite, quartz	Séjourné et al. (2005)	0
57	Canada	New Brunswick	Jones Creek Fm	Silurian	Marine shale	Calcite	Woodland (1964)	0
58	Canada	Cape Breton Island, Nova Scotia	Horton Gp	Carboniferous	Marine shale	Calcite	Woodland (1964)	0
59	U.S.A.	Alaska, Colville River	Nanushuk Fm	Late Cretaceous	Marine shale	Calcite	LePain et al. (2008)	0
60	U.S.A.	Gibson Lake, Montana	Switchback Shale	Cambrian	Marine shale	Calcite	Woodland (1964)	0
61	U.S.A.	Wyoming	Green River Fm	Eocene	Lacustrine shale	Calcite	Brown (1954)	0
62	U.S.A.	Uintah Basin, Duchesne County, Utah	Uinta Fm	Eocene	Lacustrine siltstone	Calcite	Woodland (1964)	1
63	U.S.A.	Utah	Wheeler Fm	Cambrian	Marine shale	Calcite	Woodland (1964), Brett et al., 2009	0
64	U.S.A.	Kansas	Kiowa Fm	Early Cretaceous	Marine shale	Calcite	Twenhofel and Tester (1926), Franks (1969)	0
65	U.S.A.	Kansas, Nebraska, S. Dakota	Pierre Shale, Sharon Springs Mbr	Late Cretaceous	Marine shale	Calcite	Gill et al. (1972)	0
66	U.S.A.	Ohio, Kentucky, W. Virginia, Tennessee	Ohio Shale, Cleveland Mbr	Devonian	Marine shale	Calcite	Hoover (1960), Herdendorff (1977), Provo et al. (1978), Broadhead et al. (1982)	0
67	U.S.A.	New York	Northeast Shale, Canadaway Mbr	Devonian	Marine shale	Calcite	Gilman and Metzger (1967)	0
68	U.S.A.	New York, Pennsylvania	Marcellus Shale	Devonian	Marine shale	Calcite	Taber (1918), Evans (2011)	0
69	U.S.A.	Pennsylvania	Portage Flags	Devonian	Marine limestone	Calcite	Gresley (1894)	0
70	U.S.A.	Tennessee	Holston Fm	Ordovician	Marine limestone	Calcite	Tobin et al. (1996)	0
71	U.S.A.	Parke County, Indiana	Staunton Fm	Carboniferous	Marine shale	Calcite	Woodland (1964)	0
72	U.S.A.	Oklahoma	Atoka Fm	Carboniferous	Marine shale	Calcite	Hammes et al. (2011)	0
73	U.S.A.	Fort Worth, West Texas	Barnett Shale	Carboniferous	Marine shale	Calcite	Milliken et al. (2012)	0
74	U.S.A.	West Texas	Smithwick Fm	Carboniferous	Marine shale	Calcite	Gale and Holder (2010)	0
75	U.S.A.	East Texas	Carrizo Sandstone	Eocene	Fluvial sandstone	Calcite	Enos and Kyle (2002)	0
76	U.S.A.	Louisiana	Haynesville Shale	Late Jurassic	Marine shale	Calcite	Spain and Anderson (2010), Hammes and Fréebourg (2012), Milliken and Day-Stirrat (2012)	0
77	U.S.A.	Alabama	Conasauga Shale	Cambrian	Marine shale	Calcite	Pashin (2011)	0
78	Mexico	Sierra Madre	La Casita Fm	Jurassic	Marine shale	Calcite, quartz, pyrite, bitumen	Lefticariu (2005), Fischer et al. (2005, 2009)	0
79	Mexico	Coahuila	Aurora Limestone	Late Cretaceous	Marine shale	Calcite, gypsum	Lozej and Beales (1997)	0
80	Mexico	Mexican Fold-Thrust Belt		Cretaceous	Limestone, shale	Calcite, quartz	Fitz-Diaz et al. (2011)	0
81	Colombia	Muzo, Coscuez	Paja Fm	Early Cretaceous	Marine shale	Calcite, quartz, pyrite, emerald	Branquet et al. (1999)	1
82	Colombia	Zipaquirá, Sesquilé	Lutitas del Macanal Fm	Early Cretaceous	Marine shale	Calcite	Authors' own observations	1
83	Barbados	Scotland District	Basal Complex, Joes River Fm	Eocene	Marine shale	Calcite, bitumen	Speed (1990), Parnell et al. (1994)	0
84	Trinidad & Tobago	Trinidad	Cruse Fm	Tertiary	Marine shale	Calcite	Geol. Soc. Trinidad Newsletter, March 2003.	0
85	Venezuela	Maracaibo	La Luna Fm	Late Cretaceous	Marine shale	Calcite	Pratt et al. (1993), Macsotay et al. (2003)	0
86	Venezuela	Orinoco Heavy Oil Belt	Oficina Fm	Early Miocene	Marine shale	Calcite	Hedberg et al. (1947), Renz (1957), Fary (1980), Martinius et al. (2012)	0
87	Suriname	Demerara Rise		Late Cretaceous	Marine shale	Calcite	ODP Shipboard Scientific Party (2003)	0
88	Brazil	Solimoes Basin	Jutai Fm	Devonian	Marine shale	Calcite	Rubinstein et al. (2005)	0
89	Brazil	Lower Amazon Basin	Curua Fm, Barreirinha Mbr	Devonian	Marine shale	Calcite	Stauffer (1911)	0
90	Brazil	Araripe Basin	Crato Fm	Albian	Lacustrine shale	Calcite	Silva (2003)	0
91	Peru	Talara Basin	Palegreda Fm	Eocene	Marine shale	Calcite	Iddings and Olsson (1928)	0

(continued on next page)

Table 1 (*continued*)

No.	Calcite "beef" Country	Area	Host rock name	Host rock age	Host rock type	Composition of fibres	References	Visit
92	Argentina	Yavi, Altiplano, Jujuy		Ordovician	Marine shale	Calcite (partly silicified)	Harrington and Leanza (1957), Woodland (1964)	0
93	Argentina	Neuquén Basin	Los Molles Fm	Early Jurassic	Marine shale	Calcite	Authors' own observations	1
94	Argentina	Neuquén Basin	Vaca Muerta Fm	Late Jurassic	Marine shale	Calcite, bitumen	Parnell et al. (2000), Rodrigues et al. (2009)	1
95	Argentina	Neuquén Basin	Agrio Fm	Early Cretaceous	Marine shale	Calcite, bitumen	Authors' own observations	1
96	Argentina	Magellan Basin	Rio Mayer Fm	Early Cretaceous	Marine shale	Calcite	Riccardi et al. (1987)	0
97	Chile	Magellan Basin	Rincon Negro Fm	Late Cretaceous	Marine shale	Calcite	Cecioni (1957)	0
98	Falkland Islands	Falkland Plateau		Late Jurassic	Marine shale	Calcite	Tarney and Schreiber (1976), Maillot and Bonte (1983)	0
99	Antarctica	Livingston Island	President Beaches Fm	Early Cretaceous	Marine shale	Calcite	Crame et al. (1993), Torres et al. (1997)	0
100	Antarctica	Ohio Range, Transantarctic Mountains	Discovery Ridge Fm	Devonian	Marine shale	Calcite	Doumani and Tasch (1965)	0
101	Rep. South Africa	Kalahari		Quaternary	Calcrete	Calcite	Watts (1978)	0
102	Zambia	Zambezi Valley	Madumabisa Fm, L. Karoo Gp	Permian	Marine shale	Calcite	Molyneux (1909), Nyambe and Dixon (2000)	0
103	Congo	Nyangwe, Lualaba River	Lukuga Series	Permian	Marine shale	Calcite	Denaeyer (1939c)	0
104	Tanzania	Ruhuhu Basin	Idusi Fm, Lilangu Fm	Permian	Marine shale	Calcite	Catuneanu et al. (2005)	0
105	Tanzania	Kilwa Peninsula, SE coast	Kivinje Fm, Kilwa Gp	Eocene	Marine shale	Calcite	Nicholas et al. (2006), Pearson et al. (2006)	0
106	Madagascar	Morondava Basin	Sakamena Fm	Permian	Marine shale	Calcite	Radelli (1975)	0
107	Madagascar	Morondava Basin	Isalo II Fm, Isalo III Fm	Early Jurassic	Marine shale	Calcite	Lacroix (1923), Denaeyer (1943b), Museum Collection (Geosciences-Rennes)	1
108	Australia	Lachlan Orogen, N S W.	Murrumbigee Gp	Devonian	Marine limestone, shale	Calcite	Barker et al. (2006)	0
109	Australia	Queensland, Carpentaria Basin	Rolling Downs Gp	Early Cretaceous	Marine shale	Calcite	Daintree (1872), Ingram (1972)	0
110	New Zealand	Kaipara Harbour North Auckland		Late Cretaceous	Marine shale	Calcite	Marshall (1926)	0
								15

No.	Gypsum "beef" Country	Area	Host rock name	Host rock age	Host rock type	Composition of fibres	References	Seen
1	United Kingdom	Boulby, Cleveland		Permian	Mudstone	Gypsum	Cosgrove (pers. comm., 2009)	0
2	United Kingdom	Bristol Channel	Mercia Mudstone Fm	Triassic	Mudstone	Gypsum	Cosgrove (1995, 2001), Philipp (2008)	0
3	United Kingdom	South Devon	Mercia Mudstone Fm	Triassic	Mudstone	Gypsum	Gallois (2001)	0
4	United Kingdom	Cheshire Basin	Mercia Mudstone Fm	Triassic	Mudstone	Gypsum	Richardson (1920), Gustavson et al. (1994)	0
5	United Kingdom	Cumbria, Vale of Eden	Eden Shales Fm	Permian	Mudstone	Gypsum	Shearman et al. (1972), Hughes (2003)	0
6	France	Paris Basin, Lorraine	Marnes Irisées	Triassic	Marl	Gypsum	Maubeuge (1991)	0
7	Spain	Basque-Cantabrian Basin	Zumaia-Algorri Fm	Late Cretaceous	Marl-limestone	Celestite	Abalos and Elorza (2011)	0
8	Spain	Lorca Basin	Serrata Fm	Miocene	Evaporite	Gypsum	Geel (1976), Benali et al. (1995)	0
9	Italy	Volterra Basin	Radicondoli Fm	Miocene	Evaporite	Gypsum	Testa and Lugli (2000)	0
10	Latvia	Salaspils		Devonian	Evaporite	Gypsum	Website	0
11	Tunisia	Tataouine	Zmilet Haber Fm	Early Jurassic	Marine shale/evaporite	Gypsum	Authors' own observations	1
12	Egypt	Luxor	Esna Fm	Palaeocene	Marine shale	Gypsum	Cobbold et al. (2008)	1
13	Angola	Benguela	Dombe Grande Fm	Aptian	Evaporite	Gypsum	G. Castro, pers. comm. (2012)	0
14	Israel	Dead Sea	Ora Fm	Late Cretaceous	Marine shale	Gypsum	Gross et al. (1997)	0
15	Oman	Ras-al-Hamra, Muscat		Eocene	Shale and limestone	Gypsum	Hilgers and Urai (2005)	0
16	Bolivia	Chaco Basin	Yecua Fm	Miocene	Shallow marine shale	Gypsum	Hulka et al. (2006)	0
17	U.S.A.	Fort Worth, Texas	Barnett Fm	Carboniferous	Marine shale	Barite	Gale and Holder (2010)	0
18	U.S.A.	Panoche Hills, California	Moreno Fm	Late Cretaceous	Marine shale	Gypsum	Authors' own observations	1
19	U.S.A.	Uintah Basin, Utah	Green River Fm	Eocene	Lacustrine shale	Gypsum, bitumen	Authors' own observations	1
20	U.S.A.	Capitol Reef, Utah	Moenkopi Fm	Triassic	Mudstone	Gypsum	Authors' own observations	1
21	U.S.A.	Escalante, Utah	Carmel Fm	Early Jurassic	Mudstone	Gypsum	Authors' own observations	1
22	U.S.A.	Texas Panhandle	Quatermaster Fm	Permian	Mudstone	Gypsum	Collins (1984), Gustavson et al. (1994)	0
23	U.S.A.	Appalachian Basin	Camillus Fm, Salinas Gp	Silurian	Mudstone	Gypsum	Taber (1918), Gustavson et al. (1994)	0
24	U.S.A.	Newark Basin	Passaic Fm	Triassic	Mudstone	Gypsum	El-Tabakh et al. (1998)	0

25	Canada	Western Canada Basin, Alberta	Nisku Fm	Devonian	Mudstone	Gypsum, anhydrite	Machel (1985)	0
26	Canada	Saskatchewan		Carboniferous	Mudstone	Gypsum	Kendall (1975)	0
27	Argentina	Altiplano	Sijes Fm	Miocene	Evaporite	Gypsum	Ortí and Alonso (2000)	0
28	Argentina	Neuquen Basin	Vaca Muerta Fm	Late Jurassic	Marine shale	Gypsum, oil	Authors' own observations	1
29	Australia	Amadeus Basin	Bitter Springs Fm	Late Proterozoic	Dolomite	Gypsum	Stewart (1979), Gustavson et al. (1994)	0
30	China	Qaidam Basin	Shangganchaigou Fm	Miocene	Limestone	Gypsum	Neubauer et al. (2010)	0
								7

No.	Quartz "beef"							
	Country	Area	Host rock name	Host rock age	Host rock type	Composition of fibres	References	Seen
1	United Kingdom	Devon	Culm Fm	Carboniferous	Marine turbidite	Quartz	Tanner (1989)	1
2	United Kingdom	Dolaucothi, Wales		Ordovician	Marine turbidite	Quartz, gold, sulphides	Annels and Roberts (1989)	0
3	France	Poligné, Brittany	Riadan Fm	Silurian	Marine sandstone/shale	Quartz	Authors' own observations	1
4	Germany	Ardennes	Rurberg-Heimbach	Devonian	Slate	Quartz	Van Noten et al. (2011)	0
5	Spain	Extremadura		Devonian	Slate	Quartz, gold, sulphides	Sanderson et al. (1994)	0
6	Rep. South Africa	Witwatersrand Basin	Carbon Leader Reef	Archaean	Shale	Quartz, gold, uraninite, sulphides	Parnell (1999), England et al. (2002), Grové and Harris (2010)	1
7	Rep. South Africa	Eastern Transvaal	Transvaal Supergroup	Paleoproterozoic	Dolomite and shale	Quartz, gold, sulphides	Harley and Charlesworth (1996)	0
8	Namibia	Ondundu	Kuiseb Fm	Neoproterozoic	Marine turbidite	Quartz, gold, sulphides	Forsys Metals	0
9	Australia	New South Wales	Hill End	Silurian-Devonian	Marine turbidite	Quartz, gold, sulphides	Watt (1898), Windh (1995)	0
10	Australia	Victoria	Bendigo-Ballarat Slate	Ordovician	Marine turbidite	Quartz, gold, sulphides	Jessell et al. (1994), Fowler (1996), Willman (2007)	0
11	Australia	Western Australia	Hamersley Gp	Palaeoproterozoic	Banded iron formation	Quartz, hematite (Tiger's Eye)	Brown et al. (2004), Hilgers and Urai (2005)	0
12	New Zealand	Preservation Inlet	Preservation Fm	Ordovician	Marine turbidite	Quartz, gold, sulphides	Begbie et al. (2005)	0
13	Canada	Meguma, N. Scotia	Goldenville Fm	Ordovician	Marine turbidite	Quartz, gold, sulphides	Henderson and Henderson (1986), Sangster and Smith (2007)	0
14	Canada	British Columbia	Gog Gp	Cambrian	Marine turbidite	Quartz, gold, sulphides	Foster (1987), Shaw and Morton (1990)	0
15	Argentina	Jujuy	Puna Turbidite C.	Ordovician	Marine turbidite	Quartz, gold, sulphides	Golden Arrow	1
16	Peru and Bolivia	Eastern Cordillera	San Jose Fm	Ordovician	Marine turbidite	Quartz, gold, sulphides	Fuchs (1898), Fornari and Herail (1991)	0
17	Russia	Sukhoi, Lena, Siberia	Khomolkho Fm	Neoproterozoic	Shale and silt	Quartz, gold, sulphides	Distler et al. (2004), Large et al. (2011)	0
								4

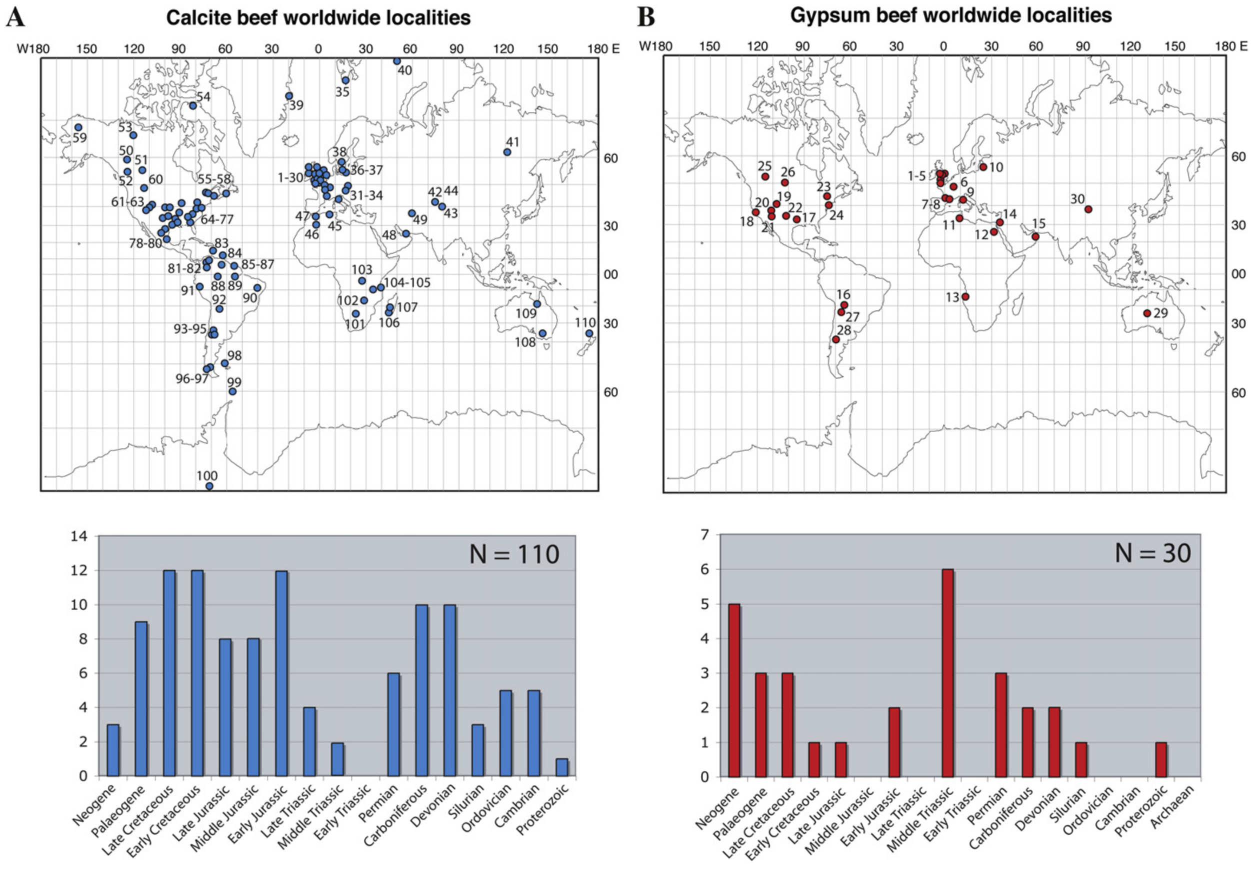

Figure 2. Worldwide localities (top) and histograms of stratigraphic ages of host rocks (bottom) for calcite beef (A), gypsum beef (B) and quartz beef (C). Numbers on maps refer to localities in Table 1 (first column). Map projection is Mercator. Locations are approximate (for more precise ones, see relevant publications). On histograms, modal ages are Cambro–Ordovician, Devonian–Carboniferous, Early Jurassic or Cretaceous, for calcite beef; Middle Triassic or Neogene, for gypsum beef; and Proterozoic or Ordovician for quartz beef.

clear to us that calcite beef and cone-in-cone layers are abundant in the area. Recent work has more than confirmed this. Across the whole of the Wessex Basin, from Dorset to Sussex, beef occurs at intervals within strata (especially mudstones) of various stratigraphic ages, from Early Jurassic to Middle Cretaceous. What is more, we have found that oil inclusions are common within the calcite fibres (Fig. 1D).

Finally, we have verified occurrences of calcite beef and cone-in-cone in outcrops at the eastern edge of the Paris Basin, France (Denaeyer, 1943b, 1944a, 1944b, 1947a). The layers occur in Lower Jurassic (Toarcian) source rocks (Schistes Carton), but also in underlying Middle Triassic limestones and overlying Middle Jurassic marls and limestones, which happen to be the main oil-producing reservoirs so far.

3. Gypsum beef worldwide

Also at the surface, or in boreholes, we have recorded 30 localities, where beef consists of gypsum fibres (Table 1, Fig. 2B), or exceptionally of anhydrite fibres (Machel, 1985). However, we are not aware of any cone-in-cone beds of the same composition. Typically, fibres of gypsum beef are less than 1 mm wide (Fig. 4), as they are for calcite beef.

The 29 localities of gypsum beef are widespread (Fig. 2B). They concentrate in the same areas as for calcite beef, except that gypsum beef is absent at high latitudes. We have documented the stratigraphic ages and lithological compositions of the host rocks (Table 1). The most frequent rock types are mudstone or evaporite and the most frequent ages are either Middle Triassic or Neogene. We notice that these were times of abundant evaporite production, under a warm dry climate. In contrast, for early Palaeozoic or Jurassic to Cretaceous host rocks, we have found few reports of gypsum beef.

At atmospheric pressure, dry gypsum is stable up to temperatures of about 60 °C. Above this it dehydrates to anhydrite (Jowett et al., 1993). However, if gypsum is in contact with an aqueous fluid, for which pressures reach lithostatic values, it may be stable at temperatures of more than 100 °C and depths of more than 3 km, depending on the salinity of the fluid.

Some gypsum beef occurs in evaporitic or continental sequences that overlie petroleum source rocks and reservoirs, good examples being those of Tunisia (Fig. 4A) or Angola (Fig. 4B). This does not necessarily mean that petroleum generation was the cause of overpressure, another possibility being the dehydration of gypsum to anhydrite at depth. Other examples of gypsum beef occur next to vertical veins, where there is independent evidence for overpressure. Thus gypsum beef is common around sills and dykes of injected sand (injectites) in the Panoche Hills, California (Fig. 4C and D). Hurst et al. (2011) have described the Panoche injectite complex in detail, inferring that it was due to overpressure. Another interesting association is between gypsum beef and vertical dykes

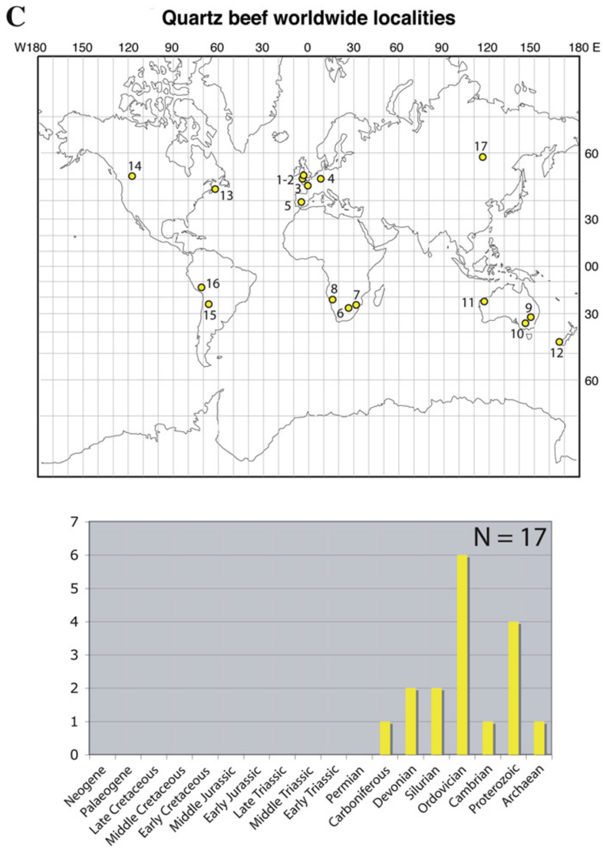

Figure 2. (*continued*).

of solid bitumen in the Neuquén Basin, Argentina (Figs. 4E and F). Cobbold et al. (2011) have discussed evidence that this bitumen was originally oil, which formed from Jurassic source rock, as a result of hydrothermal heat advection around Quaternary volcanoes, and then intruded its host rocks while under overpressure.

Of the 30 localities of gypsum beef (Table 1), we are aware of only one containing hydrocarbons, although we suspect that there may be others. In the Neuquén Basin, Argentina, where there is an active petroleum system, liquid oil is present as inclusions within gypsum fibres. This occurs at the SE edge of the basin, where facies are evaporitic. In the same area, oil occurs as surface seeps and appears to have migrated, both horizontally and vertically, from deeper parts of the basin.

4. Quartz beef worldwide

At the surface and in deep mines, we have recorded 17 localities, where bedding-parallel layers consist mainly of fibrous quartz (Table 1, Fig. 2C). Typically the fibres are several mm or even cm wide, in other words, wider than those of calcite beef or gypsum beef. Also the quartz fibres tend to be irregular in width, possibly as a result of growth competition or of recrystallization. In some examples, the fibres are perpendicular to bedding, but commonly they are oblique, indicating a component of slip along the bedding (Tanner, 1989). We have avoided recording examples of cone-in-cone that consist of quartz, because there is considerable debate as to whether such quartz is primary, or formed by secondary alteration of calcite (Woodland, 1964).

The 17 localities of quartz beef concentrate at intermediate latitudes, forming northern and southern belts. We have documented the stratigraphic ages and lithological compositions of the host rocks (Table 1, Fig. 2C). The most frequent ages are Proterozoic or Ordovician and the most frequent rock type is a meta-turbidite (that may have reached greenschist facies). For host rocks younger than Carboniferous, we have found no reports of quartz beef. We notice that the Proterozoic and Ordovician were periods of severe glaciation, which led to intense erosion and subaqueous deposition of turbidites.

The solubility of silica in water decreases strongly, as the temperature of the solution drops below 250 °C, especially if the pressure also drops (Fournier and Rowe, 1977). Thus quartz beef typically forms at depths of more than 8 km, under conditions of greenschist-facies metamorphism. For it to reach the surface by subsequent exhumation may require long periods of time and this may explain why there are no reports of quartz beef in Mesozoic or Cenozoic host rocks, even if these accumulated during periods of glaciation (such as the Quaternary).

Of the 17 localities of quartz beef, we are aware of none containing liquid oil, but some do contain solid hydrocarbons (bitumen) between the fibres. Other accessory minerals of economic importance may be uraninite, gold, or metallic sulphides. These are commonly of detrital origin, but have undergone hydrothermal remobilization, together with quartz. One of the most impressive, regionally continuous and economically valuable examples is the Carbon Leader reef of the Archaean Witwatersrand Basin, Republic of South Africa. The Carbon Leader is a conglomeratic unit with a bituminous base (Parnell, 1999; Grové and Harris, 2010). Bedding-parallel veins contain steep fibres of quartz and bitumen, as well as more equant grains of uraninite, secondary sulphides, or gold (Fig. 5). There has been considerable debate as to the origin of the uraninite and the gold, but the consensus would seem to be that (1) the bitumen represents original oil, (2) secondary uraninite precipitated around the bitumen, and (3) gold and sulphides were originally of detrital origin, but remobilized hydrothermally (Parnell, 1999; England et al., 2002; Grové and Harris, 2010). This distribution is visible under the scanning electron microscope (Fig. 5).

Of the other localities of quartz beef, many are in well-stratified turbidite sequences, which have undergone, not only metamorphism, but also folding. Early quartz veins are typically parallel to bedding, but tend to be thicker in anticlinal hinges, forming saddle reefs (Fig. 6). This indicates that flexural slip was an important mechanism of folding (Tanner, 1989). Factors that favour such a mechanism are (1) alternations of stiff and less stiff layers, which are ubiquitous in turbidites, and (2) overpressure. Many of the World’s most famous gold districts (such as Meguma in Newfoundland, or Ballarat and Bendigo in Australia) occur in such a context (see Table 1).

5. Calcite-quartz beef

At intermediate temperatures (150 °C–250 °C), calcite and quartz may precipitate almost simultaneously from aqueous fluids, accounting for bedding-parallel veins of hybrid nature (e.g. Fischer et al., 2009). Such veins tend to occur in fold-and-thrust belts, where fluid overpressure may have facilitated folding by flexural slip. We have recorded a few examples (Table 1), which we have grouped with calcite beef. Some hybrid veins may carry accessory minerals of economic importance, such as sulphides, or emerald (green beryl).

In Colombia, emeralds occur in hydrothermal veins within two belts, one on each side of the Eastern Cordillera (Branquet et al., 1999). Typically, the veins contain calcite, pyrite, quartz, bitumen,

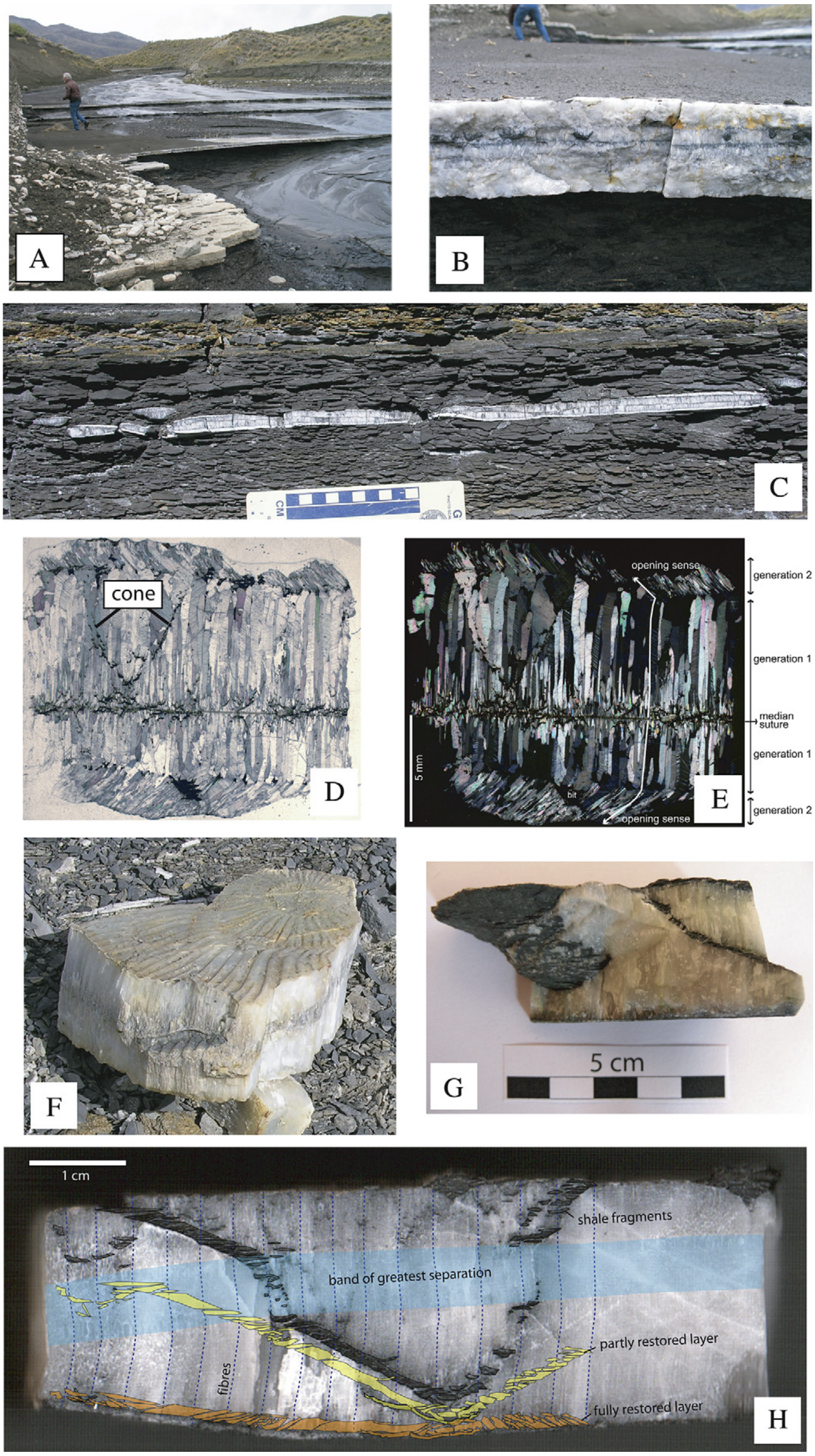
A
B
C
CM
cone
D
opening sense
generation 2
generation 1
median suture
generation 1
generation 2
5 mm
bit
opening sense
E
F
5 cm
G
1 cm
shale fragments
band of greatest separation
partly restored layer
fibres
fully restored layer
H

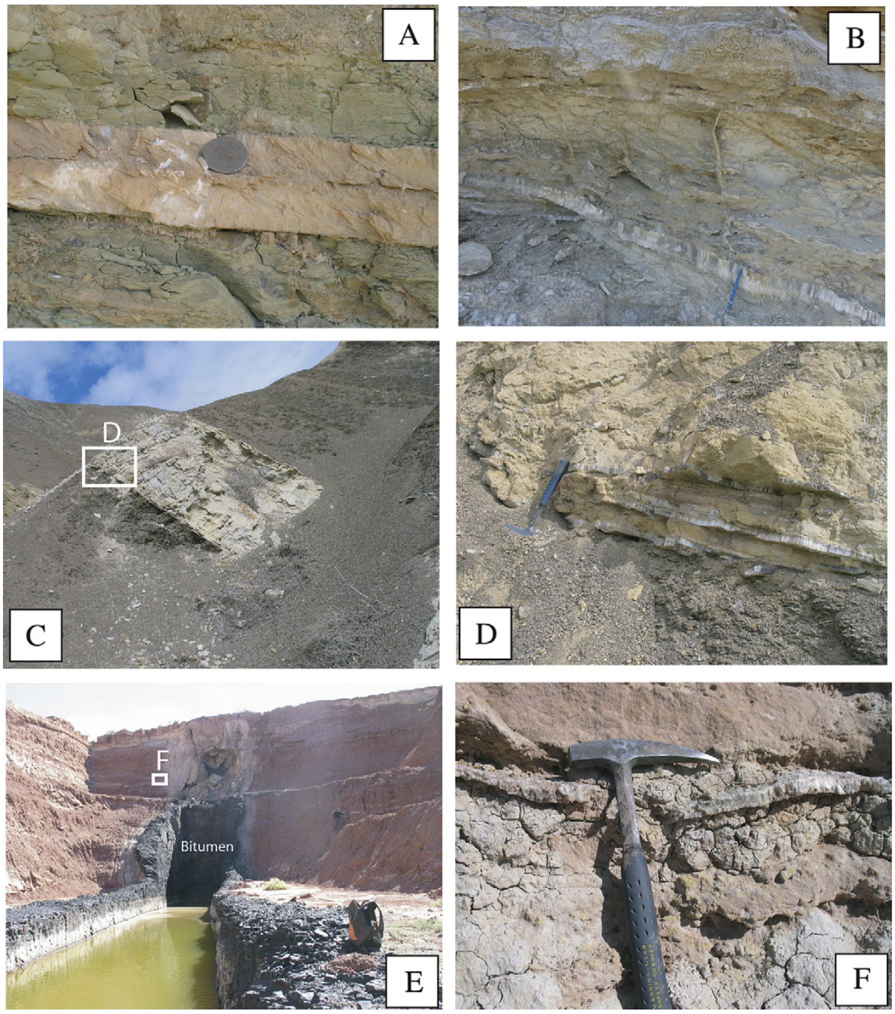

Figure 4. Gypsum beef. A. Flat-lying beef vein with oblique fibres in Cretaceous mudstone, Khanget-Aiche, Gabès, Tunisia (GPS: 34° 04′28.04″ N, 9° 51′ 40.09″ E). B. Flat-lying veins within Aptian evaporite, Benguela, Angola (photograph by courtesy of Gabriel Castro, Petrobras). C. Gently dipping sandstone sill within Tertiary mudstone, Panoche Hills, California, U.S.A. Rectangle indicates position of Figure 4D. D. Veins of gypsum beef lining upper contact of sandstone sill, Panoche Hills, California, U.S.A. E. Near-vertical dyke of bitumen (black), several m wide, within flat-lying Late Cretaceous continental strata (red), Toribia Mine, Neuquén Basin, Argentina (GPS: 37° 13′ 23.55″ S, 69° 06′ 47.86″ W). Rectangle indicates position of Figure 4F. F. Gypsum beef (parallel to bedding), near edge of bitumen dyke, Toribia Mine, Neuquén Basin, Argentina.

fluorite, dolomite, and emerald. In the western belt, around Muzo, the veins tend to be bedding-parallel. Thus they probably formed in the early stages of thrusting. The green colour of the emeralds is due to vanadium and chromium. Together with beryllium, these elements come from volcanic ash within the host rock, organic-rich marine shale of Early Cretaceous age that accumulated in a back-arc basin, above a layer of evaporite. The calcite and pyrite in the veins are products of thermo-chemical sulphate reduction. This process

Figure 3. Calcite beef and shale cones, Neuquén Basin, Argentina. A. Layers of calcite beef (white) within shale (black), Vaca Muerta Fm., Arroyo Mulichinco (GPS coordinates: 38° 01′ 14.58″ S, 70° 27′ 09.22″ W). Photograph illustrates uniform thickness of beef and parallelism with bedding. B. Close-up view of layer of calcite beef (about 20 cm thick), Arroyo Mulichinco (see A). Calcite fibres are nearly perpendicular to bedding. Darker layers in centre of vein contain organic matter. C. Layer of calcite beef within shale, Vaca Muerta Fm., Laucha, Yesera del Tromen (GPS: 37°17.347′S, 69°53.047′W; see Rodrigues et al., 2009, their fig. 6A). Inner layers, next to median suture, consist of vertical fibres of either pure calcite (white) or hydrocarbon-bearing calcite (grey), whereas thin outer layers consist of oblique fibres of purer calcite (white). D. Thin section of beef vein (C) in transmitted light, showing calcite fibres and single thin conical layer of shale. E. Same thin section of beef vein, but in polarized light. Inner zones of Generation 1 differ in thickness about median suture, but some fibres are in optical continuity across them. In outer zones of Generation 2, fibres are oblique to bedding, especially towards vein tips. From one outer zone to other, fibres are at opposite angles to vein boundaries. F. Loose fragment of beef vein, Laucha, Yesera del Tromen (GPS location 37° 18.131′ S, 69° 52.936′ W). Imprint of ammonite is on upper surface of vein, whereas part of original shell is visible along central parting. Similar imprint exists on lower surface of vein. Calcite fibres are slightly oblique to bedding-normal and they link corresponding points of shell and its imprints, proving that vein has dilated. G. Sample of calcite beef containing thin layer of shale (black) that forms cones, Arroyo Mulichinco (GPS: 38° 01′ 14.58″ S, 70° 27′ 09.22″ W; see Rodrigues et al., 2009, their fig. 8). Sample has broken, either following one of conical surfaces (left), or cutting across another (right). In both cones, small fragments of shale have separated vertically, following directions of calcite fibres. H. Vertical section across same beef sample as in G. Shale fragments (black) have separated vertically. Greatest separation is across a band (blue highlight) of paler calcite. Restoration of fragments, first by simple displacements along fibre directions, then by further displacements and rigid rotations in plane of section, yields more continuous layer (yellow or orange assemblages). For details, see text.

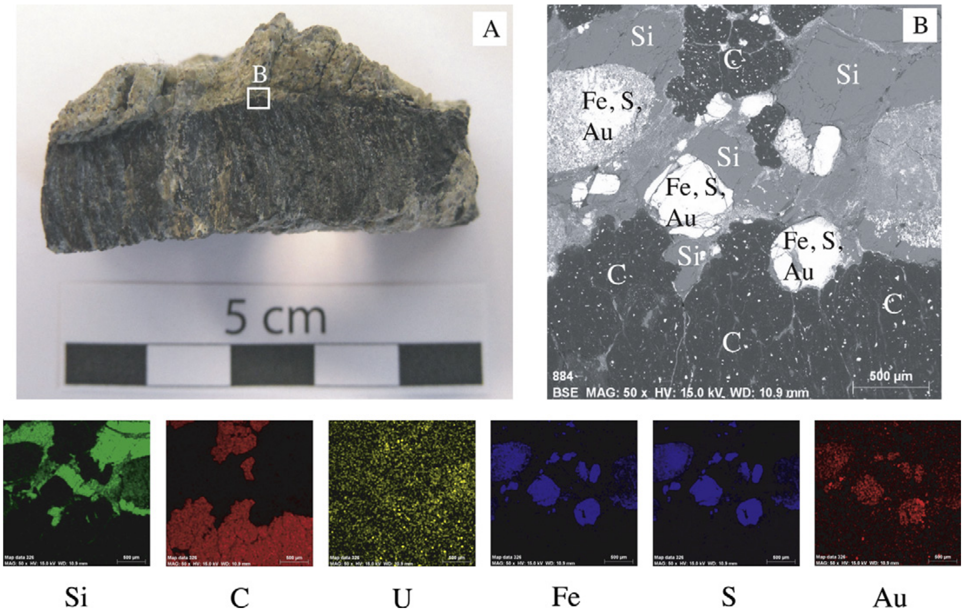

Figure 5. Carbon Leader reef, East Driefontein Mine, Witwatersrand Basin, Rep. South Africa. Sample (top left, courtesy of Goldfields Plc., year 1997) consists of bedding-parallel vein of dark fibrous material, beneath pale crystalline layer of quartz. Small white square indicates area of analysis. Composite image from Environmental Scanning Electron Microscope (top right) shows distributions of elements and mineral species. Colour images (bottom) indicate distribution of each of 6 elements across composite image. Fibrous vein consists mainly of carbon; upper pale layer is mainly quartz; uranium occurs in small particles throughout sample; whereas gold concentrates within equant crystals of iron sulphide (pyrite).

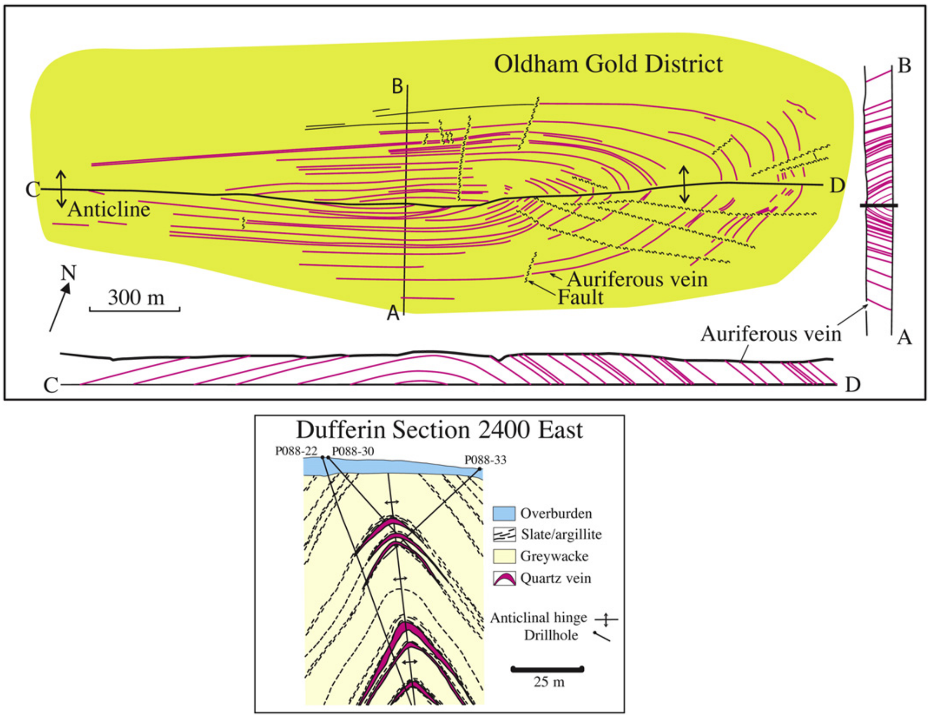

Figure 6. Gold-bearing quartz veins in meta-turbidites of the Goldenville Fm (Lower Ordovician), Meguma gold mining district, Nova Scotia, Canada (modified, after Sangster and Smith, 2007). On map of Oldham mining district (top) and vertical cross-sections (A–B, C–D), quartz veins (red) are continuous and bedding-parallel, over distances of several km and down to depths of several hundred m. On Section 2400 East at Dufferin Mine extension, Salmon River gold mining district, gold-bearing veins in sequence of meta-turbidites (greywackes and argillites of greenschist grade) locally form prominent saddle reefs across anticlinal fold hinge.

also generated large amounts of gas (carbon dioxide, methane and water vapour), which may easily have accounted for overpressure and hydraulic fractures (Branquet et al., 1999).

6. Mechanisms of development

6.1. Beef

In flat-lying sedimentary basins, fibres of beef appear to have grown vertically, or nearly so, during progressive opening of the veins. The best evidence for this probably comes from split fossils. Where shells lie along the median plane of a vein, their impressions are visible at the upper and lower surfaces. Good examples occur in the Wessex Basin, England (Lang et al., 1923) and in the Neuquen Basin, Argentina (Rodrigues et al., 2009).

More generally, for fibrous veins of any attitudes, there is a consensus that the fibres have grown incrementally, partly or totally tracking the history of relative displacement of the walls (Taber, 1918; Durney and Ramsay, 1973). In some examples, opening and infilling seem to have occurred episodically, by a crack-seal mechanism (Ramsay, 1980); whereas, in other examples, growth appears to have been more continuous (Taber, 1918; Durney and Ramsay, 1973; Means and Li, 2001). More generally, it may be possible for fibrous minerals to grow, not during the opening of a vein, but in response to concentration gradients, as in the experiments of Bons and Jessell (1997). In crack-seal, the fibrous mineral fills an open micro-crack (Ramsay, 1980), whereas in Taber growth, there is no open micro-crack, but a cohesive boundary between fibre and substrate. However, the details are subject to debate. For example, Means and Li (2001) could not exclude the possibility that micro-cracks formed during physical experiments, in which they reproduced Taber growth of fibrous minerals in veins. Also in fibrous veins, crystal faces between neighbouring fibres tend to be smooth, not serrate, and this may indicate a lack of growth competition (Mügge, 1928; Urai et al., 1991). Hilgers et al. (2001) numerically modelled the growth of fibres by crack-seal, and concluded that there should be little growth competition if the crack width is less than 10 μm. According to the positions of the growing crystals with respect to the walls, Durney and Ramsay (1973) distinguished three kinds of fibrous veins: (1) in stretched veins, fractures open and seal repeatedly in different positions across the vein; (2) in syntaxial veins, fibres grow on one or both sides of the vein and towards the middle of the vein, where there is a fracture; and (3) in antitaxial veins, the fibres grow from a median suture line towards the walls, where there are fractures. In the Neuquen Basin, there is good evidence that at least some of the veins have grown antitaxially (Rodrigues et al., 2009).

Our current understanding is that fibrous minerals in veins grow by precipitation, mainly from supersaturated aqueous solutions, as a result of chemical reactions, or changes in physical conditions, especially drops in temperature or pressure. There are two potential mechanisms for transporting the nutrients (Elburg et al., 2002). Advective fluid flow transports them over long distances, until they precipitate in a vein, which is effectively an open system (McCaig et al., 1995). Alternatively, the nutrients diffuse over shorter distances (centimetres to decimetres), in what is effectively a closed system (Durney and Ramsay, 1973; Oliver and Bons, 2001). Notice that the assumption of an open or closed system depends on the scale of observation.

A question that has arisen frequently in discussions is whether the opening of a beef vein is due to an internal agent, such as force of crystallization, or to an external agent, such as tectonic stress or pore fluid pressure. For force of crystallization, there is indeed some theoretical and experimental evidence (e.g. Taber, 1916; Means and Li, 2001; Keulen et al., 2001; Gratier et al., 2012). Keulen et al. (2001) did experiments on the hydration of anhydrite and succeeded in measuring a pressure of crystallization of as much as 11 MPa, equivalent to the vertical stress resulting from an overburden of 450–600 m. However, they did not manage to reproduce fibrous veins.

As external agents, Shearman et al. (1972) and Stoneley (1983) argued the case for overpressure, whereas Gustavson et al. (1994) favoured dissolution at depth. In theory, horizontal fractures cannot form under purely lithostatic conditions, where the greatest stress is vertical and compressive (due to gravity) and the least stress is horizontal (Sibson, 2003). However, bedding-parallel fractures may form if (1) the bedding is not horizontal and (2) the rock is anisotropic, so that its tensile strength is smallest in a direction perpendicular to bedding (Cosgrove, 1995, 2001; Lash and Engelder, 2005). Alternatively, horizontal fractures may form if the vertical stress in the solid framework (the effective stress of Von Terzaghi, 1923) becomes tensile and the horizontal stress is smaller in magnitude. This can happen if there is a vertical gradient of overpressure (Cobbold and Rodrigues, 2007). High values of pore fluid pressure are common in sedimentary basins, especially at depth (Swarbrick et al., 2002) and the term overpressure refers to a condition, in which the fluid pressure is greater than the hydrostatic pressure of an equivalent free column of water. The possible causes of such overpressure are a matter for debate. The most popular would seem to be mechanical compaction, hydrocarbon generation, or a combination of both, in other words, chemical compaction (Swarbrick et al., 2002). Another likely cause is dehydration of hydrous minerals, such as gypsum, mica, or amphibole. More generally, hydrothermal fluids may be sources of overpressure. A vertical gradient in overpressure produces seepage forces, which act vertically on every particle of the rock, as fluid migrates upward through the pores. On a graph of shear stress versus normal stress (Fig. 7), as overpressure increases, the Mohr circle, representing the state of stress, moves progressively towards the origin. However, it also decreases in size. When the fluid pressure compensates the weight of overburden, all the effective stresses in the solid framework vanish. If the overpressure exceeds the weight of overburden, the vertical effective stress becomes tensile and the rock may eventually fail in tension, producing horizontal fractures (Cobbold and Rodrigues, 2007). If there are additional tectonic stresses, their complicating effects may lead to vertical tensile fractures or to shear fractures.

6.2. Cone-in-cone

Despite an ongoing debate as to its mechanism of formation, there does seem to be a consensus, at least amongst recent reviews (Denaeyer, 1947a, c; Woodland, 1964; Selles-Martinez, 1994), that cone-in-cone has the following characteristic features.

1. It occurs most commonly in sedimentary rocks, less commonly in metamorphic rocks, and not at all in igneous rocks.
2. It is especially common in rocks of low permeability, such as shale, but less common in limestone or sandstone.
3. It commonly forms in horizontal bedding-parallel veins, not in steep ones that transect bedding.
4. However, some cone-in-cone forms in bedding-parallel lenses, or layers surrounding older concretions.
5. Cone-in-cone consists dominantly of fibrous minerals, which form nesting (coaxial) conical bundles, between one or more thin conical bands of clay or shale. The apical angles of the cones may be acute or obtuse (in the range of 25°–100°) and they may vary vertically.
6. The fibres are typically of calcite. Other minerals (such as pyrite) may be due to later alteration of calcite (Woodland, 1975).

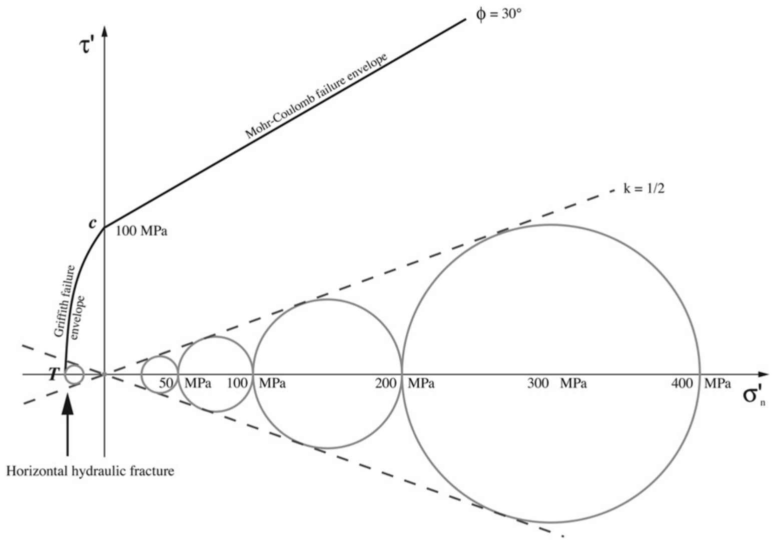

Figure 7. Mechanical explanation for origin of horizontal hydraulic fractures in porous brittle rock, as a result of seepage forces (after Cobbold and Rodrigues, 2007). Cartesian axes represent shear stress (τ) or normal stress (σ_n). Unit of stress is MegaPascal (MPa). Positive values indicate compression and negative values indicate tension. Apostrophes indicate effective stresses, acting only within solid framework. Grey Mohr circles represent states of elastic stress, before failure. Shear failure occurs if Mohr circle touches Mohr–Coulomb failure envelope, whereas tensile failure occurs if circle touches Griffith failure envelope. Failure parameters are cohesion (c) and tensile strength (*T*). Largest Mohr circle (right) represents state of stress in absence of pore fluid. Greatest principal stress (in this example, 400 MPa) is vertical, due to weight of overburden. As overpressure increases, Mohr circle shifts towards origin. However, it decreases in size, as a result of vertical seepage force (overpressure gradient). When overpressure balances weight of overburden, all effective stresses vanish (circle becomes point at origin). For even greater overpressure, Mohr circle increases in size again, but within tensile field. Finally, if Mohr circle touches failure envelope, this results in horizontal tensile fractures. For further details, see Cobbold and Rodrigues (2007).

7. Typically, the fibres show little or no signs of later deformation.
8. To a first approximation, the fibres appear to have grown vertically, or at a small angle to the vertical.
9. Where bedding-parallel veins have formed around fossils, imprints of those fossils are visible at the vein margins, indicating that the walls separated, as the fibres grew.
10. Commonly, each conical band of clay or shale has a stepped profile on one side and a smooth profile on the other side. The steps appear on one conical surface as bedding-parallel ridges.
11. Where adjacent cones form horizontal layers or lenses, their apices tend to point (become narrower) systematically in the same sense (downward or upward). The more common sense is downward.
12. Where adjacent cones form coatings around older concretions, their apices tend to point systematically inward.
13. On the surfaces of veins, the bases of cones define coaxial rings and the inner cones protrude, forming "nailheads" (nagelkalk).

To these data, we wish to add some observations of our own from the Neuquén Basin, Argentina. In some examples there (Figs. 3D and E), (1) bundles of calcite fibres have grown on each side of a thin layer of shale, which locally forms conical depressions, (2) the apical angle of each cone varies vertically, (3) the layer of shale appears to have undergone stretching and fragmentation (boudinage) in a vertical direction (Rodrigues et al., 2009, fig. 8). On vertical sections along the cone axis, where the flanks of the cone are steeper, the gaps between the fragments are greater, indicating more extension (Fig. 4E). In such a zone also, the calcite fibres are whiter than elsewhere and more oblique with respect to the pole to bedding, indicating a local zone of extension. On closing the gaps geometrically, by simple translation of the shale fragments along the corresponding fibre directions, we obtain an almost continuous band of shale, defining a cone of more regular apical angle and smaller amplitude. After a second stage of restoration, in which we also allow rigid rotations of fragments within the plane of section, we obtain an almost continuous, flat-lying, horizontal layer of shale, which we interpret to represent an original thin bed. If our restoration is geologically realistic, it means that the cone formed by warping of a shale layer between offset horizontal fractures, which opened progressively, while calcite fibres grew to fill the available spaces. According to the geometrical properties of developable surfaces, such warping should have caused the shale layer to deform internally, either by ductile strain or by fracturing. We are not in a position to affirm that all cones or cone-in-cone structures have formed in this way, but we do suspect that vertical stretching is an important factor in their genesis. In this we follow Denaeyer (1952), who, after 14 years of careful observation and at least 19 publications, concluded that most conical layers of shale within cone-in-cone structures have stretched and boudinaged vertically, as adjacent calcite fibres grew, all in a context of vertical tensile stress. Although Denaeyer did not identify the origin of such a stress, his macroscopic and microscopic observations were remarkably thorough.

To our knowledge, there has been only one successful attempt at dating cone-in-cone structures. Israelson et al. (1996) dated a sample of cone-in-cone around a concretion, from an outcrop of Alum Shale in Sweden, by the method of U–Pb. The age that they obtained for the calcite fibres (478.2 ± 4.9 Ma, early Ordovician) was younger by about 30 Ma than the stratigraphic age of the shale (510–514 Ma, Cambrian). Presumably the cone-in-cone formed during Ordovician burial and diagenesis. Clearly it would be useful to date other examples of beef or cone-in-cone worldwide.

From the above observations and because cone-in-cone typically is symmetric about a pole to bedding, we infer that the main forces at work have acted vertically, or nearly so. As for beef, so for cone-in-cone, good evidence for vertical dilation comes from (1) stretched conical shale layers (e.g. Fig. 3E), or (2) fossils and their moulds, for example in Utah (Thoral, 1942), Algeria (David, 1952), Wyoming, U.S.A. (Brown, 1954), NW Argentina (Harrington and Leanza, 1957) and other localities in the U.S.A. (Woodland, 1964). According to recent theories and experimental work, vertical seepage forces are able to induce a state of effective stress, in which the vertical stress becomes tensile (Cobbold and Rodrigues, 2007).

7. Relationship between calcite beef (or cone-in-cone) and petroleum generation

In a prescient but short note (one page of text and five references), Stoneley (1983) suggested that there might be a link between beef, overpressure and primary oil migration. The data that we have compiled do indeed provide evidence for such a link.

For example, liquid oil occurs within fluid inclusions in fibrous calcite (beef) of the Prague Basin, Czech Republic (Dobes et al., 1999; Suchy et al., 2002); the Neuquén Basin, Argentina (Parnell et al., 2000; Rodrigues et al., 2009); and the Wessex Basin, southern England (Fig. 1D; Zanella and Cobbold, 2011, 2012; work in progress). These oil inclusions indicate that the fibres grew while source rocks were generating oil, at burial depths of several km. In other words, the calcite beef in these basins is not simply of early diagenetic origin (Marshall, 1982). It is also common for such beef or cone-in-cone to have developed around earlier concretions, which originally formed around fossils (e.g. Martill, 1987).

Our worldwide catalogue (Table 1) indicates that layers of beef or cone-in-cone are common in or near source rocks for hydrocarbons. Good examples of such an association are from (1) Jurassic and Early Cretaceous strata of the Wessex and Weald basins, southern England; (2) Early Jurassic strata of the Larne Basin, Northern Ireland; (3) Middle Jurassic strata of Eastern England and the southern North Sea; (4) Late Triassic to Jurassic strata of the Paris Basin, northern France; (5) Early Jurassic strata of SW Germany; (6) Jurassic strata of Greenland, the Arctic Ocean and the Barents Sea; (7) Eocene strata of the Uintah Basin, Utah, U.S.A.; (8) Carboniferous strata of West Texas, U.S.A.; (9) Devonian strata of the Appalachian Basin, U.S.A.; (10) Eocene strata of Barbados; (11) Cretaceous strata of the Orinoco and Maracaibo basins, Venezuela; (12) Miocene strata of the Orinoco Basin, Venezuela; (13) Devonian strata of the Amazon Basin, Brazil; (14) Jurassic and Early Cretaceous strata of the Neuquén Basin, Argentina; (15) Jurassic strata of the Falklands shelf and northern Antarctica; (16) Permian strata of the Morondava Basin, Madagascar. These data indicate that overpressures were present within the source rocks and nearby. Whether or not the overpressures were due to maturation of organic matter in those same source rocks is another matter. We do not have enough data to argue for this in all examples. However, we do claim that the evidence for that is good in the Neuquén Basin, Argentina (Rodrigues et al., 2009) and the Uintah Basin, Utah, U.S.A. In the Wessex Basin, although the beef has inclusions of oil or gas, we cannot affirm from which source rocks these hydrocarbons came.

In some basins, horizontal fractures contain hydrocarbons, independently of beef. For example, bitumen occurs in horizontal fractures in the Neuquén Basin, Argentina (Borrello, 1956); the Maracaibo Basin, Venezuela (Talukdar et al., 1988); the Hils Syncline, Germany (Leythaeuser et al., 1988; Jochum et al., 1995); the accretionary prism, Barbados (Parnell et al., 1994); the Upper Devonian Dunkirk Shale, New York State, U.S.A. (Lash and Engelder, 2005); and the Upper Jurassic La Casita Formation, Sierra Madre Oriental, Mexico (Lefticariu, 2005; Fischer et al., 2009).

If hydrocarbons derive from maturation or chemical compaction of source rocks, or if fibrous material within beef or cone-in-cone layers derives from dissolution of deeper carbonates, collapse at depth may promote fracturing at shallower levels. In terms of absolute displacement, a beef vein may open because its footwall drops, rather than because its hanging wall rises. Nevertheless, significant forces should be necessary, to prevent the hanging wall from dropping, together with the footwall, and therefore the vein from closing. Indeed, such forces should more than counteract the weight of the overburden, so as to create new fractures or to allow existing ones to propagate.

To conclude this section, we have found that, in the Neuquén Basin, Argentina, the Wessex Basin, southern England, and the Paris Basin, France, calcite beef is abundant in and around Mesozoic mudstones, which are also source rocks for petroleum. In samples from the Neuquén and Wessex basins, the beef contains solid inclusions of bitumen, or fluid inclusions of oil or gas. Because we have found other examples in the literature, we suspect that an association between calcite beef, source rocks and petroleum may be common. More generally, the evidence points to calcite beef being a result of fluid overpressure and this reinforces the evidence for a link between petroleum generation, overpressure, hydrofracturing and the formation of beef or cone-in-cone layers.

However, it is clear that further work will be necessary, so as better to constrain the timing of hydrocarbon generation and beef formation, as well as the source rocks for hydrocarbon inclusions in the beef.

8. Conclusions

Bedding-parallel veins of fibrous minerals (beef or cone-in-cone) are common worldwide in sedimentary basins. The most common fibrous minerals are calcite, gypsum or quartz. Typically, the fibres are perpendicular to the bedding, or at high angles to it. In some examples, the vein has a central parting or suture, containing thin pieces of host rock or flat-lying fossils. Where imprints of a central fossil are visible at the margins of a vein, this is evidence that the fibres grew during vertical opening of the vein.

We have documented 157 worldwide localities of beef or cone-in-cone layers, as well as the compositions and ages of their host rocks. For calcite beef (110 localities), the host rock is typically a marine shale and the most common age is (1) Cambrian-Ordovician, (2) Devonian-Carboniferous, (3) early Jurassic, or (4) Cretaceous to Palaeogene. For gypsum beef (30 localities), the host rock is typically an evaporitic mudstone and the most common age is Triassic or Neogene. Finally, for quartz beef (17 localities), the host rock is typically a meta-turbidite and the most common age is Proterozoic or Ordovician. Because these ages seem to reflect climatic controls, we infer that the fibre-forming mineral species have not travelled far, vertically. The same conclusion holds for accessory minerals, such as uraninite, gold or sulphides, which in most examples derive from detrital grains.

There is also a correlation between composition and thermal maturity, typical temperatures of formation being (1) up to 60 °C for gypsum beef, (2) 70 °C to 120 °C for calcite beef, and (3) 200 °C to 350 °C for quartz beef.

In the Neuquén Basin, Argentina, the Wessex Basin, southern England, and the Paris Basin, France, calcite beef or cone-in-cone layers are abundant in Mesozoic mudstones, which are also source rocks for petroleum. In many samples, the beef contains solid inclusions of bitumen, or fluid inclusions of oil or gas. Because we have found other such examples in the literature, we suspect that an association between calcite beef, source rocks and petroleum may be common. More generally, the evidence points to calcite beef being a result of fluid overpressure and this reinforces the potential link between petroleum generation and overpressure.

Acknowledgements

We thank (1) Tony Boassen (Statoil Research Centre, Trondheim), for help with scanning electron microscopy and (2) the management of Statoil for permission to publish this paper. Ian West of Southampton University introduced us to some of the best beef localities along the coast of southern England (West, 2012).

References

Abalos, B., Elorza, J., 2011. Latest Cretaceous cone-in-cone structures and soft-sediment deformation (Basque-Cantabrian Basin, North Spain): a record of deep marine paleoseismicity? Geological Society of America Bulletin 123, 427–438.
Al-Aasm, I.S., Muir, I., Morad, S., 1993. Diagenetic conditions of fibrous calcite vein formation in black shales: petrographic, chemical and isotopic evidence. Bulletin of Canadian Petroleum Geology 41, 46–56.
Al-Aasm, I.S., Morad, S., Durocher, S., Muir, I., 1996. Sedimentology, C–S–Fe relationships and stable isotopic compositions in Devonian black mudrocks, Mackenzie Mountains, Northwest Territories, Canada. Sedimentary Geology l06, 279–298.
Andrews, W.R., 1881. Note on the Purbeck Beds at Teffont. Quarterly Journal of the Geological Society, London 37, 251–253.
Andrews, W.R., Jukes-Brown, A.J., 1894. The Purbeck Beds of the Vale of Wardour. Quarterly Journal of the Geological Society, London 50, 44–71.
Annels, A.E., Roberts, D.E., 1989. Turbidite-hosted gold mineralization at the Dolaucothi Gold Mines, Dyfed, Wales. Economic Geology 84, 1293–1314.
Barker, S.L.L., Cox, S.F., Eggins, S.M., Gagan, M.K., 2006. Microchemical evidences for episodoic growth of antitaxial veins during fracture-controlled fluid flow. Earth and Planetary Science Letters 250, 331–344.
Beadnell, J.L.B., 1905. The relations of the Eocene and Cretaceous systems in the Esna-Aswan reach of the Nile Valley. Quarterly Journal of the Geological Society, London 244, 667–678.
Becq-Giraudon, J.F., 1990. La structure cone-in-cone en milieu de dépôt siliclastique; observations nouvelles sur les cone in cone de l’Ordovicien Inférieur de la Montagne Noire, sud du Massif Central Français. Géologie de la France 1990 (2), 11–20.
Begbie, M.J., Falconer, D., Craw, D., 2005. Characteristics of gold bearing quartz veins at the historic Morning Star mine, Preservation Inlet, SW Fiordland, New Zealand. 2005 NZ Minerals Conference: Realising New Zealand’s mineral potential, 13–16 November, Auckland, pp. 320–327.
Benali, S., Schreiber, B.C., Helman, M.L., Philp, R.P., 1995. Characterization of organic matter from a restricted/evaporative sedimentary environment, southeastern Spain. American Association of Petroleum Geologists Bulletin 79, 816–830.
Bonney, T.G., 1897. A note on cone-in-cone structure. The Mineralogical Magazine and Journal of the Mineralogical Society, London 11, 24–27.
Bons, P.D., Jessell, M.W., 1997. Experimental simulation of the formation of fibrous veins by localised dissolution-precipitation creep. Mineralogical Magazine 61, 53–63.
Bonte, A., 1942. Sur l’origine sédimentaire de la structure cone-in-cone. Comptes Rendus de l’Académie des Sciences de Paris 214, 498–500.
Bonte, A., 1945a. Sur les gradins concentriques de la structure cone-in-cone. Comptes Rendus de l’Académie des Sciences de Paris 221, 507.
Bonte, A., 1945b. Observations sur les nodules à structure cone-in-cone de l’Arenig de la Montagne Noire. Bulletin de la Société Géologique de France, séries V 15, 453–478.
Bonte, A., 1952. Réflexions se le «beef», à propos d’une note de M.L. David. Comptes Rendus Sommaires de la Société Géologique de France 7, 110–112.
Bonte, A., Denaeyer, M.-E., Goguel, J., 1947. Les facteurs mécaniques dans la genèse de la structure “cone-in-cone”. Comptes Rendus sommaires de la Société Géologique de France 9, 182–184.
Borrello, A.V., 1956. Recursos minerales de la República Argentina. III. Combustibles sólidos minerales. Revista del Instituto Nacional de Investigación de las Ciencias Naturales, Ciencias Geológicas 5, 665.
Bradshaw, R., Phillips, F.C., 1967. X-ray studies of natural fabrics. I. Growth fabrics in hematite kidney ore and in fibrous calcite. Mineralogical Magazine 36, 70–77.
Branquet, Y., Cheilletz, A., Giuliani, G., Laumonier, B., Blanco, O., 1999. Fluidized hydrothermal breccia in dilatant faults during thrusting: the Colombian emerald deposits. In: McCaffrey, K.J.W., Lonergan, L., Wilkinson, J.J. (Eds.), Fractures, Fluid Flow and Mineralization. Geological Society, London, Special Publications, vol. 155, pp. 183–195.
Brett, C.E., Allison, P.A., DeSantis, M.K., Liddell, W.D., Kramer, A., 2009. Sequence stratigraphy, cyclic facies, and *lagerstätten* in the Middle Cambrian Wheeler and Marjum Formations, Great Basin, Utah. Palaeogeography, Palaeoclimatology, Palaeoecology 277, 9–33.
Broadhead, G.C., 1907. Cone in cone. Science 26 (670), 597.
Broadhead, R.F., Kepferle, R.C., Potter, P.E., 1982. Stratigraphic and sedimentologic controls of gas in shale – example from Upper Devonian of Northern Ohio. American Association of Petroleum Geologists Bulletin 66, 10–27.
Brodie, P.B., 1854. On the insect beds of the Purbeck Formation in Wiltshire and Dorsetshire. Quarterly Journal of the Geological Society, London 10, 475–482.
Brown, R.W., 1954. How does cone-in-cone material become emplaced? American Journal of Science 252, 372–376.
Brown, M.C., Oliver, N.H.S., Dickens, G.R., 2004. Veins and hydrothermal fluid flow in the Mt. Whaleback Iron Ore District, eastern Hamersley province, Western Australia. Precambrian Research 128, 441–474.
Buckland, W., De la Beche, H.T., 1835. On the Geology of the Neighbourhood of Weymouth and the Adjacent Parts of the Coast of Dorset. Transactions of the Geological Society, London, s2–4, pp. 1–46.
Cameron, A.C.G., 1892. On the continuity of the Kellaway Beds over extended areas near Bedford and on the extension of the Fuller’s Earth works at Woburn Sands. Geological Magazine 9, 66–71.
Catuneanu, O., Wopfner, H., Eriksson, P.G., Cairncross, B., Rubidge, B.S., Smith, R.M.H., Hancox, P.J., 2005. The Karoo basins of south-central Africa. Journal of African Earth Sciences 43, 211–253.
Cayeux, L., 1935. Les roches sédimentaires de France. Roches Carbonates (calcaires et dolomies). Masson, Paris, 447 pp.
Cecioni, G.O., 1957. Cretaceous flysch and molasse in Departamento Ultima Esperanza, Magallanes Province, Chile. American Association of Petroleum Geologists Bulletin 41, 538–564.
Cobbold, P.R., Rodrigues, N., 2007. Seepage forces, important factors in the formation of horizontal hydraulic fractures and bedding-parallel fibrous veins (“beef” and “cone-in-cone”). Geofluids 7, 313–332.
Cobbold, P.R., Watkinson, A.J., Cosgrove, J.W., 2008. Faults of the Pharaohs. Geoscientist 18 (6), 18–22. http://www.geolsoc.org.uk/gsl/geoscientist/features/page3994.html.
Cobbold, P.R., Ruffet, G., Leith, L., Løseth, H., Rodrigues, N., Galland, O., Leanza, H.A., 2011. Combustibles sólidos (asfaltita). XVIII Congreso Geológico Argentino, Neuquén, Relatorio, Capítulo 58, pp. 689–695.
Cobbold, P.R., Zanella, A., Ruffet, G., Rodrigues, N., Loseth, H., 2012. Beef (Bedding-parallel Fibrous Veins): Worldwide Occurrence and Significance in Terms of Fluid Overpressure, Hydrocarbon Generation and Mineralization (Including Sulfides, Emerald, Uranium or Gold). American Association of Petroleum Geologists Annual Convention, Long Beach, California. 22–25 April.
Cole, G.A.J., 1893. On some examples of cone-in-cone structure. Mineralogical Magazine 10, 136–141.
Collins, E.W., 1984. Styles of deformation in Permian strata, Texas Panhandle. Bureau of Economic Geology, Geological Circular 84-4, 32.
Cosgrove, J.W., 1995. The expression of hydraulic fracturing in rocks and sediments. In: Ameen, M.S. (Ed.), Fractography: Fracture Tomography as a Tool in Fracture Mechanics and Stress Analysis. Geological Society, London, Special Publications, vol. 92, pp. 187–196.
Cosgrove, J.W., 2001. Hydraulic fracturing during the formation and deformation of a basin: a factor in the dewatering of low-permeability sediments. American Association of Petroleum Geologists Bulletin 85, 737–748.
Cossey, P.J., Buckman, J.O., Steward, D.I., 1995. The geology and conservation of Brown End Quarry, Waterhouses, Staffordshire. Proceedings of the Geologists’ Association 106, 11–25.
Crame, J.A., Pirrie, D., Crampton, J.S., Duane, A.M., 1993. Stratigraphy and regional significance of the Upper Jurassic – Lower Cretaceous Byers Group, Livingston Island, Antarctica. Journal of the Geological Society, London 150, 1075–1087.
Daintree, R., 1872. Notes on the geology of the colony of Queensland. Quarterly Journal of the Geological Society 28, 271–317.
David, L., 1952. Présence de la structure «beef» et «cone-in-cone» dans le Crétacé de l’Est-Constantinois (Algérie). Comptes Rendus sommaires de la Société Géologique de France 3, 51–52.
Davies, G.M., 1915. Curious forms of ice. Nature 94 (2360), 563.
Dawson, J.W., 1862. On the flora of the Devonian period in north-eastern America. Proceedings of the Geological Society, London 18, 296–330.
Denaeyer, M.-E., 1938. Présentation d’un échantillon de phyllade noir à structure «cone-in-cone» provenant des carrières du Péry à Morhet (Ardennes belges). Bulletin de la Société belge de Géologie, de Paléontologie et d’Hydrologie 48, 408–410.
Denaeyer, M.-E., 1939a. A propos des gradins concentriques propres à la structure cone-in-cone. Comptes Rendus Sommaires de la Société Géologique de France 11, 154–155.
Denaeyer, M.-E., 1939b. Le reproduction expérimentale de la structure cone-in-cone. Ses conséquences au point de vue de la tectonique. Comptes Rendus de l’Académie des Sciences de Paris 208, 2004–2006.
Denaeyer, M.-E., 1939c. Les «Cone-in-Cone» de la Lufubu (Maniéma, Congo Belge). Annales de la Société géologique de Belgique, Bulletin 62 (10–11), 493–512.
Denaeyer, M.-E., 1940a. Sur la microstructure et la composition des «cone-in-cone» du Siegenien métamorphique de Morhet (Ardennes belges). Bulletin de la Société belge de Géologie, de Paléontologie et d’Hydrologie 49, 119–125.
Denaeyer, M.-E., 1940b. Résultats d’expériences relative à la genèse de la structure «cone-in-cone». Bulletin de la Société belge de Géologie, de Paléontologie et d’Hydrologie 49 (3), 313–318.
Denaeyer, M.-E., 1940c. Les schistes arénigiens à structure «cone-in-cone» de la tranchée de Sart-Bernard (province de Namur). Bulletin de la Société belge de Géologie, de Paléontologie et d’Hydrologie 49 (3), 318–326.
Denaeyer, M.-E., 1940d. Genèse des gradins concentriques propres à la structure cone-in-cone. Comptes Rendus Sommaires de la Société Géologique de France 7, 77–79.
Denaeyer, M.-E., 1942. Les miches à structure cone-in-cone du Silurien de la tranchée de Statte (Province de Namur). Bulletin de la Société belge de Géologie, de Paléontologie et d’Hydrologie 50, 74–77.
Denaeyer, M.-E., 1943a. Les cone-in-cone du Toarcien de Saint-Mard (Province de Luxembourg). Bulletin de la Société belge de Géologie, de Paléontologie et d’Hydrologie 52, 229–241.
Denaeyer, M.-E., 1943b. Les cone-in-cone de la France métropolitaine et d’outre-mer. Bulletin de la Société française de Minéralogie 66 (1–6), 173–221.
Denaeyer, M.-E., 1944a. Les marnes à structure cone-in-cone (“nagelkalk”) de la Lorraine. Comptes Rendus Sommaires de la Société Géologique de France 8, 79–81.

Denaeyer, M.-E., 1944b. Observations sur les structures cone-in-cone du Trias et du Jurassique de la Lorraine. Bulletin de la Société belge de Géologie, de Paléontologie et d'Hydrologie 53 (1 et 2), 26–43.

Denaeyer, M.-E., 1945. Essai d'une théorie mécanique de la structure cone-in-cone. Bulletin de la Société Géologique de France 15, 141–160.

Denaeyer, M.-E., 1946. Sur les cone-in-cone et les septaria. Comptes Rendus de l'Académie des Sciences de Paris 223, 953–954.

Denaeyer, M.-E., 1947a. Les gisements de cone-in-cone de France et de Grande-Bretagne. Première Partie. Bulletin de la Société belge de Géologie, de Paléontologie et d'Hydrologie 56 (1–2), 21–46.

Denaeyer, M.-E., 1947b. Sur l'existence de structures cone-in-cone dans le Siegenien inférieur, à Bastogne. Bulletin de la Société belge de Géologie, de Paléontologie et d'Hydrologie 56 (3), 272–279.

Denaeyer, M.-E., 1947c. Les gisements de cone-in-cone de France et de Grande-Bretagne. Deuxième Partie. Gisements britanniques. Bulletin de la Société belge de Géologie, de Paléontologie et d'Hydrologie 56 (3), 382–411.

Denaeyer, M., 1952. Sur la signification des «filons» transversaux à structure «beef» et «cone-in-cone». Comptes Rendus Sommaires de la Société Géologique de France 8, 138–141.

Distler, V.V., Yudovskaya, M.A., Mitrofanov, G.L., Prokof'ev, V.Y., Lioshnevskii, E.N., 2004. Geology, composition and genesis of the Sukhoi Log noble metals deposit, Russia. Ore Geology Reviews 24, 7–44.

Dobes, P., Suchy, V., Stejskal, M., 1999. Diagenetic fluid circulation through fractures: a case study from the Barrandian Basin (Lower Paleozoic), Czech Republic. Geolines (Praha) 8, 18.

Donovan, D.T., 1957. The Jurassic and Cretaceous systems in East Greenland. Meddelelser on Grœnland 155. 9–214.

Doumani, G.A., Tasch, P.A., 1965. Leaiid Conchostrachan zone (Permian) in the Ohio Range, Horlick Mountains, Antarctica. Antarctic Research Series, Geology and Paleontology of the Antarctic 6, 229–239.

Durand-Delga, M., 1952. Observations complémentaires sur le «beef». Comptes Rendus sommaires de la Société Géologique de France 7, 112–114.

Durney, D.W., Ramsay, J.G., 1973. Incremental strains measured by syntectonic crystal growths. In: De Jong, K.A., Scholten, R. (Eds.), Gravity and Tectonics. Wiley, New York, pp. 67–96.

Dypvik, H., Hvoslef, S., Bjaerke, T., Finnerud, E., 1985. The Wilhelmoya Formation (Upper Triassic – Lower Jurassic) at Bohemanflyja, Spitsbergen. Polar Research 3, 155–165.

Egenhoff, S., Fishman, N., Jackson, A., Ketki, K., Mackie, J., Newby, W., Petrowski, M.J., Ahlberg, P., 2012. High Life on the Seafloor During an Ocean Anoxic Event – the Sedimentology of Spice, Middle to Late Cambrian Alum Shale, Sweden. American Association of Petroleum Geologists Annual Convention, Long Beach. Poster 1236903.

El Albani, A., Cloutier, R., Candilier, A.-M., 2002. Early diagenesis of the Upper Devonian Escuminac Formation in the Gaspé Peninsula, Québec: sedimentological and geochemical evidence. Sedimentary Geology 146, 209–223.

Elburg, M.A., Bons, P.D., Foden, J., Passchier, C.W., 2002. The origin of fibrous veins: constraints from geochemistry. In: de Meer, S., Drury, M.R., de Bresser, J.H.P., Pennock, G.M. (Eds.), Deformation Mechanisms, Rheology and Tectonics. Current Status and Future Perspectives. Geological Society, London, Special Publications, vol. 200, pp. 103–118.

El-Tabakh, M., Schreiber, B.C., Warren, J.K., 1998. Origin of fibrous gypsum in the Newark Rift Basin, eastern North America. Journal of Sedimentary Research 68, 88–89.

England, G.L., Rasmussen, B., Krapez, B., Groves, D.I., 2002. Archaean oil migration in the Witwatersrand Basin of South Africa. Journal of the Geological Society, London 159, 189–201.

Enos, J.S., Kyle, J.R., 2002. Diagenesis of the Carrizo Sandstone at Butler Salt Dome, East Texas Basin, U.S.A.: evidence for fluid-sediment interaction near halokinetic structures. Journal of Sedimentary Research 72, 68–81.

Evans, M.A., 2011. Deformation and Fluid History of the Marcellus Shale in the Pennsylvania Valley and Ridge: Evidence From Fluid Inclusion Microthermometry of Vein Minerals. Geological Society of America, Northeastern (46th Annual) and North-Central (45th Annual) Joint Meeting (20–22 March 2011), Paper No. 56-4 (abstract).

Evans, R., Hendry, J.P., Parnell, J., Kalin, R.M., 1998. Origin and Significance of Fracture-related Dolomite in Porous Sandstones: an Example from the Carboniferous of County Antrim, Northern Ireland. In: International Association of Sedimentologists, Special Publications, vol. 26, pp. 409–435.

Fary, R.W., 1980. A Review of the Petroleum Geology of Venezuela. U.S. Geological Survey Open File Report, 80–782, 37 pp.

Fischer, M.P., Lefticariu, L., Romanek, C., Perry, E.C., 2005. Kinematics of fibrous vein growth: insights from stable isotope analyses. Eos Transactions American Geophysical Union 86 (52). Abstract T53C-1456.

Fischer, M.P., Higuera-Diaz, I.C., Evans, M.A., Perry, E.C., Lefticariu, L., 2009. Fracture-controlled paleohydrology in a map-scale detachment fold: insights from the analysis of fluid inclusions in calcite and quartz veins. Journal of Structural Geology 31, 1490–1510.

Fitches, B., 1987. Aspects of veining from the Welsh Lower Palaeozoic Basin. In: Jones, M.E., Preston, R.M.F. (Eds.), Deformation of Sediments and Sedimentary Rocks. Geological Society, London, Special Publications, vol. 29, pp. 325–342.

Fitz-Diaz, E., Hudleston, P., Siebenaller, L., Kirschner, D., Camprubí, A., Tolson, G., Puig, T.P., 2011. Insights into fluid flow and water-rock interaction during deformation of carbonate sequences in the Mexican fold-thrust belt. Journal of Structural Geology 33, 1237–1253.

Fornari, M., Herail, G., 1991. Lower Paleozoic gold occurrences in the 'Eastern Cordillera' of southern Peru and northern Bolivia. In: Ladeira, E.A. (Ed.), Brazil Gold'91: the Economics, Geology, Geochemistry and Genesis of Gold Deposits. A.A. Balkema, Rotterdam, pp. 135–142.

Fox-Strangways, C., Barrow, G., 1882. The Geology of the Country Between Whitby and Scarborough. Memoirs of the Geological Survey, Great Britain, pp. 1–60.

Foster, S.J., 1987. Geological Report, Punchbowl Property, Golden Mining Division. B.C. Geological Branch Assessment Report N° 16,242, Edmonton, Alberta, Canada.

Fournier, R.O., Rowe, J.J., 1977. The solubility of amorphous silica in water at high temperatures and high pressures. American Mineralogist 62, 1052–1056.

Fowler, T.J., 1996. Flexural-slip generated bedding-parallel veins from central Victoria, Australia. Journal of Structural Geology 18, 1399–1415.

Frandsen, N., Surlyk, F., 2003. An offshore transgressive–regressive mudstone-dominated succession from the Sinemurian of Skåne, Sweden. Geological Survey of Denmark and Greenland Bulletin 1, 543–554.

Franks, P.C., 1969. Nature, origin and significance of cone-in-cone structures in the Kiowa Formation (Early Cretaceous), North-Central Kansas. Journal of Sedimentary Petrology 39, 1438–1454.

Frizon de Lamotte, D., Leikine, M., 1985. Métamorphisme miocène du Rif Oriental et individualisation de la nappe d'Aknoul. Revue de Géologie Dynamique et de Géographie Physique 26, 29–42.

Fuchs, F.C., 1898. Estudio sobre la región aurífera de Santo Domingo en la provincia de Carabaya. Boletín de Minas, Industria y Construcciones, Lima 14.

Gale, J.F.W., Holder, J., 2010. Natural fractures in some US shales and their importance for gas production. In: Vining, B.A., Pickering, S.C. (Eds.), Petroleum Geology: From Mature Basins to New Frontiers – Proceedings of the 7th Petroleum Geology Conference. Petroleum Geology Conference Series, vol. 7, pp. 1131–1140.

Gallois, R.W., 2001. The lithostratigraphy of the Mercia Mudstone Group (mid to late Triassic) of the South Devon coast. Geoscience in south-west England. Proceedings of the Ussher Society, 195–204.

Gallois, R.W., 2008. The lithostratigraphy of the shales-with-beef member of the Charmouth Mudstone Formation, Lower Jurassic. Geoscience in South-west England 12, 32–40.

Gallois, R.W., 2009. The lithostratigraphy of the Penarth Group (late Triassic) of the Severn Estuary area. Geoscience in South-west England 12, 71–84.

Garwood, E.J., 1892. Cone-in-cone structure. Geological Magazine 9, 334–335.

Gay, R., 1942. Théorie de la formation de la structure cone-in-cone. Comptes Rendus de l'Académie des Sciences de Paris 214, 500–502.

Geel, T., 1976. Messinian gypsiferous deposits of the Lorca basin (province of Murcia, SE Spain). Memorie della Societa Geologica Italiana 16, 369–385.

Geikie, A., 1902. Text Book of Geology. Book 6. Stratigraphical Geology. American Home Library Company, New York, pp. 1419–1861.

George, T.N., 1954. Pre-seminulan main limestone of the Avonian series in Breconshire. Quaterly Journal of the Geological Society, London 110, 283–322.

Gill, J.R., Cobban, W.A., Schultz, L.G., 1972. Stratigraphy and composition of the Sharon Springs member of the Pierre shale in western Kansas. U.S. Geological Survey Professional Paper 728, 1–50.

Gilman, R.A., Metzger, W.J., 1967. Cone-in-cone concretions from western New York. Journal of Sedimentary Petrology 37, 87–95.

Gratier, J.-P., Frery, E., Deschamps, P., Røyne, A., Renard, F., Dysthe, D., Ellouz-Zimmerman, N., Hamelin, B., 2012. How travertine veins grow from top to bottom and lift the rocks above them: the effect of crystallization force. Geology, http://dx.doi.org/10.1130/G33286.1 (published online).

Gresley, W.S., 1887. Notes on "cone-in-cone structure". Geological Magazine, Decade III IV (1), 17–22.

Gresley, W.S., 1892. Cone-in-cone structure. Geological Magazine 9, 432.

Gresley, W.S., 1894. Cone-in-Cone: how it occurs in the 'Devonian' series in Pennsylvania, U.S.A. Quarterly Journal of the Geological Society, London 50, 731–739.

Gresley, W.S., 1898. Cone-in-Cone: additional facts from various countries. Quarterly Journal of the Geological Society, London 50, 196.

Gross, M.R., Becker, A., Gutiérrez-Alonso, G., 1997. Transfer of displacement from multiple slip zones to a major detachment in an extensional regime: example from the Dead Sea rift, Israel. Geological Society of America Bulletin 109, 1021–1035.

Grové, D., Harris, C., 2010. O- and H-isotope study of the Carbon Leader reef at the Tau Tona and Savuka mines (western deep levels), South Africa: Implications for the origin and evolution of Witwatersrand Basin fluids. South African Journal of Geology 113, 1–14.

Guibal, C.-F., 1841. Mémoire sur le terrain jurassique du département de la Meurthe. Mémoires de la Société Royale des Sciences, Lettres et Arts de Nancy, pp. 9–56.

Gustavson, T.C., Hovorka, S.D., Dutton, A.R., 1994. Origin of satin spar veins in evaporite basins. Journal of Sedimentary Research A64, 88–94.

Hammes, U., Frébourg, G., 2012. Haynesville and Bossier mudrocks: a facies and sequence stratigraphic investigation, East Texas and Louisiana, USA. Marine and Petroleum Geology 31, 8–26.

Hammes, U., Hamlin, H.S., Ewing, T.E., 2011. Geologic analysis of the Upper Jurassic Haynesville Shale in east Texas and west Louisiana. American Association of Petroleum Geologists Bulletin 95, 1643–1666.

Harrington, H.J., Leanza, A.F., 1957. Ordovician Trilobites of Argentina. In: University of Kansas, Department of Geology, Special Publications, vol. 1, 276 pp.

Harker, A., 1892. Cone-in-cone structure. Geological Magazine 9, 240.

Harker, A., 1908. The geology of the small isles of Inverness-shire. (Rum, Canna, Eigg, Muck, etc.). (Sheet 60, Scotland). Memoirs of the Geological Society of Great Britain, 210.

Harley, M., Charlesworth, E.G., 1996. The role of fluid pressure in the formation of bedding-parallel, thrust-hosted gold deposits, Sabie – Pilgrim's Rest goldfield, eastern Transvaal. Precambrian Research 79, 125–140.
Harnly, H.J., 1898. "Cone-in-cone" (an impure calcite). Kansas Academy of Sciences Transactions 15, 22.
Haselhurst, S.R., 1915. Some observations on cone-in-cone structure and their relation to its origin. Proceedings of the Geological Society, London 71, 7.
Hausmann, J.F.L., 1812. Ueber den sogenannten Tutenmergel von Görarp in Schonen. Annalen der Wetterauischen Gesellschaft für die gesammte Naturkunde, Hanau 3, 25–28.
Hector, J., 1861. On the geology of the country between Lake Superior and the Pacific Ocean (between the 48th and 54th parallels of latitude), visited by the Government Exploring Expedition under the command of Captain J. Palliser (1857–60). Proceedings of the Geological Society, London 17, 388–445.
Hedberg, H.D., Sass, L.C., Funkhouser, H.J., 1947. Oil fields of Greater Oficina Area, Central Anzoategui, Venezuela. American Association of Petroleum Geologists Bulletin 81, 2089–2169.
Henderson, M.N., Henderson, J.R., 1986. Constraints on the origin of gold in the Meguma Zone, Ecum Secum area, Nova Scotia. Maritime Sediments and Atlantic Geology 22, 1–13.
Hendry, J.P., 2002. Geochemical trends and palaeohydrological significance of shallow burial calcite and ankerite cements in Middle Jurassic strata on the East Midlands Shelf (onshore UK). Sedimentary Geology 151, 149–176.
Herdendorff, C.E., 1977. Cone-in-cone Structure in the Ohio Shale of Erie County. Ohio State University, Center for Lake Erie Area Research, Ohio, 7 pp.
Hilgers, C., Urai, J.L., 2005. On the arrangement of solid inclusions in fibrous veins and the role of the crack-seal mechanism. Journal of Structural Geology 27, 481–494.
Hilgers, C., Koehn, D., Bons, P.D., Urai, J.L., 2001. Development of crystal morphology during antitaxial growth in a progressively widening vein: II. Numerical simulations of the evolution of antitaxial fibrous veins. Journal of Structural Geology 23, 873–885.
Hillier, R.D., Cosgrove, J.W., 2002. Core and seismic observations of overpressure-related deformation within Eocene sediments of the Outer Moray Firth, UKCS. Petroleum Geoscience 8, 141–149.
Hoover, K.V., 1960. Devonian-Mississippian Shale Sequence in Ohio. State of Ohio Geological Survey, Information Circular N° 27, 154 pp.
Howitt, F., 1964. Stratigraphy and structure of the Purbeck inliers of Sussex (England). Quarterly Journal of the Geological Society, London 120, 77–113.
Hudson, J.D., Clements, R.G., 2007. The Middle Jurassic succession at Ketton, Rutland. Proceedings of the Geologists' Association 118, 239–264.
Hughes, R.A., 2003. Permian and Triassic Rocks of the Appleby District (Part of Sheet 30, England and Wales). British Geological Survey. Research Report RR/02/01, 15 pp.
Hulka, C., Gräfe, K.-U., Sames, B., Uba, C.E., Heubeck, C., 2006. Depositional setting of the Middle to Late Miocene Yecua Formation of the Chaco Foreland Basin, southern Bolivia. Journal of South American Earth Sciences 21, 135–150.
Hurst, A., Scott, A., Vigorito, M., 2011. Physical characteristics of sand injectites. Earth-Science Reviews 106, 215–246.
Iddings, A., Olsson, A., 1928. Geology of northwest Peru. American Association of Petroleum Geologists Bulletin 12, 1–39.
Ingram, J.A., 1972. Donors Hill, Queensland. Geological Survey of Queensland, 1:250 000 Series – Explanatory Notes, 16 pp.
Israelson, C., Halliday, A.N., Buchardt, B., 1996. U–Pb dating of calcite concretions from Cambrian black shales and the Phanerozoic time scale. Earth and Planetary Science Letters 141, 153–159.
Jessell, M.W., Willman, C.E., Gray, D.R., 1994. Bedding parallel veins and their relationship to folding. Journal of Structural Geology 16, 753–767.
Jiao, Y.Q., Wu, L.Q., He, M.C., Mason, R., Wang, M.F., Xu, Z.C., 2007. Occurrence, thermal evolution and primary migration processes derived from studies of organic matter in the Lucaogou source rock at the southern margin of the Junggar Basin, NW China. Science in China, Series D – Earth Sciences 50, 114–123.
Jochum, J., Friedrich, G., Leythaeuser, D., Littke, R., Ropertz, B., 1995. Hydrocarbon-bearing fluid inclusions in calcite-filled horizontal fractures from mature Posidonia Shale (Hils Syncline, NW Germany). Ore Geology Reviews 9, 363–370.
Jowett, D.M.S., Schröder-Adams, C.J., 2005. Paleoenvironments and regional stratigraphic framework of the Middle-Upper Albian Lepin Formation in the Liard Basin, northern Canada. Bulletin of Canadian Petroleum Geology 53, 25–50.
Jowett, E.C., 1987. Formation of sulfide-calcite veinlets in the Kupferschiefer Cu–Ag deposits in Poland by natural hydrofracturing during basin subsidence. Journal of Geology 95, 513–526.
Jowett, E.C., Cathles, L.M., Davis, B.W., 1993. Predicting depths of gypsum dehydration in evaporitic sedimentary basins. American Association of Petroleum Geologists Bulletin 77, 402–413.
Judd, J.W., 1871. On the Punfield Formation. Quarterly Journal of the Geological Society, London 27, 207–227.
Judd, J.W., 1878. On the Secondary rocks of Scotland. Third paper. The strata of the Western Coast and Islands. Quarterly Journal of the Geological Society, London 34, 660–739.
Kelling, G., Moshrif, M.A., 1977. The orientation of fossil bivalves in a pene-littoral sequence (the Rhaetian of South Wales). Journal of Sedimentary Petrology 47, 1342–1346.
Kendall, A.C., 1975. Anhydrite replacements of gypsum (satin-spar) veins in the Mississippian caprocks of southeastern Saskatchewan. Canadian Journal of Earth Sciences 12, 1190–1195.
Keulen, N. T., den Brok, S.W.J., Spiers, C.J., 2001. Force of crystallisation of gypsum during hydration of synthetic anhydrite rock. 13th DRT conference, Deformation Mechanisms, Rheology, and Tectonics, Noordwijkerhout, The Netherlands.
Keyes, C.R., 1896. Note on the nature of cone-in-cone. Iowa Academy of Science, Proceedings 3, 75–76.
Kolokol'tsev, V.G., 2002. The cone-in-cone structure and its origin. Lithology and Mineral Resources 37 (6), 523–535.
Kowal-Linka, M., 2010. Origin of cone-in-cone calcite veins during calcitization of dolomites and their subsequent diagenesis: a case study from the Gogolin Formation (Middle Triassic), SW Poland. Sedimentary Geology 224, 54–64.
Lacroix, A., 1923. Minéralogie de Madagascar, Tome 3. Augustin Chalamel, Paris.
Lamplugh, G.W., Kitchin, F.L., 1911. On the Mesozoic rocks in some of the coal explorations in Kent. Memoirs of the Geological Survey, Great Britain. 1–212.
Lang, W.D., 1914. The geology of the Charmouth Cliffs, Beach and Foreshore. Proceedings of the Geological Association 25, 293–360.
Lang, W.D., Spath, L.F., Richardson, W.A., 1923. Shales-With-'Beef', a sequence in the Lower Lias of the Dorset Coast. Quarterly Journal of the Geological Society, London 79, 47–99.
Large, R.R., Bull, S.W., Maslennikov, V.V., 2011. A carbonaceous sedimentary source-rock model for Carlin-type and orogenic gold deposits. Economic Geology 106, 331–356.
Lash, G.G., Engelder, T., 2005. An analysis of horizontal microcracking during catagenesis: example from the Catskill delta complex. American Association of Petroleum Geologists Bulletin 89, 1433–1449.
Lee, G.W., 1920. The Mesozoic Rocks of Applecross, Raasay and North-east Skye. H.M. Geological Survey, Scotland, 93 pp.
Lefticariu, L., 2005. Kinematics of Fibrous Vein Growth: Insights from Stable Isotopes and Trace Elemental Data (Abstract). American Geophysical Union. Fall Meeting, Section T26.
Leonhard, K.C. von, 1823. Charakteristik der felsarten, 418 pp.
LePain, D.L., Decker, P.L., Wartes, M.A., 2008. Measured sections and preliminary interpretations of the Nanushuk Formation exposed along the Colville River near the confluences with the Awuna and Killik rivers. In: Wartes, M.A., Decker, P.L. (Eds.), Preliminary Results of Recent Geologic Field Investigations in the Brooks Range Foothills and North Slope, Alaska. Alaska Division of Geological & Geophysical Surveys Preliminary Interpretive Report, 2008-1, pp. 41–45.
Leythaeuser, D., Littke, R., Radke, M., Schaefer, R.G., 1988. Geochemical effects of petroleum migration and expulsion from Toarcian source rocks in the Hils Syncline area, NW-Germany. In: Mattavelli, L., Novelli, L. (Eds.), Advances in Organic Geochemistry 1987. Organic Geochemistry, vol. 13, pp. 489–502.
Linck, G., 1931. Tutenmergel und Nagelkalk. Chemie der Erde 6, 227–238.
Linck, G., Noll, W., 1928. Uber Tutenmergel. Chemie der Erde 3, 699–721.
Lonsdale, W., 1832. Series 2. On the Oolitic District of Bath, vol. 3. Transactions of the Geological Society, London, pp. 241–276.
Lott, G.K., 1985. Late Triassic, Jurassic and Early Cretaceous geology of the southern North Sea Basin. PhD thesis, University of Leicester, U.K., 239 pp.
Lozej, G.P., Beales, F., 1997. Stratigraphy and structure of La Encantada mine area, Coahuila, Mexico. Geological Society of America Bulletin 88, 1793–1807.
Lugli, S., Reimold, W.U., Koeberl, C., 2005. Silicified cone-in-cone structures from Erfoud (Morocco): a comparison with impact-generated shatter cones. In: Koeberl, C., Henkel, H. (Eds.), Impact Tectonics. Impact Studies Series, vol. 6, pp. 81–110.
Machel, H.-G., 1985. Fibrous gypsum and fibrous anhydrite in veins. Sedimentology 32, 443–454.
MacKenzie, W.S., 1972. Fibrous calcite, a Middle Devonian geologic marker, with statigraphic significance, District of Mackenzie, Northwest Territories. Canadian Journal of Earth Sciences 9, 1431–1440.
Macsotay, O., Erlich, R.N., Peraza, T., 2003. Sedimentary structures of the La Luna, Navay and Quercual Formations, Upper Cretaceous of Venezuela. Palaios 18, 334–348.
Mahboubi, A., Moussavi-Harami, R., Collins, R.B., Muhling, J.R., 2010. Petrography and geochemical signatures in cracks filling calcite sequences in septarian concretions, Sanganeh Formation, Kopet-Dagh Basin, NE Iran. Journal of Applied Sciences 10, 526–534.
Maillot, H., Bonte, A., 1983. Cone-in-cone texture from Deep Sea Drilling Project Leg 71, Site 511, Falkland Plateau, south Atlantic Ocean. Initial Reports of the Deep Sea Drilling Project 71 (1), 345–349.
Mantell, G.A., 1850. Notice of the remains of the Dinornis and other birds, and of fossils and rock-specimens recently collected by Mr Walter Mantel in the Middle Island of New Zealand, etc. Quarterly Journal of the Geological Society, London 6, 319–342.
Markello, J.R., Koepnick, R.B., Waite, L.E., Collins, J.F., 2007. The carbonate analogs through time (CATT) hypothesis and the global atlas of carbonate fields – a systematic and predictive look at Phanerozoic carbonate systems. In: Controls on Carbonate Platform and Reef Development, vol. 89. Society for Sedimentary Geology (SEPM), pp. 1–31. Special Publications.
Marshall, J.D., 1982. Isotopic composition of displacive fibrous calcite veins; reversals in pore-water composition trends during burial diagenesis. Journal of Sedimentary Petrology 52, 615–630.
Marshall, P., 1926. The Upper Cretaceous ammonites of New Zealand. Philosophical Transactions of the Royal Society of New Zealand 56, 129–210.
Martill, D.M., 1987. A taphonomic and diagenetic case study of a partially articulated ichthyosaur. Palaeontology 30, 543–555.

Martinius, A.W., Hegner, J., Kaas, I., Bejarano, C., Mathieu, X., Mjús, R., 2012. Sedimentology and depositional model for the Early Miocene Oficina Formation in the Petrocedeño Field (Orinoco heavy-oil belt, Venezuela). Marine and Petroleum Geology 35, 354–380, http://dx.doi.org/10.1016/j.marpetgeo.2012.02.013.
Maubeuge, P.L., 1945. Sur quelques niveaux marneux de Lorraine à structure cône in cône. Comptes Rendus de la Société Géologique de France 9, 114–116.
Maubeuge, P.L., 1991. Le forage de Rosiéres aux Salines (M & M), un carottage continu dans le Trias moyen. Bulletin des Académie et Société Lorraines des Sciences 30, 25–33.
McCaig, A.M., Wayne, D.M., Marshall, J.D., Banks, D., Henderson, I., 1995. Isotopic and fluid inclusion studies of fluid movement along the Gavarnie Thrust, Central Pyrenees: reaction fronts in carbonate mylonites. American Journal of Science 295, 309–343.
Means, W.D., Li, T., 2001. A laboratory simulation of fibrous veins: some first observations. Journal of Structural Geology 23, 857–863.
Milliken, K.L., Day-Stirrat, R.J., 2012. Cementation in Mudrocks: Brief Review with Examples from Cratonic Basin Mudrocks.
Milliken, K.L., Esch, W.L., Reid, R.M., Zhang, T., 2012. Grain assemblages and strong diagenetic overprinting in siliceous mudrocks, Barnett Shale (Mississippian), Fort Worth Basin, Texas. American Association of Petroleum Geologists Bulletin 96, 1553–1578.
Molyneux, A.J.C., 1909. On the Karroo system in Northern Rhodesia, and its relation to the general geology. Quarterly Journal of the Geological Society, London 65, 408–439.
Morgans-Bell, H.S., Coe, A.L., Hesselbo, S.P., Jenkyns, H.C., Weedon, G.P., Marshall, J.E.A., Tyson, R.V., Williams, C.J., 2001. Integrated stratigraphy of the Kimmeridge Clay Formation (Upper Jurassic) based on exposures and boreholes in south Dorset, U.K. Geological Magazine 138, 511–539.
Mügge, O., 1928. Über die Entstehung faseriger Minerale und ihrer Aggregationsformen. Neues Jahrbuch für Mineralogie, Geologie und Paläontologie 58A, 303–348.
Neubauer, F., Liu, Y., Genser, J., Rieser, A.B., Friedl, G., Ge, X., Thöni, M., 2010. Quaternary celestine and gypsum extensional veins in a folded hypersaline lake infill: the Qaidam Basin, Western China. Austrian Journal of Earth Sciences 103, 81–91.
Newberry, J.S., 1885. On cone-in-cone. Geological Magazine, Decade III II, 559.
Newton, E.T., Teall, J.J.H., 1897. Notes on a collection of rocks and fossils from Franz Josef Land, made by the Jackson-Harmworth Experidtion during 1894–1896. Quarterly Journal of the Geological Society, London 53, 477–512.
Nicholas, C.J., Pearson, P.N., Bown, P.R., Jones, T.D., Huber, B.T., Karega, A., Lees, J.A., McMillan, I.K., O'Halloran, A., Singano, J.M., Wade, B.S., 2006. Stratigraphy and sedimentology of the Upper Cretaceous to Paleogene Kilwa Group, southern coastal Tanzania. Journal of African Earth Sciences 45, 431–466.
Nyambe, I.A., Dixon, O., 2000. Sedimentology of the Madumabisa Mudstone Formation (Late Permian), Lower Karoo Group, mid-Zambezi Valley Basin, southern Zambia. Journal of African Earth Sciences 30, 535–553.
ODP Shipboard Scientific Party, 2003. Demerara Rise: Equatorial Cretaceous and Paleogene Plaeoceanographic Transect. Leg 207 Preliminary Report. Ocean Drilling Program, Texas A&M University, 63 pp.
Oliver, N.H.S., Bons, P.D., 2001. Mechanisms of fluid flow and fluid-rock interaction in fossil metamorphic-hydrothermal systems inferred from vein-wallrock patterns, geometry, and microstructure. Geofluids 1, 137–163.
Orchard, M.J., McRoberts, C.A., Tozer, E.T., Johns, M.J., Sandy, M.R., Shaner, J.S., 2001. An intercalibrated biostratigraphy of the Upper Triassic of Black Bear Ridge, Williston Lake, northeast British Columbia. Geological Survey of Canada, Current Research 2001–A6, 21.
Ortí, F., Alonso, R.N., 2000. Gypsum-hydroboracite association in the Sijes Formation (Miocene, NW Argentina): Implications for the genesis of Mg-bearing borates. Journal of Sedimentary Research 70, 664–681.
Parnell, J., 1999. Petrographic evidence for emplacement of carbon into Witwatersrand conglomerates under high fluid pressure. Journal of Sedimentary Research 69, 164–170.
Parnell, J., Ansong, G., Veale, C., 1994. Petrology of the bitumen (manjak) deposits of Barbados: hydrocarbon migration in an accretionary prism. Marine and Petroleum Geology 11, 743–755.
Parnell, J., Honghan, C., Middleton, D., Haggan, T., Carey, P., 2000. Significance of fibrous mineral veins in hydrocarbon migration: fluid inclusion studies. Journal of Geochemical Exploration 69-70, 623–627.
Pashin, J.C., 2011. Geological Foundation for Production of Natural Gas from Diverse Shale Formations. Research Partnership to Secure Energy for America, Final Report 07122.17.01. Geological Survey of Alabama, Tuscaloosa, 156 pp.
Pearson, P.N., Nicholas, C.J., Singano, J.M., Bown, P.R., Coxall, H.K., van Dongen, B.E., Huber, B.T., Karega, A., Lees, J.A., MacLeod, K., McMillan, I.K., Pancost, R.D., Pearson, M., Msaky, E., 2006. Further Paleogene and Cretaceous sediment cores from the Kilwa area of coastal Tanzania: Tanzania Drilling Project Sites 6–10. Journal of African Earth Sciences 45, 279–317, http://dx.doi.org/10.1016/j.jafrearsci.2006.02.005.
Pedersen, G.K., 1989. The sedimentology of Lower Palaeozoic black shales from the shallow wells Skelbro 1 and Billegrav 1, Bornholm, Denmark. Bulletin of the Geological Society of Denmark 37, 151–173.
Penn, I.E., Cox, B.M., Gallois, R.W., 1986. Towards precision in stratigraphy: geophysical log correlation of Upper Jurassic (including Callovian) strata of the Eastern England Shelf. Journal of the Geological Society, London 143, 381–410.
Perrone, V., Capoa, P., de Cesarini, F., 1998. Remise en question, à propos de la Nappe du Val Varecchia, d'attributions paléogéographiques et structurales de l'Appenin nord-oriental (Italie). Comptes Rendus de l'Académie des Sciences de Paris. Sciences de la Terre et des Planètes 326, 347–353.
Philipp, S.L., 2008. Geometry and Formation of Gypsum Veins in Mudstones at Watchet, vol. 145. Geological Magazine, Somerset, SW England, pp. 831–844.
Pompeckj, J.F., 1900. The Jurassic fauna of Cape Flora, Franz Josef Land, with a geological sketch of Cape Flora and its neighbourhood by Fridtjof Nansen. In: Nansen, F. (Ed.), The Norwegian North Polar Expedition, 1893–1896, Scientific Results, vol. 1, pp. 1–147.
Pratt, L., Mompart, L., Murat, B., 1993. Hydrocarbon Generation Potential of the Cretaceous Section from Well ALP-6, Perija Region. American Association of Petroleum Geologists, Search and Discovery, Venezuela. Article 90988.
Provo, L.J., Kepferle, R.C., Potter, P.E., 1978. Division of Black Ohio Shale in eastern Kentucky. American Association of Petroleum Geologists Bulletin 62, 1703–1713.
Radelli, L., 1975. Geology and oil of Sakamena Basin, Malagasy Republic (Madagascar). American Association of Petroleum Geologists Bulletin 59, 97–114.
Raisossadat, S.N., 2004. The ammonite family Deshayesitidae in the Kopet Dagh Basin, north-east Iran. Cretaceous Research 25, 115–136.
Ramsay, J.G., 1980. The crack-seal mechanism of rock deformation. Nature 284, 135–139.
Reid, C., 1903. The geology of the country around Salisbury (Explanation of Sheet 298). Memoirs of the Geological Survey, England and Wales 298, 1–77.
Renz, H.H., 1957. Stratigraphy and geological history of Eastern Venezuela. Geologisches Rundschau 45, 728–759.
Reynolds, S.H., Vaughan, A., 1904. The Rhaetic Beds of the South Wales direct line. Quaterly Journal of the Geological Society, London 60, 194–214.
Riccardi, A.C., Aguirre Urreta, M.B., Medina, F.A., 1987. Aconeceratidae (Ammonitina) from the Hauterivian-Albian of southern Patagonia. Palaeontographica, Abt. A 196, 105–185.
Richardson, L., 1905. The Rhaetic and contiguous deposits of Glamorgan. Quarterly Journal of the Geological Society, London 61, 385–424.
Richardson, L., 1911. The Rhaetic and contiguous deposits of West, Mid, and part of East Somerset. Quarterly Journal of the Geological Society, London 67, 1–74.
Richardson, W.A., 1920. The fibrous gypsum of Nottinghamshire. Mineralogical Society Journal 19, 77–95.
Richardson, W.A., 1923. Petrology of the Shales-with-"Beef". Quarterly Journal of the Geological Society, London 79, 88–99.
Riediger, C.L., Coniglio, M., 1992. Early diagenetic calcites and associated bitumens in the "Nordegg Member"; implications for Jurassic paleogeography of the Western Canada sedimentary basin. Bulletin of Canadian Petroleum Geology 40, 381–394.
Rodrigues, N.T., 2008. Fracturation hydraulique et forces de courant: modélisation analogique et données de terrain. Mémoire de Doctorat, Université de Rennes 1, 164 pp.
Rodrigues, N., Cobbold, P.R., Løseth, H., Ruffet, G., 2009. Widespread bedding-parallel veins of fibrous calcite ("beef") in a mature source rock (Vaca Muerta Fm, Neuquén Basin, Argentina): evidence for overpressure and horizontal compression. Journal of the Geological Society, London 166, 695–709, http://dx.doi.org/10.1144/0016-76492008-111.
Rubinstein, C., Melo, J.H.G., Steemans, P., 2005. Lochkovian (earliest Devonian) miospores from the Solimões Basin, northwestern Brazil. Review of Palaeobotany and Palynology 133, 91–113.
Sach, A.J., 1892. On a sample of cone-in-cone structure found at Picton, New South Wales. Geological Magazine 9, 505–507.
Sanderson, D.J., Roberts, S., Gumiel, P., 1994. A fractal relationship between vein thickness and gold grade in drill core from La Codosera, Spain. Economic Geology 89, 168–173.
Sangster, A.L., Smith, P.K., 2007. Metallogenic summary of the Meguma gold deposits, Nova Scotia. In: Goodfellow, W.D. (Ed.), Mineral Deposits of Canada: a Synthesis of Major Deposit-types, District Metallogeny, the Evolution of Geological Provinces, and Exploration Methods. Geological Association of Canada, Mineral Deposits Division, Special Publication, vol. 5, pp. 723–732.
Schwarz, J.-O., Koehn, D., 2011. Geometry of and fluid flow in bedding parallel crack-seal veins. EGU General Assembly. Geophysical Research Abstracts 13, 5699.
Séjourné, S., Malo, M., Savard, M.M., Kirkwood, D., 2005. Multiple origin and regional significance of bedding parallel veins in a fold and thrust belt: the example of a carbonate slice along the Appalachian structural front. Tectonophysics 407, 189–209, http://dx.doi.org/10.1016/j.tecto.2005.07.009.
Selles-Martinez, J., 1994. New insights in the origin of cone-in-cone structures. Carbonates and Evaporites 9, 172–186.
Shao, L., Zhang, P., Hilton, J., Gayer, R., Wang, Y., Zhao, C., Luo, Z., 2003. Paleoenvironments and paleogeography of the Lower and lower Middle Jurassic coal measures in the Turpan-Hami oil-prone coal basin, northwestern China. American Association of Petroleum Geologists Bulletin 87, 335–355.
Shaub, B.M., 1937. The origin of cone-in-cone and its bearing on the origin of concretions and septaria. American Journal of Science 203, 331–334.
Shaw, R.P., Morton, R.D., 1990. A fluid inclusion study of quartzite-hosted lode gold mineralization at Athabasca Pass, Central Rocky Mountains, Canada. Economic Geology 85, 1881–1893.
Shearman, D.J., Mossop, G., Dunsmore, H., Martin, M., 1972. Origin of gypsum veins by hydraulic fracture. Institute of Mining and Metallurgy, Transactions B181, 149–155.
Shelton, R., 1997. Tectonic evolution of the Larne Basin. In: Meadows, N.S., Trueblood, S.P., Hardman, M., Cowan, G. (Eds.), Petroleum Geology of the Irish

Sea and Adjacent Areas. Geological Society, London, Special Publications, vol. 124, pp. 113–133.
Short, A.R., 1904. A description of some Rhaetic sections in the Bristol District, with considerations on the mode of deposition of the Rhaetic Series. Quarterly Journal of the Geological Society, London 60, 170–193.
Sibson, R.H., 2003. Brittle-failure controls on maximum sustainable overpressure in different tectonic regimes. American Association of Petroleum Geologists Bulletin 87, 901–908.
Silva, A.L. da, 2003. Estratigrafia física e deformação do sistema lacustre carbonático (Aptiano-Albiano) da Bacia do Araripe em afloramentos selecionados. Dissertação de Mestrado, Universidade Federal de Pernambuco, Pós-graduação em Geociências, 118 pp.
Sorby, H.C., 1860. On the origin of "cone-in-cone". British Association for the Advancement of Science, Report of the 29th Meeting, 1859, Transactions of Sections, Geology, 124 pp.
Spain, D.R., Anderson, G.A., 2010. Controls on reservoir quality and productivity in the Haynesville Shale, northwestern Gulf of Mexico Basin. Gulf Coast Association of Geological Studies Transactions 60, 657–668.
Speed, R., 1990. Volume loss and defluidization history of Barbados. Journal of Geophysical Research 95 (B6), 8983–8996.
Stauffer, C.R., 1911. A review of literature on the geology of South America. The Ohio Naturalist 11, 273–285.
Stewart, A.J., 1979. A barred-basin marine evaporite in the Upper Proterozoic of the Amadeus Basin, central Australia. Sedimentology 26, 33–62.
Stoneley, R., 1983. Fibrous calcite veins, overpressures, and primary oil migration. American Association of Petroleum Geologists Bulletin 67, 1427–1428.
Stow, G.W., 1874. Geological notes upon Griqualand west. Quarterly Journal of the Geological Society, London 30, 581–680.
Suchy, V., Dobes, P., Filip, J., Stejskal, M., Zeman, A., 2002. Conditions for veining in the Barrandian Basin (Lower Palaeozoic), Czech Republic: evidence from fluid inclusion and apatite fission track analysis. Tectonophysics 348, 25–50.
Swarbrick, R.E., Osborne, M.J., Yardley, G.S., 2002. Comparison of overpressure magnitude resulting from the main generating mechanisms. In: Huffman, A.R., Bowers, G.L. (Eds.), Pressure Regimes in Sedimentary Basins and Their Prediction. American Association of Petroleum Geologists Memoir, vol. 76, pp. 1–12.
Taber, S., 1916. The growth of crystals under external pressure. American Journal of Science 41 (246), 532–556. Series 4.
Taber, S., 1918. The origin of veinlets in the Silurian and Devonian strata of New York. Journal of Geology 26, 56–63.
Taber, S., 1930. The mechanics of frost heaving. Journal of Geology 38, 303–317.
Talukdar, S., Gallango, O., Vallejos, C., Ruggiero, A., 1988. Observations on the primary migration of oil in the La Luna source rocks of the Maracaibo Basin, Venezuela. Oil & Gas Science and Technology (Revue de l'Institut Français du Pétrole) 43, 357–370.
Tanner, P.W.G., 1989. The flexural-slip mechanism. Journal of Structural Geology 11, 635–655.
Tarney, J., Schreiber, B.C., 1976. Cone-in-cone and beef-in-shale textures from DSDP site 330, Falkland Plateau, South Atlantic. In: Barker, P.F., Dalziel, I.W.D., et al. (Eds.), Initial Reports of the Deep Sea Drilling Project, vol. 36. U.S. Government Printing Office, Washington, D.C, pp. 865–870.
Tarr, W.A., 1922. Cone-in-Cone. American Journal of Science 4, 199–213.
Testa, G., Lugli, S., 2000. Gypsum-anhydrite transformations in Messinian evaporites of central Tuscany (Italy). Sedimentary Geology 130, 249–268.
Thickpenny, A., 1984. The Sedimentology of the Swedish Alum Shales. In: Geological Society, London, Special Publications, vol. 15, pp. 511–525.
Thompson, B., 1902. Geology. In: Adkins, W.R.D., Serjeantson, R.M. (Eds.), A History of the County of Northampton, vol. 1. University of London, Institute for Historical Research, pp. 1–40.
Thoral, M., 1942. A propos de la structure "cone-in-cone". Comptes Rendus de la Société Géologique de France 13, 144–146.
Tobin, K.J., Walker, K.R., Steinhauff, D.M., Mora, C.I., 1996. Fibrous calcite from the Ordovician of Tennessee: preservation of marine oxygen isotopic composition and its implications. Sedimentology 43, 235–251.
Torres, T., Barale, G., Méon, H., Philippe, M., Thévenard, F., 1997. Cretaceous floras from Snow Island (South Shetland Islands, Antarctica) and their biostratigraphic significance. In: Ricci, C.A. (Ed.), The Antarctic Region: Geological Evolution and Processes. Terra Antarctica Publication, Siena, pp. 1023–1028.
Trabucho-Alexandre, J., Dirkx, J., Veld, H., Klaver, G., De Boer, P.L., 2012. Toarcian black shales in the Dutch Central Graben: record of energetic, variable depositional conditions during an oceanic anoxic event. Journal of Sedimentary Research 82, 104–120.
Turner, E.C., Kamber, B.S., 2012. Arctic Bay Formation, Borden Basin, Nunavut (Canada): basin evolution, black shale, and dissolved metal systematics in the Mesoproterozoic ocean. Precambrian Research 208-211, 1–18.
Twenhofel, W.H., Tester, A.C., 1926. New data on the Comanchean strata of central Kansas. American Association of Petroleum Geologists Bulletin 10, 553–561.
Urai, J.L., Williams, P.F., van Roermund, H.L.M., 1991. Kinematics of crystal growth in syntectonic fibrous veins. Journal of Structural Geology 13, 823–836.
Ure, D., 1793. History of Rutherglen and East Kilbride. David Niven, Glasgow, 334 pp.
Van Noten, K., Muchez, P., Sintubin, M., 2011. Stress-state evolution of the brittle upper crust during compressional tectonic inversion as defined by successive quartz vein types (High-Ardenne slate belt, Germany). Journal of the Geological Society, London 168, 1–16, http://dx.doi.org/10.1144/0016-76492010-112.
Vincent, S.J., Allen, M.B., 2001. Sedimentary record of Mesozoic intracontinental deformation in the eastern Junggar Basin, northwest China: response to orogeny at the Asian margin. Geological Society of America Memoir 194, 341–360.
Volk, H., Horsfield, B., Mann, U., Suchy, V., 2002. Variability of petroleum inclusions in vein, fossil and vug cements – a geochemical study in the Barrandian Basin (Lower Palaeozoic, Czech Republic). Organic Geochemistry 33, 1319–1341.
Von Terzaghi, K., 1923. Die Berechnung der Durchlâssigkeitsziffer des Tones aus dem Verlauf der hydrodynamischen Spannungerscheinungen. Sitzungsberichte der Akademie der Wissenschaften in Wien, mathematischnaturwissenschaftliche Klasse, Abteilung IIa 132, 125–138.
Warrington, G., Whittaker, A., Scrivener, R.C., 1986. The late Triassic succession in central and eastern Somerset. Proceedings of the Ussher Society 6, 368–374.
Watt, J.A., 1898. Saddle reefs at Hargraves. New South Wales Geological Survey Records 5, 153–160.
Watts, N.L., 1978. Displacive calcite: evidence from recent and ancient calcretes. Geology 6, 699–703.
Webster, T., 1826. Observations on the Purbeck and Portland Beds. In: Transactions of the Geological Society, London, Series 2, vol. 2, pp. 37–44.
West, I.M., 2012. Geology of the Wessex Coast of Southern England – the World Heritage Jurassic Coast – and More. Internet page. http://www.southampton.ac.uk/~imw/index.htm.
Wignall, P.B., Pickering, K.T., 1993. Palaeoecology and sedimentology across a Jurassic fault scarp, NE Scotland. Journal of the Geological Society, London 150, 323–340.
Willman, C.E., 2007. Regional structural controls on gold mineralisation, Bendigo and Castlemaine goldfields, Central Victoria, Australia. Mineralium Deposita 42, 449–464.
Windh, J., 1995. Saddle reef and related gold mineralization, Hill End Gold Field, Australia: evolution of an auriferous vein system during progressive deformation. Economic Geology 90, 1764–1775.
Woodland, B.G., 1964. The nature and origin of cone-in-cone structure. Fieldiana: Geology 13 (4). 187–305.
Woodland, B.G., 1975. Pyritic cone-in-cone concretions. Fieldiana Geology 33, 125–139.
Woodward, H.B., 1893. The Jurassic Rocks of Britain. In: The Lias of England and Wales (Yorkshire Excepted), vol. 3. Memoir of the Geological Survey of the United Kingdom, 399 pp.
Yates, J., 1821. Account of a variety of argillaceous limestone, found in connexion with the iron-stone of Staffordshire. Transactions of the Geological Society of London 5, 375–378. Series 1.
Young, J., 1885. Notes on "cone-in-cone" Structure, vol. 8. Transactions of the Geological Society, Glasgow, Part 1, pp. 1–27.
Young, J., 1886. Cone-in-cone. Geological Magazine 2, 139–140. Decade 3.
Young, J., 1892a. Cone-in-cone structure. Geological Magazine 9, 138–139. Decade 3.
Young, J., 1892b. Cone-in-cone structure. Geological Magazine 9, 278–279. Decade 3.
Young, J., 1892c. Cone-in-cone structure. Geological Magazine 9, 480. Decade 3.
Zanella, A., Cobbold, P.R., 2011. Influence of Fluid Overpressure, Maturation of Organic Matter, and Tectonic Context during the Development of 'beef ': Physical Modelling and Comparison With the Wessex Basin, SW England, vol. 13. EGU General Assembly, Vienna, Austria. Geophysical Research Abstracts.
Zanella, A., Cobbold, P.R., 2012. 'Beef': Evidence for Fluid Overpressure and Hydraulic Fracturing in Source Rocks During Hydrocarbon Generation and Tectonic Events: Field Studies and Physical Modelling. Geofluids VII International Conference, Rueil-Malmaison, May 2012.

Chapitre 2

Etude du bassin du Wessex, Angleterre du sud

2.1 Introduction

Dans le chapitre précédent, nous avons pu voir l'étendu du phénomène beef. Ce dernier trouve son origine dans le bassin du Wessex au sud de l'Angleterre (Buckland & De la Bèche, 1835). Nous avons donc choisi de faire de ce bassin un de nos objets d'étude. Le choix d'étudier ce dernier ne repose pas uniquement sur le caractère historique, mais également sur le fait que ce bassin possède un système pétrolier.

À notre connaissance, seule une étude publiée existe sur la détermination de l'origine des fluides liés au beef (Marshall, 1982). Pourtant, les affleurements de beef ne manquent pas le long de la côte anglaise. Nous apprenons dans cette étude que l'origine du beef est peu profonde, dans les premières centaines de mètres lors de l'enfouissement de la roche. Au regard des nouvelles théories sur les surpressions de fluides et le beef, nous nous sommes intéressés aux critères de développement du beef et au fluide responsable de sa formation. En effet, si le beef est issu des phénomènes de surpression de fluides, en partie dûs à la génération d'hydrocarbures, alors son origine peut être beaucoup plus profonde.

Nous avons donc cherché dans cette étude si le beef était porteur de critères structuraux qui pourraient nous renseigner sur son développement, c'est à dire de la création de la fracture jusqu'à la fin de la croissance des fibres minérales qui le composent. Puis, il nous a semblé intéressant de regarder plus précisément le fluide lié au beef. Pour ceci, nous avons utilisé la géochimie isotopique et les analyses sur inclusions de fluide. Ces techniques ont fait preuve d'un grand potentiel auparavant. En effet, Rodrigues dans sa thèse (2008) montre que ces techniques sont très adaptées pour l'étude du beef. Il démontre ainsi que le fluide à l'origine du beef dans le bassin de Neuquén en Argentine est marin, et qu'il dérive spécifiquement des eaux marines contenues au sein même de la roche mère des hydrocarbures. Ainsi, nous avons voulu étudier la génération, la circulation (ou migration) et les effets de la surpression d'un fluide dans le bassin du Wessex.

2.2 Article#2: 'Beef' of the Wessex Basin, SW England: Widespread distribution and some new interpretations

L'étude du bassin du Wessex est rédigée sous la forme d'un article scientifique. Ce dernier est soumis dans la revue *Journal of the Geological Society of London*.

2.2.1 Résumé de l'article

Les veines de calcite fibreuse parallèles à la stratification de la roche (beef) sont très répandues dans le bassin du Wessex, Angleterre du sud-ouest. Ces veines sont communes dans les silts et argiles mésozoïques, et plus particulièrement ceux d'âge liassique à Crétacé moyen. Les structures cone-in-cone, qui consistent en de multiples cônes emboités les uns dans les autres, sont aussi très présentes à l'intérieur du beef. Ces veines sont typiquement formées par de la calcite, mais des inclusions ou patches d'hydrocarbures (liquides ou solides) sont nombreux, respectivement à l'intérieur des cristaux de calcite ou entre les fibres. Pour étudier le contexte de formation du beef dans ce bassin, nous avons tout d'abord mené une étude structurale. Nous avons trouvé deux variétés de beef dans le bassin : (1) ceux ne montrant aucun signe de déformation et (2) ceux montrant des évidences de plissement et de fracturation, durant la croissance des veines. Alors que le beef non déformé est très répandu dans le bassin, celui montrant des signes de déformation est particulièrement présent à l'approche des failles majeures. Nous avons aussi étudié la nature du fluide responsable de la formation du beef au moyen d'analyses isotopiques et d'une étude sur les inclusions de fluide. Les résultats montrent que le fluide à l'origine du beef est de source marine, typiquement dérivé d'argiles marines. Par conséquent, nous proposons que le beef du bassin du Wessex se soit formé d'une manière synchrone à la génération d'hydrocarbures, notamment durant l'inversion Cénozoïque du bassin.

2.2.2 Article#2

'Beef' of the Wessex Basin, SW England: widespread distribution and some new interpretations

A. Zanella[1]*, O. Prévost-Bourré[1], P. Boulvais[1], J. Pironon[2], P.R. Cobbold[1] and T. Boassen[3]

[1]Géosciences-Rennes (UMR-6118), CNRS and Université de Rennes 1, Campus de Beaulieu, 35042 Rennes Cedex, France

[2] Géoressources, Université de Lorraine, Nancy, France

[3] Statoil ASA Research Center, Norway

*Corresponding author, e-mail: alain.zanella@univ-rennes1.fr

Abstract

Bedding-parallel veins of fibrous calcite (beef) are widespread in the Wessex Basin of SW England. The veins are common in Mesozoic mudstones and shales, especially of Liassic to Mid-Cretaceous age. Cone-in-cone structures, which consist of multiple nested cones, are also well developed within the beef. The veins are typically of calcite, but inclusions or patches of hydrocarbons (liquid or solid) are numerous within calcite crystals or between fibres, respectively. To investigate the context of formation of beef in the basin we first did a structural study. We found two varieties of beef in the basin: (1) showing no signs of deformation and (2) showing evidence for folding and faulting, during growth of the veins. Whereas undeformed beef is widespread within the basin, deformed beef is especially well developed near major tectonic faults. We also investigated the nature of the fluid responsible for the formation of beef, via isotopic analyses and studies of fluid inclusions. According to the results, the original fluid was of marine origin, as is typical for marine shales. Thus, we argue that beef in the Wessex Basin formed at the same time as hydrocarbons, especially during Meso-Cenozoic inversion of the basin.

Keywords: Wessex Basin, 'beef', overpressure development, organic matter, stable isotopes, fluid inclusions

Introduction

Bedding-parallel fibrous calcite veins, or ‘beef’ called, are common worldwide in sedimentary basins, in particular in shales or mudstone rocks (see the recent review by Cobbold et al., 2013). Historically, Buckland and De la Beche (1835) introduced the term ‘beef’ for calcite veins in the Wessex Basin, SW England. Workmen there had adopted the term, because of the resemblance between the fibrous veins and the fibres of animal muscle. Some veins of ‘beef’ also contain ‘cone-in-cone’ structures, which consist of multiple nested cones of fibres. In what follows we will use the term ‘beef’ for all bedding-parallel fibrous calcite veins and only mention ‘cone-in-cone’ as an internal structure of these. In the Wessex Basin (Fig. 1), Mesozoic strata crop out well along the coast.. Between the localities of Lyme-Regis and Charmouth, Devon. ‘beef’ is so common that Lang et al. (1923) named a sequence of Liassic age (now a Member of the Charmouth Mudstone Formation) the ‘Shales-with-Beef’. Not until much later did Marshall (1982) study the isotopic composition of the veins, so as to elucidate their conditions of formation.

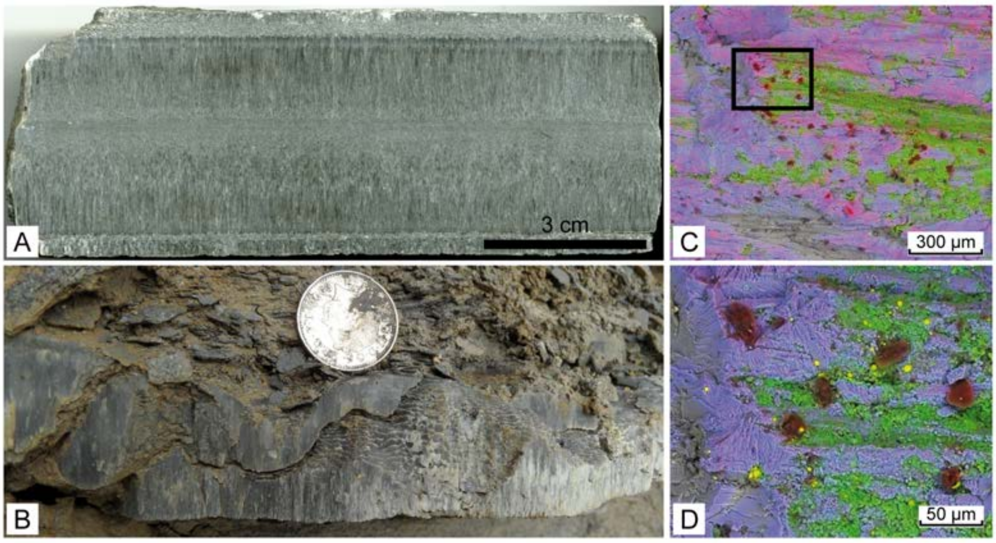

Figure 1. A. Photograph of a ‘beef’ vein from the Blue Lias Formation between the localities of Lyme Regis and Charmouth, Dorset. The ‘beef’ consists of crystalline calcite and its fibrous structure is typical. The grey colour is mainly due to the presence of pyrite and shale fragments between the fibres of calcite. Note the horizontal symmetry plane at the centre of the vein from which the ‘beef’ began to grow. A second generation is visible at both edges of the vein (below and above). B. Photograph of ‘cone-in-cone’ structure from the Chief Beef Member at Swanage, Dorset. C. & D Composite BSE and X-ray images, both showing the typical composition of ‘beef’ for the Wessex Basin. Intensities of colours reveal

concentrations of elements (red = carbon; green = aluminium; yellow = sulfur and blue = calcium).

More generally, during the last two centuries, numerous scientists have studied the mechanisms of formation of fibrous veins , distinguishing (1) mechanisms of fracturing and (2) mechanisms of fibre growth within fractures. Fibres may grow by a crack-seal mechanism (Ramsay 1980), or in a continuous manner (Taber 1918; Durney & Ramsay 1973; Means & Li 2001). Bons & Jessel (1997) argued that fibrous minerals grow under the effects of concentration gradients. Indeed, fibrous crystals grow by precipitation from supersaturated aqueous solutions, under various conditions of temperature and pressure.

For the generation and opening of fractures, some authors have privileged internal agents, such as force of crystallization (Keulen et al. 2001). It seems however, from theoretical and experimental data (Taber 1918; Means & Li 2001; Keulen et al. 2001), that this force is not always great enough enough to open a fracture. Otherwise, there are several potential external agents, especially tectonic stress and pore fluid pressure. For developing horizonal fractures, Gustavson et al. (1994) advocated dissolution at depth, whereas Shearman et al. (1972) and Stoneley (1983) highlighted the role of fluid overpressure. Several authors have argued that the tensile strength of the rock should be smallest in a direction perpendicular to bedding (Cosgrove 1995, 2001; Lash & Engelder 2005) and certainly this should help. However, Cobbold & Rodrigues (2007) argued and demonstrated experimentally that an upward-decreasing overpressure gradient leads to the development of vertical seepage forces and therefore horizontal fractures. In the Neuquen Basin of Argentina, Rodrigues et al. (2009) have described fossil prints in the centre and on both sides of ‘beef’ veins, as evidence for antitaxial growth and opening perpendicular to bedding.

One mechanism for obtaining fluid overpressure is by load transfer during chemical compaction (Swarbrick & Osborne, 2002). Part of the solid framework collapses and the weight of the overburden transmits to the pore fluid. This leads to hydraulic fracturing, provided that the total fluid pressure becomes greater than the sum of the lithostatic pressure and the tensile strength of the rock.

In many sedimentary basins worldwide, ‘beef’ occurs in or near potential source rocks for petroleum (Cobbold et al. 2013). This is particularly true in basins where the source rock is or has been mature. In this context, several authors have described liquid oil or bitumen as inclusions within fibrous veins of calcite (Stoneley 1983; Dobes et al. 1999; Parnell et al. 2000; Rodrigues et al. 2009; Zanella & Cobbold 2011, 2012). Crystallization of ‘beef’, maturation of organic matter and migration of hydrocarbons may thus be synchronous phenomena. In turn, 'beef' veins may contain physical and chemical information that is relevant to our understanding of hydrocarbon generation in sedimentary basins (see, for example, Rodrigues et al., 2009). In particular, the composition of calcite (in terms of stable isotopes of oxygen and carbon) and the properties of fluid inclusions provide first-order information on fluid sources and conditions of trapping. The oxygen isotope composition of beef relates to the one of the local fluid, provided that the temperature of calcite precipitation is known, the relative amount of fluid over rock (the so-called fluid/rock ratio), and in the conditions of large fluid/rock ratios under which fluids preserve their original isotopic composition, provides information of fluid sources. To be complete, an isotopic study should also consider the host rocks, so as to check how these may have influenced the composition of the flowing fluid. The carbon isotope composition gives information on the relative contribution of marine-derived carbon ($\delta^{13}C$ around 0‰) and organic matter-derived carbon ($\delta^{13}C$ between -15 and -30‰). The fluid inclusion tools allow discussing the physical (pressure, temperature) and chemical (fluid composition) of the fluid at the time of entrapment. In this paper, we present new O and C stable isotopes and fluid inclusion data for 'beef' in the Wessex basin. Our work is complementary to the pioneering work of Marshall (1982), who presented detailed isotopic variations at the decimetre scale in 'beef' around dolomitic nodules at Charmouth and to the work of Rodrigues et al. (2009), who studied "beef" in the Neuquén Basin. We have visited and sampled numerous 'beef' veins and host rocks throughout the Wessex Basin and provide new field observations, stable isotopes and fluid inclusions data that allow us discussing the origin of fluids involved in the 'beef' formation, at the scale of the whole Wessex Basin.

Geological context

The Wessex Basin lies along the coast of South-West England (Fig. 2). It contains a Permian to Oligocene sedimentary sequence, which post-dates the Devonian-Carboniferous sequence of the Proto-Tethys ocean (Glennie & Underhill 1998; Fig. 3). The structural development of the basin finds its origins in the late Carboniferous-early Permian apogee of the Variscan orogeny (Chadwick et al. 1983). The deposition of sediments of the basin took place during the fragmentation of the Pangaean megacontinent and so the Permo-Triasic extensional period of the central Channel rifting and then continued during the Mesozoic period. Several structural features subdivide the Wessex Basin. They are mainly extensional E-W tectonic structures developed during the late Palaeozoic-Mesozoic times and inverted during late Cretaceous-Tertiary times (e.g. Stoneley 1982; Chadwick 1993; Underhill & Paterson 1998; Underhill & Stoneley 1998). Among these structures, the Purbeck - Isle of Wight fault system is the major one (Fig. 2). This fault system accommodated much of the compressional deformation during the late Cretaceous and Tertiary, producing major monoclinal flexures. On its southern side, the hangingwall,has undergone a regional uplift of about 1.5 km (Bray et al. 1998). As a result of such Late Cretaceous to Cenozoic inversion, the sedimentary fill of the Wessex Basin crops out well, all along the coasts of Devon, Dorset and Hampshire and on the Isle of Wight. Thus, several generations of geologists have studied this area, which is now part of a World Heritage Site.

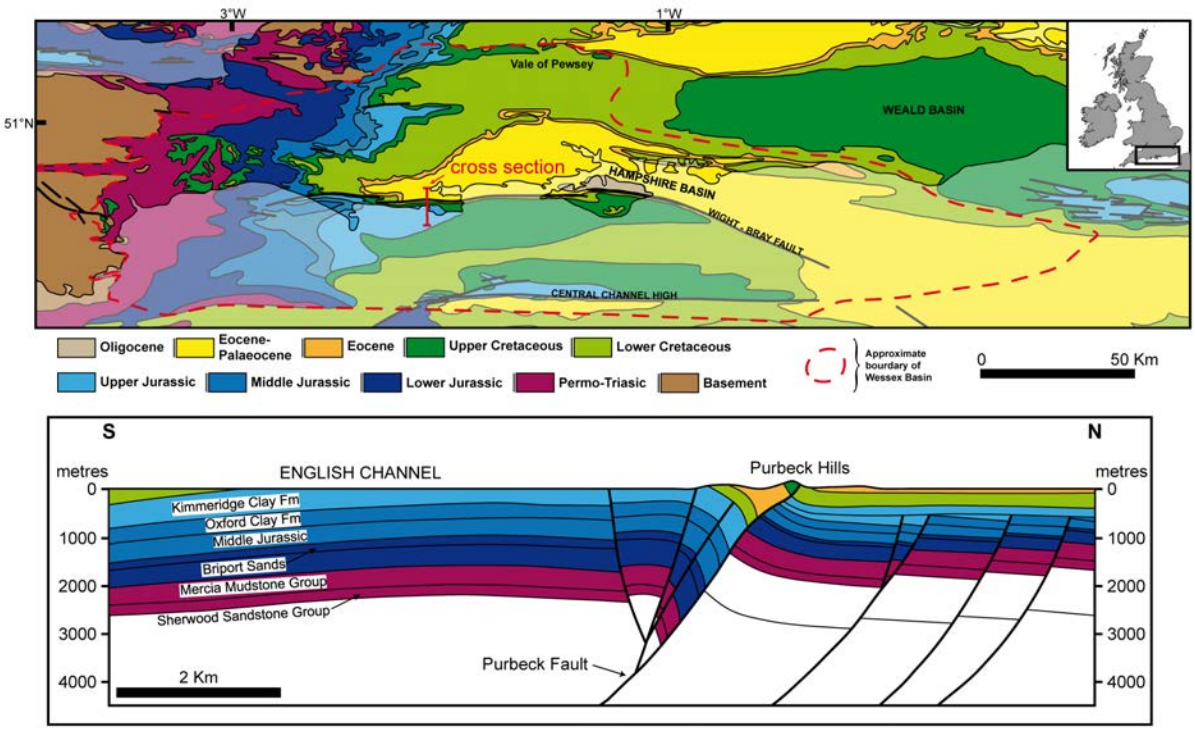

Figure 2. (A), Geological map of the Wessex Basin, SW England. (B), North-South cross-section of the Wessex Basin showing the Purbeck Fault, the major structure of the basin. (Modified after Underhill & Stoneley 1998).

The sedimentary fill of the Wessex Basin consists of three megasequences (Permian to Lower Cretaceous, Upper Cretaceous; and Tertiary; Fig. 3) with intervening erosional unconformities (Hawkes et al. 1998). The corresponding sedimentary environments were, successively, continental, deepshore marine and near-shore to non-marine.

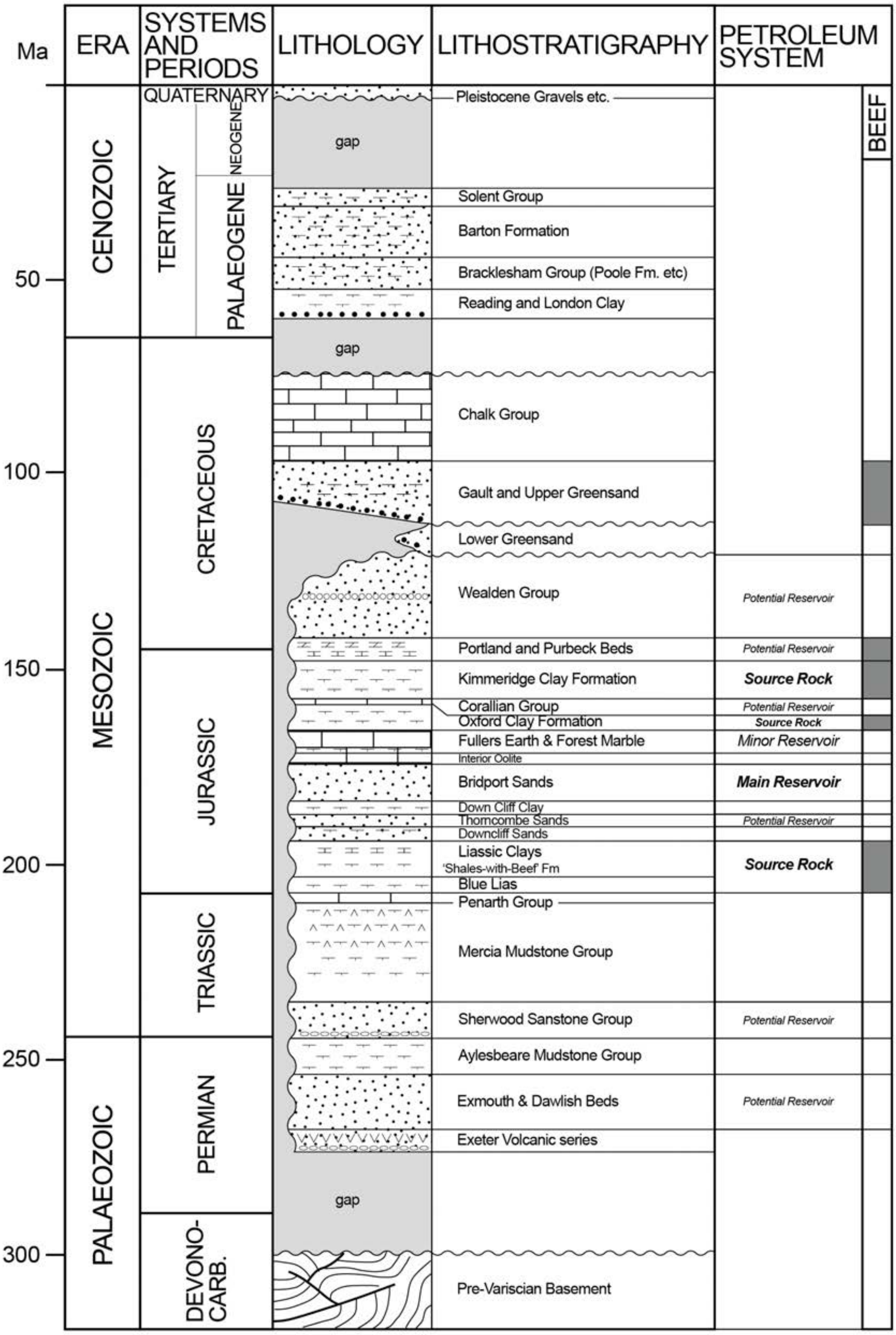

Figure 3. Generalized stratigraphical column of the Wessex Basin, (modified after Underhill & Stoneley 1998; West 2010). For the petroleum system, potential source rocks and conventional reservoirs are mainly within Mesozoic srata (especially Jurassic and Early Cretaceous). Beef is also present, especially in or near the potential source rocks.

The Mesozoic strata concentrate the majority of the petroleum system of the Wessex Basin (Fig. 3). Exploration for petroleum led in 1937 to the first exploration well, Poxwell-1 (Buchanan 1998). One of the historical discoveries was the Kimmeridge oilfield, on the Dorset coast, which is still in production (Buchanan 1998). The major onshore oilfield of the Wessex Basin is Wytch Farm on the Isle of Purbeck (Fig. 2). The petroleum system of the basin has three potential source rocks: (1) the Blue Lias Fm and Lias Clays, (2) the Oxford Clay Fm and (3) the Kimmeridge Clay Fm, (Fig. 3). In the Liassic and Kimmeridgian clays, the organic matter is of Type II, with a minor amount of Type III (Ebukanson & Kinghorn 1986). Organic matter is quite abundant (Ebukanson & Kinghorn 1985): up to 8% of Total Organic Carbon (TOC) for the Liassic Clays and about 20% for the Kimmeridge Clays. Vitrinite reflectance measurements point out that at outcrops these source rocks are immature; only 0.48% for the Kimmeridge Clay (Ebukanson & Kinghorn 1985). In contrast, Bray et al. (1998) demonstrated via Apatite Fission Track Analyses (AFTA) that the source rocks have been mature over time and that the hydrocarbon generation is linked to the burial and uplift history. These authors also argued that the Wessex Basin has gone through a very complex thermal history related to several phases of uplift and erosion. These events have affected the generation of hydrocarbons. The study of Bray et al. (1998) reveals that the timing of hydrocarbon generation is widespread through times, from the mid-Jurassic (~170 Ma) to the late Tertiary (~20Ma). Nevertheless, the peak hydrocarbon generation is more and more recent eastward.

In this petroleum context, ‘beef’ has a key place. At the beginning of its historical discovery, ‘beef’ seemed to be just anecdotic veins in muddy sediments. With times, ‘beef’ have gained interest. Indeed, ‘beef’ have been identified in several stratigraphic levels of the sedimentary succession: in the Blue Lias and Liasic Clays of Early Jurassic age at Lyme Regis and Charmouth (Sorby 1860; Lang 1914; Lang et al. 1923; Marshall 1982; Gallois 2008), in the Kimmeridge Clays of Late Jurassic age at Kimmeridge Bay (Morgans-Bell et al. 2001), in the Purbeck beds of Early Cretaceous age at Swanage (Webster 1826; Buckland and De la Beche 1835), in the area of the Vale of Wardour (Andrews & Jukes-Brown 1894; Reid 1903) and in the Vectis Formation of Early Cretaceous age on the Isle of Wight (Judd 1871). But even if well known, ‘beef’ have been poorly characterized in order to specify their origin of formation. The most complete study is likely the isotopic study of Marshall (1982). This author identified large variations in $\delta^{18}O$ along fibres and suggested that external fluid flowed in a bedding-parallel direction, supplanting precipitation from connate waters. Correlatively, variations in $\delta^{13}C$ values are also large (from nearly -17 ‰ to 0 ‰; Marshall, 1982, his

Figure 5). Marshall attributed these variations to the successive involvement of carbon deriving mainly from organic matter and marine waters.

Field Data

In the Wessex Basin, ‘beef’ is visible along many of the coastal cliffs. Previous studies have described ‘beef’ within shales or mudstones of several stratigraphic levels of the basin. Here, we have investigated the whole stratigraphic sequence throughout the Basin. We have identified other occurrences of ‘beef’: in the Blue Lias at Chippel Bay, in the Oxfordian Clays at Ringstead Bay, in the Purbeck Beds at Durdle Door, Stair Hole, Lulworth Cove (see the website of West) and Mupe Bay, and in the Early Cretaceous at Sandown on the Isle of Wight. It seems then that ‘beef’ is limited to Mesozoic strata, from the Lias to the Early Cretaceous (Fig. 3). The limits of these occurrences match those of the petroleum system (Fig. 3). Calcite is the main mineral of ‘beef’ but we also observed pyrite and shale particles within them; the grey colour of ‘beef’ likely is due to these elements. Throughout the Wessex Basin, we have found no correlation between the size of beef veins, their amount and the stratigraphic position. The size of ‘beef’ is mainly between a few millimetres to 3-4 decimetres in thickness (reaching two tens of centimetres at Lyme Regis and Charmouth) and from several centimetres to tens of meters in length, providing sometimes a very planar aspect of the beef. At the outcrop scale, ‘beef’ can appear at several levels in the same Formation, or can be also disseminated in smaller occurrences within the shales, as in the ‘Shale-with-beef’ Fm at Lyme Regis for example (Fig. 4). Structurally, if most ‘beef’ occurrences are parallel to the bedding (Fig. 3), locally ‘beef’ can be deformed and/or faulted (Fig. 5).

Several authors have shown that the formation of ‘beef’ seems to be correlated with the nature of the host rock, impermeable shales or mudstones. During our fieldwork, systematic HCl attack on host rocks has revealed that the more the host rock is carbonate-rich, the more the beef are abundant. As an extreme, carbonate-free levels of clayey sediments are devoid of beef. This observation points to a local chemical control of the fluid-rock system by the mineralogical composition of the host rock.

Two sites are worthy to be described: Lyme Regis and Lulworth Cove areas. They correspond to historical accessible areas with beautiful easily observable ‘beef’. Furthermore, both sites are very different in terms of morphology for the ‘beef’. At Lyme Regis ‘beef’ is undeformed while at Lulworth cove the ‘beef’ is deformed and faulted. Such deformation is likely related to the vicinity of the Purbeck-Isle of Wight system fault. Numerous vertical calcite veins also occur in Lulworth Cove and attest of vertical fluid migration, a feature that is absent in Lyme Regis. In addition, the Lyme Regis area exposes formations of the Lower Jurassic and thus corresponds to the base of the petroleum system in the Wessex Basin.

Lyme Regis outcrop

About 600 metres west of the Lyme Regis port, , the beautiful outcrop of Chippel Bay composes the cliff until Seven Rock Point. Strata are from the Blue Lias Formation (Top of Hettangian) to the ‘Shale-with-beef’ Formation (Sinemurian), and are mainly shales and limestone beds (Fig. 4A). The global structure consists of a gentle anticline (N-S) and the bedding of rocks remains nearly flat (Fig. 4A). We identified only one vertical strike-slip fault on outcrop, but this fault does not affect the global geometry of strata.

As previously describe in this area, ‘beef’ is abundant within the ‘shale-with-beef’ Fm (Lang et al. 1923; Fig. 4C). In this Formation, visible on the top of the cliff, ‘beef’ are well preserved, numerous and continuous, including the level of ‘beef’ that Marshall (1982) had studied (Fig. 4C). This level of ‘beef is remarkable on the outcrop because its hardness brings them out and sampling is made possible because of continuous landslides. In addition of these continuous levels of ‘beef’, the formation contains a lot of ‘beef’ disseminated through the organic-rich shales.

In the Blue Lias Formation we have identified 9 levels of ‘beef’ (Fig. 4B, D). ‘Beef’ is present in organic matter-rich dark marly shales, and is parallel to the bedding. Calcite fibres are easily visible and oriented perpendicular to the axis vein, which is well expressed. In some examples, ‘beef’ is splited and forms ‘en échelon’ structures (Fig. 4B). The thickness of ‘beef’ is from several millimetres to 1 - 2 centimetres (Fig. 4D). The length of each ‘beef’ is very variable, from several centimetres up to decametres. Some thin beef are hard to distinguish, especially those at first levels between the 2nd Tape and the 3rd Quick stratigraphic strata (Fig. 4B).

In the area of Lyme Regis and especially between Lyme Regis and Charmouth, Lees & Cox (1937) described bitumen veins in the Black Ven Marls, the Beleminite Marls and the Blue Marls (Liasic Clays). Nevertheless, they did not specify localities for them. We also identified small particles of bitumen veins in shales between those localities but there were only loose fragments in the coastal landslides of the area.

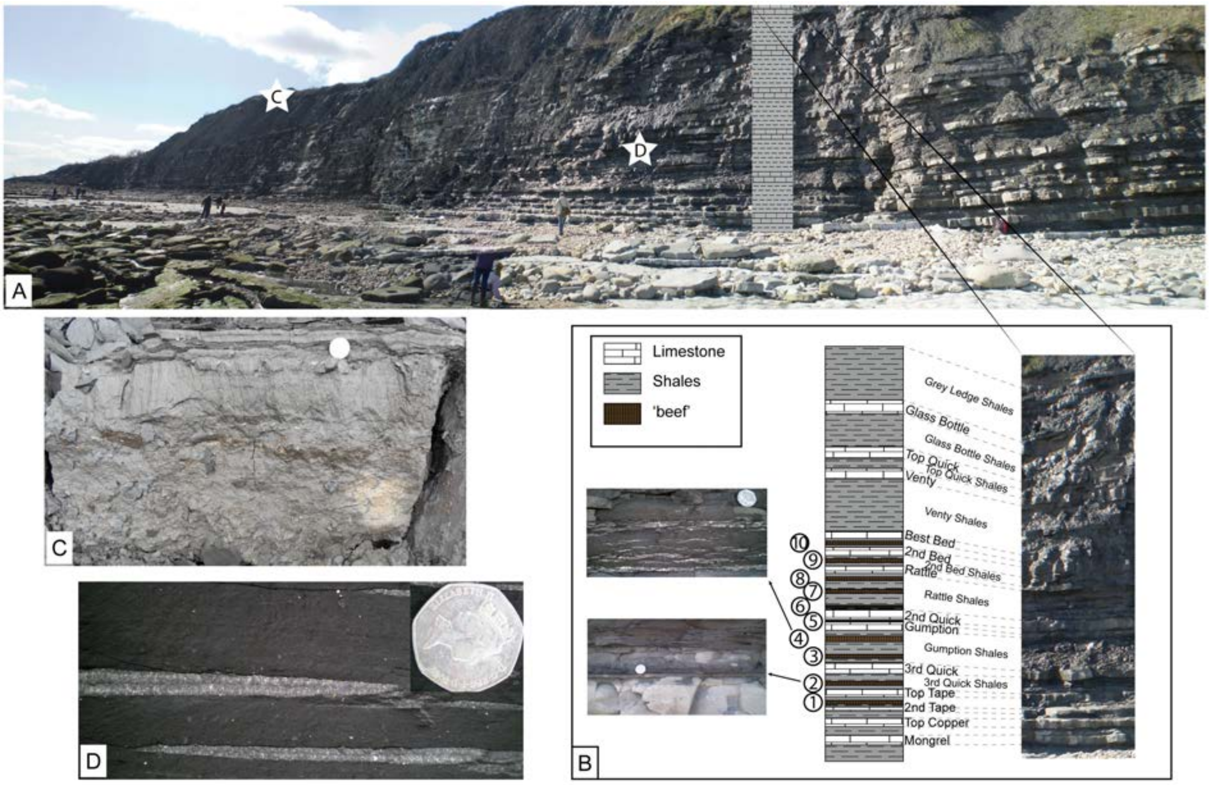

Figure 4. Lyme-Regis outcrop observations. A. Panorama of Chippel Bay (East of Lyme Regis). Strata form a very gentle anticline. B. Schematic representation of the local stratigraphic nomenclature of the Blue Lias Fm. Notice the occurrence of 'beef' layers. C. Photograph of the main 'beef' level in the 'Shales-with-Beef' Fm. D. Photograph of typical 'beef' from the Blue Lias Fm.

Lulworth cove outcrop

Outcrops of the Lulworth Cove area are easily accessible, at low tide. Along an E-W trend around this area, the Purbeck-Isle of Wight fault system cuts through the entire sedimentary pile, which now dips towards the North and forms a monocline, well known to be a great example of a basin inversion (Fig. 5A). From the locality of Durdle Door in the West, through Stair Hole and Lulworth Cove and to Mupe Bay in the East, outcrops consist of Cretaceous strata from the Portland Beds to the Chalk Group. The spectacular outcrop of 'beef' is in the east side of Lulworth Cove (box in the Fig. 5A), immediaetly above the last Upper Purbeck limestone bed (Fig. 5A). Nevertheless stratigraphically, we have observed 'beef' at about 2 metres beneath the Cinder Bed at Stair hole, but their became numerous from the Upper Purbeck Beds (for example those of Lulworth cove Fig. 5B). In all occurrences of this area, ‘beef’ is concentrated within mudstones, (i.e. in an impermeable sedimentary level).

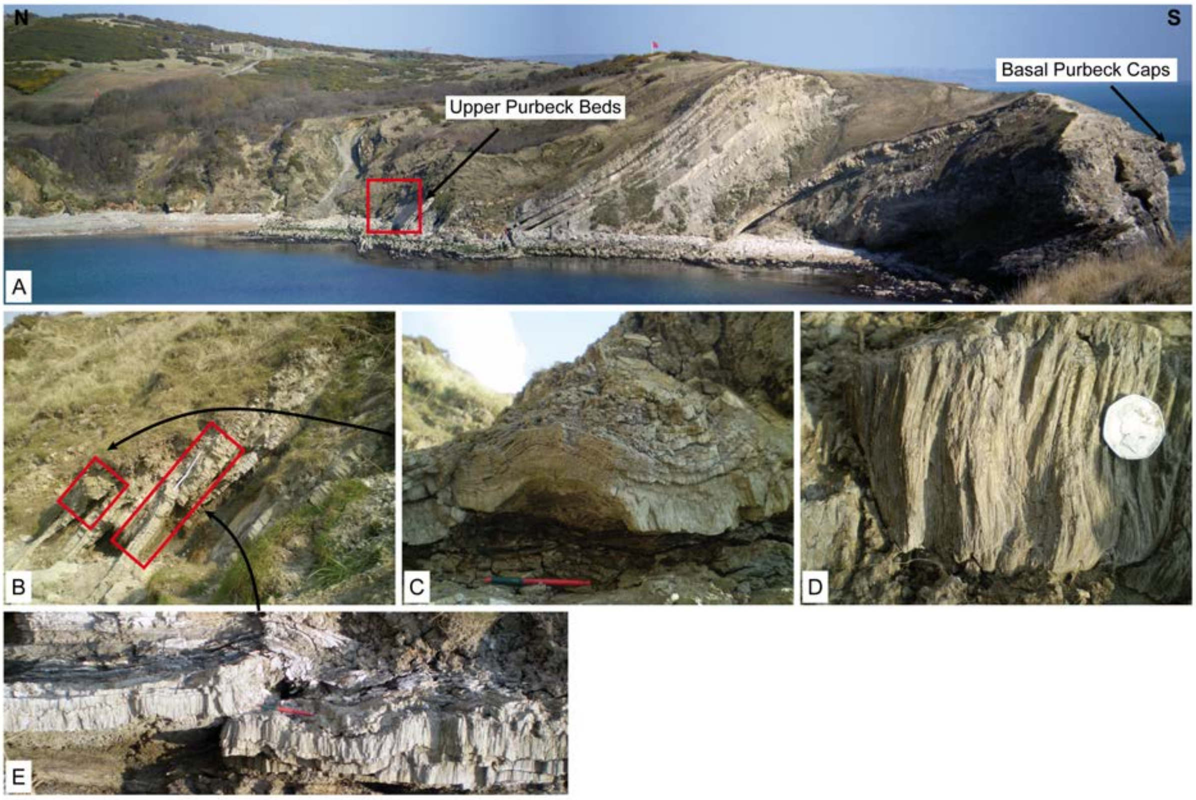

Figure 5. Lulworth Cove outcrop observations. A. Panorama of the eastern side of Lulworth Cove (red box refers to Figure B). B. Main outcroup for beef veins. C. Folded beef. The thickness of beef is variable (thicker in the syncline form). D. Curved calcite fibres, which compose beef. Cone-in-cone is visible as well. E. Folded and faulted beef veins. The fault cut through the beef but the shales arount it are not faulted.

The morphology of ‘beef’ is distinct from to those of the Lyme Regis area, despite ‘beef’ is also parallel to the bedding. It is generally thicker and deformed (Fig. 5C) and/or faulted (Fig. 5E). The thickness reaches several centimetres until frequently 20 or 30 centimetres and the length of ‘beef’ is difficult to estimate while continuous (Fig. 5B). By internal structural arguments, ‘beef’ seems to be synchronous with a compressional deformation. Examples are the thickening of ‘beef’ syncline, a feature attesting fibres growth during deformation (Fig. 5C) and sigmoidal calcite fibres. The analysis of this outcrop thus suggests that ‘beef’ grew during horizontal shortening associated with inversion of the basin (Fig. 5C & 5E).

Vertical veins of white and sparritic calcite are also visible, especially at Stair Hole (West of Lulworth Cove). These veins cut through shales and calcareous beds of the Purbeck Fm and do not reach the main ‘beef’ level (just above the Upper Purbeck limestones bed). Veins are metric in length but are thin, only 1 or 2 centimetres of thickness. They are perpendicular to the direction of the regional anticline structure.

Sampling

The objective of our sampling strategy was to get a comprehensive view of the beef-related fluid system at the basin scale. This strategy is complementary to the one of Marshall (1982) who detailed the small-scale evolution of the O and C isotope compositions at the beef scale. We have thus sampled seven sites through the entire stratigraphic pile, from the Blue Lias Fm (Lyme Regis) to lower Cretaceous (Swanage) (Fig. 3). For each site, we collected several beef samples in order to specify the local variability of isotopic compositions. When possible, we also sampled the most representative host rock, close to the beef or a few metres away from it. At Stair hole, we also sampled vertical calcite veins as these veins may record fluid circulations in the vertical direction, perpendicular to bedding. Three materials were selected for the fluid inclusion investigation: two beef coming from the outcrops detailed above (Lyme Regis and Lulwoth cove) and one vertical vein coming from Stair hole. The fluid inclusion dataset may then look rather limited but considering the difficulty in preparing the thick sections, the scarcity of preserved fluid inclusion and the equivocal aspect related to the interpretation of fluid inclusion data, we do believe that our fluid inclusion data, which are the first published on beef in the Wessex Basin, are worthy to be presented and discussed in the frame of the present paper.

Samples

Our collected samples are hand-sized specimen (Fig. 6). We collected them directly on cliffs or on large blocks fallen from the cliffs. In that case, we ensured in the field that the sampled blocks did correspond to what is still present in cliffs. On beef samples, we made a total of 25 thin sections for the petrographic description and 20 thick sections for fluid inclusion analyses. For isotopic analyses, we sawed samples in order to get planar surfaces perpendicular to beef-shale contacts, and got a few tens of mg by microdrilling or scratching these surfaces. We performed powders on both the beef and the shales sides (fig. 6A). For vertical veins (7 samples), calcite was separated manually and crushed in a boron carbide mortar. A total number of 75 isotopic analyses was obtained.

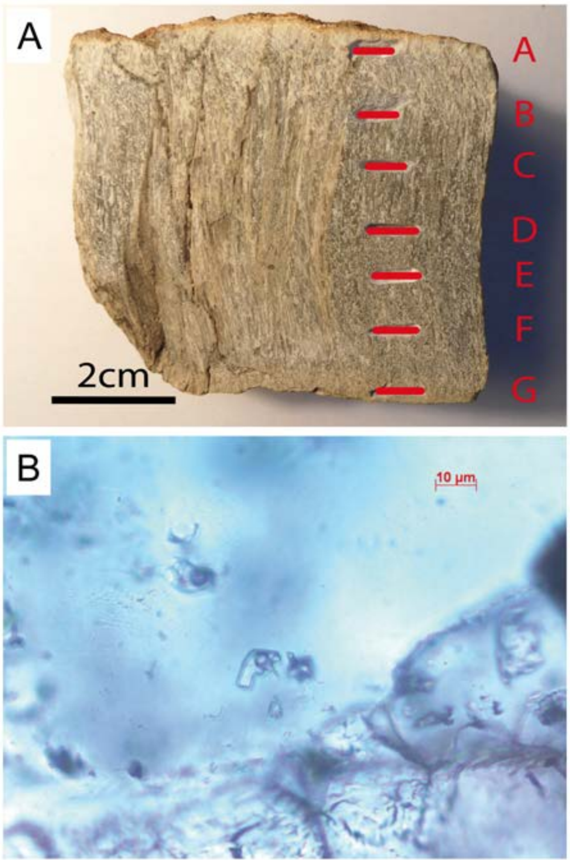

Figure 6. A. Sampling of 'beef' for isotope studies. Red lines indicate micro drillings. B. Photograph of a typical fluid inclusion in 'beef' from Lyme Regis (LR-12-02).

We analysed 'Beef' veins with an ESEM, at the Statoil Research Center, Trondheim Norway (Fig. 1 & Annexe 1). We worked directly on sawed faces of samples rather than on thin or thick sections to avoid contamination by substances used for the elaboration of sections. We also imaged some beef by cathodoluminescence, which allows distinguishing growth stages of calcite fibres.

For the fluid inclusions analyses, we performed uncovered thick sections (200-300 µm) of two 'beef' at the bottom and the top of the petroleum system (respectively Lyme Regis, sample LR-12-02, and Lulworth Cove, sample LUL-12-13, Table. 1) and one vertical vein (Stair Hole, sample STA-12-20, Table. 1). For 'beef', we orientated thick section parallel to the calcite fibres. During preparation of thick sections, we did not exceed the temperature of 60°C, so as not to damage the fluid inclusions within the calcite fibres.

Results and interpretation

Calcite fibres are the main component for 'beef' veins, but we identified some others (Fig. 1c & 1D & Annexe 1). Shales seem and pyrite grains are disseminated through spaces between calcite crystals. We also observed that a thin discontinuous layer of shales delimits 'cone-in-cone' structures, as Denaeyer (1943) has already described. Finally, 'beef' contains a lot of liquid or solid hydrocarbons (Fig. 1C & 1D & Annexe 1). These hydrocarbons are

				Veines					Encaissants					
				'Beef'			Veines sécantes		Shales				calcaire/dolomie	
		Echantillon		d1	$\delta^{18}O$	$\delta^{13}C$	$\delta^{18}O$	$\delta^{13}C$	d2	% $CaCO_3$	$\delta^{18}O$	$\delta^{13}C$	$\delta^{18}O$	$\delta^{13}C$
Swanage	C.B.M	SWA-12-24	A	0	24,2	1,8								
		-	B	0	24,6	1,3								
		SWA-12-26	A				22,6	1,8						
		-	B						1				26,8	0,8
Lulworth Cove	Purbeck beds	LUL-12-17							500				25,8	0,2
		LUL-12-18		0	26,2	0,9								
		LUL-12-19							700				25,8	0,2
		LUL-12-14	A	2	25,9	1,3								
		-	B	0	25,4	1,4								
		-	C	1,5	24,5	0,9								
		LUL-12-13	A	2,5	21,1	0,7								
		-	B	1,5	24,0	1,7								
		-	C	0,5	23,9	1,6								
		-	C	0,5	23,7	1,6								
		-	D	0,5	24,1	1,6								
		-	E	1,2	24,5	1,5								
		-	F	2,2	24,3	1,4								
		-	G	3,5	24,1	1,2								
		LUL-12-16	B	0			23,7	-5,4						
		-	A						0,5				23,8	-2,9
Stair Hole		STA-12-23	A	0,8	24,3	-2,7								
		-	B	0,7	24,3	-2,6								
		-	C	0,7	24,7	-0,6								
		STA-12-22	A	1,5	25,5	-0,7								
		-	B	0,8	24,8	-0,5								
		-	C	0,5	20,7	-1,4								
		STA-12-21	C						2				25,6	-1,9
		-	B						0				25,4	-2,0
		-	A	0			22,5	-4,2						
		STA-12-20	E	0,8			23,0	-7,8						
		-	D	0			23,1	-7,3						
		-	C	0,8			23,3	-7,4						
		-	B						0				25,4	-2,4
		-	A						2				26,1	-1,8
Kimmeridge bay	Kimmeridge clay	KIM-12-43							100	0,9	26,6	-0,9		
		KIM-12-42	B						0	5,3	28,0	-2,4		
		-	A	0	25,9	0,4								
		KIM-12-40	B						0	12	26,7	-0,4		
		-	A	0	25,7	0,0								
		KIM-12-39							100	10,1	26,7	-2,3		
		KIM-12-34	B	0			25,4	-3,9						
		-	A						2	1,8			29,3	6,3
Osmington mills	Oxford clay	OSM-12-56	B	0	29,1	-7,3								
		OSM-12-55	B	0	29,2	-11,0								
		-	A	0	28,2	-8,9								
		OSM-12-51							0	10,6	28,5	-2,0		
		OSM-12-52	A						0	54,9	26,7	-10,5		
		-	B	0,9	27,2	-14,2								
		-	C	0	27,1	-16,7								
		-	D	0,7	26,3	-12,9								
		OSM-12-53	A	1	28,1	-7,7								
		-	B	1,2	27,0	-17,0								
		OSM-12-54							100	0,2	22,1	-7,1		
Charmouth	Blue Lias	CHA-12-08	D						5	6,4	24,3	0,5		
		-	A	0	20,8	2,9								
		-	B	1	26,3	-0,4								
		-	C						0	4,5	24,9	-0,2		
		CHA-12-09		0	22,9	1,2								
Lyme Regis		LR-12-07	A	0	23,0	1,0								
		LR-12-06							300	10,2	25,5	-0,5		
		LR-12-03	A						0	12,8	24,9	-0,9		
		-	B	0,3	27,6	-0,3								
		-	C	0,3	26,7	-0,6								
		-	D						0	10,4	25,3	-0,3		
		LR-12-02	J	4,7	27,1	-0,4								
		-	F	4,1	22,4	1,6								
		-	E	4,1	22,2	0,8								
		-	D	3,7	23,3	1,1								
		-	I	4,7	26,0	0,0								
		-	C	4,4	22,0	2,3								
		-	B	3,8	20,7	2,6								
		-	A	3,1	20,4	2,1								
		-	G	2	22,2	-4,0								
		-	H	2,2	24,9	-3,3								
		LR-12-01	A	0	24,9	-16,3								

Table 1. Stable isotope compositions of veins ("beef" and vertical veins) and host rocks (shales and limestone; sample KIM 12-34 is a dolostone). "Dist" is the distance to the contact between vein and the host rock. "%CacO3" refers to the amount of calcite in shales.

either disseminated within spaces between fibres or into crystals as inclusions. All ‘beef’ in the sedimentary sequence has the same composition and contains hydrocarbons.

Fluid inclusions

In beef samples, fluid inclusions are aqueous. They are scarce and small (Fig. 6d). They do not occur all along the calcite fibres but rather in zones of clear white calcite. The results presented here are thus not representative of the entire fluid history associated with beef growth, but rather, they record instantaneous fluid composition at some time during beef formation.

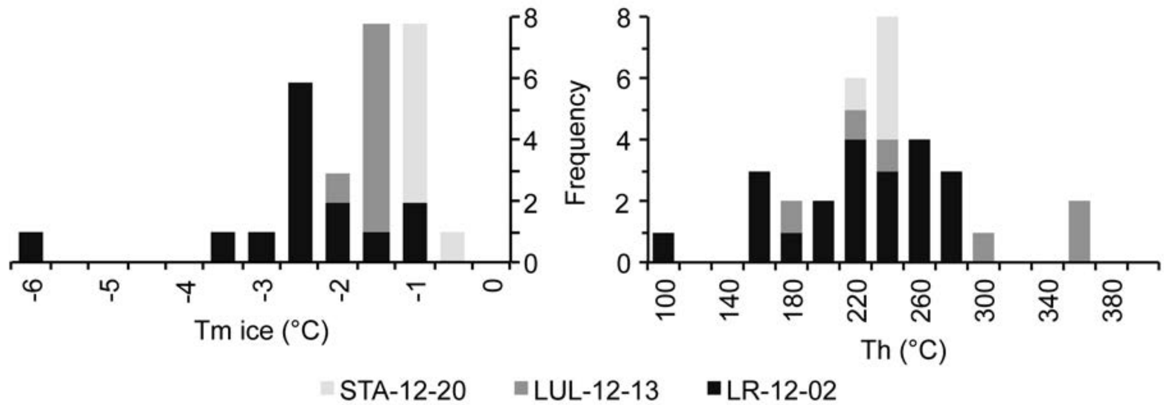

Figure 7. Graphs showing the results of microthermometric analyses on the fluid inclusions.

Aqueous inclusions in beef display a last ice melting temperature (*T*m ice) ranging from -1 to -5.6 °C (Table 2, Fig. 7), with a majority of data in the range -1/-3.5°C (the corresponding salinity being in the range 2/3.8 wt% eq. NaCl; Table TT). The Lulworth cove inclusions have Tm centered around -2°C, the Lyme Regis inclusions show a wide range of Tm between -6°C and -1°C, whereas STA samples show the lowest Tm near -1°C. Homogenization histograms are very broad for samples SR and LUL. Homogenization temperatures (*T*h) range from 104 to 380 °C. Th values recorded for STA sample are all located in the 220-240°C range. Broad Th histograms can be the results of several reasons: impact of sample preparation, stretching or leakage of inclusion induced during microthermometry measurements, or complex thermal history of the rock formation. In our case, sample preparation has been carefully made with heating not exceeding 60°C. However some decrepitated inclusions are observed, probably due to mechanical stress during sample preparation. Homogenization temperatures have been measured after congelation, a procedure which could have induced some “leakage/disturbance” of the inclusions. However, reproducibility of microthermometric measurements has been checked on several inclusions: reproducibility is rather good, in most cases less than a few degrees.

Sample		Th(°C)	Tm ice(°C)	Salinity (wt%)
LUL-12-13	range	192.0/379.2	-1.9/-1	2.0/3.8
-	mode	280.7	-2.3	2.0
-	n	6	8	5
LR-12-02	range	104.1/290.4	-5.6/-0.9	2:3.8
-	mode	339.9	-2.2	6
-	n	21	14	0.3/2.0
STA-12-20	range	237.8/247.5	-0.9/-0.5	1.2
-	mode	242.9	-0.6	1.2
-	n	5	7	4

Table 2. Microthermometric data for fluid inclusions in beef (samples LUL 12-13 and LR 12-02) and a secant vein (STA 12-20). Tm ice: melting temperature of ice; Th: homogenization temperature; n: number of measurements.

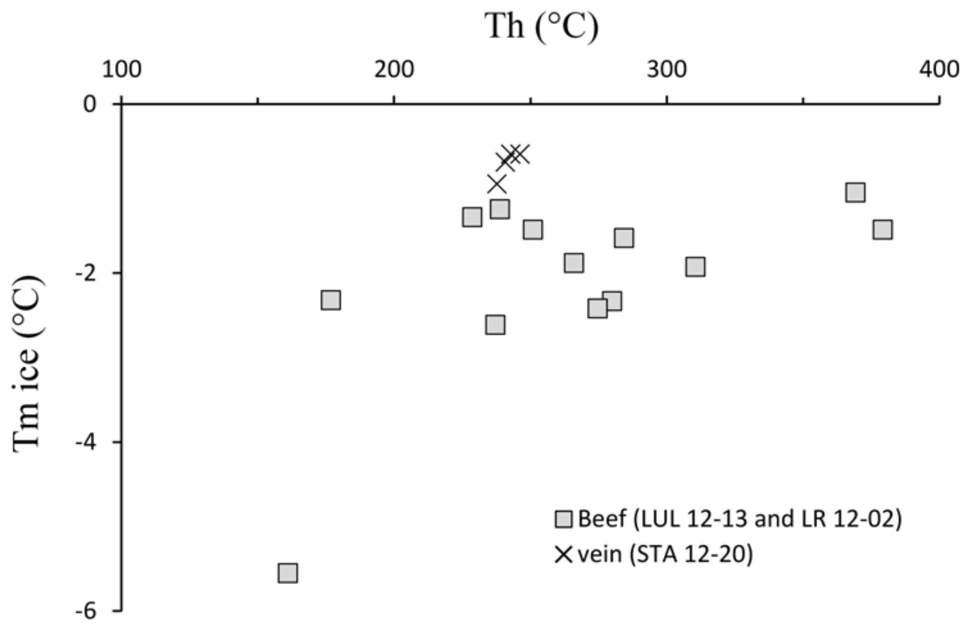

Figure 8. Melting temperature of ice (Tm ice) vs. homogenization temperature (Th) diagram applied to fluid inclusions studied in beef and secant veins.

No gases were identified by Raman spectroscopy analyses. These analyses were difficult to perform because of elevated fluorescence of fibrous calcite. As a consequence, we also had large uncertainties on the salinity estimates obtained during this methodology and thus present only salinity estimates obtained by microthermometry.

On the secant vein STA 12-20, the last ice melting temperature is slightly higher than in beef (*T*m ice in the range -0.5/0.9°C (Table 2, Fig. 7), corresponding salinity in the range 0.3/2.0 wt% eq. NaCl (Table 2)). Homogenization temperatures are centered on 240°C (Table 2, Fig. 7), a value comparable to the ones obtained on beef and thus also suspicious. All IF microthermometric are summarized in the Tm vs. Th diagramme (Fig. 8), where we can see the difference in Tm ice between beef and secant veins.

Stable isotopes

We presented the stable isotope compositions of beef, shales, vertical veins and limestones in table. 1 and in Fig. 9.

Beef display a very large range of both $\delta^{13}C$ values (between +3 and -17‰) and $\delta^{18}O$ values (between 20.5 and 29‰). The Osmington Mills group of beef is distinguishable fron the other sites by lower $\delta^{13}C$ values and somewhat higher $\delta^{18}O$ values. Considering the other sites, most of the beef data plots along a trend that extends the one defined by shales (increasing $\delta^{13}C$ values from -2 to 0.5‰ with decreasing $\delta^{18}O$ values from 28.5 to 24.5‰). The isotopic data obtained by Sælen et al. (2000) on oil shale close to the White Stone Band (close to Kimmeridge) compare well the data presented here. Two shales and five beef differ from the general trend by displaying negative $\delta^{13}C$ values. The most negative values (samples LR 12-01 and LR-12-02G and F; Table. 1) were sampled at the extreme base of a beef vein and thus correspond to the early stage of beef growth. This result is consistent with Marshall (1982) who also obtained very negative values ($\delta^{13}C$ down to -16.6‰) in comparable samples.

The two shales with negative values also have extreme carbonate contents. Sample OSM 12-52A has 55 wt% calcite and was collected in close contact with beef (itself displaying very negative $\delta^{13}C$ value near -14‰). It is likely that this shale sample was contaminated either mechanically during sample preparation or carbonated during beef development. On the other hand, sample OSM 12-54 ($\delta^{13}C$ = -7.1‰), which also has a low d18O value, compared to other shales ($\delta^{18}O$ = 22.1‰) has only 0.2 wt% calcite. With such a low carbonated content one cannot exclude that late carbonation associated with meteoric infiltration is the main process responsible for the specific isotopic values. These two samples can thus reasonably be excluded from further discussion, and to sum up beef and shales isotopic compositions, it comes that, excluding Osmington Mills which deserves a specific discussion, beef display a negative trend in the $\delta^{13}C$ – $\delta^{18}O$ space (Fig. 9) which extends to the left a comparable trend defined by the shales of the Wessex Basin.

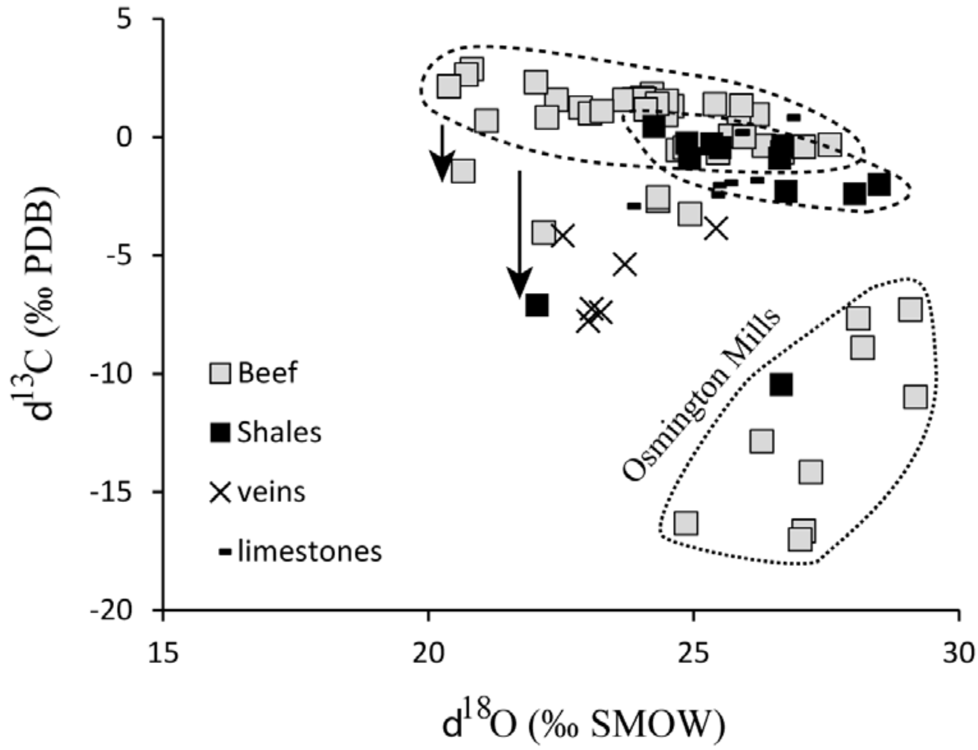

Figure 9. d13C vs d18O diagram showing the isotopic compositions of veins (beef and verticla veins) and host rocks (shales and limstones; sample KIM 12-34 not plotted). The arrows show the tendency of some rocks towards low d13C values at constant d18O value. See text for discussion.

Vertical veins show more homogeneous C and O isotopes composition than beef. Their $\delta^{18}O$ value is between 23 and 25‰ and compare well with the $\delta^{18}O$ mean value of beef (Fig. 9). On the other hand, vertical veins show more $\delta^{13}C$ negative values than the majority of beef, excluding again Osmington mills site.

Sedimentary limestones (plus one dolomite) have isotopic values comparable with shales, with however a notable positive correlation between $\delta^{18}O$ and $\delta^{13}C$ values. The dolomite sample from Kimmeridge Bay is distinguishable with a high $\delta^{18}O$ value (29.3‰) and a very positive $\delta^{13}C$ value (+6.3‰).

Discussion

Fluid regime in the Wessex basin

Beef forms during fluid overpressure in impermeable beds (Rodrigues et al. 2009; Zanella et al. 2011; Cobbold et al. 2013). In the Wessex Basin, our field observations confirm that beef are localized in marly shales. Also, the more carbonated the marly shale, the more abundant and wide are the beef. This observation was made at several stratigraphic layers. It seems then that if marly shales have a physical first-order control on beef formation, their carbonate content is a fundamental chemical factor for beef development and that the calcium necessary to feed the growing fibres come from the local host shale. Rodrigues (2008) provides some examples of carbonate depletion in host shales toward the contact with beef in the Neuquen Basin (Argentina). He interpreted this evolution as a calcium migration from the shale towards the vein. In the Wessex basin, we can then propose a physical-chemical mechanism of beef formation. Fluid overpressure induces vertical opening of horizontal hydraulic fractures. The transient pressure drop associated with fracturing led to precipitation of minute amounts of calcite, as calcite solubility decreases with decreasing pressure. The calcium necessary for calcite growth is first taken from the dissolved calcium in the fluid. At this time, the beef forming fluid is thus depleted in Ca whereas the fluid present in the porosity of the shale is in equilibrium with the local mineralogy. A chemical gradient of calcium activity in the fluid phase thus appears. Energetically, to erase such a gradient, it is more efficient to dissolved small grains, like the calcite ones present in the shale, than large ones, like the ones just appeared in the beef. It comes then that dissolution of calcite in the shale enriched the fluid phase, this calcium being used to feed the growing calcite fibres in the still opening veins.

Stable isotopes are consistent with this model. The large majority of beef define a trend that extends the trend defined by the marly shales of the Wessex Basin (the Osmington case and the low $\delta^{13}C$ beef being excluded). The isotope compositions of shales likely correspond to original marine values, only slightly altered during diagenetic recrystallization. Sælen et al. (2000) confirm this statement in their exhaustive geochemical study of the Whitby Mudstone Formation (Lower Jurassic) and Kimmeridge Clay Formation (Upper Jurassic). In our study, shales preserve C isotope signature close to typical marine ones ($\delta^{13}C$ around 0‰) and also compare rather well with the O isotope composition of limestones (Fig. 9). The only difference lies in the positive correlation exhibited by limestones whereas shales show a negative correlation. Actually, the negative correlation of limestones may be well due to diagenetic recrystallization and porosity infilling, as already documented in the Paris Basin (France) (e.g., Vincent et al., 2007; Brigaud et al., 2009) or on the East Midlands Shelf (Hendry, 2002). It is reasonable then to consider that the carbonate fraction of shales preserved their original marine pristine signature. In a fluid-rock interaction system, the fluid/rock ratio can vary between two extremes, zero (where rocks dominate over fluids and impose their isotopic signature) to infinity (where fluids buffer the infiltrated rock). In the first case, the fluid and the minerals precipitated from it, like the calcite fibres in beef, acquire the isotopic composition of the rock. They however get distinct composition because of isotopic equilibrium fractionation reasons and because of temperature dependency of this fractionation. If a set of rocks displays a variable isotopic composition, the minerals formed in veins also display a comparable variability, but possibibly displaced to distinct values. In the case of fluid-dominated system on the other hand, veins shall have rather constant isotopic compositions (the ones of the fluid taking into account fractionation) irrespective of any variation of isotopic compositions in the host rock. In figure. 8, the cloud of data depicted by beef mimics the one depicted by shales, a situation, which that corresponds to a rock, dominated fluid-rock system, where rocks impose their signature to the fluid, and to the fluid-related beef. In turns, this relationship shows that the fluids that induced fracturation by overpressure and beef formation likely derived from local rocks. At the scale of the Wessex Basin, we have no evidence of externally derived fluids, which would have generated the network of beef veins.

Fluid inclusion data showed that, in some instances (we have FI data for only two beef), the salinity of fluids was around 2 to 4 wt% eq. NaCl. For comparison, present-day seawater contains 3.5 wt% NaCl. The most straightforward observation of the salinity calculated for beef-related fluids is that they have a seawater-like salinity. Connate waters buried together with sediments are originally seawater, more or less modified by fluids liberated during diagenesis, for example during clay aggradation. The geological and isotopic characteristics of ‘beef’ depicted above allow us inferring that the beef-related fluids originated within the Wessex basin. Our fluid inclusion data on beef are thus consistent with this inference, as their salinity properties point to a seawater-derived fluid. The vertical veins collected at Stair Hole may well represent such a diagenetic fluid because their salinity (05/2 wt% eq. NaCl) is somewhat lower that the one of the beef-related fluid. Their stable isotopes signature is not straightforward to interpret, despite the rather homogeneity of isotopic compositions point to a fluid domintated fluid-rock interaction system. Indeed, we have some uncertainty with the homogenization temperature, which precludes a pertinent discussion using the mean $\delta^{18}O$ value. Also, the $\delta^{13}C$ value of the vertical veins are lower than the ones of beef, which shows that the fluid leading to vertical veins carried more organic carbon than the fluid leading to beef. Moreover, it is also possible that the vertical veins are genetically related to the Bray-Wight fault system that accommodated inversion in the Wessex Basin during Upper Cretaceous – Tertiary and that emerges a few tens of metres from the sampled outcrop.

The general model that beef-related fluids are originated form the Wessex Basin itself is not at variance with the study of Marshall (1982), who identified an evolution in the fluid composition during the growth of calcite fibres. In the early stages, Marshall (1982) identified a fluid with very low $\delta^{13}C$ values that shows that the C budget was buffered by organic matter-derived carbon (with a very low $\delta^{13}C$ signature). During fracture opening and along fibres of calcite, he then documented isotopic shifts, which he interpreted as the result of some lateral fluid flow. What we propose here is that such lateral flows must have originated from neighbouring rocks, within the basin, with the consequence for the carbon budget that the organic matter-derived carbon mixed with time (and incoming fluid) with marine water-derived carbon (with a $\delta^{13}C$ around 0‰).

The Osmington Mills case

In figure 9, beef from Osmington Mills is distinguishable from other beef by very negative $\delta^{13}C$ values and slightly higher $\delta^{18}O$ values. On a geological point of view, the Osmington Mills outcrop is indistinguishable from others sites where beefs have been observed. The isotopic specificity of Osmington is thus likely due to the particularities of the local fluid-rock system. Actually, we have only one valid isotopic measurement for the host rocks, as two shales exhibit either anomalously high or low carbonate content (see above). This normal shale (with a carbonate content of 10.6 wt.% calcite) has a $\delta^{18}O$ value 28.5‰, which is actually the highest value measured for a shale in this study; this property is likely due to specific sedimentary conditions at the time of deposition of the shale (see discussion in Sælen et al., 2000). It could be then that the oxygen composition of the Osmington beef was buffered by the local rocks, as in the general case discussed above. For the carbon, the large variation of $\delta^{13}C$ values (more than 10‰) implies two sources of carbon, an organic matter-derived carbon and a seawater-derived one. The measured value ($\delta^{13}C$ between -7 and -17‰)

let us infer that the organic matter contribution is more important here than in other sites in the Wessex Basin. The reason for that is not straightforward, and specific new studies should be engaged to specify this point, notably by reinforcing the stable isotope data set on shales and by measuring the carbon budget in the host shales (Total Organic Carbon vs. Inorganic Carbon).

Conclusions

(1) In the Wessex Basin, calcite ‘beef’ is widespread within shales and mudstones of the Mesozoic strata. Shales and mudstones encouraged the formation of bedding-parallel veins (‘beef’).

(2) The composition of ‘beef’ is globaly homogeneous. It is composed by calcite fibres with pyrite grains and shales between fibres. Liquid or solid hydrocarbons are present between fibres as well as in inclusion into crytals of calcite. This observation demonstrates that during ‘beef’ veins crystallization liquid hydrocarbons were present.

(3) The formation of ‘beef’ is synchronous to the migration of hydrocarbons in the basin. This is why ‘beef’ contains such hydrocarbons. We have so to envisaged the synchronous migration of two fluid phases: acqueous phase and hydrocarbons.

(4) The geometry of ‘beef’ is undeformed in areas where the deformation is gentle, but highly deformed near major tectonic accidents. Indeed, ‘beef’ of the area of Lulworth Cove are folded and faulted, suggesting a development during the compressional deformation and so the Upper Cretaceous-Tertiary inversion of the Wessex Basin.

(5) The isotopes revealed that the fluid responsable of the ‘beef’ crystallization has a rock signature. The origin of calcium for ‘beef’ veins is the marine marly shales of the Wessex Basin. The emplacements of ‘beef’ veins are so controled by the calcitic disponibility and the nature of the host rocks.

(6) The salinity calculated for beef-related fluids is around 2 to 4 wt% eq. NaCl. This value is consistent with isotopes analyses and argues the marine oringin of the fluid.

(7) From observations and analyses we infer a general model of formation for the ‘beef’ veins of the Wessex Basin. During the maturation organic matter, chemical compaction leads to fluid overpressure and then to hydraulic fracturing. The migration of two fluid phases (acqueous and liquid hydrocarbons) was synchronous to the inversion of the basin

during the Late Cretaceous-Teriary. The migration was in particular facilitating by the presence of discontinuité as the Wight-Bray Fault System. Indeed, ‘beef’ veins (bedding-partallel hydraulic fractures) at Lulworth Cove area have strong structural arguments to infer that ‘beef’ is synchronous to the contraction of the basin.

From the study of the Wessex Basin and with the other study on the Neuquén Basin, we believe that the generation of ‘beef’ is a strong marker for fluid overpressure development and hydrocarbon generation. We infer that ‘beef’ constitute a powerfull geological object for the study and the understanding of a petroleum system.

Appendix

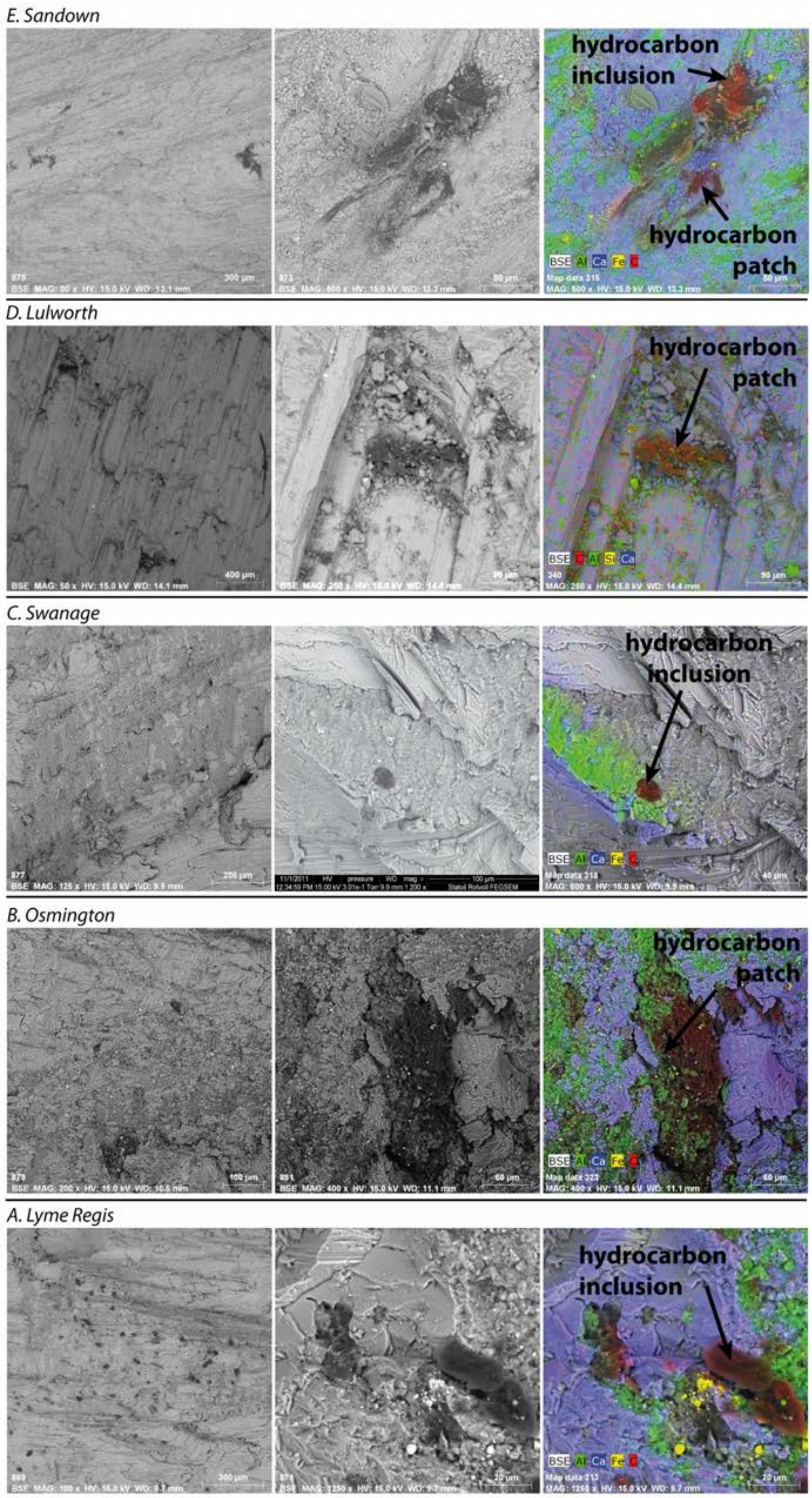

Appendix 1. ESEM analyses on 'beef' samples of the Wessex Basin for each locality identified. Images are composite BSE and X-ray images, showing the typical composition of 'beef' for the Wessex Basin. Intensities of colours reveal concentrations of elements (red = carbon; green = aluminium; yellow = sulfur and blue = calcium).

References

Andrews, W.R. 1881. Note on the Purbeck Beds at Teffont. *Quarterly Journal of the Geological Society, London*, 37, 251-253.

Andrews, W.R. & Jukes-Brown, A.J. 1894. The Purbeck Beds of the Vale of Wardour. *Quarterly Journal of the Geological Society, London*, 50, 44-71.

Bons, P.D. & Jessell, M.W.1997. Experimental simulation of the formation of fibrous veins by localised dissolution-precipitation creep. *Mineralogical Magazine*, 61, 53-63.

Bray, R.J., Duddy, I.R. & Green, P.F. 1998. Multiple heating episodes in the Wessex Basin: implications for geological evolution and hydrocarbon generation. *Geological Society, London, Special Publications*, 133, 199-213.

Brigaud, B., Durlet, C., Deconinck, JF., Vincent, B., Thierry, J. & Trouiller A. 2009. The origin and timing of multiphase cementation in carbonates: Impact of regional scale geodynamic events on the Middle Jurassic Limestones diagenesis (Paris Basin, France). *Sedimentary Geology*, 222, 161–180

Buchanan, J.G. 1998. The exploration history and controls on hydrocarbon prospectivity in the Wessex basins, southern England, UK. *Geological Society, London, Special Publications*, 133, 19-37.

Buckland, W. & De la Beche, H.T. 1835. On the Geology of the Neighbourhood of Weymouth and the Adjacent Parts of the Coast of Dorset. *Transactions of the Geological Society, London*, s2-4, 1-46.

Chadwick, R.A., Kenoulty, N. & Whittaker, A. 1983. Crustal structure beneath southern England from deep seismic reflection profiles. Journal of the Geological Society, London, 140, 893-912.

Cobbold, P.R., Rodrigues, N., 2007. Seepage forces, important factors in the formation of horizontal hydraulic fractures and bedding-parallel fibrous veins (‘beef’ and ‘cone-in-cone’). Geofluids 7, 313-332.

Cobbold, P.R., Zanella, A., Rodrigues, N., Løseth, H. 2013. Bedding-parallel fibrous veins (beef and cone-in-cone): worldwide occurrence and possible significance in terms of fluid overpressure, hydrocarbon generation and mineralization. Marine and Petroleum Geology 43, 1-20, doi: 10.1016/j.marpetgeo.2013.01.010.

Cosgrove, J.W., 1995. The expression of hydraulic fracturing in rocks and sediments. In: Ameen, M.S. (Ed.), Fractography: Fracture Tomography as a Tool in Fracture Mechanics and Stress Analysis. Geological Society, London, Special Publications, 92, 187-196.

Cosgrove, J.W., 2001. Hydraulic fracturing during the formation and deformation of a basin: a factor in the dewatering of low-permeability sediments. American Association of Petroleum Geologists Bulletin 85, 737-748.

Denaeyer, M.-E., 1943. Les cone-in-cone de la France métropolitaine et d’outre--mer. Bulletin de la Société française de Minéralogie 66 (1-6), 173-221.

Dobes, P., Suchy, V., Stejskal, M., 1999. Diagenetic fluid circulation through fractures: a case study from the Barrandian Basin (Lower Paleozoic), Czech Republic. Geolines (Praha) 8, 18.

Durney, D.W., Ramsay, J.G., 1973. Incremental strains measured by syntectonic crystal growths. In: De Jong, K.A., Scholten, R. (Eds.), Gravity and Tectonics. Wiley, New York, pp. 67-96.

Ebukanson, E.J. & Kinghorn, R.R.F. 1985. Kerogen Facies in the Major Mudrock Formations of Southern England and the Implication on the Depositional Environments of their Precursors. Journal of the Petroleum Geology, 8, 435-462.

Ebukanson, E.J. & Kinghorn, R.R.F. 1986. Maturity of organic matter in Jurassic of Southern England and its relation to the burial history of the sediments. Journal of the Petroleum Geology 9, 259-280.

Gallois, R.W. 2001. The lithostratigraphy of the Mercia Mudstone Group (Mid to Late Triassic) of the south Devon coast. Geoscience in south-west England, Proceedings of the Ussher Society 10, 195-204.

Glennie, K.W. & Underhill, J.R. 1998. Origin, development and evolution of structural styles. In: Glennie, K.W. (ed.) Petroleum Geology of the North Sea. Blackwell Scientific Publications, Oxford.

Gratier, J.-P., Frery, E., Deschamps, P., Røyne, A., Renard, F., Dysthe, D., Ellouz-Zimmerman, N., Hamelin, B., 2012. How travertine veins grow from top to bottom and lift the rocks above them: the effect of crystallization force. Geology, http://dx.doi.org/10.1130/G33286.1 (published online).

Gustavson, T.C., Hovorka, S.D., Dutton, A.R., 1994. Origin of satin spar veins in evaporite basins. Journal of Sedimentary Research A64, 88-94.

Hawkes, P. W., Fraser, A. J., & Einchcomb, C. C. G. 1998. The tectono-stratigraphic development and exploration history of the Weald and Wessex basins, Southern England, UK. Geological Society, London, Special Publications, 133(1), 39-65.

Hendry, J., 2002. Geochemical trends and palaeohydrological significance of shallow burial calcite and ankerite cements in Middle Jurassic strata on the East Midlands Shelf (onshore UK). Sedimentary Geology 151, 149–176.

Judd, J.W., 1871. On the Punfield Formation. Quarterly Journal of the Geological Society, London 27, 207-227.

Keulen, N. T., den Brok, S.W.J., Spiers, C.J., 2001. Force of crystallisation of gypsum during hydration of synthetic anhydrite rock. 13th DRT conference, Deformation Mechanisms, Rheology, and Tectonics, Noordwijkerhout, The Netherlands.

Lang, W.D., 1914. The geology of the Charmouth Cliffs, Beach and Foreshore. Proceedings of the Geological Association 25, 293e360.

Lang, W.D., Spath, L.F., Richardson, W.A., 1923. Shales-With-‘Beef’, a sequence in the Lower Lias of the Dorset Coast. Quarterly Journal of the Geological Society, London 79, 47-99.

Lash, G.G., Engelder, T., 2005. An analysis of horizontal microcracking during catagenesis: example from the Catskill delta complex. American Association of Petroleum Geologists Bulletin 89, 1433-1449.

Lees, G.M. & Cox, P.T. 1937. The geological basis of the present search for oil in Great Britain by the D'Arcy Exploration Compagny. Limited, Quarternary Journal of The Geological Society, London, XCIII, 156-194.

Marshall, J.D., 1982. Isotopic composition of displacive fibrous calcite veins; reversals in pore-water composition trends during burial diagenesis. Journal of Sedimentary Petrology 52, 615-630.

Means, W.D., Li, T., 2001. A laboratory simulation of fibrous veins: some first observations. Journal of Structural Geology 23, 857-863.

Morgans-Bell, H.S., Coe, A.L., Hesselbo, S.P., Jenkyns, H.C., Weedon, G.P., Marshall, J.E.A., Tyson, R.V. & Williams, C.J. 2001. Integrated stratigraphy of the Kimmeridge Clay Formation (Upper Jurassic) based on exposures and boreholes in south Dorset, U.K. Geological Magazine 138, 511-539.

Parnell, J., Honghan, C., Middleton, D., Haggan, T., Carey, P., 2000. Significance of fibrous mineral veins in hydrocarbon migration: fluid inclusion studies. Journal of Geochemical Exploration 69-70, 623-627.

Ramsay, J.G., 1980. The crack-seal mechanism of rock deformation. Nature 284, 135e139.

Reid, C., 1903. The geology of the country around Salisbury (Explanation of Sheet 298). Memoirs of the Geological Survey, England and Wales, 298, 1-77.

Rodrigues, N. 2008. Fracturation hydraulique et forces de courant : Modélisation analogique et données de terrain. Mémoire de doctorat, Université de Rennes 1, 164 pp.

Rodrigues, N., Cobbold, P.R., Løseth, H., Ruffet, G., 2009. Widespread bedding-parallel veins of fibrous calcite ('beef') in a mature source rock (Vaca Muerta Fm, Neuquén Basin, Argentina): evidence for overpressure and horizontal compression. Journal of the Geological Society, London, 166, 695-709, http:// dx.doi.org/10.1144/0016-76492008-111.

Sælen, G., Tyson, R.V., Telnæs, N., Talbot M.R., 2000. Contrasting watermass conditions during deposition of the Whitby Mudstone (Lower Jurassic) and Kimmeridge Clay (Upper Jurassic) formations, UK. Palaeogeography, Palaeoclimatology, Palaeoecology 163, 163–196

Shearman, D.J., Mossop, G., Dunsmore, H., Martin, M., 1972. Origin of gypsum veins by hydraulic fracture. Institute of Mining and Metallurgy, Transactions B181, 149-155.

Sorby, H.C. 1860. On the origin of "cone-in-cone". British Association for the Advancement of Science, Report of the 29th Meeting, 1859, Transactions of Sections, Geology, p. 124.

Stoneley, R. 1982. The structural development of the Wessex Basin. Journal of the Geological Society, London, 139, 543-554.

Stoneley, R., 1983. Fibrous calcite veins, overpressures, and primary oil migration. American Association of Petroleum Geologists Bulletin 67, 1427-1428.

Swarbrick, R.E., Osborne, M.J., Yardley, G.S., 2002. Comparison of overpressure magnitude resulting from the main generating mechanisms. In: Huffman, A.R., Bowers, G.L. (Eds.), Pressure Regimes in Sedimentary Basins and Their Prediction. American Association of Petroleum Geologists Memoir 76, 1-12.

Taber, S., 1918. The origin of veinlets in the Silurian and Devonian strata of New York. Journal of Geology 26, 56-63.

Underhill, J.R. & Paterson, S. 1998. Genesis of tectonic inversion structures: seismic evidence for the development of key structures along the Purbeck-Isle of Wight Disturbance. Journal of the Geological Society, London, 155 (6), 975-992.

Underhill, J. R. & Stoneley, R. 1998. Introduction to the development, evolution and petroleum geology of the Wessex Basin. *Geological Society, London, Special Publications*, *133*(1), 1-18.

Vincent, B., Emmanuel, L., Houel, P., Loreau, JP., 2007. Geodynamic control on carbonate diagenesis: Petrographic and isotopic investigation of the Upper Jurassic formations of the Paris Basin (France). Sedimentary Geology 197, 267–289

Webster, T., 1826. Observations on the Purbeck and Portland Beds. In: Transactions of the Geological Society, London, s2-2, 37-44.

West, I.M. 2013. Geology of the Wessex Coast of Southern England – the World Heritage Jurassic Coast – and More. Internet page: http://www.southampton.ac.uk/~imw/index.htm

Zanella, A., Cobbold, P.R., 2011. Influence of Fluid Overpressure, Maturation of Organic Matter, and Tectonic Context during the Development of ‘beef ’: Physical Modelling and Comparison With the Wessex Basin, SW England, vol. 13. EGU General Assembly, Vienna, Austria. Geophysical Research Abstracts.

Zanella, A., Cobbold, P.R., 2012. ‘Beef’: Evidence for Fluid Overpressure and Hydraulic Fracturing in Source Rocks During Hydrocarbon Generation and Tectonic Events: Field Studies and Physical Modelling. Geofluids VII International Conference, Rueil-Malmaison, May 2012.

Chapitre 3

Etude du bassin de Neuquén, Argentine

3.1 Introduction

Dans le précédent chapitre nous avons montré la synchronicité entre la génération des hydrocarbures, le développement de surpression de fluides et la génération de fractures hydrauliques parallèles à la stratification des roches matérialisées par le beef. Pour ce chapitre, nous allons développer l'étude du bassin de Neuquén en Argentine, et plus particulièrement la partie nord du bassin où les évidences de surpression de fluides sont nombreuses.

Le bassin sédimentaire de Neuquén est de plus en plus convoité par les sociétés pétrolières. En effet, ce bassin est le centre d'un système pétrolier relativement important. La nouvelle cible à laquelle les pétroliers s'intéressent est le potentiel non-conventionel du bassin, et particulièrement les huiles et gaz de schistes situés au sein même de sa principale roche mère, la Formation Vaca Muerta. De ce fait, les études sur ce bassin se sont largement multipliées. Cependant, dans la partie nord du bassin les études ne sont pas aussi nombreuses que dans les autres parties. Une des raisons est que cette zone est très affectée par la tectonique andine et que sa position au cœur de la ceinture de chevauchements diminue les chances de trouver un gisement non-conventionel très important. Néanmoins, cette zone montre des évidences de surpressions, matérialisées notamment par la présence de veines d'hydrocarbures solides (bitume) et de beef. Cette zone fut un lieu d'exploitation relativement intense de bitume dans de nombreuses mines découvertes et exploitées entre la fin du 19ème et la première moitié du 20ème siècle. Une des particularités du nord du bassin de Neuquén est l'intense volcanisme Tertiare et Quaternaire. Le fait que la majeure partie des évidences de surpression de fluides soit aux alentours de ce phénomène nous a alors fortement intéressé. Ce constat a déjà été réalisé par plusieurs auteurs qui se sont ainsi intérogés sur cette particularité, mais sans jamais démontrer de relations entre les différents objets géologiques (Meyerhoff 1948 ; Borrello 1956). Un peu plus au sud de la région de Malargűe, Rodrigues et al. (2009) et Cobbold et al. (2011) ont également souligné ce fait, respectivement pour la région de Loncoché et la région du Tromen.

3.2 Article#3: Geological evidence for fluid overpressure and hydraulic fracturing during maturation and migration of hydrocarbons in the northern Neuquén Basin, Mendoza Province, Argentina

L'étude du bassin de Neuquén en Argentine est rédigée sous forme d'un article scientifique. Ce dernier est soumis dans la revue *AAPG Bulletin*.

3.2.1 Résumé de l'article

Dans le nord du bassin de Neuquén de l'Argentine (en particulier dans la province de Mendoza), il existe une évidence en faveur de paléo-surpression de fluide. Cette dernière prend la forme de veines de bitume et de veines de calcite fibreuse parallèles à la stratification de ("beef"). Ces veines sont très répandues dans la chaîne d'avant pays de la zone malargue, où l'exploitation minière de bitume a été active pendant plus d'un siècle. Afin de recueillir des informations sur le développement de surpression de fluide dans cette partie du bassin du Neuquén, nous avons visité et étudié plusieurs anciennes mines dans la région de Malargűe. À cet endroit, les veines de bitume ont intrudé principalement les roches du Jurassique supérieur au Crétacé inférieur du Mendoza Group, mais aussi celles du Neuquén Group d'âge Crétacé supérieur. Les veines ont la forme de sills, parallèles à la stratification, ou de dykes et sont particulièrement épaisses dans les anticlinaux, formant des saddle-reefs à plusieurs endroits. Les 'beef' sont également nombreux dans la région Malargűe. Ils contiennent du bitume et par conséquent semblent avoir été formé en même temps que les veines de bitume. Près de nombreux affleurements de bitume et de 'beef', nous avons trouvé des corps intrusifs volcaniques. Les meilleurs exemples sont présents dans le synclinal de La Valenciana. D 'après les datations 39Ar - 40Ar, ces corps intrusifs sont principalement d'âge Miocène moyen. Plus généralement, le volcanisme, la déformation et la maturation des roches mères semblent avoir atteint leur paroxisme au Miocène, lorsque le slab de la plaque Pacifique, en subduction, est devenu relativement plat.

3.2.2 Article#3

Geological evidence for fluid overpressure and hydraulic fracturing during maturation and migration of hydrocarbons in the northern Neuquén Basin, Mendoza Province, Argentina

Alain Zanella[a]*, Peter R. Cobbold[a], Gilles Ruffet[a] and Hector Leanza[b]

[a] Geosciences (UMR-6118), CNRS and Université de Rennes 1, 35042 Rennes, France
[b] CONICET, Buenos-Aires, Argentina
*Corresponding author, e-mail: alain.zanella@univ-rennes1.fr

Abstract

In the northern Neuquén Basin of Argentina (especially in Mendoza Province), there is strong geological evidence for fluid overpressure in the past. The evidence takes the form of bitumen veins and bedding-parallel veins of fibrous calcite (‘beef’). Such veins are widespread in the fold-and-thrust belt of the Malargűe area, where bitumen mining has been active for a century or so. So as to collect information on the development of fluid overpressure in this part of the Neuquén Basin, we visited and studied several old mines in the Malargűe area. Here the bitumen veins have intruded mainly the Late Jurassic to Early Cretaceous Mendoza Group, but also the Late Cretaceous Neuquén Group. The veins have the forms of bedding-parallel sills or dikes and they are especially thick within anticlines, forming saddle-reefs in several places. Beef veins are also numerous in the Malargűe area. They contain bitumen and therefore seem to have formed at the same time as the bitumen veins. Near many outcrops of bitumen and beef, we have found fine-grained volcanic intrusive bodies. The best examples are from the La Valenciana syncline. According to ^{39}Ar-^{40}Ar dating, these bodies are mainly of Mid-Miocene age. More generally, volcanism, deformation and maturation of source rocks seems to have reached a climax in Miocene times, when the subducting Pacific slab became relatively flat.

Keywords: Neuquén Basin, Mendoza Province, ‘beef’, bitumen veins, hydrocarbon migration, fluid overpressure

Introduction

'Beef' (bedding-parallel veins of fibrous calcite) and solid bitumen veins seem to be common in sedimentary basins worldwide. According to the recent review by Cobbold et al. (2013) 'beef' or 'cone-in-cone' are common, especially within shale and/or mudstone in sedimentary basins that have generated petroleum. Asphalts and bituminous substances have been known for a long time, long before 'beef' or the onset of hydrocarbon production. Abraham (1960) compiled an inventory, showing that solid bitumen veins occur in some well-known sedimentary basins, for example in Utah and Oklahoma (United States), in the State of Vera Cruz (Mexico), or in the Province of Pinar del Rio (Cuba) for North America; in the Tolima Department (Colombia), in the Province of Canta and Yauli (Peru), or in Neuquén and Mendoza provinces (Argentina), for Central and South America; and in the Province of Hanover (Germany), or the Ural Mountains (Russia), for Europe and Asia. Nevertheless, the Neuquén Basin, Western Argentina, may contain the most widespread bitumen veins in the world (Parnell & Carey 1995), as well as being known for its high potential in oil and gas. Veins of solid bitumen (often named 'asphaltite' or less often 'neuquenite' or 'rafaelite') and of 'beef' crop out, together with source rocks for petroleum, especially in the central and northern part of the basin. There the bitumen veins have been subject to intense mining for fuel, especially during World War II. Hence the veins and mines figure in a book by Borrello (1956), as well as in many reports by the government agency, Yacimientos Carboníferos Fiscales (YCF). Today these reports are not readily available, but with help from the Geological Survey of Argentina (SEGEMAR), we managed to access some of them. According to all this information, bitumen veins are numerous in three main areas, (1) Auca Mahuida, (2) Chos Malal or Pum Mahuida and (3) the Malargüe area (Meyerhoff, 1948). These three areas are also regions where magmatic rocks are common. Indeed, several authors in the past suggested relationships between magmatic activity and the development of bitumen veins (Groeber 1923, Rassmuss 1923; Fester and Cruellas 1941, Piscione 1947, Meyerhoff 1948; Borrello 1956). In the Chos Malal area, Cobbold et al. (2011) demonstrated such relationships, by showing that vertical veins of bitumen form a radial pattern around Tromen volcano, which is of Plio-Pleistocene age, conical in shape and 4114 m high.

In the Malargűe area, there is no such obvious topographic feature as Tromen volcano, but the area does contain a large amount of volcanic and magmatic rocks, mostly of Neogene or Quaternary ages (Fig. 1). Furthermore, bitumen mines are numerous and some of them are

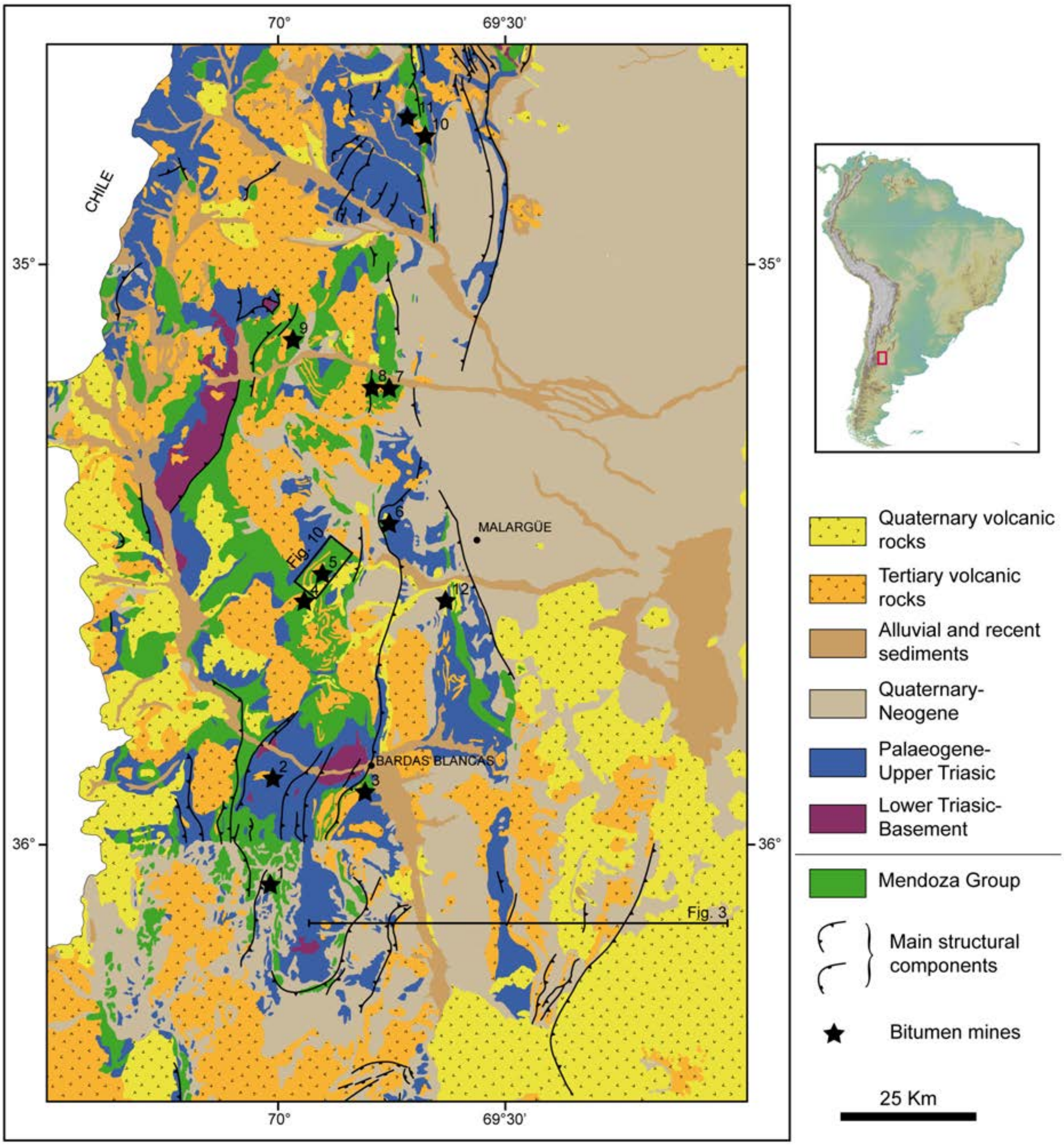

Figure 1. Geological map of the northern Neuquén Basin, Mendoza Province. Data are from the following geological maps: Volcan Maipo, Malargűe and Barrancas (SEGEMAR). Stars refer to bitumen mines visited in this study (1 = Mercedes; 2 = Minacar; 3 = Aida; 4 = La Malarguiña; 5 = La Valenciana; 6 = El Toki; 7 = Mallin Largos; 8 = Los Castaños; 9 = Santa Rosa; 10 = General Mitré; 11 = Eloise; 12 = Loncoché). The Mendoza Group (Early Cretaceous) includes source rock of the Vaca Muerta Fm.

exceptionally large. Some authors have suggested that maturation and migration of petroleum in the northern Neuquén Basin could be, at least in part, due to volcanic or magmatic activity (Rodriguez et al., 2007, 2009; Witte et al. 2012). Nevertheless, there are still many questions about such a possible correlation. As a result, we decided to revisit the bitumen mines of the Malargűe area, as well as others in Mendoza province. We worked at two different scales, first by comparing as many mines as possible in the region, then by studying in detail La Valenciana Mine, which for many years was the most productive, in the area to the West of Malargűe city. As part of this work, we have used the ^{39}Ar-^{40}Ar method, to date magmatic rocks near the main bitumen occurrences.

Geological setting

The Neuquén Basin lies mainly on the eastern side of the Andes (Fig. 1). The complex history of the basin began by the development of a series of Permo-Triassic grabens during a phase of continental extension, when the Choiyoi Group accumulated (Vergani et al. 1995), (Fig. 2). Then, during the Jurassic and Early Cretaceous, the basin was subject to thermal subsidence and a eustatic rise in sea level, so that marine transgressions from the Pacific Ocean led to deposition of a thick stratigraphic sequence (some 5000 m), from the Remoredo Fm to the top of the Mendoza Group (Vergani et al. 1995; Franzese and Spalletti 2001; Franzese et al. 2003). In the Late Cretaceous a change in tectonic setting led to inversion of the basin and formation of a fold-and-thrust belt in the foothills of the Andes (Cobbold and Rossello 2003), (Fig. 1). At the same time, uplift and erosion provided clastic material for deposition of the Neuquén Group, further eastward (Fig. 2). The last marine deposits in the area (the Malargűe Fm of Maastrichtian to Palaeogene age) were due to transgression from the Atlantic Ocean (Legarreta and Gulisano 1989), (Fig. 2). Sedimentation then continued under continental conditions, producing synorogenic Tertiary strata (Fig. 2). In the foothills of Mendoza Province and the northernmost Neuquén Province, volcanic rocks of Tertiary or Quaternary ages are also widespread (Fig. 1). The most common ages are Miocene and their geochemical characteristics led Kay et al. (2006) to suggest that they formed during a period, when the subducting Pacific plate was flatter than normal.

In the northern part of the Neuquén Basin, the petroleum system is simpler than it is in the central or southern parts. In Mendoza Province, there is only one potential source rock (the Vaca Muerta Fm), which consists of deep-marine organic-rich black shales (Fig.2). This formation is also the main source rock of the entire Neuquén Basin (Urien and Zambrano 1994; Villar et al. 2006). In Mendoza Province, the kerogen of the Vaca Muerta Fm is intermediate between Types II and III (Parnell and Carey 1995). The TOC values are very variable for the source rock in this area, from 7.57 % (area of Los Castaños) to 14.20 % (area of La Valenciana). Contrary to the central part of the basin, Tmax values indicate that, in the Mendoza Province, the Vaca Muerta Fm has not surpassed the oil window (Parnell and Carey 1995).

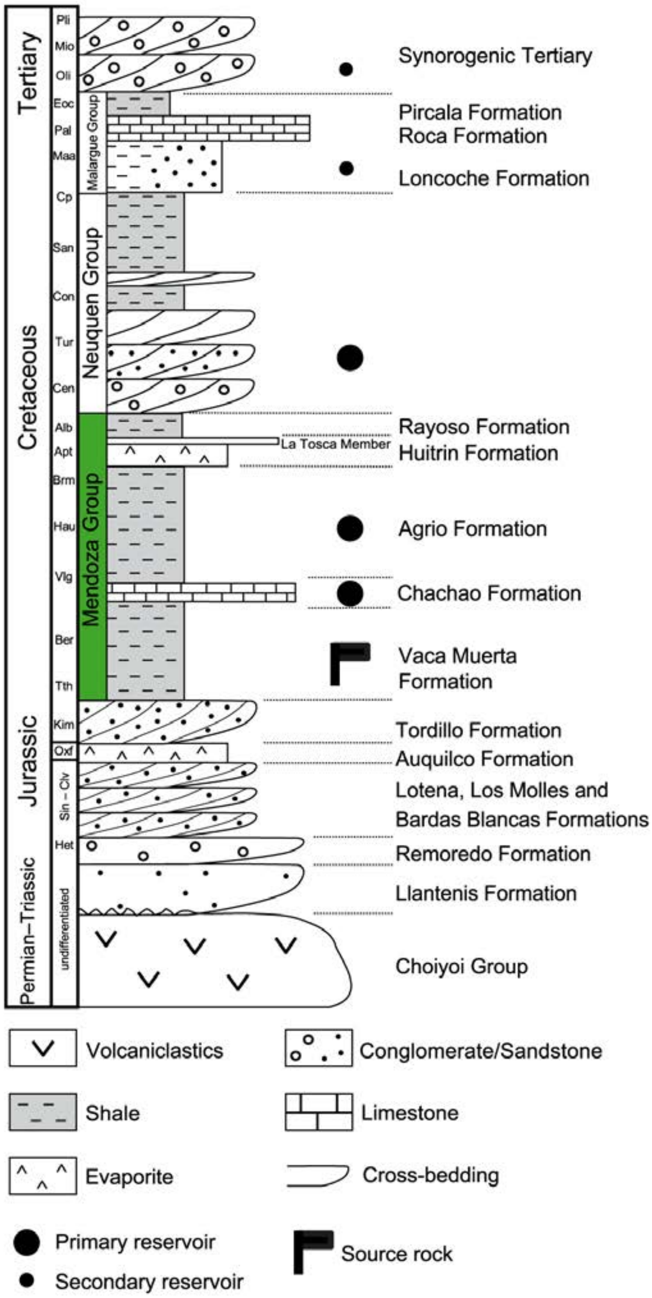

Figure 2. Generalized stratigraphic column of the northern Neuquén Basin (modified, after Witte et al. 2012). Pli = Pliocene; Mio = Miocene; Oli = Oligocene; Eoc = Eocene; Pal = Palaeogene; Maa = Maastrichtian; Cp = Campanian; San = Santonian; Con = Coniacian; Tur = Turonian; Cen = Cenomanian; Alb = Albian; Apt = Aptian; Brm = Barremian; Hau = Hauterivian; Vlg = Valanginian; Ber = Berriasian; Tith = Tithonian; Kim = Kimmeridgian; Oxf = Oxfordian; Sin-Clv = Sinemurian to Callovian; Het = Hettangian.

In the Malargűe area, the foothills of Andes have the typical structure of a foreland basin, where a series of fore-thrusts and back-thrusts affect the whole sedimentary sequence (Fig. 3). Pre-existing extensional basins (grabens and half-grabens) have been inverted, so that the Vaca Muerta source rock now crops out in the cores of anticlines (Fig. 3). According to recent work, the Malargűe fold and thrust belt formed between 15 Ma and 1 Ma and appears to have migrated progressively southward into the basin (Koslowski et al. 1993; Silvestro and Kraemer 2005; Giambiagi et al. 2008; Giambiagi et al. 2009).

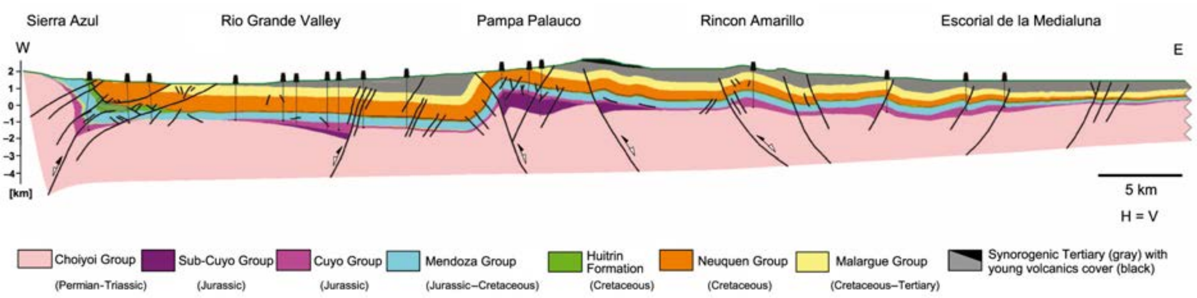

Figure 3. Regional E-W section of the southern Malargűe fold and thrust belt (modified, after Witte et al. 2012). For location, see Figure 1.

Geological evidence for fluid overpressure, while the petroleum system was active, is widespread in the Neuquén Basin. Rodrigues et al. (2009) have already shown the importance of fluid overpressures within the Vaca Muerta source rock, but essentially in the Mulichinco area, further to the south in Neuquén Province. They concluded that maturation and generation of hydrocarbons led to fluid overpressures. They evoked chemical compaction, during transformation of solid kerogen to oil or gas, as a possible mechanism for the development of fluid overpressure. Indeed, solid hydrocarbon veins and palaeo-hydraulic fractures are widespread, in particular within or near the Vaca Muerta source rock (Borrello 1956; Parnell and Carey 1995), (Fig. 1). Examples are bedding-parallel veins of fibrous calcite, or 'beef' (Buckland and De la Beche 1835, Stoneley 1983; Cobbold et al., 2013). These fractures and the emplacement of bitumen veins, parallel to the bedding, suggest that high fluid pressure initiated and then opened the fractures, which then filled with calcite and/or bitumen. For both kinds of veins, Parnell and Carey (1995) estimated the timing of formation to be Eocene-Oligocene.

In the Malargűe area, the foothills of Andes have the typical structure of a foreland basin, where a series of fore-thrusts and back-thrusts affect the whole sedimentary sequence (Fig. 3). Pre-existing extensional basins (grabens and half-grabens) have been inverted, so

that the Vaca Muerta source rock now crops out in the cores of anticlines (Fig. 3). According to recent work, the Malargűe fold and thrust belt formed between 15 Ma and 1 Ma and appears to have migrated progressively southward into the basin (Koslowski et al. 1993; Silvestro and Kraemer 2005; Giambiagi et al. 2008; Giambiagi et al. 2009).

Bitumen mines

Bitumen mines of the Malargűe area are within the fold and thrust belt, especially between latitudes 35°S and 36°S (Fig. 1 and Table. 1). The Vaca Muerta Fm is the main host rock for the mines, but some of them occur in the Neuquén Group or in the Malargűe Group (Table. 1). Within the mines, the bitumen veins are either sills or dikes. The bitumen varies in composition and maturity, from impsonite to gilsonite, but there are no obvious correlations with location or host rock (Parnell and Carey 1995), (Fig. 4). The mines are old and we had difficulty in finding some of them, although mostly they lie close to roads or footpaths.

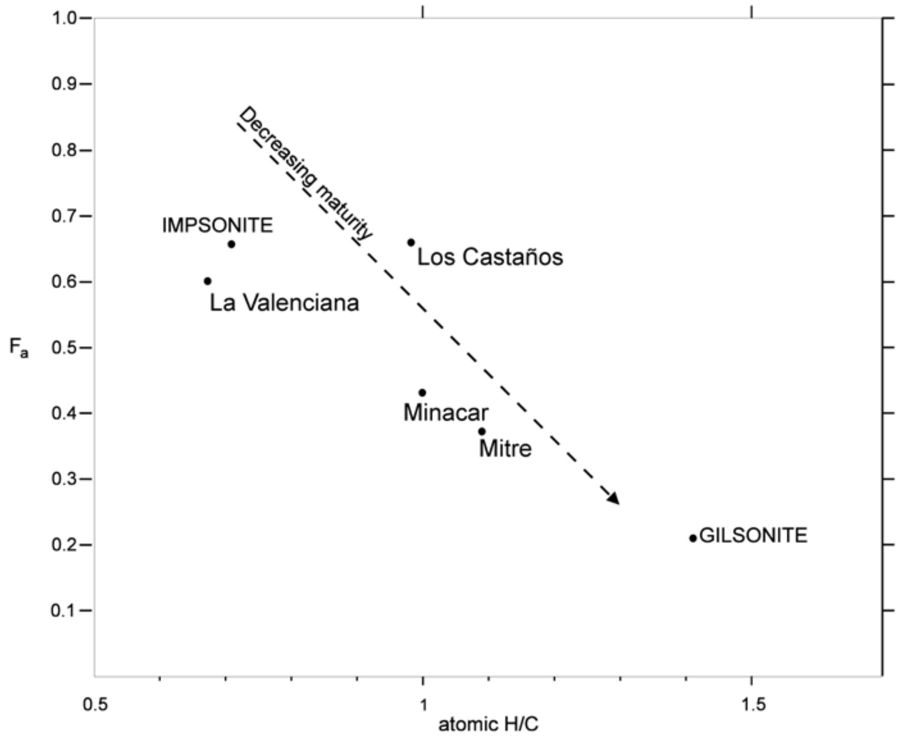

Figure 4. Aromaticity (Fa) as a function of atomic ratio (H/C) and for bitumen from various localities of the northern Neuquén basin, relative to standard bitumen subtypes (see Jacob, 1989).

In the following section we will briefly describe some of the mines, outcrops of bitumen veins and other features, such as the presence of ‘beef’ veins or magmatic bodies. La Valenciana Mine figures in a separate section.

n°-	Name	Coordonates			Host rock
		Latitude S	Longitude W	Elevation (m)	
1	Mercedes	36° 4' 30"	70° 1' 19"	2024	Vaca Muerta
2	Minacar	35° 51' 58"	70° 4' 5"	2138	Vaca Muerta
3	Aida	35° 54' 36"	69° 48' 30"	1648	Mendoza Group
4	La Malarguiña	35° 35' 18"	69° 56' 06"	2146	Vaca Muerta
5	La Valenciana	35° 33' 2"	69° 54' 11"	2000	Vaca Muerta
6	El Toki	35° 27' 11"	69° 46' 51"	1736	Malargue Group
7	Mallin Largo	35° 14' 4"	69° 45' 23"	1850	Vaca Muerta
8	Los Castaños	35° 13' 54"	69° 47' 19"	2137	Vaca Muerta
9	Santa Rosa	35° 7' 38"	69° 59' 20"	2740	Vaca Muerta
10	General Mitré	34° 45' 2"	69° 40' 6"	2552	Neuquen Group
11	Eloisa	34° 41' 21"	69° 42' 37"	3242	Vaca Muerta

Table 1. Bitumen mines of the Malargűe fold-and-thrust belt that we were able to visit. For location on regional map, see Figure 1.

Mercedes, Los Vascos, Minacar and Aida mines

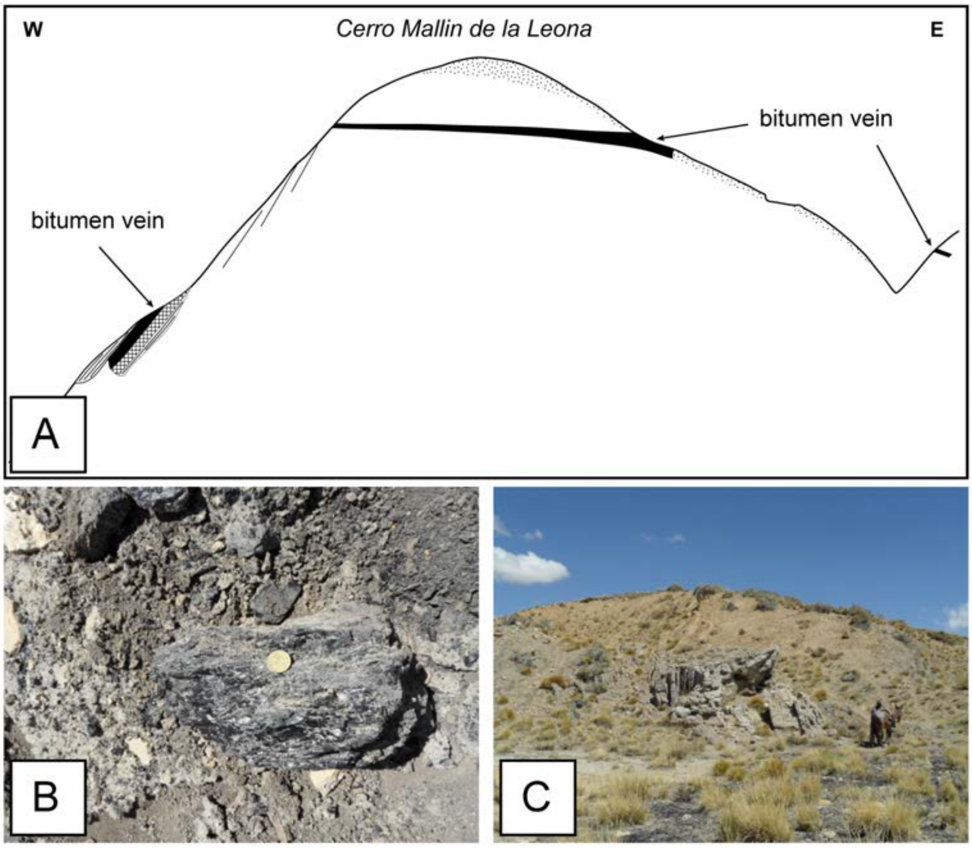

Figure 5. A. Schematic E-W section of Cerro Mallin de la Leona, including bitumen veins of Mercedes Mine (modified, after Biondi 1942a). The main bitumen vein is a sill parallel to the bedding in an anticline structure. The thickness of the bitumen is variable and is thicker in the hinge of anticline. B. Loose fragment of bitumen near the main gallery entry of the Mercedes Mine. C. Remains of entrance to main gallery, Mercedes Mine.

In the southern part of the Malargűe area, three main bitumen mines are visible. The first is Mercedes Mine on "Cerro Rahui" or "Monte de la Leona" mountain (n°1 in Fig. 1 and Table. 1). Nowadays, this mine is easily accessible on foot, but outcrops of old workings are poor and have almost disappeared. Nevertheless, descriptions of the mine exist in YCF reports (Biondi, 1942a, 1942b) and in the book of Borrello (1956). The mine exploited mainly one bitumen sill, 0.70 to 1.50 m thick, parallel to bedding, the host rock being the Mendoza Group (Lower Cretaceous). The mine lies at the top of a hill, on an anticline, which is in fact a box-fold (Fig. 5A). According to old descriptions (Biondi, 1942a), at the hinge the vein is flat-lying and as much as 4.5 m thick, forming a saddle-reef. We found the old mine entrance (Fig. 5C) and many loose fragments of bitumen (Fig. 5B).

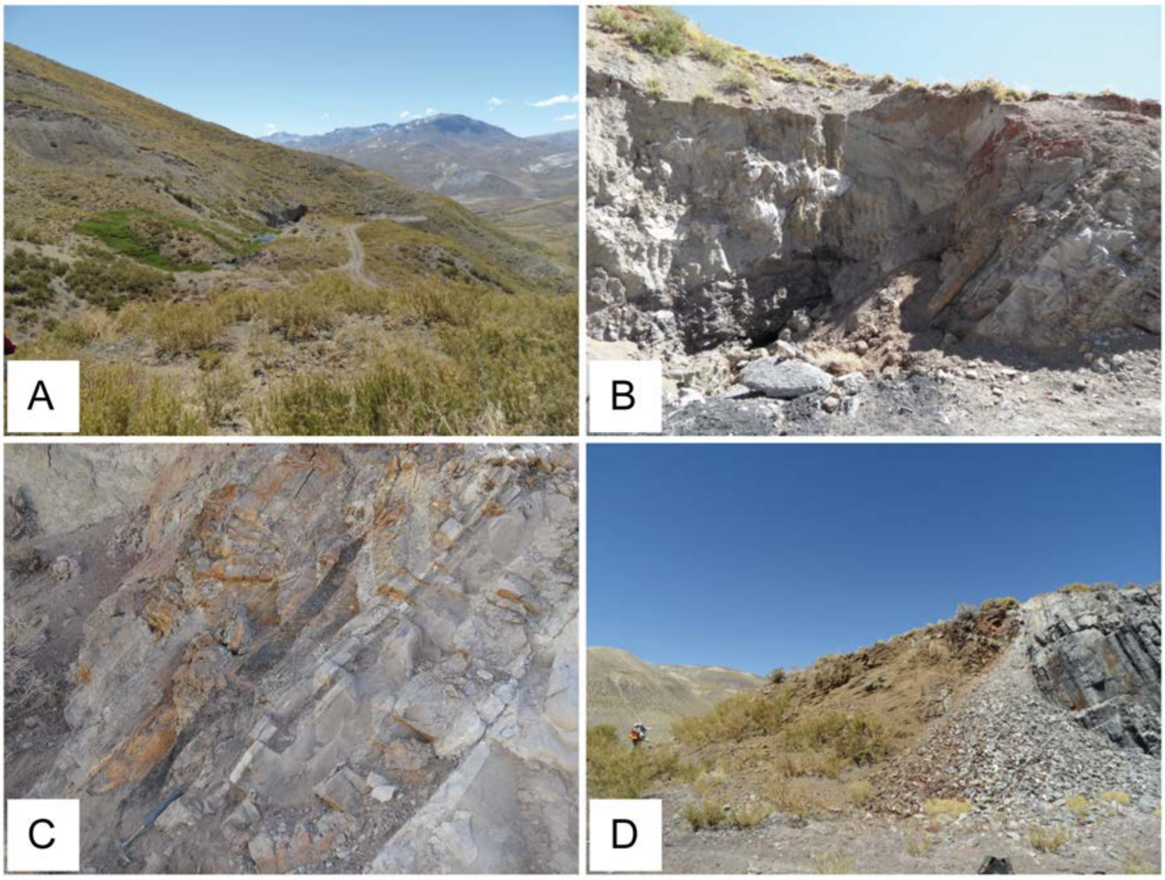

Figure 6. A. General view of Minacar (or General San Martin) Mine. B. Recent quarry, showing two bitumen veins. Vein at left cuts across strata, whereas sill at right intruded parallel to bedding. C. Close-up view of bitumen sill, which has pencillate structure. D. Main igneous intrusive body (andesite), Minacar area. Body has metamorphic aureole.

At about 2 km westward of Mercedes Mine, on the other side of the Rio de la Leona, we explored another old mine, Los Vascos or Santa Maria (Borrello, 1956). This lies within shale of the Mendoza Group, at the bottom of a deeply incised river valley. The old workings are still visible in part and they follow vertical veins of bitumen (up to 2.2 m thick), which strike approximately E-W. Possibly these veins were feeders for the sills at Mercedes Mine. At Los Vascos we also found many loose fragments of beef. When we broke these samples, they released strong odors of hydrocarbons.

The third mine in the southern area is Minacar (or General San Martin); (n°2 in Fig. 1; Fig. 6A and Table 1). The remains of this mine, which was active from 1942 to 1951, follow an anticlinorium and several bitumen veins, some of which are parallel to bedding in Lower Cretaceous strata, others of which are transverse (Borrello 1956); (Fig. 6B & C). The main vein, which is no longer visible at outcrop, was in fact a sill or laccolith, as much as 30 m thick, which was just beneath gypsum-bearing evaporite of the Huitrin Fm, or even in places reached the surface (Fester and Cruellas, 1941; Nicolas Davis, personal communication). As in Mercedes mine, so at Minacar, the bitumen was thicker at the hinge of the anticline, than on its flanks (Borrello, 1956), so that it formed a saddle-reef. At depth was a bitumen dike, striking N-S, as well as shows of liquid oil (Fester and Cruellas, 1941). At Minacar, the bitumen is about half way in composition between impsonite and gilsonite, indicating moderate maturity (Parnell and Carey 1995, their fig. 5). Moreover, the ash that remains after burning the bitumen contains as much as 70% of vanadium pentoxide. As previously described by Parnell and Carey (1995), the bitumen has a pencillate internal structure (Fig. 6C). Near the main bitumen vein (about 50 meters from it) an andesitic body has intruded the Agrio Fm (Fig. 6D). The body is massive and it has metamorphosed the shales at its edges. The relationships between bitumen veins and magmatic activity are not very clear but the proximity of both structures seems to be no accident, so much so, that Fester and Cruellas (1941) inferred that magmatic activity was responsible for the bitumen veins.

The last mine that we visited in this area was Aida. This mine lies about 3 kilometres southward of the town of Bardas Blancas (n°3 on the Fig. 1; Table. 1). Outcrops are not of good quality, but the remains of gallery entrances are still identifiable. The mine is on the eastern side of the Bardas Blancas anticline (Gross 1950). Bitumen occurs in the Agrio Fm, just beneath the transition with the Huitrin Fm, and it consists of veins or impregnations within shale and calcareous stata, as well as evaporites. Andesitic dikes are also present in this area (Gross 1950; Borrello 1956).

Mallin Largo, Los Castaños and El Toki mines

Between latitudes 35°S and 36°S, bitumen mines were numerous in the first half of the last century. Borrello (1956) mentioned not less than 25 bitumen mines in this part of the Malargűe fold and thrust belt. The biggest mine was La Valenciana, which we will describe later in this paper. Here we will describe three other mines (Mallin Largo, Los Castaños and El Toki), to illustrate bitumen occurrences.

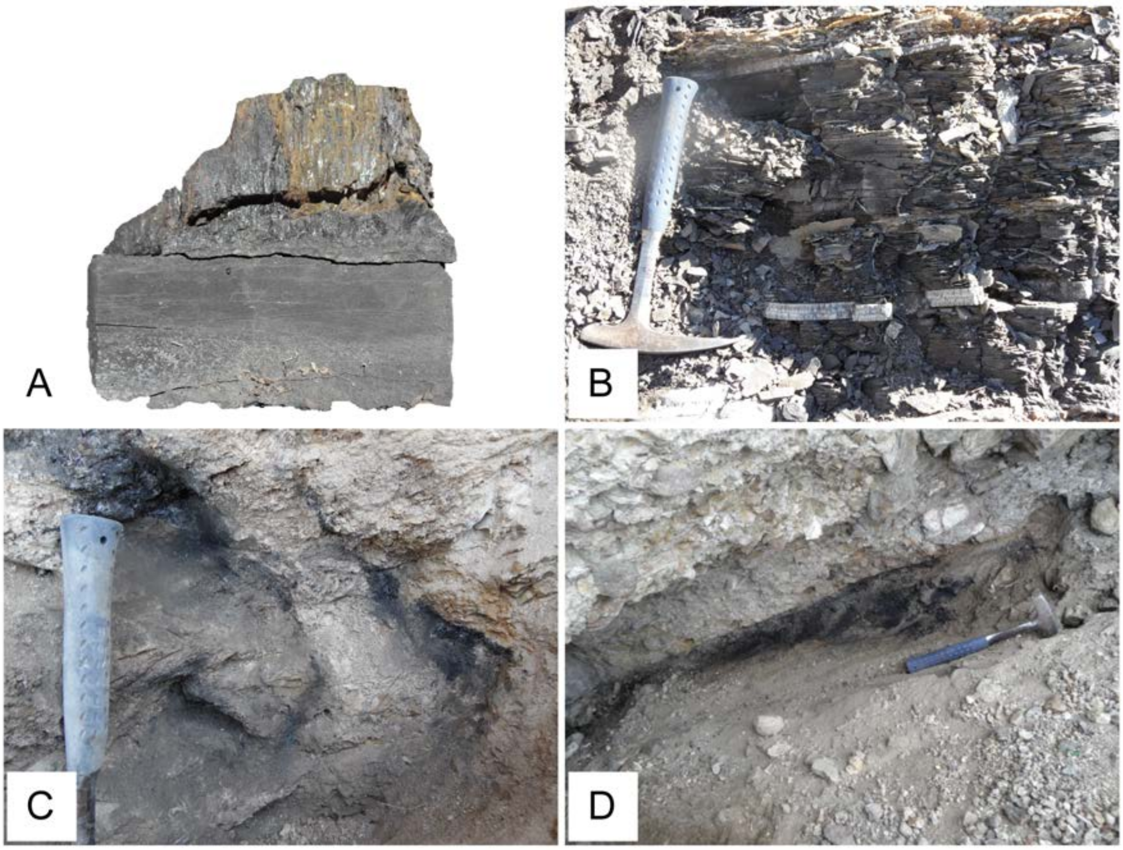

Figure 7. A. Pencillate bitumen vein, from near gallery entrance, Los Castaños Mine. Edges of vein (horizontal) are parallel to bedding in Vaca Muerta shale, whereas 'fibres' of bitumen are perpendicular to it. B. Beef veins within Vaca Muerta shale near Los Castaños Mine. Veins are strictly parallel to bedding and contain hydrocarbons. C. Outcropping bitumen vein, Mallin Largo Mine. Bitumen cross-cuts and impregnates Mendoza Group. D.

Outcropping bitumen vein, El Toki Mine. Vein is parallel to bedding in Early Tertiary conglomerate.

Los Castaños and Mallin Largo mines are close to one another (n° 7 and 8 in Fig. 1; Table. 1). They lie to the south of the Rio Salado, on an anticlinal structure. Los Castaños is on the western side and Mallin Largo on the eastern side of the anticline. The bitumen veins of Los Castaños consist mainly of sills, parallel to bedding in the Vaca Muerta Fm (Borrello 1956). Outcrops are rare, but one sample that we found illustrates the pencillate structure of the bitumen within a vein parallel to bedding in shale (Fig. 7A). At Los Castaños, the bitumen is relatively mature, being closer to impsonite, than to gilsonite (Parnell and Carey 1995, their fig. 5). Also within shale of the Vaca Muerta Fm, around the site of Los Castaños, we found several bedding-parallel veins of fibrous calcite (beef) (Fig. 7B). The veins are typically 1 to 5 cm thick and contain dark patches. When we broke the beef with a hammer, we noticed strong odours of hydrocarbons, which came from within it.

Mallin Largo Mine lies within Neocomian strata, including the Vaca Muerta Fm. Videla Leaniz (1946) has described the mine in some detail. Bitumen forms irregular veins (up to 3 m thick), which dip at about 70° to the NW and cut across the bedding. We saw only some of these (Fig. 7C), because the mine is now only partly accessible.

El Toki is the third mine that we visited in this central part of the Malargűe area (n°6 on the Fig. 1; Table. 1). Here bitumen veins cut through the Neuquén Group (Late Cretaceous) and Tertiary strata (Borrello 1942a, 1956). Veins are typically 0.50 to 1.50 m thick. During our study, we observed one sill of bitumen, which was 40 cm thick, within Tertiary conglomerate (Fig. 7D). Nearby was an oblique vein, which followed an eastward-verging thrust fault. Further W we found some thin bitumen veins (less than 1 cm thick), lining a right-lateral flower structure, which had horizontal strike-slip striations, trending at 035°. Thus in this area there is evidence for bitumen generation during Tertiary transpressional tectonics.

Eloisa and General Mitre mines

In the northern Malargűe area, two mines caught our attention, Eloisa and General Mitre. Eloisa lies at an altitude of 3100 m, at the northern head of a valley (about 7 km long) and it is accessible on foot or on horseback (n°11 on the Fig. 1; Table. 1). Salas (1892) identified bitumen in this area. Today the mine workings have almost disappeared, but we found some good outcrops (Fig. 8A). Borrello (1942b, 1956) has provided a detailed description of the area. The sedimentary sequence is Mid-Jurassic to Mid-Cretaceous in age. However, it has been overturned above an eastward-verging thrust fault and now dips gently westward. In the East, mine workings follow bitumen dikes (trending about 075°), which have intruded continental sandstones of the Neuquén Group, beneath clays and evaporites of the stratigraphically older Huitrín Fm (Fig. 8A). Further W, bitumen sills (up to 2 m thick) lie parallel to bedding within the Huitrín evaporites (Borrello, 1956, figure 92). Above them, the Mendoza Group contains an andesite sill, which has fractured, allowing small dikes of bitumen to crosscut it. Similar dikelets of bitumen also crosscut the Vaca Muerta Fm. Finally, to the E of Eloisa Mine, Tertiary volcanic rocks (andesites) overlie the sedimentary sequence unconformably. We were not able to find any bitumen within them.

General Mitre is the last mine that we will briefly describe in this section (n°10 on the Fig. 1; Table. 1). This mine is easily accessible, lying as it does near a farmhouse, along a provincial road. Again, Salas (1892) was the discoverer. Bitumen there forms several dikes, 50-60 cm thick, which strike at about 70°N, cutting through the Late Cretaceous Neuquén Group (Fig. 8B), (Borrello 1956). At Mitre mine, the bitumen is the least mature, being closer in composition to gilsonite, than to impsonite (Parnell and Carey 1995, their fig. 5). Structurally the mine is to the S of a thrust fault (Fig. 1).

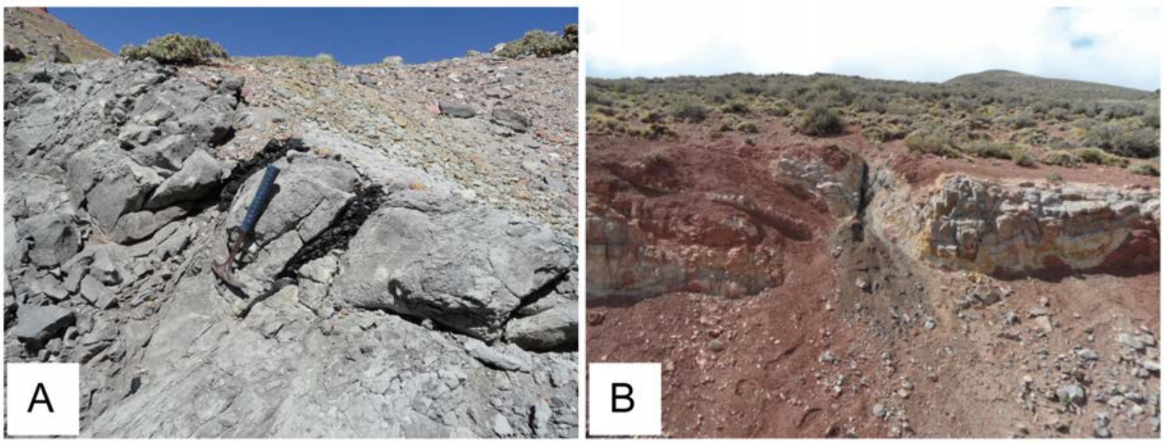

Figure 8. A. Outcropping bitumen vein, Eloisa Mine. Vein cross-cuts Agrio Fm, just beneath gypsum of Huitrin Fm. B. Bitumen vein, General Mitré Mine. Vein cross-cuts strata of Neuquén Group (Late Cretaceous).

Volcanic rocks

In the Malargűe fold and thrust belt, volcanic rocks are abundant (Fig. 1). Most of them are of Tertiary or Quaternary ages. During our field study, we noticed that bitumen mines lie, in general, near local volcanic provinces. This is so for the mines (previously described) Minacar, Aida, El Toki, Los Castaños and Eloisa, but also for La Valenciana Mine that we will describe in the following section. On the basis of these observations, we decided to investigate the volcanic rocks. We did not observe any direct structural relationships between bitumen veins and igneous rocks. However, we sampled them for ^{39}Ar-^{40}Ar dating (Table 2, Fig. 9). In detail, we obtained ^{39}Ar-^{40}Ar age spectra for 42 samples of whole rock or phenocrysts, from 7 localities (Figs. 9 & 13; Table 2). Nonetheless, some samples did not provide any plateau ages. That is why Table 2 shows only 38 analyses. The results fall into two main groups. The first group is of Miocene age and ranges from 10.3 to 14.2 Ma. The second group is of Quaternary age, from 0.75 Ma to 0.20 Ma (Fig. 9). Only one area, near Eloisa Mine and the Rio Diamante, yielded different ages, between 3.6 Ma and 6.2 Ma (Fig. 9).

La Valcenciana Mine

The discovery of La Valenciana (n°5 in Fig. 1; Table. 1) dates back to 1922. It soon became the biggest bitumen mine of the Malargűe fold and thrust belt (Ljungner 1931). That was one reason why we decided to give it special attention. For this mine (and the adjacent exploration sites of La Porteña, La Cordobesa, York, Invisible, La Poderosa, La Francesa and La Malargűina) there have been many descriptions of bitumen occurences (e.g. Ljungner 1931; Meyerhoff 1948; Borrello 1956; Parnell and Carey, 1995). The main mine entrance was on the southeastern flank of the La Valenciana syncline, which trends approximately NE-SW (Fig. 10). The main occurrence of bitumen was in the form of a sill, as much as 4 m thick and 150-200 m long. This is no longer visible, although one of us (PRC) saw it in the year 2000. The old mine workings have collapsed in recent years, but photographs and mine plans remain (Ljungner 1931; Meyerhof 1948; Borrello 1956). By comparison with Mercedes and Minacar, the bitumen at La Valenciana has a composition that is much closer to impsonite, than to gilsonite (Parnell and Carey 1975, their fig. 5). This indicates a relatively high maturity.

Site	Sample	Latitude (S)	Longitude (W)	Ages (Ma)	Type or mineral
Aida	11-AIDA-1	35 54 33.2	69 48 24.5	12,5 ± 0.1	Whole rock
				14,2 ± 0.1	Amphibole
Minacar	11-MINACA-1			13 ± 0.29	Whole rock
	11-MINACA-2	35 51 54.9	70 04 10.8	14,7 ± 0.18	Whole rock
	11-MINACA-3	35 51 55.7	70 04 03.2	13,67 ± 0.08	Amphibole
	11-MINACA-4	35 50 35.3	70 02 41.7	0,228 ± 0.12	Whole rock
	11-MINACA-5	35 46 25.9	70 06 30.3	0,301 ± 0.022	Whole rock
	11-MINACA-6	35 45 21.1	70 06 39.7	0,722 ± 0.028	Whole rock
				0,751 ± 0.06	Biotite
El Toki	TOKI-1	35 26 48.4	69 46 47.9	12,91 ± 0.09	Whole rock
	TOKI-3	35 26 48.0	69 46 55.8	10,64 ± 0.05	Whole rock
	TOKI-4	35 27 05.2	69 46 43.9	12,01 ± 0.11	Whole rock
	TOKI-5	35 27 03.6	69 47 17.4	10,3 ± 0.05	Whole rock
	TOKI-6			13,13 ± 0.12	Whole rock
La Valenciana	PLOMO-1	35 30 33.3	69 55 47.4	9,87 ± 0.05	Whole rock
	M11-003A	35 33 09.8	69 54 20.7	0,165 ± 0.025	Whole rock
	M11-003B	35 33 09.8	69 54 20.7	0,177 ± 0.019	Whole rock
	11-VA-1	35 33 02.2	69 54 24.3	10,21 ± 0.14	Whole rock
				9,99 ± 0.2	Amphibole
	11-VA-2	35 32 55.1	69 54 06.6	14,63 ± 0.13	Whole rock
	11-VA-3	35 32 36.9	69 53 54.4	12,88 ± 0.36	Whole rock
	M12-028	35°31'40.75"	69°55'37.01"	12,63 ± 0.43	Whole rock
				11,39 ± 0.36	Amphibole
	M12-029	35°31'40.75"	69°55'37.01"	10,74 ± 0.11	Whole rock
	M12-038	35 31 50.9	69 53 52.3	10,84 ± 0.2	Whole rock
	M12-039	35 31 30.5	69 54 17.8	9,44 ± 0.04	Whole rock
				9,64 ± 0.45	Sanidine
	M12-042	35 31 07.2	69 54 32.6	9,92 ± 0.1	Whole rock
	M12-043	35 31 16.6	69 54 44.9	10,77 ± 0.36	Whole rock
	M12-046	35 31 43.5	69 53 47.3	10,92 ± 0.28	Whole rock
				9,56 ± 0.33	Amphibole
	M12-052	35 31 50.5	69 55 07.7	10,65 ± 0.35	Whole rock
				9,67 ± 0.17	Amphibole
Malarguina	M11-019	35 34 18.3	69 55 16.5	0,195 ± 0.013	Whole rock
	M12-030	35 35 20.3	69 56 01.3	0,216 ± 0.009	Whole rock
Eloisa	M12-018	34 41 18.9	69 42 38.8	3,61 ± 0.05	Whole rock
Rio Diamante	M12-023	34 40 51.6	69 34 10.4	6,09 ± 0.03	Whole rock
				6,24 ± 0.16	Amphibole

Table 2. ^{39}Ar-^{40}Ar ages for volcanic rocks in the Malargűe fold and thrust belt area.

Around La Valenciana mine, bedding-parallel veins of fibrous calcite (beef) are also widespread within the Vaca Muerta source rock, which occupies the core of the syncline (Parnell and Carey 1995). The calcite fibers are in general perpendicular to the walls of the veins (Figs. 11A & 11D), but in some examples they curve sigmoidally towards the edges, indicating deformation during growth (Figs. 11B & 11D). Cone-in-cone structures, consisting of shale fragments, occur near the centers of some beef veins (Fig. 11D).This beef also contains patches of bitumen (Figs. 11D & 11E)., which follow an irregular surface, approximately parallel to the edges of the vein and where the calcite fibers start to curve (Fig. 11E). This would indicate that bitumen was forming at the onset of deformation. We also observed that beef is more common around igneous intrusive bodies. Near some of these, the beef appears to be less fibrous, indicating that it has recrystallized, at least in part (compare Figs. 11A & 11B). Each sample that we broke in the field had a strong odour of hydrocarbons. Near volcanic intrusions, we also identified some travertine (Fig. 11C), attesting to fluid circulation around igneous rocks.

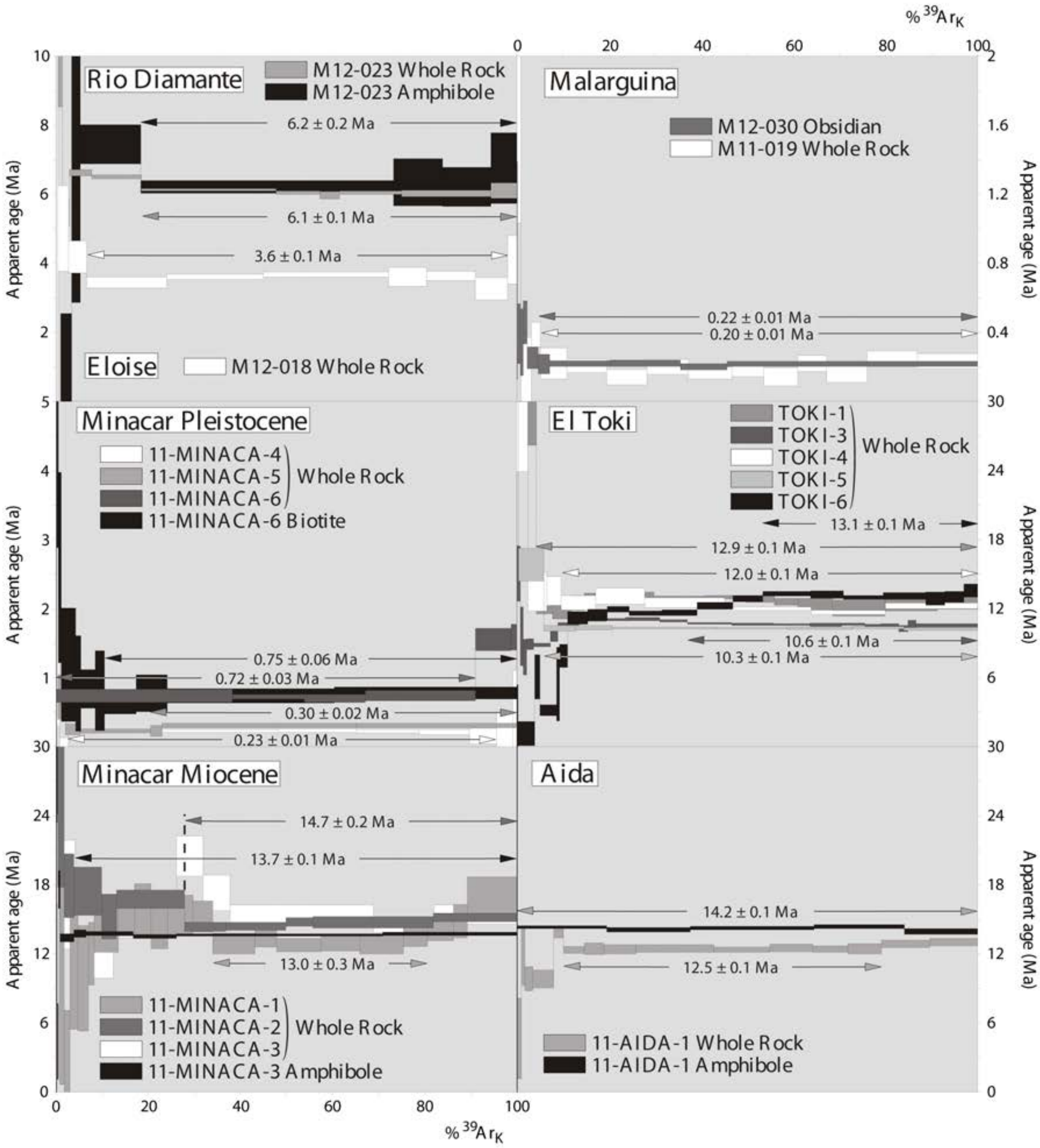

Figure 9. Results for the ^{39}Ar-^{40}Ar datings. ^{39}Ar-^{40}Ar spectra are for 20 samples of volcanic rocks. For analytical procedure, see Ruffet et al. (1995, 1997). Irradiation standard was sanidine TCR-2 (28.34 Ma, according to Renne et al. 1998). For each temperature, error bars are at 1σ level.

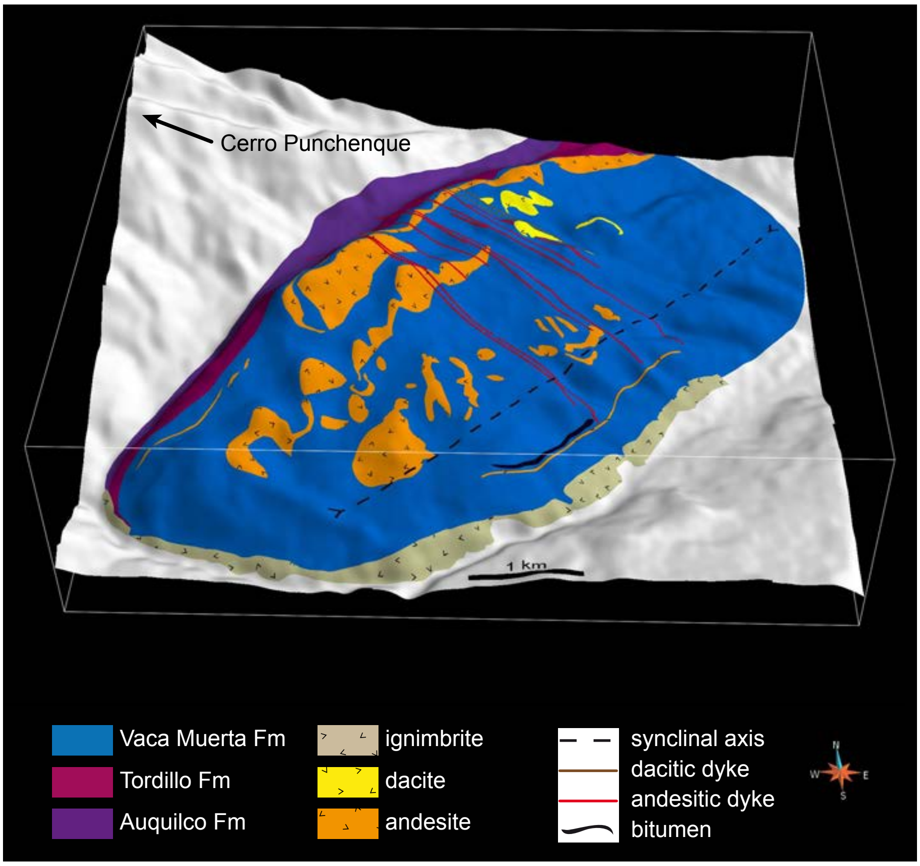

Fig. 10. La Valenciana Mine. Oblique 3D view shows geological map (in colour), on a background of topographic relief (grey tones). Cutting across sedimentary sequence (blue for Vaca Muerta Fm) are main bitumen sill (black) and multiple intrusive bodies of igneous rocks, including dikes and sills of andesite (red) or dacite (orange). Dikes appear to radiate southeastwards from Cerro Puchenque volcanic edifice. For location, see Fig. 1.

In the central and southern parts of the La Valenciana syncline, large amounts of igneous rocks have intruded Mesozoic strata of the Mendoza Group (Figs. 10 & 12). Most of the intrusive bodies are dikes, but some of them are wide-ranging bedding-parallel sills. The dikes are of andesitic composition and typically 2 to 15 m thick (Fig. 12C). They have an average strike of 100-110°N and cut though the entire syncline. In detail, however, they appear to form a somewhat radial pattern, as if they emanated from a large intrusive pluton, the Cerro Puchenque (Fig. 10). In general, the sills are somewhat thinner (1 to 10 m thick).

In contrast, in the northern part of the La Valenciana syncline, intrusive rocks are not andesites, but dacites (Fig. 12D). Structurally, these dacites (sills and dikes) seem to cut the andesitic bodies, but the relationships are not clear. At its northeastern end,, the main bitumen sill seems to terminate against a major andesitic dike (Fig. 10; see also Meyerhoff 1948, his fig. 3), but we have seen no evidence allowing us to determine the relative timing of the sill and dike.

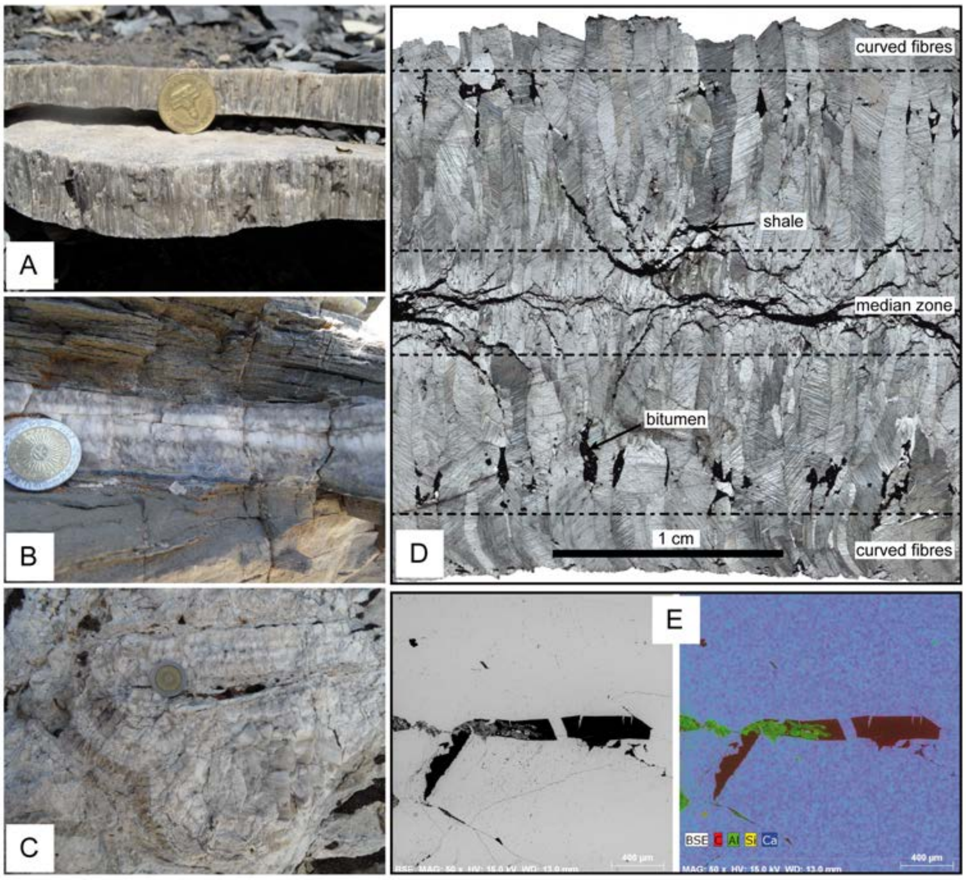

Figure 11. A. Vein of calcite beef within Vaca Muerta Fm, La Valenciana syncline. B. Calcite beef near andesitic sill (60 cm beneath intrusion). Beef seems to be metamorphosed. C. Patch of travertine near an andesitic dyke (40 cm from intrusion). D. Thin section of beef from La Valenciana. Calcite fibres curve at edges of veins. Nearby are patches of bitumen, between calcite fibres. E. ESEM image of bitumen (left). Composite BSE and X-ray image sohing the composition of a part of beef vein (right). Intensities of colours reveal concentrations of elements (carbon = red; aluminum = green; silica = yellow; calcium = blue).

More generally, so as to try to constrain the relative and absolute ages of volcanic and bitumen intrusions, we used ^{39}Ar-^{40}Ar dating (Fig. 13 and Table. 2). For 20 samples from the La Valenciana area, 18 have yielded Miocene ages (14.6 to 9.4 Ma, Langhian to Tortonian,

Fig. 13). This corroborates the stratigraphic chart and geological map (at a scale of 1:250,000) for the Malargue area (Nullo et al. 2005), which have these volcanic rocks ("Ciclo Eruptivo Huincán") as "Lower to Upper Miocene" in age (14 to 5 Ma). In contrast, the two very recent ages (0.18 and 0.17 Ma, Fig. 13) correspond to Quaternary ignimbrites in the valleys.

About 5 km SW of La Valenciana is another small mine, La Malarguina (Table 1, Fig. 1). According to Borrello (1956), bitumen veins of high thermal grade, 2 to 5 cm thick, were visible there, at the edges of a dike and sill of Tertiary andesite. Similarly, at another locality (La Francesa), some 2.5 km NNE of La Valenciana, small bitumen veins (up to 2 cm thick) occupied joints within a large sill of andesite. Thus the evidence in this region is for bitumen generation during volcanic activity.

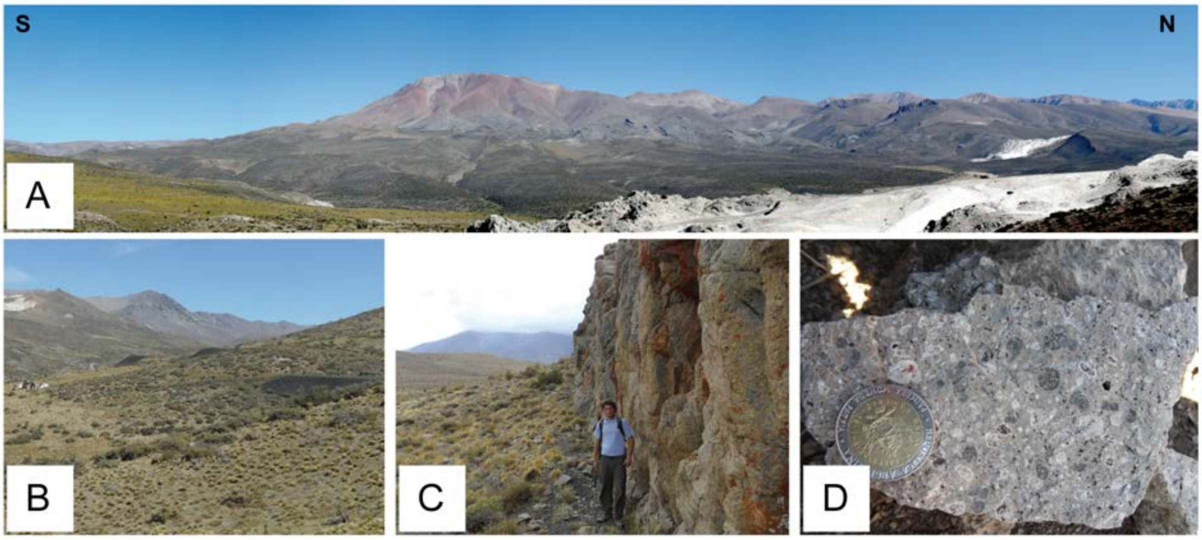

Figure 12. A. Westerly panoramic view (N to S), La Valenciana syncline. White outcrops in foreground are of evaporites (Auquilco Fm). Mountain in background is of intrusive andesite .B. Remains of La Valenciana Mine. Dark mounds are mine dumps of bitumen and shale, close to old mine galleries. C. One of main vertical andesitic dykes cutting approximately E-W through Vaca Muerta Fm. D. Dacite from northern La Valenciana syncline.

Discussion

Evidence for hydrocarbon migration is abundant in the Malargűe fold and thrust belt. Most obvious at the surface are the bitumen mines and veins. Nevertheless, the timing of generation of the bitumen is still uncertain. From the burial history and assuming a standard thermal gradient (30°C/km), Parnell and Carey (1995) suggested that oil and therefore bitumen veins formed in the Eocene to Oligocene. However, some of our data are inconsistent with this timing. Furthermore, Kay et al. (2006) have shown that magmatic activity in the

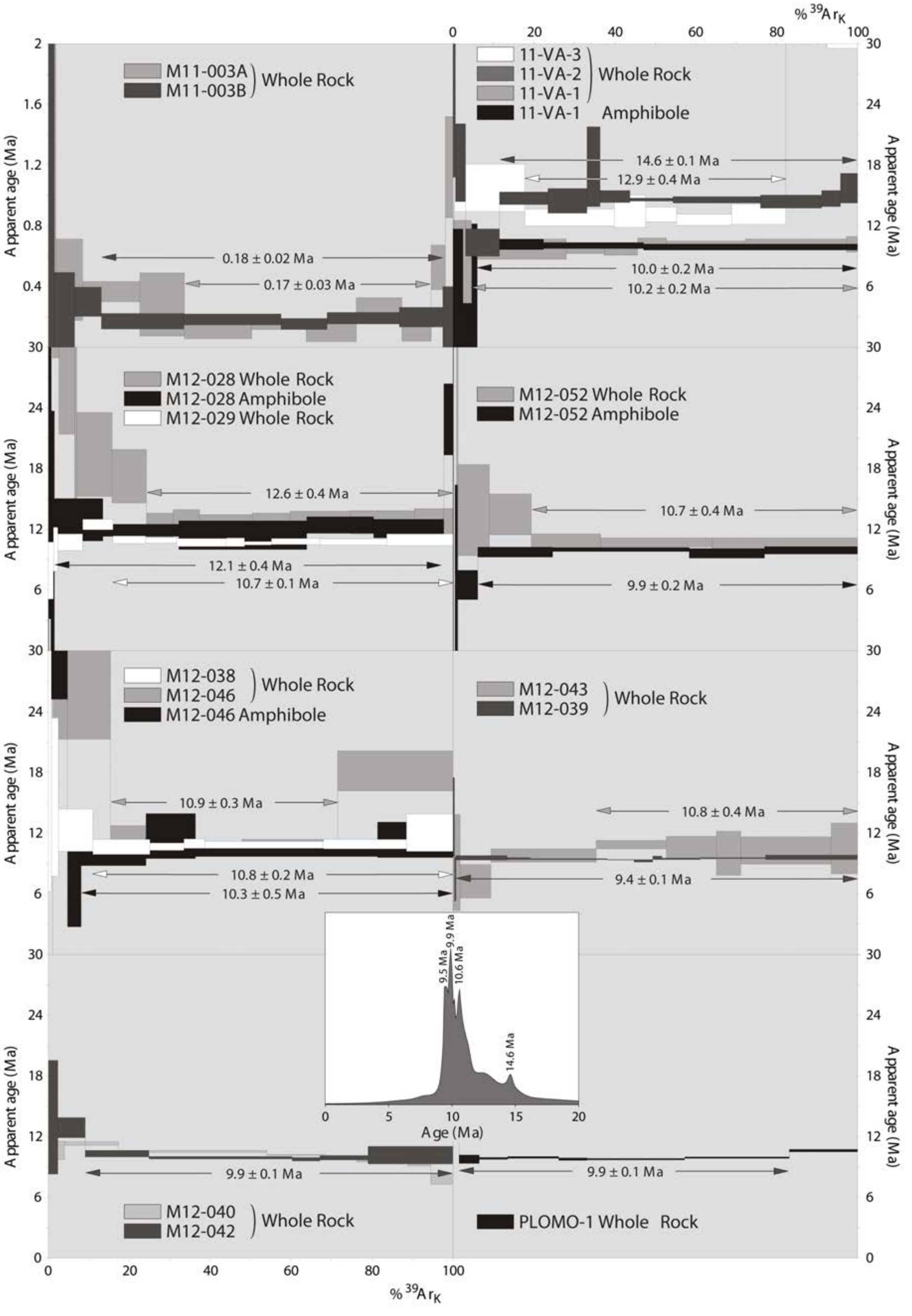

Figure 13. Results of ^{39}Ar-^{40}Ar dating, La Valenciana area. Spectra are for 20 samples of volcanic rocks. For analytical procedure, see Ruffet et al. (1995, 1997). Irradiation standard was sanidine TCR-2 (28.34 Ma, according to Renne et al. 1998). For each temperature, error bars are at 1σ level.

northern Neuquén Basin reached a peak in the Miocene, at a time when the subducting slab at the Pacific margin became relatively flat.

Bitumen sills of the Malargűe area tend to occur within anticlines as saddle-reefs, a good example being Mercedes Mine. This is evidence that hydrocarbons were migrating during a phase of compressional tectonics. Furthermore, the bitumen tends to have a pencillate internal structure, which suggests progressive opening of veins, as a result of high fluid pressure (Parnell and Carey 1995). Further evidence for overpressure is the presence of beef veins along the fold and thrust belt. These bedding-parallel veins of fibrous calcite also indicate progressive opening, as a result of high fluid overpressure within the enclosing strata, which commonly are source rocks for petroleum (Rodrigues et al. 2009; Cobbold et al. 2013). At La Valenciana, curving calcite fibers provide evidence for ongoing deformation, during opening of the veins. Possibly this was another result of compressional tectonics.

Like previous authors, we have observed that bitumen veins tend to occur near volcanic intrusive bodies, good examples being at La Valenciana and Minacar mines. This could be simply a coincidence, but probably it is not. Volcanism could provide the heat that is necessary for maturation of source rock and especially for the formation of high-grade pyrobitumen (Abraham 1960). This is all the more likely in that volcanic activity in the northern Neuquén Basin reached a peak in the Miocene (Kay et al., 2006).

We explain the overpressure, which led to hydraulic fracturing and the formation of bitumen and beef veins within Vaca Muerta source rock, mainly by a mechanism of chemical compaction and load transfer (see Swarbrick et al., 2002). However, we would admit that the presence of evaporite layers might have enhanced the overpressure and retained the hydrocarbons within the source rock. From what we have seen so far, we would infer that volcanic activity, compressional tectonics and hydrocarbon generation are probably all of Miocene age in the Malargüe fold-and-thrust belt. Indeed Kay et al. (2006) attributed volcanic activity and compressional tectonics to flattening of the subducting Pacific slab during the Miocene.

Conclusions

(1) In the northern part of the Neuquén Basin, bitumen veins are widespread, especially within strata of the Mendoza Group, including the Vaca Muerta source rock.

(2) In the Malargűe fold and thrust belt, new argon-argon dating has confirmed Miocene ages (Langhian to Tortonian) for volcanic rocks, which lie near bitumen veins.

(3) In the La Valenciana area especially, there seems to be a strong link between volcanic intrusions and the emplacement of bitumen and beef veins.

(4) Bitumen veins and calcite beef veins are a consequence of hydrocarbon generation, which led to fluid overpressure and hydraulic fracturing. Veins of bitumen and beef formed during Andean compression in the Tertiary. Like previous authors, we consider that the bitumen veins and beef veins formed in the Early to Middle Miocene.

(5) In the Miocene, the synchronicity of volcanic activity, compressional tectonics and hydrocarbon generation may well have been a result of flattening of the subducting Pacific slab.

Acknowledgements

We are grateful to Statoil, for funding the PhD research project of Alain Zanella. Tony Boassen of the Statoil Research Centre in Trondheim was instrumental in obtaining images of beef under the scanning electron microscope (ESEM). We thank the SEGEMAR for making available to us copies of hitherto unpublished reports by Yacimientos Carboníferos Fiscales. Christian Le Carlier de Veslud helped in the construction of Fig. 10. Juan Spacapan (Universidad Nacional de La Plata) provided very useful assistance in field mapping, especially around La Valenciana Mine. Nicolas Davies was kind enough to provide unpublished information, from the time when he worked on some of the bitumen mines.

References

Abraham, H., 1960. Asphalt and allied substances. Volume 1, Sixth Edition, D. Van Nostrand Company, New York, U.S.A., 325 pages.

Biondi, J.L. 1942a. Informe preliminar de la zona de Mina Mercedes, Provincia de Mendoza. Yacimientos Carboníferos Fiscales, Informe, 97, 1-6.

Biondi, J.L., 1942b. Informe de la Comisión Carbón Mineral N° 52, correspondiente al mes de abril de 1942. Yacimientos Carboníferos Fiscales, Informe (unpublished report).

Borrello, A.V., 1942a. El yacimiento de asfaltita “El Toki”, Mendoza. Yacimientos Carboníferos Fiscales, Informe, 65, 1-4 (unpublished report).

Borrello, A.V. 1942b. Informe sobre la mina “Eloisa” (San Rafael) Provincia de Mendoza. Yacimientos Carboníferos Fiscales, Informe, 91, 1-7..

Borrello, A.V., 1956. Recursos minerales de la República Argentina. III. Combustibles sólidos minerales. Revista del Instituto Nationales de Investigación de la Ciencias Naturales y Museo Argentino de Ciencias Naturales “Bernardino Rivadavia”, Ciencias Geológicas, 5: 1-665.

Buckland, W., De la Beche, H.T., 1835. On the geology of the neighbourhood of Weymouth and the adjacent parts of the coast of Dorset. Transactions of the Geological Society, London, s2-4, 1-46.

Cobbold, P.R., Rossello, E.A., 2003. Aptian to recent compressional deformation, foothills of the Neuquén Basin, Argentina. Marine and Petroleum Geology, 20, 429–443.

Cobbold, P.R., Zanella, A., Rodrigues, N., Løseth, H., 2013. Bedding-parallel fibrous veins (beef and cone-in-cone): worldwide occurrence and possible significance in terms of fluid overpressure, hydrocarbon generation and mineralization. Marine and Petroleum Geology, 43, 1-20, doi: 10.1016/j.marpetgeo.2013.01.010.

Fester, G.A. y Cruellas, J. 1941. Yacimientos de asfaltitas de carácter especial. Revista de Minería y Geología Minera, 12 (1,2), 31-37.

Giambiagi, L., Bechis, F., García, V., Clark, A.H., 2008. Temporal and spatial relationships of thick- and thin-skinned deformation: A case study from the Malargue fold-and-thrust belt, southern Central Andes. Tectonophysics, 459, 123–139, doi:10.1016/j.tecto.2007.11.069.

Giambiagi, L., Ghiglione, M., Cristallini, E., Botesi, G., 2009. Kinematic models of basement-cover interaction: Insights from the Malargue fold and thrust belt, Mendoza, Argentina. Journal of Structural Geology, 31, 1443–1457, doi:10.1016/j.jsg.2009.10.006

Groeber, P., 1923. Origen del petróleo de Barrancas. Deducciones que sugiere su estudio. Boletín de la Dirección General de Minas, Geología e Hidrología, Serie F (Informes Preliminares y Communicaciones), 6 (1), 3-14.

Gross, W.G., 1950. Examen geológico-minero de mina Aída, Llano Blanco - Mendoza. Yacimientos Carboníferos Fiscales, Informe, 714, 1-6 (unpublished).

Jacob, H., 1989. Classification, structure, genesis and practical importance of natural solid oil bitumen (“migrabitumen”). International Journal of Coal Geology, 11, 65-79

Kay, S. M., Burns, W. M ., Copeland, P., Mancilla, O. 2006. Upper Cretaceous to Holocene magmatism and evidence for transient Miocene shallowing of the Andean subduction zone under the northern Neuquen Basin. In: Kay, S.M., Ramos, V.A. (eds), Evolution of an Andean Margin: A tectonic and magmatic view from the Andes to the Neuquén Basin (35° - 39°S lat), Geological Society of America, Special Paper, 407, 19-60.

Kozlowski, E.E., Manceda R., Ramos, V.A., 1993. Estructura: XII Congreso Geológico Argentino, Geología y Recursos Naturales de Mendoza, Relatorio 1, 235–256.

Legarreta, L., Gulisano, C.A., 1989. Análisis estratigráfico de la cuenca Neuquina (Triásico superior–Terciario inferior). In: Chebli, G.A. & Spalletti, L.A. (eds), Cuencas Sedimentarias Argentinas. Universidad Nacional de Tucumán, Serie de Correlación Geológica, 6, 221–244.

Ljungner, E. 1931. El carbón asfáltico de Las Romanas (Mina La Valenciana) en el Distrito de Malargüe (Departamento de San Rafael). Dirección General de Minas, Geología e Hidrología, Informe, 1-11 (unpublished report).

Meyerhoff, H.A., 1948. The occurrence and mining of solid bitumens in western Argentina. Transactions of the American Institute of Mining Engineers, 181, 403-412.

Nullo, F.E., Stephens, G., Combina, A., Dimieri, L., Baldauf, P., Bouza, P., 2005. Hoja geológica 3569-III/3572-IV, Malargüe, Provincia de Mendoza. Programa Nacional de Cartas Geológicas de la República Argentina, 1:250.000, Servicio Geológico Minero Argentino, Instituto de Geología y Recursos Minerales, Boletín, 346, 1-85.

Parnell, J., Carey, P.F., 1995. Emplacement of bitumen (asphaltite) veins in the Neuquén Basin, Argentina. American Association of Petroleum Geologist Bulletin 79, 1798-1816.

Piscione, C.A.S., 1947. Asfaltitas y pirobitumen asfáltico. Revista de la Sociedad Geológica Argentina, 2, 65-87.

Rassmuss, J., 1923. Breves apuntes geológicos sobre la parte del territorio del Neuquén entre Auca Mahuida y El Tromen. Dirección General de Minas, Geológia e Hidrogeología, Serie F (Informes Preliminares y Communicaciones), 6 (1), 15-20.

Renne, P.R., Swisher, C.C., Deino, A.L., Karner, D.B., Owens, T.L., De Paolo, D.J., 1998. Intercalibration of standards, absolute ages and uncertainties in $^{40}Ar/^{39}Ar$ dating. Chemical Geology, 145, 117-152.

Rodrigues, N., Cobbold, P.R., Løseth, H., Ruffet, G. 2009. Widespread bedding-parallel veins of fibrous calcite (“beef”) in a mature source rock (Vaca Muerta Fm, Neuquén Basin, Argentina): evidence for overpressure and horizontal compression. Journal of the Geological Society, London, 166 (4), 695-709, doi 10.1144/0016-76492008-111.

Rodriguez, F., Villar, J. H., Baudino, R. 2007. Hydrocarbon generation, migration, and accumulation related to igneous intrusions: An atypical petroleum system from the Neuquén Basin of Argentina. SPE Paper 107926-PP, 4 p.

Rodriguez Monreal, F., Villar, H.J., Baudino, R., Delpino, D., Zencich, S. 2009. Modeling an atypical petroleum system: A case study of hydrocarbon generation, migration and accumulation related to igneous intrusions in the Neuquen Basin, Argentina. Marine and Petroleum Geology, 26, 590-605.

Ruffet, G., Féraud, G., Ballèvre, M., Kiénast, J-R., 1995. Plateau ages and excess argon in phengites: an ^{40}Ar-^{39}Ar laser probe study of Alpine micas ‘Sesia Zone, Western Alps, northern Italy). Chemical Geology (Isotopic Geosciences Section), 121, 327-343.

Ruffet, G., Gruau, G., Ballèvre, M., Féraud, G., Philippot, P., 1997. Rb-Sr and ^{40}Ar-^{39}Ar laser probe dating og high-pressure phengites from the Sesia zone (western Alps): underscoring of excess argon and new age constraints on the high-pressure metamorphism. Chemical Geology, 141, 1-18.

Salas, J., 1892. Noticias y documentos sobre el carbón de piedra de San Rafael (Mendoza). Revista del Museo de La Plata, 4, 138-.

Silvestro, J., Kraemer, P., 2005. Evolución tecto-sedimentaria de la Cordillera Principal en el sector surmendocino a los 35° 30′ S, Faja plegada de Malargüe, Republica Argentina. 6° Congreso de Exploración y Desarrollo de Hidrocarburos, Artículo 25, Mar del Plata, CD-ROM.

Stoneley, R., 1983. Fibrous calcite veins, overpressures, and primary oil migration. American Association of Petroleum Geologists Bulletin, 67, 1427-1428.

Swarbrick, R.E., Osborne, M.J., Yardley G.S., 2002. Comparison of overpressure magnitude resulting from the main generating mechanisms. In: Huffman, A.R., Bowers, G.L. (Eds.), Pressure regimes in sedimentary Basins and their Prediction. American Association of Petroleum Geologists Memoir 76, 1-12.

Urien, C.M., Zambrano, J.J., 1994. Petroleum systems in the Neuquén Basin, Argentina. In: Magoon, L.B. & Dow, W.G. (eds) The Petroleum System — from Source to Trap. American Association of Petroleum Geologists, Memoirs, 60, 513–534.

Vergani, G.D., Tankard, A.J., Belotti, H.J., Welsink, H.J., 1995. Tectonic evolution and paleogeography of the Neuquén Basin, Argentina. In: Tankard, A.J., Suárez S., R., Welsink, H.J. (eds), Petroleum Basins of South America. American Association of

Petroleum Geologists, Memoirs, 62, 383–402.

Videla Leaniz, J.R., 1945. Informe mensual sobre los trabajos efectuados en abril 1945 (Comisión Carbón Mineral n° 55). Yacimientos Carboníferos Fiscales (unpublished report).

Villar, H.J., Legarreta, L., Cruz, C.E., Laffitte, G., Vergani, G., 2006. Los cinco sistemas petroleros coexistentes en el sector sudeste de la Cuenca Neuquina: definición geoquímica y comparación a lo largo de una transecta de 150 km. Boletín de Informaciones Petroleras, Cuarta época, 3, 50–66.

Witte, J., Bonora, M., Carbone, C., Oncken, O., 2012. Fracture evolution in oil-producing sills of the Rio Grande Valley, northern Neuquén Basin, Argentina. American Association of Petroleum Geologists Bulletin, 96 (7), 1253-1277.

Chapitre 4

Etude du bassin de Magellan, Argentine-Chili

4.1 Introduction

Dans ce Chapitre, nous abordons l'étude que nous avons réalisée dans le bassin sédimentaire de Magellan à l'extrême sud de l'Amérique du sud. Ce bassin d'avant-pays de la chaîne andine est l'un des plus épais du monde avec pas moins de 9 km de sédiments à certains endroits. Ce dernier subit une compression horizontale très intense qui affecte toute la série sédimentaire et en particulier la roche mère des hydrocarbures du bassin, la Formation Rio Jackson. Nous avons donc choisi d'étudier ce bassin pour appréhender les relations entre la maturation de la matière organique, les surpressions de fluides, la fracturation hydraulique et la déformation.

Des études précédentes ont montré que les surpressions de fluides pouvaient totalement modifier le style de déformation dans les sédiments. Ainsi, Cobbold et al. (2004) montrent que les décollements à la base de la roche mère dans le delta de l'Amazone sont vraissemblablement liés à la présence de surpression de fluides. Plus récemment et à la vue des nouvelles données sur le bassin de Magellan, Cobbold (2005) et Rojas et Mpodozis (2006) démontrent que les décollements de ce bassin sont situés à la base de la roche mère. Dans notre étude nous avons donc voulu savoir si des évidences de surpression de fluides étaient visibles, notamment dans les affleurements de la roche mère d'âge Crétacé. Des données pétrolières (cartes, coupes sismiques interprétées, et données de maturité) de la société ENAP, viennent compléter l'étude. Dans ce chapitre nous faisons le rapprochement entre la génération d'hydrocarbures, la déformation et les surpressions de fluides au sein même de la roche mère. Ainsi, dans la région de Vicuña (en Terre de feu, Chili), nous apportons des données inédites qui attestent de niveaux de décollements à la base de la roche mère. Les données de maturité, également fournies par ENAP, montrent que les décollements sont présents aux endroits où la roche mère est mature et a donc généré des hydrocarbures. De part la distribution des veines de beef, spécialement aux alentours des chevauchements connectés aux niveaux de décollements en profondeur, nous avons pu faire le lien entre les surpressions de fluides et l'apparition des niveaux de décollement dans la roche mère.

4.2 Article#4 Beef veins and thrust detachments in Early Cretaceous source rocks, foothills of Magallanes-Austral Basin, southern Chile and Argentina: structural evidence for fluid overpressure during hydrocarbon maturation

Notre étude du bassin de Magellan nous a conduit à la rédaction d’un article scientifique publié dans une édition spéciale de la revue *Marine and Petroleum Geology*. Cet article est disponible via le lien suivant :

http://www.sciencedirect.com/science/article/pii/S0264817213002584

4.2.1 Résumé de l’article

Nous décrivons (1) des veines de calcite fibreuse parallèles à la stratification de la roche (beef) et (2) des niveaux de décollement, tous deux traduisant des évidences de surpression de fluides dans les roches mères d’hydrocarbures. Nos exemples portent sur des données de surface ou de subsurface du bassin de Magellan se situant à l’extrême sud de l’Amérique du sud. Dans ce bassin, les meilleures roches mères sont d’âge Crétacé inférieur. Dans les parties centrales du bassin, les roches mères sont déjà surmatures, alors que sur la bordure est de ce dernier, en onshore et offshore, elles sont actuellement immatures ou en fenêtre de génération d’huile.

En Terre de feu, l’avant-pays des Andes consiste principalement en des roches sédimentaires affectées par des chevauchements de type ‘thin-skin’. Dans la région de Vicuña (Chili), les roches mères du Crétacé inférieur atteignent la surface juste au-dessus des niveaux de décollement. Ces derniers étant visibles sur les données sismiques et les données de puits. À la surface, nous avons identifié du ‘beef’, contenant des hydrocarbures (solides et/ou liquides) dans les formations de Rio Jackson et Vicuña qui ont atteint la fenêtre de génération de gaz humide. Dans la région de Rio Gallegos (Argentine), les roches mères n’ont pas atteint la surface. Cependant, les données de puits et de sismiques fournissent des évidences en faveur de chevauchements ‘thin-skin’ au-dessus de niveaux de décollement horizontaux dans la roche mère d’âge Crétacé inférieur, située dans la fenêtre à huile. À l’inverse, il n’y a aucune, ou très peu, de déformation dans les roches mères encore immatures. Ainsi, le front de déformation coincide avec le front de maturité. À proximité des zones centrales du bassin, où les roches mères ont atteint la surface, à l’intérieur de la chaîne centrale Andine, ces dernières ont subi un métamorphisme de bas-grade. À l'intérieur de ces roches mères, nous avons trouvé des veines de 'beef', mais cette fois constituées de quartz et non de calcite. À l'est, à l'intérieur de la chaîne d'avant-pays, les données de sismiques et de forages fournissent des évidences de quelques structures compressives, incluant des décollements 'thin-skin' dans les roches mères les plus enfouies. Finalement, dans la partie nord du bassin (province de Santa Cruz, Argentine), où ce dernier est moins profond, les roches mères ont atteint la surface dans la zone de la chaîne d'avant-pays au dessus de séries de rétro-chevauchements. Au Lago San Martin, les roches mères sont entrées dans la fenêtre à huile et contiennent du 'beef' de calcite.

En conclusion, dans les endroits où nous avons observé les roches mères d'âge Crétacé inférieur à la surface, celles-ci contenaient toutes du 'beef' de calcite (si elles avaient atteint la fenêtre de génération de l'huile ou du gaz humide) ou du 'beef' de quartz (si elles étaient surmatures). Indépendemment, des évidences de surpressions de fluides, sous la forme de niveaux de décollement, viennent des données de subsurface, en particulier dans la région de l'extrême sud du bassin où les roches mères ne sont pas surmatures et que la déformation est assez intense. De part les observations de cette étude, nous pensons que la génération d'hydrocarbures a conduit à une surpression de fluides, par le mécanisme de compaction chimique et le transfert de charge, ou de part des changements de volume, ou les deux.

4.2.2 Article#4

ARTICLE IN PRESS

Marine and Petroleum Geology xxx (2013) 1–12

Contents lists available at ScienceDirect

Marine and Petroleum Geology

journal homepage: www.elsevier.com/locate/marpetgeo

Beef veins and thrust detachments in Early Cretaceous source rocks, foothills of Magallanes-Austral Basin, southern Chile and Argentina: Structural evidence for fluid overpressure during hydrocarbon maturation

Alain Zanella [a,*], Peter R. Cobbold [a], Lisandro Rojas [b]

[a] Geosciences (UMR-6118), CNRS and Université de Rennes 1, 35042 Rennes, France
[b] ENAP-SIPETROL, Avenida Vitacura 2736, Santiago, Chile

ARTICLE INFO

Article history:
Received 31 July 2013
Received in revised form
9 October 2013
Accepted 15 October 2013
Available online xxx

Keywords:
Magallanes-Austral basin
Fluid overpressure
Beef veins
Thrust detachments
Source rocks

ABSTRACT

We describe (1) bedding-parallel veins of fibrous calcite (beef) and (2) thrust detachments, which we believe provide good evidence for fluid overpressure in source rocks for petroleum. Our examples are from the surface or subsurface of the Magallanes-Austral Basin, which lies at the southern tip of South America. There, the best source rocks for petroleum are of Early Cretaceous age. In the central parts of the basin these source rocks have become overmature, but at the eastern edge, onshore and offshore, they are today either immature or in the oil window.

In Tierra del Fuego, the foothills of the Andes consist mainly of sedimentary rocks, which have undergone thin-skinned thrusting. In the Vicuña area (Chile), Early Cretaceous source rocks have reached the surface above thrust detachments, which are visible on seismic data and well data. At the surface, we have found calcite beef, containing hydrocarbons (solid and/or fluid), in the Rio Jackson and Vicuña formations, which have reached the wet gas window. In the Rio Gallegos area (Argentina), the source rocks have not reached the surface, but seismic and well data provide good evidence for thin-skinned thrusting above flat-lying detachments in Early Cretaceous source rock, where it is in the early oil window. In contrast, there is little or no deformation where the source rock is still immature. Thus the deformation front coincides with the maturity front. Next to the central parts of the basin, where the source rocks have reached the surface within the Andes proper, they have undergone low-grade metamorphism. Within these source rocks, we have found beef veins, but of quartz, not calcite. To the east, within the foreland basin, seismic and well data provide evidence for a few compressional structures, including thin-skinned detachments in the deeply buried source rock. Finally, in the northern part of the basin (Santa Cruz province, Argentina), where it is shallower, the source rocks have reached the surface in the foothills, above a series of back-thrusts. At Lago San Martín, the source rocks have reached the oil window and they again contain calcite beef.

In conclusion, where we have examined Early Cretaceous source rocks at the surface, they contain either calcite beef (if they have reached the late oil window or wet gas window) or quartz beef (if they are overmature). Independent evidence for overpressure, in the form of source-rock detachments, comes from subsurface data, especially at the southern end of the basin, where the source rocks are not overmature and deformation is relatively intense. Thus we argue that hydrocarbon generation has led to overpressure, as a result of chemical compaction and load transfer, or volume changes, or both.

1. Introduction

Over the last few decades, there has been an increasing interest in mesoscopic structures, which provide evidence for overpressure within mature source rocks for petroleum. Examples of such structures are fault detachments within foreland basins (Cobbold, 1999, 2005) or deltas (Cobbold et al., 2004, 2009). Other

* Corresponding author.
E-mail addresses: alain.zanella@univ-rennes1.fr, zanella.alain@gmail.com (A. Zanella).

0264-8172/$ – see front matter © 2013 Elsevier Ltd. All rights reserved.
http://dx.doi.org/10.1016/j.marpetgeo.2013.10.006

Please cite this article in press as: Zanella, A., et al., Beef veins and thrust detachments in Early Cretaceous source rocks, foothills of Magallanes-Austral Basin, southern Chile and Argentina: Structural evidence for fluid overpressure during hydrocarbon maturation, Marine and Petroleum Geology (2013), http://dx.doi.org/10.1016/j.marpetgeo.2013.10.006

examples are hydrofractures, in other words, dilatant veins, which formed as a result of fluid overpressure, but filled progressively with solid material, such as fibrous minerals or bitumen. Physical modelling of the consequences of fluid overpressure (Cobbold and Castro, 1999) led to ideas on the importance of seepage forces (Mourgues and Cobbold, 2003), which can explain why veins form horizontally, for example parallel to bedding, as a result of fluid overpressure and tensile fracturing (Cobbold and Rodrigues, 2007). More recently, we have constructed more complex physical models, which include source layers of granular material (silica powder), containing, for example, 50% by volume of organic material (beeswax microspheres). On placing such models under water and heating the source layers up to 62 °C, the beeswax melts and the pressure of the pore fluid increases, from hydrostatic to lithostatic values, while horizontal hydrofractures form in the mixture and fill with migrating molten beeswax (Lemrabott and Cobbold, 2009; Zanella et al., 2010; Zanella and Cobbold, 2011, 2012, 2013; Zanella et al., 2013). Because the volume change, from solid to liquid wax, is no more than 15% or so (as it is for catagenesis of kerogen to oil), we infer that the overpressure is mainly due to load transfer, from the overburden to the pore fluid, as the solid framework collapses (compacts), by a process that is physically analogous to chemical compaction (Swarbrick et al., 2002).

Source rocks of the Neuquén Basin, Argentina, contain bedding-parallel hydrofractures, which have filled with bitumen (Borrello, 1956). On searching for similar features in the southern part of this basin, we discovered large numbers of bedding-parallel veins, not of bitumen, but of fibrous calcite (Rodrigues et al., 2009). Such veins are also common in the Wessex Basin of SW England, where in the early 1800s they received the names “beef”, or “cone-in-cone” (see historical review by Cobbold et al., 2013). Thus, the term ‘beef’ refers to fibrous minerals in bedding-parallel veins, where the fibres are approximately perpendicular to the margins. It turns out that calcite beef is also common in many other sedimentary basins worldwide, especially within layers of shale (Cobbold et al., 2013). In some examples, such shale layers also happen to be mature source rocks for petroleum and the beef contains hydrocarbons, either within fluid inclusions or as solid inclusions of bitumen between calcite fibres (Rodrigues et al., 2009; Cobbold et al., 2013).

On the strength of this work, we decided to visit the Magallanes-Austral Basin of Patagonia, one of the foreland basins in which thrust faults appear to have detached within mature source rock (Cobbold, 2005; Rojas and Mpodozis, 2006). Our aims were to confirm those detachments, but also to look for the possible presence of beef. On searching through the geological literature for the key words, “beef” or “cone-in-cone”, we discovered a few references to the latter within the Magellan Basin (Cobbold et al., 2013, Table 1). The earliest reference that we found was to cone-in-cone within Late Cretaceous strata on the western edge of the basin, near Puerto Natales, Chile (Cecioni, 1957). Later references were to cone-in-cone in Early Cretaceous source rock (Rio Mayer Fm) of Santa Cruz province, Argentina, at the northern end of the basin (Aguirre Urreta and Ramos, 1981; Riccardi et al., 1987). This area therefore became one of our strategic objectives.

2. Magallanes-Austral Basin

The Magallanes-Austral Basin lies in Patagonia, near the southern tip of South America (Fig. 1). Even before 1990, the area had a long history of geological exploration, including the search for petroleum (see, for example, Darwin, 1846; Hatcher, 1897; Windhausen, 1931; Kranck, 1932; Thomas, 1949; Feruglio, 1949; Katz, 1962, 1963; Scott, 1966; Barker, 1970; Riccardi, 1971; Leanza, 1972; Butterlin, 1972; Natland et al., 1974; Dalziel et al., 1974, 1979; Suárez and Pettigrew, 1976; Nelson et al., 1980; Riccardi and Rolleri, 1980; Dalziel, 1981; Caminos et al., 1981; Winslow, 1981, 1982, 1983; Mingramm, 1982; Ramos, 1982, 1989; Wilson and Dalziel, 1983; Dalziel, 1985; Lesta et al., 1985; Biddle et al., 1986; Laffitte et al., 1986; Milnes, 1987; Cagnolatti et al., 1987; Soffia et al., 1988; Dalziel and Brown, 1989).

In southern Patagonia, the Andes curve around, from an N–S to an E–W trend (Fig. 1). The bend reflects a special plate tectonic setting, between the Pacific plate in the W, the South American plate in the E and the Scotia plate in the S (Barker, 1970; Dalziel, 1981; Wilson, 1991). Currently, most of the Magallanes-Austral Basin lies on the eastern or northern sides of the Andes, but in the past the basin was wider, before the mountains encroached upon it, deforming its sedimentary infill. At the surface today, the infill is mostly of Cenozoic age. However, at depth the strata range in age from Late Jurassic to Cenozoic. In the central parts of the basin, near the Magellan Straits, the sedimentary infill is as thick as 8 km or more (Figs. 1B, 2). However, the basin shallows progressively to N and S, as well as to E and W.

The underlying basement, as visible in the Andes and a few deep wells, consists mainly of Palaeozoic metamorphic rocks, Jurassic volcanic rocks and plutonic rocks of various ages. In the Early Cretaceous, a marine transgression, in a tectonic context of rifting, led to deposition of organic-rich marine shale, which forms the main petroleum source rock of the basin. In contrast, in the Late Cretaceous, the basin became subject to multi-phase compression, in the foreland of the Andes. This context continued throughout the Tertiary and is ongoing today. As a result, in the western and southern parts of the basin, thrust faulting, strike-slip faulting and resulting exhumation have brought basement rocks and cover rocks to the surface, forming the foothills and main cordillera of the Andes (for details, see Caminos et al., 1981; Ramos, 1982, 1989, 2005; Lesta et al., 1985; Cagnolatti et al., 1987; Dalziel and Brown, 1989; Cunningham, 1993; Alvarez-Marrón et al., 1993; Kraemer, 1993, 1998, 2003; Uliana et al., 1995; Kraemer and Riccardi, 1997; Kraemer et al., 2002; Klepeis, 1994a, 1994b; Klepeis and Austin, 1997; Diraison et al., 1996, 1997a, 1997b, 2000; Coutand et al., 1999; Olivero et al., 1999; Olivero and Malumián, 1999, 2008; Olivero and Martinioni, 2001; Ghiglione, 2002; Ghiglione et al., 2002, 2009, 2012; Harambour, 2002; Fildani et al., 2003; Lodolo et al., 2003; Ghiglione and Ramos, 2005; Tassone et al., 2005; Ghiglione and Cristallini, 2007; Mpodozis and Rojas, 2006; Rojas and Mpodozis, 2006; Michel et al., 2008; Hubbard et al., 2008; Barbeau et al., 2009; Suárez et al., 2000; Torres Carbonell et al., 2011; Fosdick et al., 2011, 2013; Romans et al., 2011; Sánchez et al., 2010; Giacosa et al., 2012).

3. Petroleum systems

Exploration for petroleum has shown that the main source rocks in the Magallanes-Austral Basin are Early Cretaceous marine shales (Lower Palermo Aike or Lower Inoceramus Fm, Pampa Rincón Fm, Margas Verdes Fm, Rio Mayer Fm, Zapata Fm or Rio Jackson Fm, the name depending on the area), although a secondary source rock is lacustrine to marginal marine shale of the upper Jurassic Springhill Fm (Thomas, 1949; Laffitte et al., 1986; Biddle et al., 1986; Pittion and Gouadain, 1992; Urien et al., 1995; Pittion and Arbe, 1999; Zilli et al., 2002; Peroni et al., 2002; Rodríguez and Miller, 2005; Rodriguez and Cagnolatti, 2008; Rodríguez et al., 2008; Rossello et al., 2008; Legarreta and Villar, 2011; Ministerio de Planificación Federal, 2012). The main conventional reservoirs for oil and gas are Jurassic sands of the Springhill Fm. Other conventional reservoirs are in Upper Cretaceous or even Tertiary formations. For hydrocarbons to have reached the Springhill Fm requires either downward migration, or lateral migration across gently dipping strata (Pittion and Gouadain, 1992). In offshore Tierra del Fuego,

Please cite this article in press as: Zanella, A., et al., Beef veins and thrust detachments in Early Cretaceous source rocks, foothills of Magallanes-Austral Basin, southern Chile and Argentina: Structural evidence for fluid overpressure during hydrocarbon maturation, Marine and Petroleum Geology (2013), http://dx.doi.org/10.1016/j.marpetgeo.2013.10.006

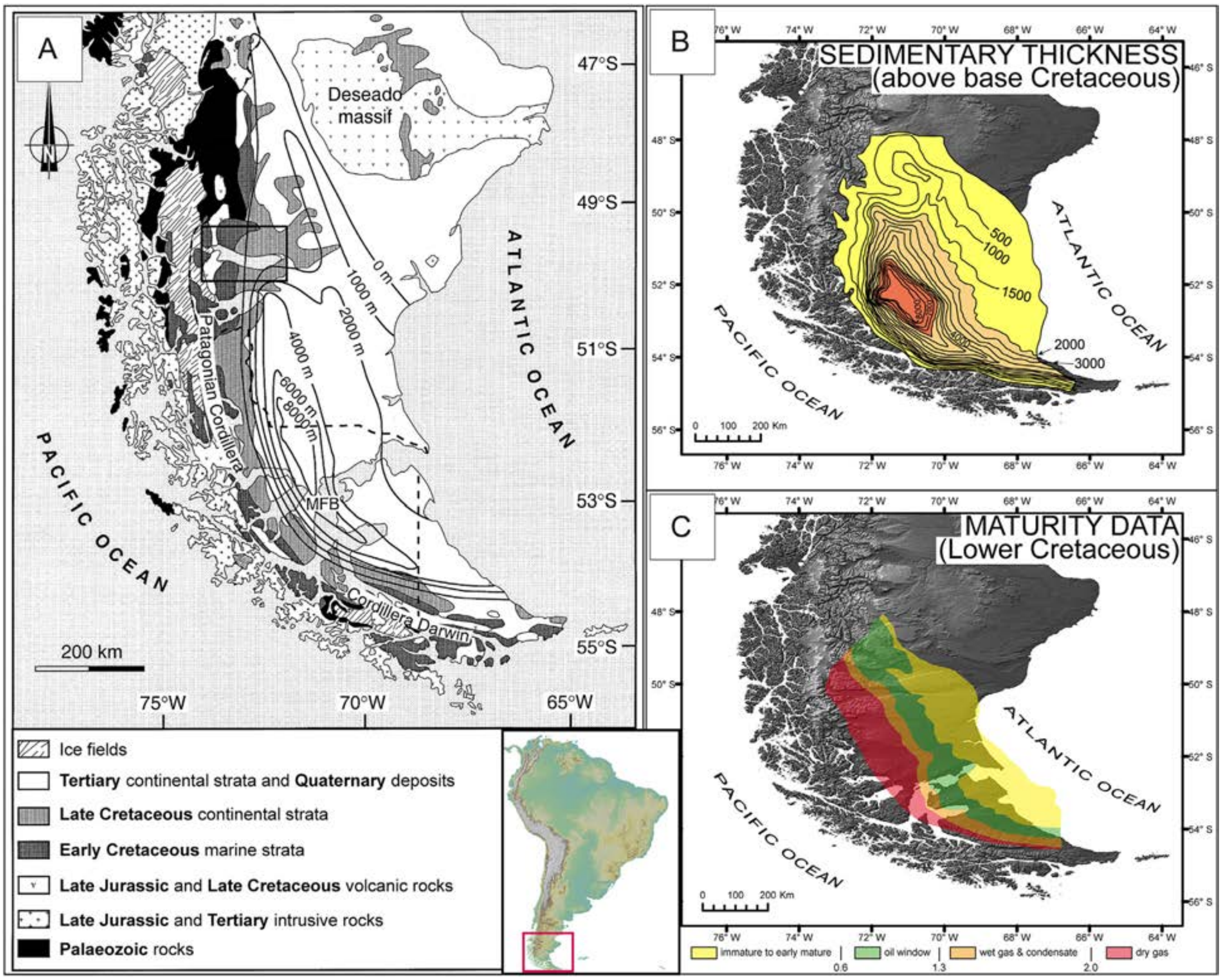

Figure 1. Magallanes-Austral Basin. A. Simplified geological map (modified, after Coutand et al., 1999). Inset (centre bottom) shows location of area (rectangle) in southern South America, against a background of altitude contours. B. Sedimentary thickness. Contours (in m below sea level) are on base Cretaceous (modified, after Ministerio de Planificación Federal, 2012). C. Maturity of Lower Cretaceous source rocks (modified, after Legarreta and Villar, 2011).

Argentina, oil production has come mainly from Springhill sands within a shallow foreland bulge, where Early Cretaceous source rock is immature. Thus migration must have occurred over horizontal distances of 20–150 km. It is likely that fluid overpressure within mature source rock assisted such migration. Indeed, some wells in the southern Magallanes-Austral Basin have encountered overpressures within conventional reservoirs or within source rock (see Law and Spencer, 1998; their Fig. 1). Independent evidence for

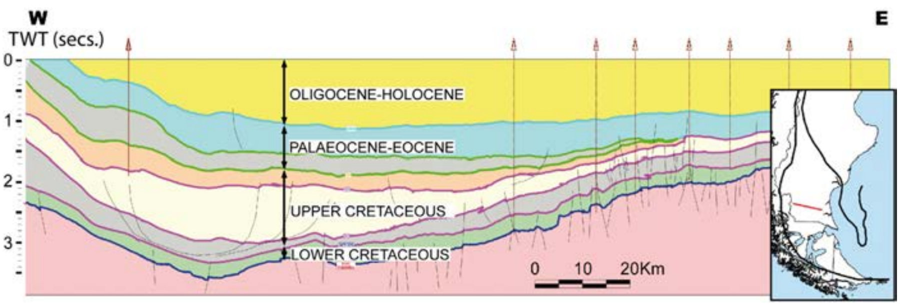

Figure 2. Geoseismic section, Magallanes-Austral Basin (modified, after Rodríguez et al., 2008). Vertical scale is in seconds, two-way time (TWT). Notice positions of 8 vertical wells, which provide good control on seismic data. Inset (bottom right) shows location of section (red line). (For interpretation of the references to colour in this figure legend, the reader is referred to the web version of this article.)

Please cite this article in press as: Zanella, A., et al., Beef veins and thrust detachments in Early Cretaceous source rocks, foothills of Magallanes-Austral Basin, southern Chile and Argentina: Structural evidence for fluid overpressure during hydrocarbon maturation, Marine and Petroleum Geology (2013), http://dx.doi.org/10.1016/j.marpetgeo.2013.10.006

overpressure at depth comes from an abundance of clastic dykes (sand injectites), for which the source material was Cretaceous sand at depths of several km (Winslow, 1983). An important question today is whether or not the Early Cretaceous source rock qualifies as an unconventional reservoir, containing commercially significant reserves of oil or gas (Ministerio de Planificación Federal, 2012).

4. Structures in Early Cretaceous source rock, Tierra del Fuego, Chile

The island of Tierra del Fuego lies at the southern end of the Magallanes-Austral Basin, where Early Cretaceous source rocks have undergone relatively little burial (Fig. 1B). In the foothills of the Andes, thin-skinned thrusting and exhumation have brought those same source rocks and their overburden to exposure, or close to it (Fig. 3A). In contrast, in the foreland, deformation has been less intense and the strata at the current surface are mostly Cenozoic. However, many years of hydrocarbon exploration have resulted in abundant sub-surface data. In the area around Rio Grande, Argentina, according to sub-surface data, thin-skinned thrusts have detached within Early Cretaceous source rock (Diraison et al., 1997b, Fig. 3C). On the strength of maturity data (mainly from Pittion and Gouadain, 1992), Cobbold (2005) inferred that the deformation front of the thrusts coincides relatively well with the maturity front (entry into the oil window), suggesting links between maturation, overpressure and detachment.

In Chile, on the basis of proprietary data from ENAP (2D seismic sections and geological maps), Alvarez-Marrón et al. (1993) described the structure of the thin-skinned fold-and-thrust belt in the Vicuña area, near the Lago Blanco (Fig. 3B). However, at that time the authors did not have access to well data. Therefore they interpreted the seismic profiles by line balancing or area balancing of cross sections. Although such methods limit the range of acceptable solutions, they do not provide unique answers. Thus Alvarez-Marrón et al. (1993) concluded that thin-skinned thrusts in the Vicuña area detached within Jurassic volcanic rocks of the Tobífera Fm. In contrast, by analogy with what has happened in Argentine Tierra del Fuego (Diraison et al., 1997b), Cobbold (2005) suggested that detachment in the Vicuña area occurred within Early Cretaceous source rock, as a result of overpressure during hydrocarbon generation. Rojas and Mpodozis (2006) confirmed this higher stratigraphical level of detachment, on the strength of newly available well data.

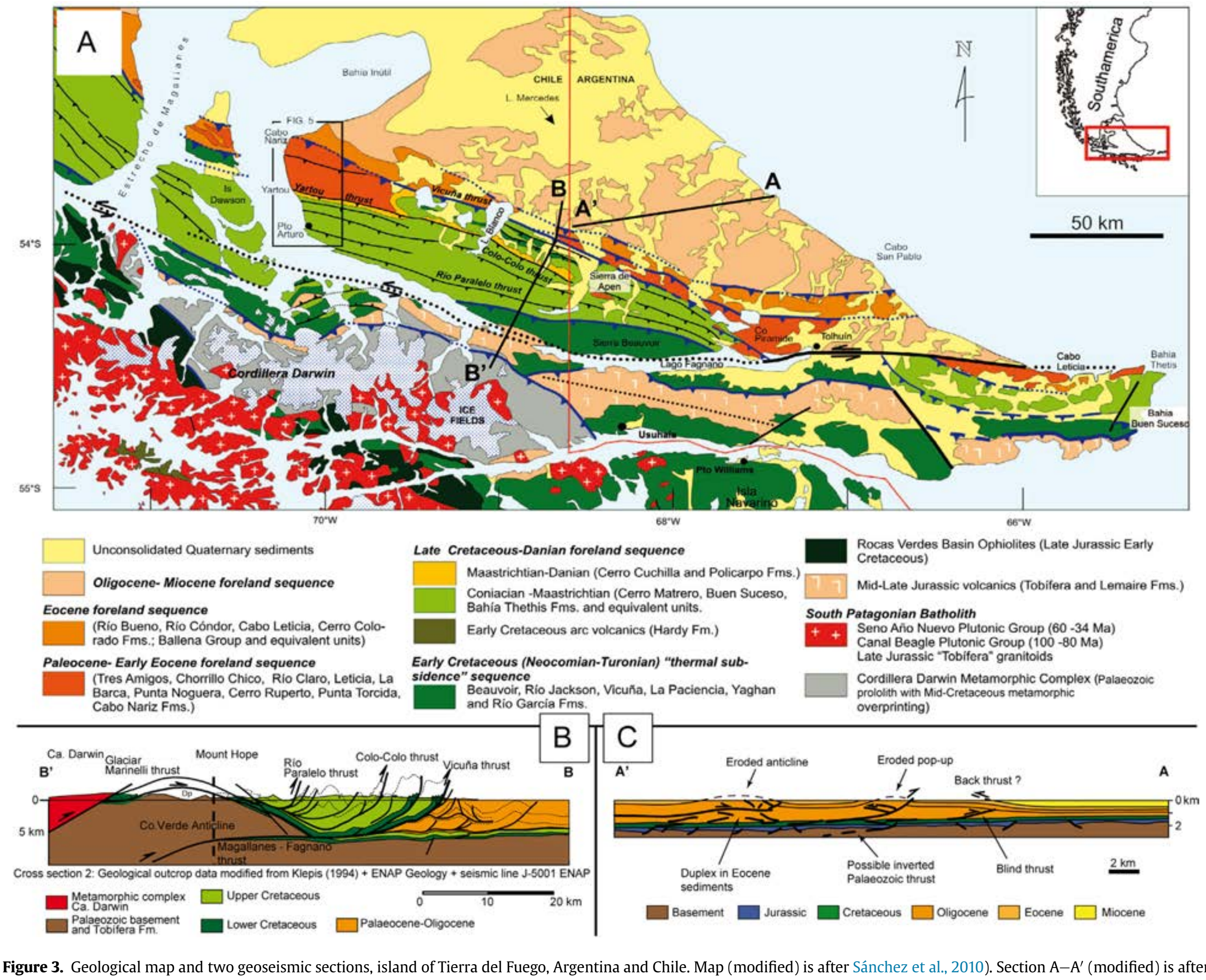

Figure 3. Geological map and two geoseismic sections, island of Tierra del Fuego, Argentina and Chile. Map (modified) is after Sánchez et al., 2010). Section A–A′ (modified) is after Diraison et al. (1997b). Section B–B′ (modified) is after Mpodozis and Rojas (2006). For corresponding section lines, see map.

Please cite this article in press as: Zanella, A., et al., Beef veins and thrust detachments in Early Cretaceous source rocks, foothills of Magallanes-Austral Basin, southern Chile and Argentina: Structural evidence for fluid overpressure during hydrocarbon maturation, Marine and Petroleum Geology (2013), http://dx.doi.org/10.1016/j.marpetgeo.2013.10.006

In such a context and to search for the possible presence of beef within source rocks, we visited the Vicuña area in January 2012. Here the sedimentary sequence (Early Cretaceous to Tertiary) dips southward, above a series of northward-verging thrust faults (Figs. 4 to 7A). We paid particular attention to the eastern shoreline of the Lago Blanco, where the sedimentary sequence and the structures crop out well. Next to thrust faults (major or minor), we found veins of beef, parallel or almost parallel to bedding (Fig. 7B). Under the optical microscope, such beef consists of calcite fibres, forming bedding-parallel zones or, locally, cone-in-cone structures (Fig. 7C). The beef also contains fragments of the surrounding host rock and dark inclusions. On breaking beef samples at outcrop with a geological hammer, we encountered strong odours of aromatic and volatile hydrocarbons, odours which are typical of hydrocarbons that have reached the wet gas window. In contrast, the surrounding shale did not yield such odours. We infer that the hydrocarbons were from inclusions within the calcite beef, as in other oil-producing basins (see Cobbold et al., 2013). Indeed, later analysis of beef samples from Vicuña, under a scanning electron microscope, confirmed the presence of hydrocarbons within dark patches, where carbon was the dominant element (Fig. 7D). In the future, geochemical analyses may be able to demonstrate whether or not such hydrocarbons derive from the surrounding Early Cretaceous shale.

So as better to constrain the geological context of our samples and our field observations, the Empresa Nacional del Petróleo (ENAP) provided us with (1) geological maps of the Vicuña area at a scale of 1:50,000 (e.g. Fig. 4), (2) 3 geological sections, one of which (Section 4, Fig. 5) follows a regional seismic section and 4 later wells, and (3) maturity data from one of those wells (Vicuña 2, Fig. 6). The maps and sections show thrust faults and multiple detachments, mostly within source rock of the marine Rio Jackson Fm (Early Cretaceous). At a depth of about 4 km, two major thrusts (Vicuña and Bahía Bell) diverge upward. Nearer the surface, these

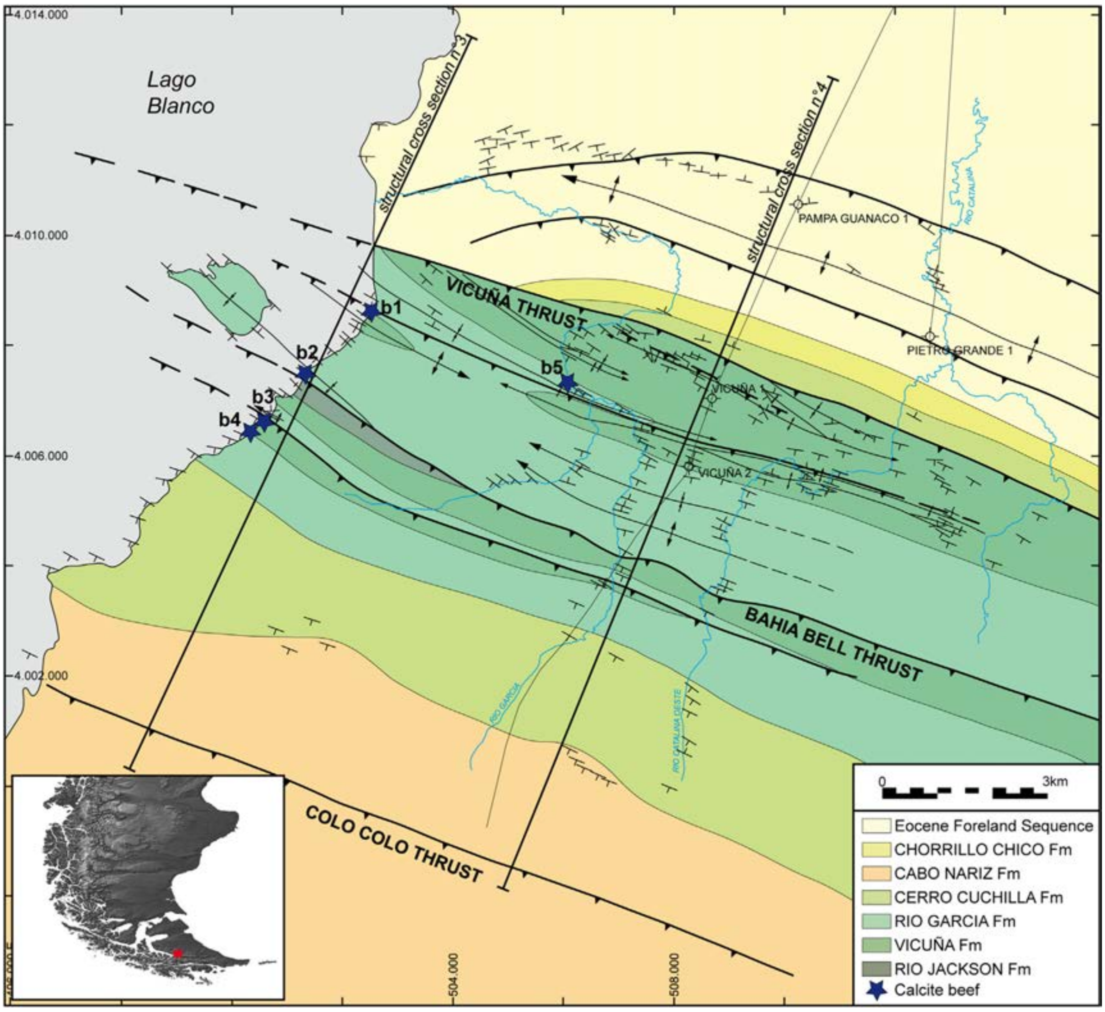

Figure 4. Geological map of western Vicuña area, Tierra del Fuego, Chile (data by courtesy of ENAP). Grey area (left) is the Lago Blanco. Black stars indicate localities (mainly along eastern shore of Lago Blanco) where we found calcite beef (see key). Sample numbers and their GPS coordinates are: b1 (54° 4′ 9.93″ S; 68° 57′ 29.12″ W), b2 (54° 4′ 31.83″ S; 68° 57′ 57.90″ W; b3 (54° 5′ 16.88″ S; 68° 59′ 25.38″ W), b4 (54° 5′ 21.76″ S; 68° 59′ 30.43″ W), b5 (54° 4′ 38.03″ S; 68° 54′ 21.97″ W). For structural cross sections (3 and 4), see Fig. 5. Circles indicate locations of wells (Vicuña 1, Vicuña 2, Pampa Guanaco 1, Pietro Grande 1). Inset (bottom left) shows location of map (red box). (For interpretation of the references to colour in this figure legend, the reader is referred to the web version of this article.)

Please cite this article in press as: Zanella, A., et al., Beef veins and thrust detachments in Early Cretaceous source rocks, foothills of Magallanes-Austral Basin, southern Chile and Argentina: Structural evidence for fluid overpressure during hydrocarbon maturation, Marine and Petroleum Geology (2013), http://dx.doi.org/10.1016/j.marpetgeo.2013.10.006

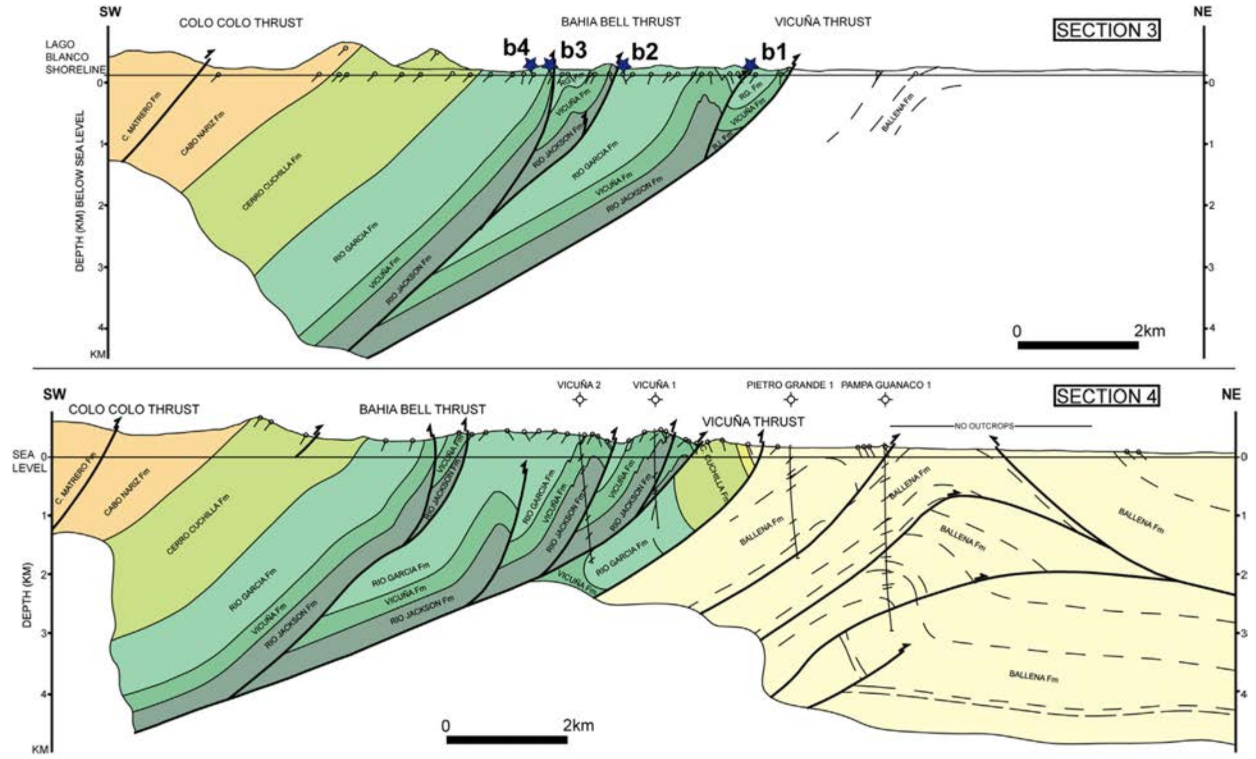

Figure 5. Geoseismic Sections 3 and 4, Vicuña area, Tierra del Fuego, Chile. Data are by courtesy of Empresa Nacional del Petróleo (ENAP). For section lines, see Fig. 4. Section 3 follows eastern shore of Lago Blanco, whereas Section 4 follows a seismic section and 4 steep wells (Pampa Guanaco 1, Pietro Grande 1, Vicuña 1, Vicuña 2). Major thrust faults have detached at base of Rio Jackson Fm (Early Cretaceous). Black stars (Section 3) indicate where we found calcite beef (see Fig. 4).

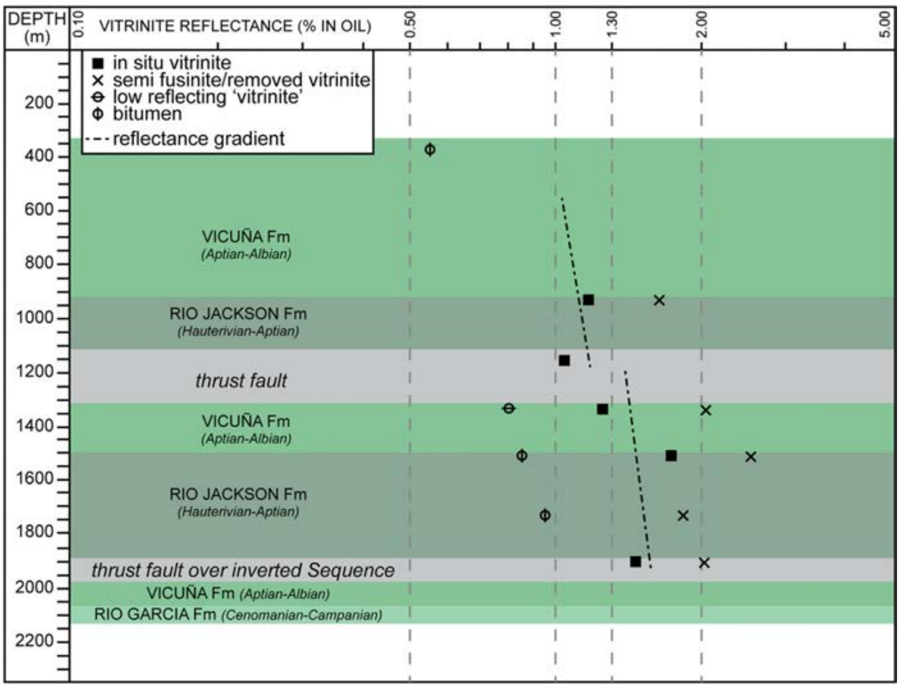

Figure 6. Maturity of source rock (% vitrinite reflectance) as a function of depth (in m) for Vicuña 2 well, Vicuña area, Tierra del Fuego, Chile (data by courtesy of ENAP). For location of well, see Figures 4 and 5.

Please cite this article in press as: Zanella, A., et al., Beef veins and thrust detachments in Early Cretaceous source rocks, foothills of Magallanes-Austral Basin, southern Chile and Argentina: Structural evidence for fluid overpressure during hydrocarbon maturation, Marine and Petroleum Geology (2013), http://dx.doi.org/10.1016/j.marpetgeo.2013.10.006

ARTICLE IN PRESS

A. Zanella et al. / Marine and Petroleum Geology xxx (2013) 1–12

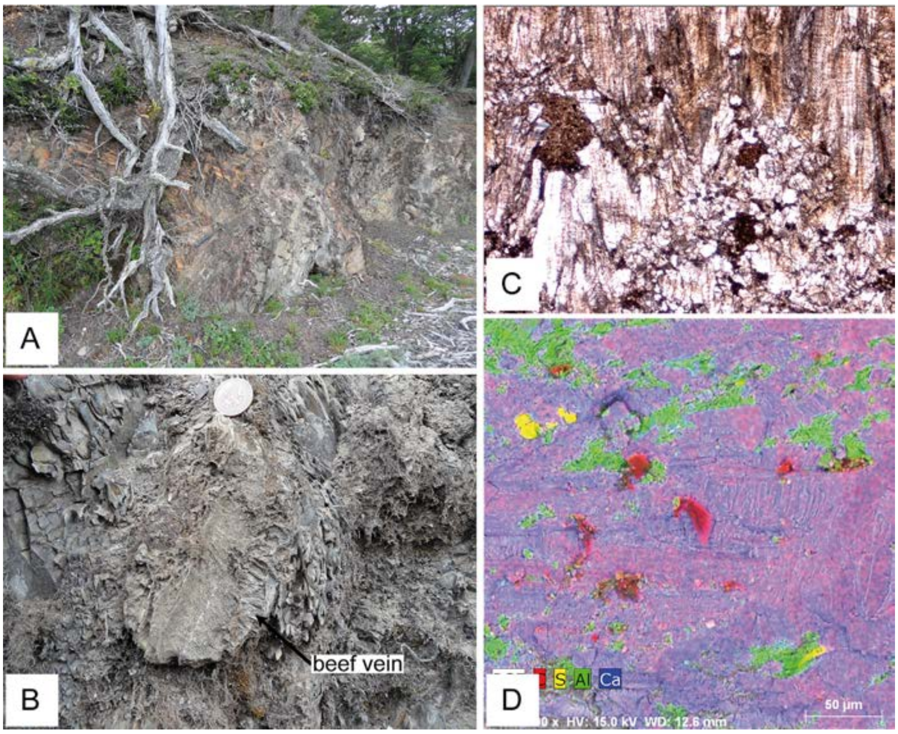

Figure 7. Calcite beef, shore of Lago Blanco, Vicuña area, Tierra del Fuego, Chile. A. View of Early Cretaceous shale and limestone, cropping out along low cliffs, eastern shore of Lago Blanco (locality b1, Fig. 4). B. Close-up of vein of calcite beef (centre of photograph, beneath coin for scale), within steeply dipping shale (locality b1, Fig. 4). C. Thin section of beef vein (here horizontal), showing calcite fibres (vertical), horizontal zonation of vein and opaque inclusions of country rock, minerals or hydrocarbons (locality b1, Fig. 4). D. Composite BSE (back-scattered electrons) and X-ray image showing the composition of part of beef vein (locality b2, Fig. 4). Intensities of colours reveal concentrations of elements (carbon, sulphur, aluminium, calcium). Concentration of carbon in dark patches is beyond that of calcite and is due to hydrocarbons.

major thrusts branch into a series of minor thrusts and hanging-wall anticlines. Two of the wells (Vicuña 1 and Vicuña 2) passed through the Vicuña Thrust and a hanging-wall splay, traversing the Rio Jackson Fm, before encountering overturned younger rocks (Section 4, Fig. 5). Thus there can be little doubt as to the structure and the stratigraphic level of the detachments. Moreover, the maturity data (vitrinite reflectance) for the Vicuña 2 well indicate that the source rock there, in the anticline and beneath the uppermost thrust (Fig. 5), reached the wet gas window (Fig. 6). Independently, available maturity data at the scale of the basin confirm that the source rock in the Vicuña area did indeed reach the wet gas window (Fig. 1C; Legarreta and Villar, 2011). At nearby Cabo Nariz (Fig. 3A), Sánchez et al. (2010) showed that the sedimentary sequence attained maximal burial during the Upper Palaeocene, when the Cerro Cuchilla Fm accumulated, prior to the onset of Neogene deformation and exhumation. The Cerro Cuchilla Fm also occurs, near the top of the sequence, in the southern Vicuña area (Figs. 4 and 5), lending credence to the idea of maximal burial, there as well, during the Upper Palaeocene. At that time, according to the stratigraphic thicknesses on geoseismic sections (Fig. 5), the Rio Jackson Fm would have reached a depth of about 4 km, which would have been enough to generate oil or wet gas, under normal thermal gradients (30 °C/km). On superimposing our beef localities and the geoseismic sections (Fig. 5), we found a good correlation between beef and detachments, all within the Early Cretaceous source rock. Thus the structural evidence at Vicuña is in favour of overpressure development during migration of aqueous fluids and hydrocarbons.

5. Structures in Early Cretaceous source rock, Lago San Martín

The area around Lago San Martín (49°S, Province of Santa Cruz, Argentina) is in the foothills of the Andes, at the northern end of the Magallanes-Austral Basin (Fig. 8A). Here (as in Tierra del Fuego), Early Cretaceous source rocks have undergone relatively little burial. According to a recent compilation by Giacosa et al. (2012), basement-involved faults functioned as thrusts in the Palaeozoic, reactivated as normal faults during Mesozoic rifting, then reactivated once again as thrusts in the Late Cretaceous to Present (Fig. 8B). Thus the thrusts have brought to the surface Palaeozoic metamorphic basement and igneous intrusive rocks of various ages. Overlying these unconformably are either Jurassic volcanic rocks (Tobífera Fm), or sedimentary strata of the Magallanes-Austral Basin. In general, the sedimentary strata dip gently eastward (Fig. 8B). However, thrust faults have caused repetitions. At the surface, many of the thrusts verge westward and involve basement (Giacosa et al., 2012). However, according to seismic sections along Lago Viedma, other thrusts would appear to detach at depth within the Early Cretaceous Rio Mayer Fm, which is the source rock for this part of the basin (Coutand et al., 1999). For elsewhere in the area of Lago San Martín, subsurface data are as yet unavailable to us, so that it is difficult for us to judge how much of the deformation may be thin-skinned. Further E, next to the Lago Cardiel, Early Cretaceous shale reaches the surface locally, in the core of a recumbent anticline, above a W-verging thrust fault. According to Ramos (1982), this fault involves basement. However, at the surface the fault would appear to dip gently eastward, so that an

Please cite this article in press as: Zanella, A., et al., Beef veins and thrust detachments in Early Cretaceous source rocks, foothills of Magallanes-Austral Basin, southern Chile and Argentina: Structural evidence for fluid overpressure during hydrocarbon maturation, Marine and Petroleum Geology (2013), http://dx.doi.org/10.1016/j.marpetgeo.2013.10.006

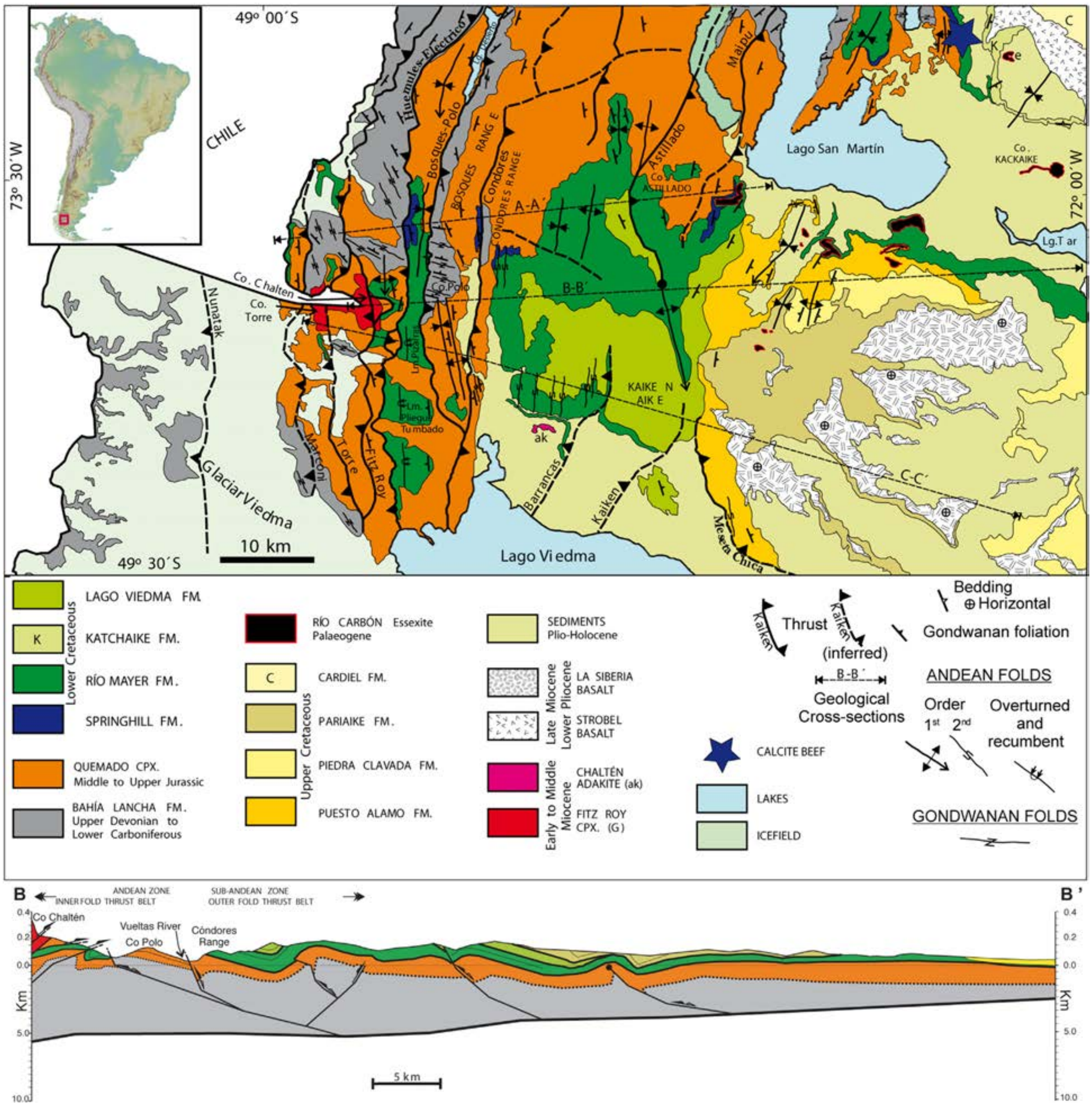

Figure 8. Geological map and section, area between Lago San Martín and Lago Viedma, Santa Cruz province, Argentina (modified, after Giacosa et al., 2012). Inset (top left) shows location of area (red rectangle). Section (B–B′) is from surface data only. Dark blue star (top right) indicates locality (GPS coordinates 49° 1′ 56.95″ S; 72° 11′ 22.36″ W), where we found calcite beef (see Fig. 9). (For interpretation of the references to colour in this figure legend, the reader is referred to the web version of this article.)

alternative interpretation is that it detaches, at least in part, within the Early Cretaceous sequence. In the future, new seismic data may help to define the structure more fully at depth.

To the N of Lago San Martín, near Bahía de La Lancha, the Cretaceous sequence crops out well, along the side of a wide glacial valley (Riccardi, 1971; Richiano, 2012; Richiano et al., 2012, Fig. 8A). In particular, the Early Cretaceous Rio Mayer Fm crops out along an incised river valley, where it consists of dark laminar shale and a few beds of limestone (Fig. 9A; Richiano, 2012). In general, the sequence here dips gently to the E. However, it also contains asymmetric folds and thrust faults, verging to the W, which appear to detach within it. At this locality we found several veins of fibrous calcite (beef), as well as a few veins of bitumen, all parallel or nearly parallel to bedding (Fig. 9B). Possibly the bitumen has resulted from abnormal heating, due to igneous intrusion of basaltic sills and dykes (the Rio Carbón essexite of Palaeogene age, Fig. 8A; Giacosa et al., 2012). As in the Vicuña area of Tierra del Fuego, so near Lago San Martín, scanning electron

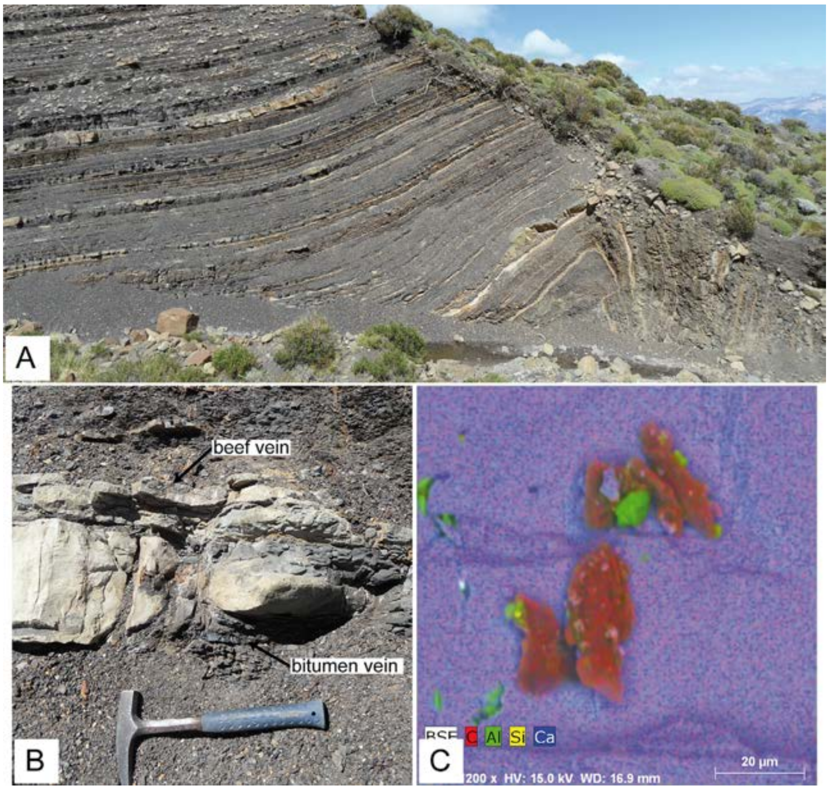

Figure 9. Calcite beef and bitumen veins near Bahía La Lancha, Lago San Martín (for map position, see Fig. 8). A. Outcrop of Lower Cretaceous shale (Rio Mayer Fm) in river valley (GPS coordinates: 49° 1′ 55.90″ S; 72°11′ 24.20″ W). B. Photograph of beef vein and bitumen vein. C. Composite BSE (back-scattered electrons) and X-ray image showing the composition of beef vein. Intensities of colours reveal concentrations of elements (carbon, aluminium, silica, calcium). Concentration of carbon in dark patches is beyond that of calcite and is due to hydrocarbons.

microscopy has revealed that the beef contains hydrocarbons (Fig. 9C). Thus the evidence at Lago San Martín is for overpressure development within Early Cretaceous source rock, during migration of aqueous fluids and hydrocarbons. Independently, available maturity data at the scale of the basin indicate that the source rock in this area has reached the late oil window (Fig. 1C; Legarreta and Villar, 2011).

6. Structures in other parts of the basin and at other stratigraphical levels

During our reconnaissance of the Magallanes-Austral Basin, we confirmed the presence of thrust detachments in many areas and we also found beef at other stratigraphical levels (Fig. 10). In western areas of the Andean foothills or cordillera, where Early Cretaceous source rock has reached high levels of maturity (dry gas window or beyond), we found beef, but of quartz, not of calcite. The quartz beef is in places somewhat fibrous, although not as strongly so as the calcite beef. Of the quartz beef that we found, the most numerous and continuous examples were in the Rio Jackson Fm of southern Tierra del Fuego, Chile, near the Lago Fagnano. However, other examples came to light on the mainland, within the cordillera of Chile and Argentina or to the W of it. Thus there would seem to be a direct correlation, between the mineralogical composition of beef and the maturity of the Early Cretaceous host rock.

In those same areas of the foothills or cordillera, on searching at higher stratigraphical levels, where Late Cretaceous strata have reached low degrees of maturity, we found calcite beef. According to the results of scanning electron microscopy (not shown here), some of that calcite beef contains hydrocarbons, raising obvious questions. For example, did overpressure and hydrocarbons originate within Late Cretaceous source rock, or did they form at deeper stratigraphic levels (within Early Cretaceous source rock) and at earlier stages of burial? In the future, geochemical studies may help to answer these questions.

7. Discussion

In general, throughout the Magellan-Austral Basin, we have found beef of various kinds within Early Cretaceous source rock. The mineralogical composition of the beef (calcite or quartz) correlates with the maturity of the source rock. Thus calcite beef occurs where the source rock has reached the oil window or the wet gas window, whereas quartz beef occurs where the source rock has reached the late gas window or is overmature. At the northern and southern ends of the basin, calcite beef in source rock contains hydrocarbons. We have not yet investigated the provenance of these hydrocarbons, but it is clear that they were migrating together with aqueous fluids, which were responsible for dissolving, transporting and precipitating calcite. Thus the evidence is for overpressure during hydrocarbon migration.

At the southern end of the basin (Vicuña area of Tierra del Fuego), calcite beef occurs in source rock, together with thrust detachments, which are visible at the surface and on subsurface data (from a seismic section and well core). Thus the evidence

Please cite this article in press as: Zanella, A., et al., Beef veins and thrust detachments in Early Cretaceous source rocks, foothills of Magallanes-Austral Basin, southern Chile and Argentina: Structural evidence for fluid overpressure during hydrocarbon maturation, Marine and Petroleum Geology (2013), http://dx.doi.org/10.1016/j.marpetgeo.2013.10.006

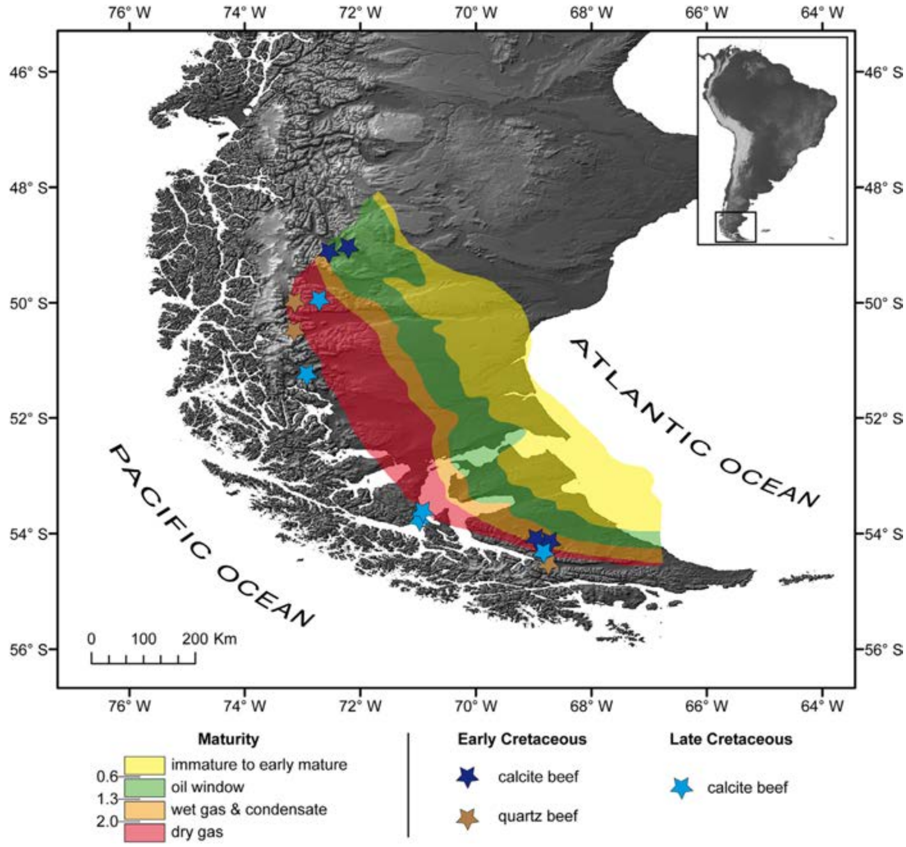

Figure 10. Composition and provenance of beef, by comparison with maturity of Early Cretaceous source rock, Magallanes-Austral Basin. Maturity data (background colours, see Fig. 1C) are after Legarreta and Villar (2011). For Early Cretaceous source rock, beef is of calcite (dark blue stars) or of quartz (yellow stars), depending on thermal maturity. For Late Cretaceous shale, beef is of calcite (light blue stars). (For interpretation of the references to colour in this figure legend, the reader is referred to the web version of this article.)

there, for overpressure during hydrocarbon migration, is doubly strong.

By comparison of our field data with the results of physical modelling (Zanella et al., 2013), we argue that hydrocarbon generation in the Magallanes-Austral Basin has led to overpressure as a result of chemical compaction and load transfer, or volume changes, or both.

8. Conclusions

Throughout the Magallanes-Austral basin, where we have been able to examine Early Cretaceous source rocks at the surface, they contain either calcite beef (if they have reached the late oil window or wet gas window) or quartz beef (if they are overmature). Independent evidence for overpressure, in the form of source-rock detachments, comes from subsurface data, especially at the southern end of the basin, where the source rocks are not overmature and deformation is relatively intense. Thus we infer that hydrocarbon generation has led to overpressure. By comparison with physical models, we suspect that the mechanism of overpressuring is load transfer during chemical compaction, although volume changes probably contributed.

Acknowledgements

We are especially grateful to (1) Empresa Nacional del Petróleo (ENAP), Chile, for providing data for the Vicuña area, and (2) Statoil, for funding the PhD project of Alain Zanella. Gilles Ruffet and Fernando Poblete provided assistance in the field and with shipping samples from Chile, whereas Héctor Leanza helped to ship samples from Argentina. At the Statoil Research Centre in Trondheim, Norway, A. Boassen conducted analyses under an environmental scanning electron microscope (ESEM).

References

Aguirre Urreta, M.B., Ramos, V.A., 1981. Estratigrafía y paleontología de la alta cuenca del Río Roble, provincia de Santa Cruz. 8° Congreso Geológico Argentino. Actas 3, 101–138.
Alvarez-Marrón, J., McClay, K.R., Harambour, S., Rojas, L., Skarmeta, J., 1993. Geometry and evolution of the frontal part of the Magallanes Foreland Thrust and Fold Belt (Vicuña area), Tierra del Fuego, southern Chile. Am. Assoc. Pet. Geol. Bull. 77, 1904–1921.
Barbeau, D.L., Olivero, E.B., Swanson-Hysell, N.L., Zahid, K.M., Murray, K.E., Gehrels, G.E., 2009. Detrital-zircon geochronology of the eastern Magallanes foreland basin: implications for Eocene kinematics of the northern Scotia Arc and Drake Passage. Earth Planet. Sci. Lett. 284, 489–503.
Barker, 1970. Plate tectonics of the Scotia Sea region. Nature 228, 1293–1296.
Biddle, K.T., Uliana, M.A., Mitchum, R.M., Fitzgerald, M.G., Wright, R.C., 1986. The stratigraphic and structural evolution of the central and eastern Magallanes Basin, southern South America. In: Allen, P.A., Homewood, P. (Eds.), Foreland Basins, International Association of Sedimentologists, Special Publication, 8, pp. 41–66.
Borrello, A.V., 1956. Recursos minerales de la República Argentina. III. Combustibles sólidos minerales. Revista del Instituto Nacional de Investigación de las Ciencias Naturales y Museo Argentino de Ciencias Naturales «Bernardino Rivadavia». Ciencias Geol. 5, 1–665.
Butterlin, J., 1972. Comparaison des caractères structuraux de la cordillère Caraïbe (Vénézuela) et de la cordillère Magellanienne (Chili-Argentine). In: 6th Caribbean Geological Conference, Transactions, 6, pp. 265–273.

Please cite this article in press as: Zanella, A., et al., Beef veins and thrust detachments in Early Cretaceous source rocks, foothills of Magallanes-Austral Basin, southern Chile and Argentina: Structural evidence for fluid overpressure during hydrocarbon maturation, Marine and Petroleum Geology (2013), http://dx.doi.org/10.1016/j.marpetgeo.2013.10.006

Cagnolatti, M., Covellone, G., Erlicher, J., Fantin, F., 1987. Fallamiento y plegamiento de cobertura al suroeste del Rio Grande, Cuenca Austral, Tierra del Fuego, Argentina. In: 10° Congreso Geológico Argentino, San Miguel de Tucumán, Actas, 1, pp. 149–152.
Caminos, R., Haller, M., Lapido, O., Lizuain, A., Page, R., Ramos, V.A., 1981. Reconocimiento geológico de los Andes Fueguinos, Territorio Nacional de Tierra del Fuego. In: 8° Congreso Geológico Argentino (San Luis), Actas, 3, pp. 759–786.
Cecioni, G.O., 1957. Cretaceous flysch and molasse in Departamento Ultima Esperanza, Magallanes province, Chile. Am. Assoc. Pet. Geol. Bull. 41, 538–564.
Cobbold, P.R., 1999. Hydrocarbon Generation, Fluid Overpressure and Source Rock Detachments in Thrust Belts. Thrust Tectonics 99, Egham, Extended Abstracts, pp. 7–9.
Cobbold, P.R., 2005. Hydrocarbon Generation, a Mechanism of Detachment in Thin-skinned Thrust Belts. Joint Earth Science Meeting on Thrust belts and Foreland basins. Société Géologique de France and Sociedad Geológica de España, Rueil-Malmaison, France, pp. 104–107. Abstracts Volume.
Cobbold, P.R., Castro, L., 1999. Fluid pressure and effective stress in sandbox models. Tectonophysics 301, 1–19.
Cobbold, P.R., Rodrigues, N., 2007. Seepage forces, important factors in the formation of horizontal hydraulic fractures and bedding-parallel fibrous veins ("beef" and "cone-in-cone"). Geofluids 7, 313–322. http://dx.doi.org/10.1111/j.1468-8123.2007.00183.x.
Cobbold, P.R., Mourgues, R., Boyd, K., 2004. Mechanism of thin-skinned detachment in the Amazon Fan: assessing the importance of fluid overpressure and hydrocarbon generation. Mar. Pet. Geol. 21, 1013–1025.
Cobbold, P.R., Clarke, B.J., Løseth, H., 2009. Structural consequences of fluid overpressure and seepage forces in the outer thrust belt of the Niger Delta. Pet. Geosci. 15, 3–15.
Cobbold, P.R., Zanella, A., Rodrigues, N., Løseth, H., 2013. Bedding-parallel fibrous veins (beef and cone-in-cone): worldwide occurrence and possible significance in terms of fluid overpressure, hydrocarbon generation and mineralization. Mar. Pet. Geol. 43, 1–20. http://dx.doi.org/10.1016/j.marpetgeo.2013.01.010.
Coutand, I., Diraison, M., Cobbold, P.R., Gapais, D., Rossello, E.A., Miller, M., 1999. Structure and kinematics of a foothills transect, Lago Viedma, southern Andes (49°30'S). J. South Am. Earth Sci. 12, 1–15.
Cunningham, W.D., 1993. Strike-slip faults in the southernmost Andes and the development of the Patagonian Orocline. Tectonics 12, 169–186.
Dalziel, I.W.D., 1981. Back-arc extension in the southern Andes, a review and critical reappraisal. Phil. Trans. R. Soc. Lond. A 300, 319–335.
Dalziel, I.W.D., 1985. Collision and cordilleran orogenesis: an Andean perspective. In: Coward, M.P., Ries, A.C. (Eds.), Collision Tectonics, Geological Society, London, Special Publications, 19, pp. 389–404.
Dalziel, I.W.D., Brown, R.L., 1989. Tectonic denudation of the Cordillera Darwin metamorphic core complex in the Andes of Tierra del Fuego, southernmost Chile: implications for Cordilleran Orogenesis. Geology 17, 699–703.
Dalziel, I.W.D., Palmer, F.K., 1979. Progressive deformation and orogenic uplift at the southern extremity of the Andes. Geol. Soc. Am. Bull. 90, 259–280.
Dalziel, I.W.D., de Wit, M.J., Palmer, F.K., 1974. Fossil marginal basin in the southern Andes. Nature 250, 291–294.
Darwin, C., 1846. Geological Observations on South America: Being the Third Part of the Geology of the Voyage of the Beagle. Smith, Elder and Co, London, p. 279.
Diraison, M., Cobbold, P.R., Gapais, D., Rossello, E.A., 1996. Tertiary kinematics of the southern Andes and the development of the Magellan foreland basin (Patagonia). In: Andean Geodynamics. O.R.S.T.O.M. éditions, Paris, pp. 347–350.
Diraison, M., Cobbold, P.R., Gapais, D., Rossello, E.A., 1997a. Magellan Strait: part of a Neogene rift system. Geology 25, 703–706.
Diraison, M., Cobbold, P.R., Gapais, D., Rossello, E.A., Gutiérrez Pleimling, A., 1997b. Neogene tectonics within the Magellan basin (Patagonia). 6° Simposio Bolivariano, Petroleum exploration in the Subandean basins, Cartagena de Indias, Colombia. Memorias 1, 1–14.
Diraison, M., Cobbold, P.R., Gapais, D., Rossello, E.A., Le Corre, C., 2000. Cenozoic crustal thickening, wrenching and rifting in the foothills of the southernmost Andes. Tectonophysics 316, 91–119.
Feruglio, E., 1949. Descripción geológica de la Patagonia. In: Dirección General Y.P.F., 1, pp. 1–334.
Fildani, A., Cope, T.D., Graham, S.A., Wooden, J.L., 2003. Initiation of the Magallanes foreland basin: timing of the southernmost Patagonian Andes orogeny revised by detrital zircon provenance analysis. Geology 31, 1081–1084.
Fosdick, J.C., Romans, B.W., Fildani, A., Bernhardt, A., Calderón, M., Graham, S.A., 2011. Kinematic evolution of the Patagonian retroarc fold-and-thrust belt and Magallanes foreland basin, Chile and Argentina, 51°30'S. Geol. Soc. Am. Bull. 123, 1679–1698. http://dx.doi.org/10.1130/B30242.1.
Fosdick, J.C., Grove, M., Hourigan, J.K., Calderón, M., 2013. Retroarc deformation and exhumation near the end of the Andes, southern Patagonia. Earth Planet. Sci. Lett. 361, 504–517.
Ghiglione, M.C., 2002. Diques clásticos asociados a deformación transcurrente en depósitos sinorogénicos del Mioceneo inferior de la cuenca Austral. Asoc. Geol. Argentina Rev. 57, 103–118.
Ghiglione, M.C., Cristallini, E.O., 2007. Have the southernmost Andes been curved since Late Cretaceous time? an analog test for the Patagonian orocline. Geology 35, 13–16.
Ghiglione, M.C., Ramos, V.A., 2005. Progression of deformation and sedimentation in the southernmost Andes. Tectonophysics 405, 25–46.
Ghiglione, M.C., Ramos, V.A., Cristallini, E.O., 2002. Fuegian Andes foreland fold and thrust belt: structure and growth strata. Revista Geol. Chile 29, 17–41.
Ghiglione, M.C., Suárez, F., Ambrosio, A., Da Poian, G., Cristallini, E.O., Pizzio, M.F., Reinoso, R.M., 2009. Structure and evolution of the Austral Basin fold-thrust belt, southern Patagonian Andes. Asociación Geológica Argentina. Revista 65, 215–226.
Ghiglione, M.C., Navarrete-Rodríguez, A.T., González-Guillot, M., Bujalesky, G., 2012. The opening of the Magellan Strait and its geodynamic implications. Terra Nova 25, 13–20.
Giacosa, R., Fracchia, D., Heredia, N., 2012. Structure of the southern Patagonian Andes at 49°S, Argentina. Geol. Acta 10, 265–282.
Harambour, S.M., 2002. Deep-seated Thrusts in the Frontal Part of the Magallanes Fold and Thrust Belt, Ultima Esperanza, Chile. In: 15° Congreso Geológico Argentino, Actas, 3, p. 232.
Hatcher, J.B., 1897. On the geology of Southern Patagonia. Am. J. Sci. 4, 321–354.
Hubbard, S.M., Romans, B.W., Graham, S.A., 2008. Deep-water foreland basin deposits of the Cerro Toro Formation, Magallanes Basin, Chile: architectural elements of a sinuous basin axial channel belt. Sedimentology 55, 1333–1359.
Katz, H.R., 1962. Fracture patterns and structural history in the sub-Andean belt of southernmost Chile. J. Geol. 70, 593–603.
Katz, H.R., 1963. Revision of Cretaceous stratigraphy in Patagonian cordillera of Ultima Esperanza, Magallanes province, Chile. Am. Assoc. Pet. Geol. Bull. 47, 506–524.
Klepeis, K.A., 1994a. Relationship between uplift of the metamorphic core of the southernmost Andes and shortening in the Magallanes foreland fold and thrust belt, Tierra del Fuego, Chile. Tectonics 13, 882–904.
Klepeis, K.A., 1994b. The Magallanes and Deseado fault zones: major segments of the South American-Scotia transform plate boundary in southernmost South America, Tierra del Fuego. J. Geophys. Res. 99, 22001–22014.
Klepeis, K.A., Austin, J.A., 1997. Contrasting styles of superposed deformation in the southernmost Andes. Tectonics 16, 755–776.
Kraemer, P.E., 1993. Perfil estructural de la Cordillera Patagónica Austral a los 50° L.S., Santa Cruz. In: 12° Congreso Geológico Argentino y 2° Congreso de Exploración de Hidrocarburos, Buenos Aires, Actas, 3, pp. 119–125.
Kraemer, P.E., 1998. Structure of the Patagonian Andes: regional balanced cross section at 50°S, Argentina. Int. Geology. Rev. 40, 896–915.
Kraemer, P.E., 2003. Orogenic shortening and the origin of the Patagonian orocline (56°S. Lat). J. South Am. Earth Sci. 15, 731–748.
Kraemer, P.E., Riccardi, A.C., 1997. Estratigrafía de la región comprendida entre los lagos Argentino y Viedma (49° 40'–50° 10' lat. S), Provincia de Santa Cruz. Asoc. Geol. Argentina Rev. 52, 333–360.
Kraemer, P.E., Ploskiewicz, Ramos, V.A., 2002. Estructura de la Cordillera Patagónica Austral entre los 46° y 52° S. In: Haller, M.J. (Ed.), Geología y Recursos Naturales de Santa Cruz, 15° Congreso Geológico Argentino, El Calafate, Relatorio, pp. 353–364.
Kranck, E.H., 1932. Geological investigations in the Cordillera of Tierra del Fuego. Acta Geogr. (Helsinki) 4, 1–231.
Laffitte, G.A., Arias, W.E., Marinelli, R.V., 1986. Caracterización térmica de la F. Springhill, Cuenca Austral. Relación con el entrampamiento de hidrocarburos. In: 60 Reunión Anual a Nivel de Expertos, Lima, Perú, Exploración, Actas, pp. 70–78.
Law, B.E., Spencer, C.W., 1998. Abnormal pressures in hydrocarbon environments. In: Law, B.E., Ulmishek, G.F., Slavin, V.I. (Eds.), Abnormal Pressures in Hydrocarbon Environments, American Association of Petroleum Geologists, Memoir, 70, pp. 1–11.
Leanza, A.F., 1972. Andes Patagónicos Australes. In: Geología Regional Argentina. Academia Nacional de Ciencias, Córdoba, pp. 689–706.
Legarreta, L., Villar, H.J., 2011. Geological and Geochemical Keys of the Potential Shale Resources, Argentina Basins. American Association of Petroleum Geologists, Geoscience Technology Workshop, "Unconventional Resources: Basics, Challenges, and Opportunities for New Frontier Plays, " Buenos Aires, Argentina. June 26-28, 2011, Search and Discovery Article # 80196(2011) http://www.searchanddiscovery.com.
Lemrabott, A., Cobbold, P.R., 2009. Physical Modeling of Fluid Overpressure and Compaction during Hydrocarbon Generation in Source Rock of Low Permeability. American Association of Petroleum Geologists, International Conference and Exhibition, Rio de Janeiro, Brazil, 15–18 November. Search and Discovery Article #40518 (2010) http://www.searchanddiscovery.com.
Lesta, P.J., Digregorio, J., Mozetic, M.E., 1985. Presente y futuro de la exploración de petróleo en las cuencas subandinas, Argentina. In: 2° Simposio Bolivariano, Exploración Petrolera en las Cuencas Subandinas, Asociación Colombiana de Geólogos y Geofísicos del Petróleo (ACGGP), Bogotá, Publicaciones, 3, pp. 1–35.
Lodolo, E., Menichetti, M., Bartole, R., Ben-Avraham, Z., Tassone, A., Lippai, H., 2003. Magallanes-Fagnano continental transform fault (Tierra del Fuego, southernmost South America). Tectonics 22, 1076.
Michel, J., Baumgartner, L., Putlitz, B., Schaltegger, U., Ovtcharova, M., 2008. Incremental growth of the Patagonian Torres del Paine laccolith over 90 k.y. Geology 36, 459–462.
Milnes, A.G., 1987. Tectonic evolution of the southern Andes, Tierra del Fuego: a summary. In: Schaer, J.P., Rodgers, J. (Eds.), The Anatomy of Mountain Ranges. Princeton University Press, pp. 173–177.
Mingramm, A.R.G., 1982. Evolution scheme of Fueguian Andes along Los Cerros - Pla Hardy Section, Shell Compañía Argentina de Petróleo (unpublished report).
Ministerio de Planificación Federal, 2012. Cuenca Austral. http://www.energia.gov.ar/contenidos/verpagina.php?idpagina=814.
Mourgues, R., Cobbold, P.R., 2003. Some tectonic consequences of fluid overpressures and seepage forces as demonstrated by sandbox modelling. Tectonophysics 376, 75–97.

Please cite this article in press as: Zanella, A., et al., Beef veins and thrust detachments in Early Cretaceous source rocks, foothills of Magallanes-Austral Basin, southern Chile and Argentina: Structural evidence for fluid overpressure during hydrocarbon maturation, Marine and Petroleum Geology (2013), http://dx.doi.org/10.1016/j.marpetgeo.2013.10.006

Mpodozis, C., Rojas, L., 2006. Orogénesis en los Andes Patagónicos Australes de Tierra del Fuego: cierre de una “cuenca marginal” o colisión intracontinental?. In: 11° Congreso Geológico Chileno, Actas, 1, pp. 329–332.
Natland, M.L., González, E., Cañón, A., Ernst, M., 1974. A system of stages for correlation of Magallanes Basin sediments. Geol. Soc. Am. Mem. 139, 1–126.
Nelson, E.P., Dalziel, I.W.D., Milnes, A.G., 1980. Structural geology of the Cordillera Darwin – collision style orogenesis in the southernmost Andes. Eclo. Geol. Helvet. 73, 727–751.
Olivero, E.B., Malumián, N., 1999. Eocene stratigraphy of southeastern Tierra del Fuego island, Argentina. Am. Assoc. Pet. Geol. Bull. 83, 295–313.
Olivero, E.B., Malumián, N., 2008. Mesozoic-cenozoic stratigraphy of the Fuegian Andes, Argentina. Geol. Acta 6, 5–18.
Olivero, E.B., Martinioni, D.R., 2001. A review of the geology of the Argentinian Fueguian Andes. J. South Am. Earth Sci. 14, 175–188.
Olivero, E.B., Martinioni, D.R., Malumián, N., Palamarczuk, S., 1999. Bosquejo geológico de la Isla Grande de Tierra del Fuego, Argentina. In: 14° Congreso Geológico Argentino, Salta, Actas, 1, pp. 291–294.
Peroni, G., Cagnolatti, M., Pedrazzini, M., 2002. Cuenca Austral: Marco geológico y reserva histórica de la actividad petrolera. In: Schiuma, M., Hinterwimmer, G., Vergani, G. (Eds.), Rocas reservorio de las cuencas productivas de la Argentina, 5° Congreso de Exploración y Desarrollo de Hidrocarburos, Mar del Plata, pp. 11–26.
Pittion, J.-L., Arbe, H.A., 1999. Sistemas petroleros de la Cuenca Austral. In: 14° Congreso de Exploración y Desarrollo de Hidrocarburos, Mar del Plata, Actas, 1, pp. 239–262.
Pittion, J.L., Gouadain, J., 1992. Source-rocks and Oil Generation in the Austral Basin. Thirteenth World Petroleum Congress, Buenos Aires, Proceedings. John Wiley & Sons, New York, 2, pp. 113–120.
Ramos, V.A., 1982. Geología de la region del Lago Cardiel, Provincia de Santa Cruz. Asoc. Geol. Argentina Rev. 37, 23–49.
Ramos, V.A., 1989. Andean foothills structures in the northern Magallanes Basin, Argentina. Am. Assoc. Pet. Geol. Bull. 73, 887–903.
Ramos, V.A., 2005. Seismic ridge subduction and topography: foreland deformation in the Patagonian Andes. Tectonophysics 399, 73–86.
Riccardi, A.C., 1971. Estratigrafía en el oriente de Bahía La Lancha, Lago San Martín, Santa Cruz, Argentina. Rev. Museo La. Plata 7, 245–318.
Riccardi, A.C., Rolleri, E.O., 1980. Cordillera Patagónica Austral. In: Segundo Simposio de Geología Regional Argentina, Actas, 2, pp. 1173–1306.
Riccardi, A.C., Aguirre Urreta, M.B., Medina, F.A., 1987. Aconeceratidae (Ammonitina) from the Hauterivian-Albian of southern Patagonia. Palaeontogr., Abt. A 196, 105–185.
Richiano, S., 2012. Sedimentología e icnología de la formación Rio Mayer, cuenca Austral, provincia de Santa Cruz, Argentina. Tesis de doctorado. Facultad de Ciencias Naturales y Museo, Universidad Nacional de La Plata, Argentina, p. 278.
Richiano, S., Varela, A.N., Cereceda, A., Poiré, D.G., 2012. Evolución paleoambiental de la Formación Rio Mayer, Cretácico Inferior, Cuenca Austral, Provincia de Santa Cruz, Argentina. Latin Am. J. Sedimentol. Basin Anal. 19, 3–26.
Rodrigues, N., Cobbold, P.R., Løseth, H., Ruffet, G., 2009. Widespread bedding-parallel veins of fibrous calcite (“beef”) in a mature source rock (Vaca Muerta Fm, Neuquén Basin, Argentina): evidence for overpressure and horizontal compression. J. Geol. Soc. Lond. 166 (4), 695–709. http://dx.doi.org/10.1144/0016-76492008-111.
Rodriguez, J.F., Cagnolatti, M.J., 2008. Source Rocks and Paleogeography, Austral Basin, Argentina. American Association of Petroleum Geologists Convention, San Antonio, Texas, pp. 1–24. April 20-23, 2008, Search and Discovery Article # 10173.
Rodríguez, J., Miller, M., 2005. Cuenca Austral. In: Frontera Exploratoria de la Argentina. VI Congreso de Exploración y Desarrollo de Hidrocarburos, pp. 307–324.
Rodríguez, J.F., Miller, M., Cagnolatti, M.J., 2008. Sistemas petroleros de Cuenca Austral, Argentina y Chile. In: Cruz, C.E., Rodríguez, J.F., Hechem, J.J., Villar, H.J. (Eds.), Sistemas Petroleros de las Cuencas Andinas. Instituto Argentino del Petróleo y del Gas, pp. 1–31.
Rojas, L., Mpodozis, C., 2006. Geología estructural de la Faja Plegada y Corrida de Tierra del Fuego, Andes Patagónicos Chilenos. In: 11° Congreso Geológico Chileno, Actas, 1, pp. 325–328.
Romans, B.W., Fildani, A., Hubbard, S.M., Covault, J.A., Fosdick, J.C., Graham, S.A., 2011. Evolution of deep-water stratigraphic architecture, Magallanes Basin, Chile. Mar. Pet. Geol.. 28, 612–628.
Rossello, E.A., Haring, C.E., Cardinali, G., Suárez, F., Laffitte, G.A., Nevistic, A.V., 2008. Hydrocarbons and petroleum geology of Tierra del Fuego, Argentina. Geol. Acta 6, 69–83. http://dx.doi.org/10.1344/105.000000242.
Sánchez, A., Pavlishina, P., Godoy, E., Hervé, F., Fanning, C.M., 2010. On the presence of Upper Paleocene rocks in the foreland succession at Cabo Nariz, Tierra del Fuego, Chile: geology and new palynological and U-Pb data. Andean Geol. 37, 413–432.
Scott, K.M., 1966. Sedimentology and dispersal patterns of a Cretaceous flysch sequence, Patagonian Andes, southern Chile. Am. Assoc. Pet. Geol. Bull. 50, 72–107.
Soffia, C., José, M., Harambour, P., Salvador, S., 1988. Estructuras en el cinturón plegado y fallado de Ultima Esperanza, Magallanes, Chile. In: Departamento de Geología, Facultad de Ciencias Físicas y Matemáticas, Universidad de Chile, Comunicaciones, Serie 22, pp. 36–39.
Suárez, M., Pettigrew, T.H., 1976. An Upper Mesozoic island-arc backarc system in the southern Andes and South Georgia. Geol. Mag. 113, 305–328.
Suárez, M., de la Cruz, R., Bell, C.M., 2000. Timing and origin of deformation along the Patagonian fold and thrust belt. Geol. Mag. 137, 345–353.
Swarbrick, R.E., Osborne, M.J., Yardley, G.S., 2002. Comparison of overpressure magnitude resulting from the main generating mechanisms. In: Huffman, A.R., Bowers, G.L. (Eds.), Pressure Regimes in Sedimentary Basins and Their Prediction, American Association of Petroleum Geologists Memoir, 76, pp. 1–12.
Tassone, A., Lippai, H., Lodolo, E., Menichetti, M., Comba, A., Hormaechea, J.L., Vilas, J.F., 2005. A geological and geophysical crustal section across the Magallanes-Fagnano fault in Tierra del Fuego. J. South Am. Earth Sci. 19, 99–109.
Thomas, C.R., 1949. Geology and petroleum exploration in Magallanes Province, Chile. Am. Assoc. Pet. Geol. Bull. 33, 1553–1578.
Torres Carbonell, P.J., Dimieri, L.V., Olivero, E.B., 2011. Progressive deformation of a Coulomb thrust wedge: the eastern Fuegian Andes Thrust-Fold Belt. In: Poblet, J., Lisle, R.J. (Eds.), Kinematic Evolution and Structural Styles of Fold-and-thrust Belts, Geological Society, London, Special Publications, 349, pp. 123–147. http://dx.doi.org/10.1144/SP349.7.
Uliana, M.A., Arteaga, M.E., Legarreta, L., Cerdán, J.J., Peroni, G.O., 1995. Inversion structures and hydrocarbon occurrences in Argentina. In: Buchanan, J.G., Buchanan, P.G. (Eds.), Basin Inversion, Geological Society, London, Special Publication, 88, pp. 211–233.
Urien, C.M., Zambrano, J.J., Yrigoyen, M.R., 1995. Petroleum basins of southern South America: an overview. In: Tankard, A.J., Suárez Soruco, R., Welsink, H.J. (Eds.), Petroleum Basins of South America, American Association of Petroleum Geologists Memoir, 62, pp. 63–77.
Wilson, T.J., 1991. Transition from back-arc to foreland basin development in the southernmost Andes: stratigraphic record from the Ultima Esperanza District, Chile. Geol. Soc. Am. Bull. 103, 98–111.
Wilson, T.J., Dalziel, I.W.D., 1983. Geology of the Ultima Esperanza fold-thrust belt, southernmost Andes. U.S. Antarc. J., Annu. Rev. 18, 75–76.
Windhausen, A., 1931. Geología Argentina. Segunda Parte. Geología histórica y regional del territorio argentino. Buenos Aires, Jacobo Peuser, p. 645.
Winslow, M.A., 1981. Mechanisms for basement shortening in the Andean foreland fold belt of southern South America. In: McClay, K.R., Price, N.J. (Eds.), Thrust and Nappe Tectonics, Geological Society, London, Special Publications, 9, pp. 513–528.
Winslow, M.A., 1982. The structural evolution of the Magallanes Basin and neotectonics in the southernmost Andes. In: Craddock, C. (Ed.), Antarctic Geoscience. University of Wisconsin Press, Madison, pp. 143–154.
Winslow, M.A., 1983. Clastic dike swarms and the structural evolution of the foreland fold and thrust belt of the southern Andes. Geol. Soc. Am. Bull. 94, 1073–1080.
Zanella, A., Cobbold, P.R., Lemrabott, A., 2010 27–29 September. Physical Models of Chemical Compaction, Overpressure Development and Hydraulic Fracturing in Various Tectonic Contexts. GeoMod2010, Lisbon, Portugal.
Zanella, A., Cobbold, P.R., 2011. In: Influence of Fluid Overpressure, Maturation of Organic Matter, and Tectonic Context during the Development of ‘Beef ’: Physical Modelling and Comparison with the Wessex Basin, SW England, vol. 13. EGU General Assembly, Vienna, Austria. Geophysical Research Abstracts.
Zanella, A., Cobbold, P.R., 2012. ‘Beef’: evidence for fluid overpressure and hydraulic fracturing in source rocks during hydrocarbon generation and tectonic events: field studies and physical modelling. In: Geofluids VII International Conference, Rueil-malmaison, 6–8 June.
Zanella, A., Cobbold, P.R., 2013, 19–22 May. Physical Modeling of Fluid Overpressure and Hydraulic Fracturing in Source Rocks in Various Tectonic Contexts. American Association of Petroleum Geologists Annual Convention, Pittsburgh, Tennessee.
Zanella, A., Cobbold, P.R., Le Carlier de Veslud, C., 2013. Physical modelling of chemical compaction, overpressure development, hydraulic fracturing and thrust detachments in organic-rich source rock. Mar. Pet. Geol. submitted for publication.
Zilli, N., Pedrazzini, M., Peroni, G., 2002. La cuenca Austral. In: Haller, M.J. (Ed.), Geología y Recursos Naturales de Santa Cruz, 15° Congreso Geológico Argentino, El Calafate, Relatorio, pp. 607–662.

Please cite this article in press as: Zanella, A., et al., Beef veins and thrust detachments in Early Cretaceous source rocks, foothills of Magallanes-Austral Basin, southern Chile and Argentina: Structural evidence for fluid overpressure during hydrocarbon maturation, Marine and Petroleum Geology (2013), http://dx.doi.org/10.1016/j.marpetgeo.2013.10.006

Chapitre 5

Modélisation analogique

5.1 Introduction

Dans les précédents chapitres, nous avons pu voir l'étude de différents bassins sédimentaires. Ces derniers, de part leur position géographique et leur structure géologique, illustrent bien la complexité des sytèmes géologiques sédimentaires. Tout au long de leur histoire, les bassins sédimentaires sont au cœur de processus physico-chimiques qu'il est très difficile d'étudier par des analyses purement analytiques ou des études de terrain, et ce, même en intégrant des degrés de complexité extrême. Dans ce contexte, la modélisation analogique a trouvé sa place dans le monde de la géologie en offrant la possibilité d'observer, d'étudier, et de prédire (dans certains cas) les phénomènes géologiques, aussi divers et variés soient-ils. Cependant, cette technique de modélisation des systèmes géologiques ne peut se réaliser en reproduisant à l'identique la nature. En effet, les processus qui régissent ces systèmes sont eux aussi complexes et ne peuvent en aucun cas faire l'objet d'une copie intégrale du système naturel concerné. Un modèle analogique représente donc un modèle d'échelle réduite et très simplifié d'un système géologique naturel. La simplification de ces systèmes découle également de la technicité des modèles analogiques. En effet, l'un des plus grands défis de cette méthode est de trouver les matériaux analogues adéquats pour représenter la nature. Une grande partie des avancées scientifiques en modélisation analogique dépend donc de la découverte de nouveaux matériaux analogues.

Une alternative à la modélisation analogique réside dans la modélisation numérique. Ce type de modélisation, largement utilisé de nos jours, offre des possibilités d'étude très larges dans le monde des Sciences de la Terre et remplace petit à petit la méthode historique de modélisation que les géologues, en particulier, ont développé depuis presque deux siècles. Néanmoins, l'utilisation de la modélisation analogique s'avère être un outil clé dans la compréhension de certains phénomènes, comme les systèmes sédimentaires en surpression de fluides dont il est question dans cette partie.

5.2 Modélisation analogique des systèmes en surpression de fluides

Précédemment dans notre étude, nous avons montré que les veines fibreuses parallèles à la stratification de la roche (beef), ainsi que les veines de bitume, étaient des marqueurs de paléo-fracturation hydraulique sous l'effet de surpression de fluides au sein des bassins sédimentaires et plus particulièrement au sein des roches mères d'hydrocarbures. Dans cette partie, nous avons choisi de développer une nouvelle technique de modélisation analogique pour tenter de comprendre les mécanismes mis en jeu lors de la génération des surpressions de fluides et de la fracturation hydraulique.

La modélisation des systèmes en surpression de fluides en géologie a commencé au début des années 2000 notamment avec les modèles de Cobbold et al. (2001). Depuis, plusieurs études ont mis en avant la modélisation analogique dans l'étude des surpressions de fluides et de la fracturation hydraulique (e.g. Mourgues & Cobbold 2003 ; Cobbold & Rodrigues 2007 ; Rodrigues et al. 2009). Tous ces modèles ont généré des surpressions de fluides par un système d'injection de fluide (air ou eau) à la base des modèles. Cependant au regard des chapitres précédents, nous avons constaté que l'origine des fluides qui circulent dans les bassins sédimentaires peut être externe ou interne. Dans les fluides internes au système sédimentaire on peut dissocier les fluides aqueux, qui se retrouvent piégés dans les sédiments lors de la diagenèse, mais également ceux qui sont produits au sein même des roches. Dans ces derniers il y a les hydrocarbures. Nous avons donc cherché un moyen de modéliser les surpressions de fluides dans un système capable de générer son propre fluide, et donc de ne pas utiliser d'injecteurs. Pour ceci, nous sommes partis de l'étude de Lemrabott & Cobbold (2010). Cette étude a montré que l'utilisation de microbilles de cire d'abeille, mélangées à de la poudre de silice, constituait un mélange très adéquat pour représenter une roche mère. Ainsi, nous avons développé un dispositif analogique d'échelle métrique pour étudier les mécanismes qui interviennent lors de la génération des surpressions de fluides et de la fracturation hydraulique. Dans nos modèles, nous nous sommes également intéressés à l'intéraction entre ces phénomènes et la déformation. Le but étant de montrer l'effet de ces processus sur la déformation des bassins sédimentaires.

5.3 Article#5: Physical modelling of chemical compaction, overpressure development, hydraulic fracturing and thrust detachments in organic-rich source rock.

Le travail effectué dans cette partie a abouti à la rédaction d'un article scientifique publié dans une édition spéciale de la revue *Marine and Petroleum Geology*. Cet article est disponible via le lien suivant :

http://www.sciencedirect.com/science/article/pii/S0264817213003231

5.3.1 Résumé de l'article

Les évidences de surpression de fluides sont communes à travers le monde, en particulier dans les bassins sédimentaires riches en hydrocarbures. Devant l'accroissement de l'intérêt face aux ressources non-conventionnelles, de nouvelles données sont disponibles sur les roches mères d'hydrocarbures. Celles-ci montrent que les valeurs anormalement élevées de pression de fluide aux pores sont communes à travers le monde et particulièrement dans les roches mères matures, probablement en conséquence de la compaction chimique et des accroissements de volume durant la génération d'hydrocarbures. Pour tenter d'approcher les phénomènes que sont la compaction chimique, le développement des surpressions de fluides et la fracturation hydraulique, nous avons développé de nouvelles techniques de modélisation analogique en système fermé. Dans les premiers stades de notre travail, nous avons construit et déformé nos modèles dans une petite boîte rectangulaire (40x40x10 cm), qui reposait sur une plaque électrique chauffante. Cependant plus récemment, nous avons utilisé une boîte beaucoup plus grande (77x75x10 cm) afin de pouvoir déformer plus facilement les modèles par un raccourcissement horizontal. Les modèles consistent en plusieurs couches horizontales de deux matériaux : (1) un mélange à volume égal de poudre de silice et de microbilles de cire d'abeille, représentant la roche mère, et (2) de la poudre de silice pure, représentant la couverture imperméable. En submergeant les matériaux sous eau, nous évitons des surfaces de tension trop importantes, qui s'expriment notamment à l'intérieur des pores contenant à la fois de l'air et des liquides. Ainsi, nous avons pu mesurer la pression de fluide aux pores à l'aide de puits verticaux. Lors du chauffage, la température basale du modèle a dépassé le point de fusion de la cire d'abeille (~62°C), jusqu'à un maximum de 90°C. Pour étudier différents contextes tectoniques comme la compression et l'extension, nous avons utilisé un piston pour appliquer des déplacements horizontaux.

Dans les expériences où le piston n'était pas présent, la fusion rapide de la cire a conduit à la compaction verticale de la couche source basale, due au poids de la couverture, et à une surpression de fluides (lithostatique ou supérieure). Les coupes faites à travers le modèle après refroidissement ont montré que la cire fondue avait migré à travers l'espace poral jusque dans des fractures hydrauliques ouvertes (sills). La plupart de ces sills étaient horizontaux et induisaient un bombement de la topographie du modèle, probablement en réponse à une surpression interne et à une perte de la contrainte dans le mélange. Nous avons aussi constaté que les sills étaient moins nombreux aux alentours des bords du modèle, vraissemblablement en conséquence des effets de bords. Dans les autres expériences, pour lesquelles le piston a causé la compression horizontale du modèle, des sills se sont également formés. Cependant, l'épaisseur de ces derniers était plus importante que celle des sills dans les expériences sans déformation. De plus, les sills étaient plissés ou faillés. Pour les expériences où nous avons causé le raccourcissement horizontal du modèle, avant le commencement de la fusion de la cire d'abeille, des chevauchements et des rétro-chevauchements se sont développés à travers toute l'épaisseur du modèle, affectant ainsi toutes les couches près du piston et produisant un prisme de haut angle. Au contraire, dès que la cire a commencé à fondre, une surpression de fluides s'est développée à l'intérieur des couches sources et un décollement à la base de ces dernières est apparu. Ainsi, des chevauchements 'thin-skin' se sont propagés plus loin dans le modèle, produisant un prisme de bas angle. Dans quelques expériences, des corps de cire se sont formés dans des zones imbriquées à l'intérieur des couches sources.

Ainsi dans nos expériences, c'est la transformation, de la cire solide à la cire liquide, qui a conduit à la compaction chimique, au développement de surpression de fluides et à la fracturation hydraulique. Tous ces mécanismes se sont développés dans un système fermé. Les mesures de surpression de fluides indiquent que le transfert de charge a été le principal mécanisme, mais que les changements de volumes ont aussi contribué, produisant ainsi des surpressions de fluides supérieures à la valeur lithostatique et ainsi provoqué la fracturation en tension du mélange.

5.3.2 Article#5

ARTICLE IN PRESS

Marine and Petroleum Geology xxx (2014) 1–13

Contents lists available at ScienceDirect

Marine and Petroleum Geology

journal homepage: www.elsevier.com/locate/marpetgeo

Physical modelling of chemical compaction, overpressure development, hydraulic fracturing and thrust detachments in organic-rich source rock

A. Zanella*, P.R. Cobbold, C. Le Carlier de Veslud

Géosciences-Rennes (UMR-6118), CNRS and Université de Rennes 1, Campus de Beaulieu, 35042 Rennes Cedex, France

A R T I C L E I N F O

Article history:
Received 1 August 2013
Received in revised form
20 December 2013
Accepted 23 December 2013
Available online xxx

Keywords:
Fluid overpressure
Physical modelling
Chemical compaction
Thrust detachments

A B S T R A C T

Geological evidence for overpressure is common worldwide, especially in petroleum-rich sedimentary basins. As a result of an increasing emphasis on unconventional resources, new data are becoming available for source rocks. Abnormally high values of pore fluid pressure are especially common within mature source rock, probably as a result of chemical compaction and increases in volume during hydrocarbon generation. To investigate processes of chemical compaction, overpressure development and hydraulic fracturing, we have developed new techniques of physical modelling in a closed system. During the early stages of our work, we built and deformed models in a small rectangular box (40 × 40 × 10 cm), which rested on an electric flatbed heater; but more recently, in order to accommodate large amounts of horizontal shortening, we used a wider box (77 × 75 × 10 cm). Models consisted of horizontal layers of two materials: (1) a mixture of equal initial volumes of silica powder and beeswax micro-spheres, representing source rock, and (2) pure silica powder, representing overburden. By submerging these materials in water, we avoided the high surface tensions, which otherwise develop within pores containing both air and liquids. Also we were able to measure pore fluid pressure in a model well. During heating, the basal temperature of the model surpassed the melting point of beeswax (~62 °C), reaching a maximum of 90 °C. To investigate tectonic contexts of compression or extension, we used a piston to apply horizontal displacements.

In experiments where the piston was static, rapid melting led to vertical compaction of the source layer, under the weight of overburden, and to high fluid overpressure (lithostatic or greater). Cross-sections of the models, after cooling, revealed that molten wax had migrated through pore space and into open hydraulic fractures (sills). Most of these sills were horizontal and their roofs bulged upwards, as far as the free surface, presumably in response to internal overpressure and loss of strength of the mixture. We also found that sills were less numerous towards the sides of the box, presumably as a result of boundary effects. In other experiments, in which the piston moved inward, causing compression of the model, sills also formed. However, these were thicker than in static models and some of them were subject to folding or faulting. For experiments, in which we imposed some horizontal shortening, before the wax had started to melt, fore-thrusts and back-thrusts developed across all of the layers near the piston, producing a high-angle prism. In contrast, as soon as the wax melted, overpressure developed within the source layer and a basal detachment appeared beneath it. As a result, thin-skinned thrusts propagated further into the model, producing a low-angle prism. In some experiments, bodies of wax formed imbricate zones within the source layer.

Thus, in these experiments, it was the transformation, from solid wax to liquid wax, which led to chemical compaction, overpressure development and hydraulic fracturing, all within a closed system. According to the measurements of overpressure, load transfer was the main mechanism, but volume changes also contributed, producing supra-lithostatic overpressure and therefore tensile failure of the mixture.

* Corresponding author. Tel.: +33 243833522.
E-mail addresses: alain.zanella@univ-rennes1.fr, zanella.alain@gmail.com (A. Zanella).

0264-8172/$ – see front matter © 2014 Elsevier Ltd. All rights reserved.
http://dx.doi.org/10.1016/j.marpetgeo.2013.12.017

Please cite this article in press as: Zanella, A., et al., Physical modelling of chemical compaction, overpressure development, hydraulic fracturing and thrust detachments in organic-rich source rock, Marine and Petroleum Geology (2014), http://dx.doi.org/10.1016/j.marpetgeo.2013.12.017

1. Introduction

Fluid overpressures are common worldwide, especially within petroleum-rich sedimentary basins (Swarbrick et al., 2002). Osborne and Swarbrick (1997) described three main mechanisms for the generation of fluid overpressures in sedimentary basins: diagenetic reactions, disequilibrium compaction and hydrocarbon generation. Several authors have described geological hydrofractures within source rocks for petroleum, these fractures having filled with solid materials, such as pyrobitumen or fibrous calcite. The solid infills have therefore preserved the fractures. Good examples come from the 'Vaca Muerta' source rock of the Neuquén Basin, western Argentina. In the northern part of this basin, bitumen veins are relatively common and tend to be parallel to bedding (Borrello, 1956; Abraham, 1960); whereas in the southern part, veins are commonly of fibrous calcite, but may also contain hydrocarbons (Parnell and Carey, 1995; Parnell et al., 2000; Rodrigues et al., 2009). In general, calcite veins that are parallel to bedding go under the name of "beef" (see historical and worldwide review by Cobbold et al., 2013). Cobbold and Rodrigues (2007) managed to reproduce open horizontal fractures in physical models, attributing them to the action of seepage forces, which result from vertical gradients in overpressure.

More generally, in the last decade or so, techniques of physical modelling have evolved, so as to take into account pore fluids and overpressures within granular materials and their structural effects (e.g. Cobbold and Castro, 1999; Cobbold et al., 2001; Mourgues and Cobbold, 2003; Cobbold and Rodrigues, 2007; Rodrigues et al., 2009). Other authors have used physical models to study processes of magmatic intrusion, especially during horizontal shortening (Benn et al., 1998; Galland et al., 2003, 2006, 2007; Gressier et al., 2010; Román-Berdiel, 1999). However, in all of these physical models, the fluid pressures came from outside, via injectors. This technique has the advantage of allowing good controls on boundary conditions of pressure and flow rate, but it cannot investigate the causes of overpressure or the possible feedback between overpressure generation and hydrofracturing. For this purpose, Lemrabott and Cobbold (2010) developed another technique, in which model materials were of solid particles, of which some (beeswax microspheres) were able to melt, thus simulating the catagenesis of kerogen to hydrocarbons. The experiments resulted in fluid overpressure, partly as a result of volume changes (15% for beeswax), but more as a result of load transfer, from the solid overburden to the pore fluid, during a process that was physically analogous to the chemical compaction of Swarbrick et al., 2002.

In what follows, we describe the results of similar experiments, but involving new apparatus and more detailed observations. We have studied the effects of overpressure development in various tectonic settings, in particular that of horizontal shortening, so as to simulate what happens to fold and thrust belts within foreland basins. A relevant example is the Magellan (Magallanes–Austral) Basin of southern Patagonia, South America, where detachments have occurred within source rock (Diraison et al., 1997; Cobbold, 2005; Rojas and Mpodozis, 2006; Zanella et al., 2013).

2. Experimental materials

In all of our physical models, the scaling was such that 1 cm in the model represented something between 100 m and 1 km in nature. To model brittle rock, we therefore used weak frictional material, which failed according to a Mohr-Coulomb envelope. However, we required two such materials, one representing a source rock, the other representing an overburden of low permeability.

As an analogue material for the overburden, we used a pure silica powder (Millisil C4, available from Sifraco, Compiègne, France). This material has a grain size of less than 150 μm, a porosity of about 40%, a bulk density of about 1.34 g/cm^3 and an intrinsic permeability of about 1.6 Darcy (Table 1B; see also Rodrigues et al., 2009, their Table 2A). Because the grains are angular, they tend to lock together, so that the dry material is cohesive. It fails according to a Coulomb criterion, the cohesive strength being about 300 Pa and the angle of internal friction about 40° (see Galland et al., 2006; their Table 1B). In tension, the material has a strength of about 100 Pa and fails by forming open fractures. However, in our experiments, we saturated the silica powder with water, by fully submerging it. Thus we avoided the high surface tensions, which otherwise develop within pores that simultaneously contain air and one or more liquids, rendering the material cohesive (as in sand castles on a beach). As yet, we have not measured the mechanical properties of the silica powder in an under water state. However, Graveleau et al. (2011, Table 1B) have done so, for a similar silica powder. In their tests, capillary cohesion was absent or very small and the behaviour of the water-saturated material was analogous to that when it was dry. Currently, we are developing new techniques for measuring the mechanical properties of silica powder or similar materials, when fully under water.

For the source rock, following Lemrabott and Cobbold (2010), we used a mixture of silica powder and beeswax microspheres (Table 1). The microspheres (about 1 mm in diameter) are readily available in France for making candles and pharmaceutical products. The variety that we used (cire d'abeille blanche en microbilles, from La Marchande de Couleurs) is solid at room temperature, but melts at 62–64 °C to a liquid of low viscosity (14×10^{-3} Pa s, Table 1B). The density of the solid beeswax is 0.95 g/cm^3 and the density of the melt is 0.82 g/cm^3 at 80 °C. Melting therefore implies a decrease in density and an increase in volume. The coefficient of linear expansion is 350×10^{-6}/°C, corresponding to a volume change of no more than 15% or so (similar to that for catagenesis of kerogen to oil). These properties mean that the beeswax is a useful analogue material for organic matter in sediment. For the mixture, we used equal initial volumes of beeswax and of silica powder. However, the initial porosity of the beeswax powder was about 40% and the microspheres were much larger than the particles of silica, so that, on mixing the two materials, much of the silica occupied the original pore space between the microspheres. Thus the volume percentage of beeswax in the final mixture was about 40%.

3. First experiments (Series I)

3.1. Apparatus and experimental procedure

During the early stages of our work on the development of fluid overpressures, we built our models in a small apparatus, similar to that of Lemrabott and Cobbold (2010). It consisted mainly of a rectangular plastic box, 30 cm long, 20 cm wide and 10 cm high (Fig. 1). The aim was to heat the model from the base, until the temperature of the beeswax exceeded its melting point (~62–64 °C). The baseplate of the box was therefore of aluminium, to facilitate transfer of heat, whereas the sidewalls were of transparent plastic, for better observation and thermal insulation (Fig. 1). The box rested on a flatbed electric heater, which was able to deliver a maximum power of 1 W/m^2. In our experiments, we used only 30% of this power, in order to reach a maximum temperature of 90 °C. To investigate the influence of tectonic compression or extension, we used a piston to apply horizontal displacements.

We built each model in three layers. The two basal layers, each 1 cm thick, consisted of a mixture of coloured silica powder (blue or

Please cite this article in press as: Zanella, A., et al., Physical modelling of chemical compaction, overpressure development, hydraulic fracturing and thrust detachments in organic-rich source rock, Marine and Petroleum Geology (2014), http://dx.doi.org/10.1016/j.marpetgeo.2013.12.017

Table 1
Properties of the modelling materials. A. Properties of beeswax microspheres, as used in this study. B. Mechanical properties of dry silica powder (from Rodrigues et al. (2009)).

A. Beeswax microspheres

Material	Grain size, µm	Melting point, °C	Density (solid), g cm^{-3}	Density (liquid), g cm^{-3}	Viscosity (liquid), Pa. s	Thermal expansion coefficient, °C^{-1}	Thermal conductivity, W m^{-1} K^{-1}	Latent heat of fusion, J g^{-1}
Beeswax microspheres	≈1000	≈62–64	0.95 (at 20 °C)	0.82 (at 80 °C)	14 × 10^{-3} (at 80 °C)	350 × 10^{-6}	0.4	175.8

B. Silica powder

Material	Variety	Roughness	Grain size, µm	d10, µm	d50, µm	d90, µm	Particle density, g cm^3	Bulk density, g cm^{-3}	Permeability to water, m^2 Pa^{-1} s^{-1}	Intrinsic permeability, m^2	Intrinsic permeability, Darcy
Silica powder	Millisil C4	Angular	0–150	177	64	8.8	2.65	1.34	8.00 × 10^{-8}	1.6 × 10^{-12}	1.621

yellow) and beeswax microspheres, whereas the overlying third layer, 1.5 cm thick, was of pure silica powder. We deposited each layer carefully and then scraped its surface flat. Thereby, the total thickness of the model was 3.5 cm. Finally we submerged the model, by slowly pouring water onto its surface, in one corner of the box, until the water level was 1 cm above the top of the third layer. Before heating or deforming the model, we waited for several hours, so that any air bubbles would have time to rise to the surface.

During each experiment, we used several vertical wells (glass tubes), to measure the pore fluid pressure at depth. In fact, we recorded the hydraulic head (difference in water level, inside and outside the tubes). The tubes were at the sides of the models, in order to minimize disturbances (which might have triggered horizontal hydraulic fractures). We also plugged the bottom of each tube with a piece of metallic mesh, to prevent any solid particles from penetrating it. Temperatures were recorded (with a precision of ±0.1 °C) by transducers or thermocouples in three positions: (1) the heater itself, (2) within the aluminium plate and (3) at the base of the model.

After each experiment, we drained the model and left it for one night to dry on a hot plate at 50 °C. Then, before cutting the model, we impregnated it with gelatine solution and dried it again. With a knife we then cut cross-sections every 2 cm. This technique has the advantage of preserving the slices for long periods of time.

3.2. Results of experiments

With this first apparatus we did 11 experiments. The results were consistent and here we will describe four representative examples (Fig. 2).

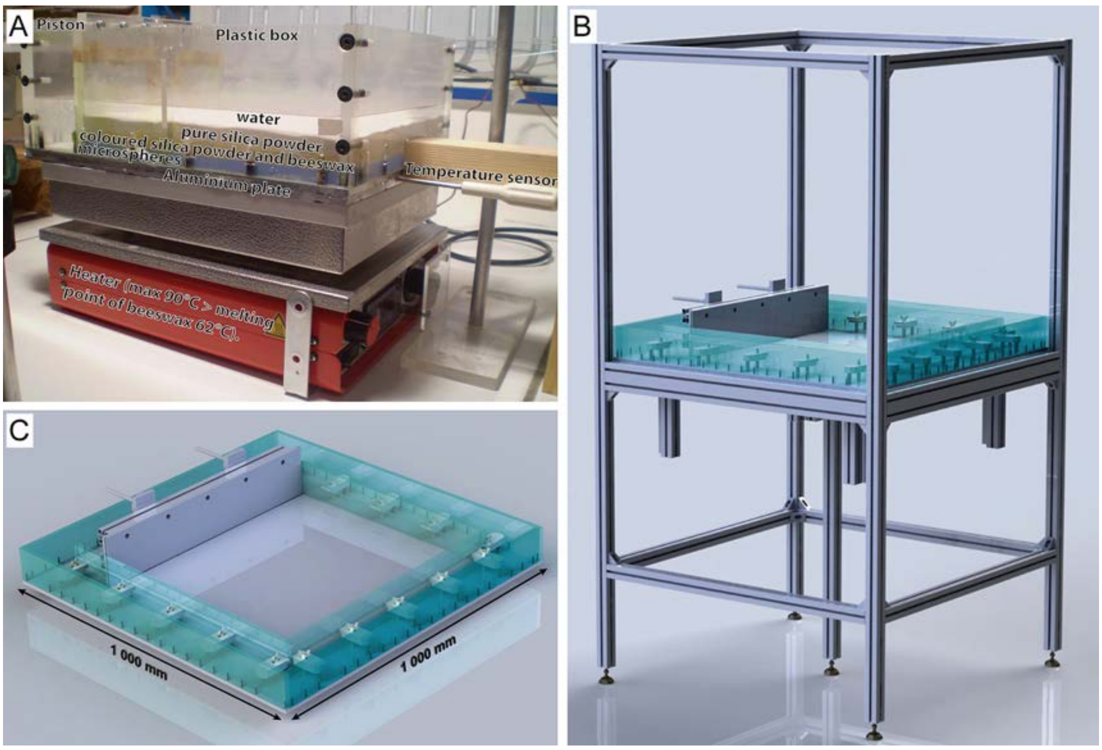

Figure 1. A. Photograph of the first (small) apparatus. Plastic box (30 cm × 20 cm × 10 cm) with an aluminium baseplate rests on an electric heater. Piston (left) can deform model horizontally. During heating, beeswax microspheres melt. Vertical well (not visible) measures pore fluid pressure at base of model. For description of layers, see Figure 2. B. Photograph (3D view) of the new (large) apparatus. Outer plastic box (1 m × 1 m) rests on aluminium table and has three hot plates beneath it. C. 3D view of outer and inner plastic boxes of the new apparatus. Inner box (77 cm × 75 cm) houses models. Piston (top left), driven by two electric motors, can deform model horizontally.

Please cite this article in press as: Zanella, A., et al., Physical modelling of chemical compaction, overpressure development, hydraulic fracturing and thrust detachments in organic-rich source rock, Marine and Petroleum Geology (2014), http://dx.doi.org/10.1016/j.marpetgeo.2013.12.017

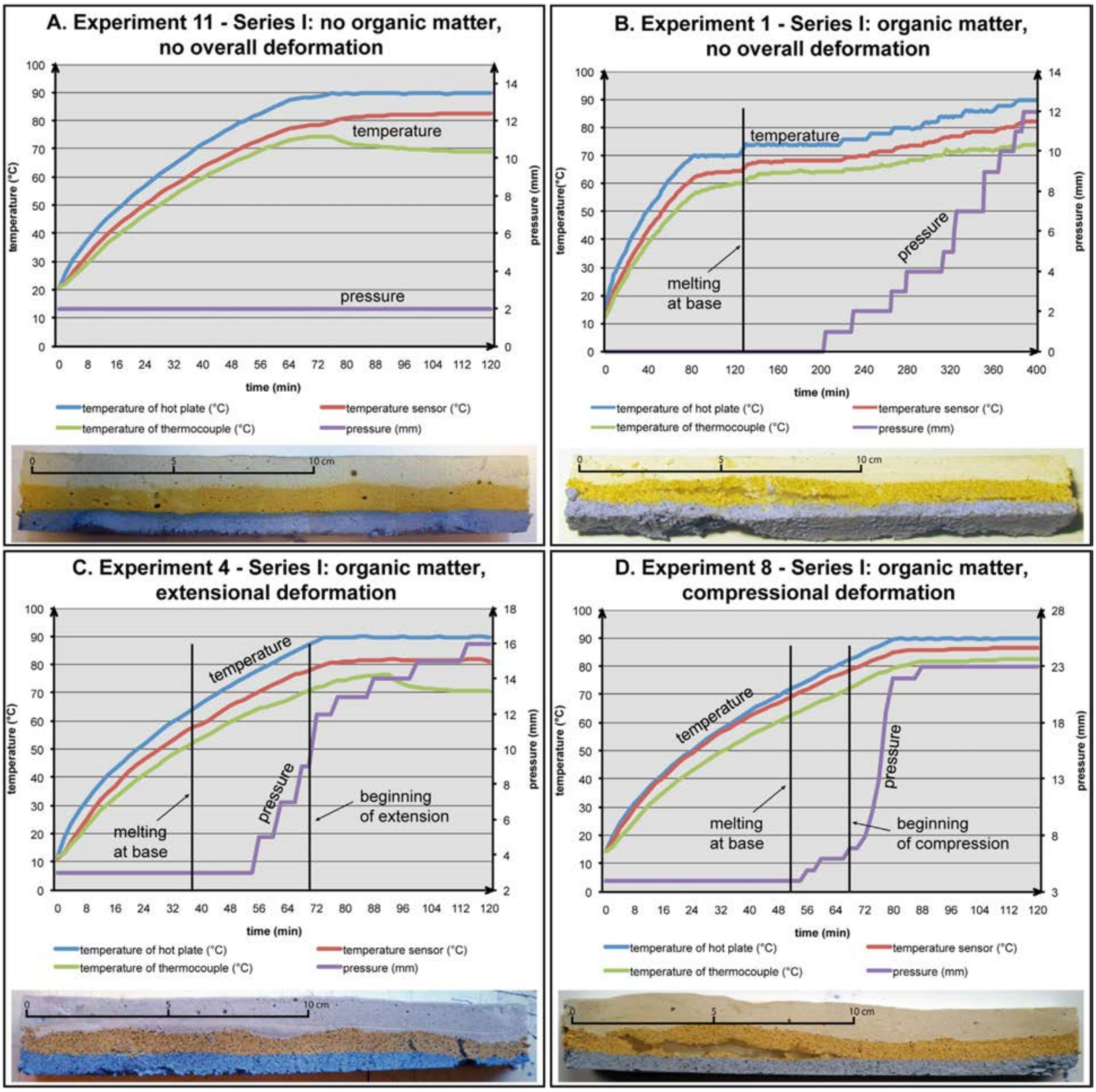

Figure 2. Results of 4 experiments with first apparatus. Graphs show variation with time (in minutes) of temperature (at 3 points, see text for details) and fluid pressure (at base of model) since beginning of each experiment. Photographs show longitudinal sections. Results are for no organic matter and no overall deformation (A. Experiment 11 – Series I); organic matter and no overall deformation (B. Experiment 1 – Series I); organic matter and extensional deformation (C. Experiment 4 – Series I); or organic matter and compressional deformation (D. Experiment 8 – Series I). For Experiment 4, piston was at right and moved outward (to right) at 2.5 cm/h; whereas, for Experiment 8, piston was at left and moved inward (to right) at 2.5 cm/h.

3.2.1. Experiment 1 (containing 'organic matter', but with no overall tectonic deformation)

In Experiment 1 (Fig. 2B) the lower two layers contained beeswax and the boundaries were static, so that the model did not change shape externally. During heating, the temperature rose over a period of 400 min to a maximum of 74 °C at the base of the model. By also measuring the temperature at the surface of the model, we deduced a vertical thermal gradient of 10 °C/cm at the centre of the model. Some 80 min after the temperature at the base surpassed the melting point of wax (~62–64 °C), the hydrostatic head (difference in water level, inside and outside the glass tube) began to increase. After another 3 h or so, the hydrostatic head had reached a value of 12 mm. This was comparable to the vertical stress, due to the weight of overburden and source layers, at the base of the model. Indeed, if we assume for the granular material an average density (when dry) of 1.3 g/cm^3, subtract the density of water (1 g/cm^3), to account for buoyancy, then take a total thickness of 3.5 cm, this yields a vertical stress of 10.5 g/cm^2 (about 100 Pa), which is equivalent to the weight of 10 mm of water. We therefore infer that melting produced an approximately lithostatic overpressure at the base of the model. Indeed, cross-sections (Fig. 2B) showed horizontal bodies (sills) of wax, which formed by horizontal hydraulic fracturing within the yellow layer. In addition, by this stage the blue layer had become thinner than the yellow layer, although originally the thicknesses of the two layers were the same. This thinning (compaction) of the blue layer was thus due to loss of beeswax by melting and upward migration.

3.2.2. Experiment 11 (no 'organic matter' and no 'tectonic' deformation)

Here the conditions were the same as in Experiment 1, except that there was no wax in either of the two basal layers (Fig. 2A). The temperature rose in a similar way, but the water level in the glass tube remained steady (2 mm of hydrostatic head). We suspect that this small value may have been due to a wax plug at the base of the tube. On cross-sections (Fig. 2A), no internal structures were visible and the thicknesses of the various layers did not change.

3.2.3. Experiment 4 ('organic matter' and extensional deformation)

In Experiment 4 (Fig. 2C), we used a piston to induce horizontal extension. The piston velocity was 2.5 cm/h. We decided to start it moving only after the wax had begun to melt, to see if extension might have an effect on fluid overpressure. We heated the model as in both previous experiments. Just after the wax began to melt, the hydrostatic head started to increase within the glass tube. When extension began, the hydrostatic head continued to increase, but more slowly than in Experiment 1. On cross-sections (Fig. 2C), various structures were visible. Near the piston there were several wax dykes, steeply dipping or vertical, whereas away from the piston there were some small sills (a few mm long) at the base of the yellow layer.

3.2.4. Experiment 8 ('organic matter' and compressional deformation)

For Experiment 8 we used the piston to apply horizontal shortening at a velocity of 2.5 cm/h (Fig. 2D). As in the previous two experiments, melting of the wax led to a hydrostatic head, which we attribute to fluid overpressure at the base of the model. However, when horizontal compressional started, the hydrostatic head rose at a rate that was faster than in the previous experiments, to a value of 23 mm. Thus we infer that shortening contributed to overpressure, perhaps via horizontal tectonic compaction. The cross-sections (Fig. 2D) show that sills of wax became thicker and longer than those in Experiment 1 (involving no 'tectonic' deformation). Moreover, the sills were subject to folding and reverse faulting, especially near the piston. The blue layer became slightly thinner than the yellow layer, as a result of compaction.

3.3. Conclusions for first experiments

From the first four experiments (Series I), we infer that it was the transformation from solid to liquid wax that resulted in fluid overpressure and horizontal hydraulic fracturing. Indeed, such overpressure arose when there were source layers in the model (Fig. 2B, C, D), but not when source layers were absent (Fig. 2A). Because the volume change, from solid to liquid wax, was no more than about 15%, we attribute the overpressure to a mechanism of load transfer, from the overburden to the pore fluid, as the solid framework collapsed and compacted. The molten wax migrated through pore space and into open hydraulic fractures, where it solidified, when the temperature was low enough. Compressional deformation had an amplifying effect on this process (Experiment 8, Fig. 2D) and produced more complex structures (folds and faults) around the hydrofractures.

4. New experiments (Series II)

Although the results for the first apparatus were encouraging, we did observe some edge effects along the transparent sidewalls, especially when the piston advanced, producing compressional deformation. These effects we attribute to high friction against the sidewalls. In order to avoid this and to be able to model larger amounts of horizontal deformation, we decided to build a longer and wider box (Fig. 1).

4.1. Apparatus and experimental procedure

The new apparatus consists of a square box, 1 m wide and 10 cm high, resting on an aluminium table (Fig. 1B). The size of the model is 77 × 75 cm (dimensions of the internal box, Fig. 1C). For such a large box, we were unable to find a single electric heater that was powerful enough. Instead, we mounted one circular heating plate (15 cm in diameter) beneath the centre of the model and two identical rectangular plates, 75 cm long and 37.5 cm wide, beneath each half of the model. Each of these heating plates can deliver 1 W/m^2, as in the first apparatus, and has its own electrical control system, incorporating several thermocouples.

As before, we built the models with two source layers (1 cm thick) and one overlying layer of pure silica powder (1.5 cm thick). In all the experiments, the models were under water. For details of construction, See part 3.1. In one experiment, where a piston was to cause horizontal shortening of the model, we added a basal black layer of quartz sand (e.g. Fig. 9B) and strips of pure silica powder at the sides of the mode. Because the black sand contained no wax, heating did not lead to an internal increase in fluid overpressure and therefore the frictional resistance of the material remained high. In contrast, along the sides of the model, the frictional resistance of the silica powder, when under water, was much lower than that of the mixture of sand and beeswax microspheres. Because the models were so large, we did not impregnate them with a gelatine solution. Instead, we wet them with water, cut serial cross-sections (every 2 cm) with a knife, and made a panoramic image of each section, using a sequence of overlapping photographs (Figs. 4 and 9).

As before, we used vertical wells, to measure the pressure in the model. To record the temperature, we used thermocouples, but in three positions at the base of the model: (1) at the centre; (2) at 20 cm from the edge; and (3) at the edge. The aim was to check for horizontal thermal gradients during the experiments.

4.2. Results of experiments

So far, we have done 8 experiments with this new apparatus, under conditions of (1) no 'tectonic' deformation or (2) horizontal shortening (compressional deformation). In what follows, we will describe one example from each context, giving particular attention to Experiment 4, for which we used a gOcad 3D modeller to define the shapes of layers and wax bodies.

4.2.1. No tectonic deformation

Of the experiments that we did under static conditions (no applied horizontal deformation), Experiment 4 was the one that yielded the most data. To estimate the pore fluid pressure, we recorded the hydrostatic head in five wells, which penetrated both source layers to different depths (every 0.5 cm, from the base to the top; Fig. 3). To record the temperature, we placed thermocouples at 3 different horizontal positions along the base of the model. About

Please cite this article in press as: Zanella, A., et al., Physical modelling of chemical compaction, overpressure development, hydraulic fracturing and thrust detachments in organic-rich source rock, Marine and Petroleum Geology (2014), http://dx.doi.org/10.1016/j.marpetgeo.2013.12.017

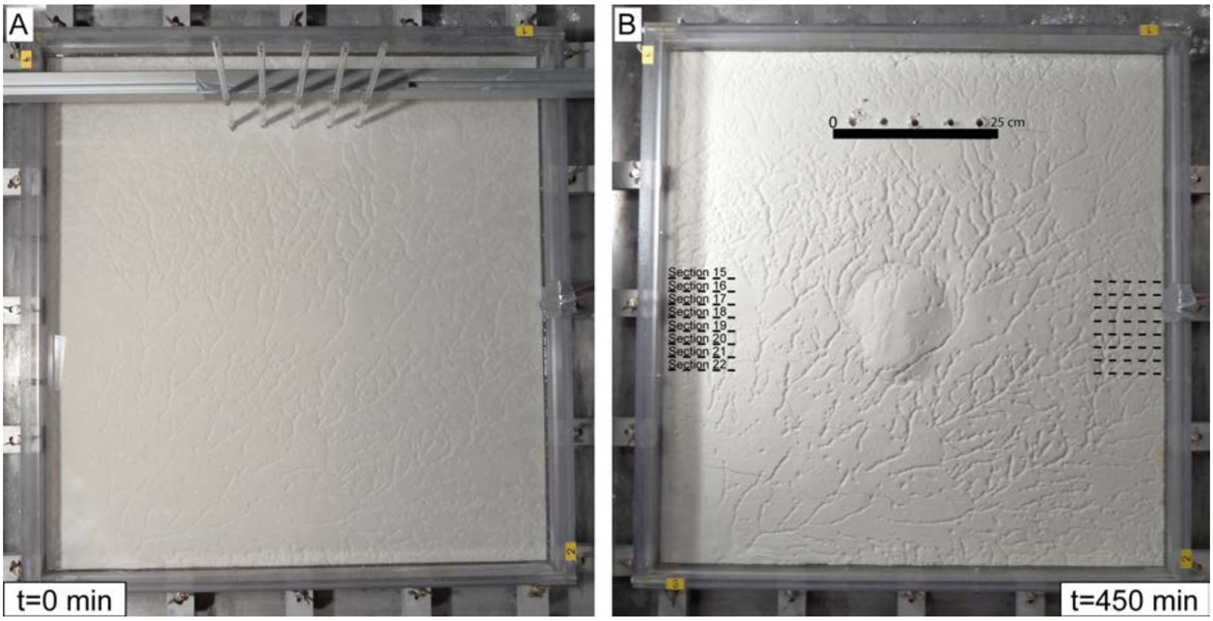

Figure 3. Photographs of top surface, Experiment 4 – Series II, (A) before deformation ($t = 0$) and (B) after 450 min. Five vertical glass tubes (A, top) are for measuring pore fluid pressure (every 5 cm, from bottom to top of source layer). After deformation (B), wax migrated into central horizontal hydraulic fracture, uplifting surface of model. Runnels, visible at the surface, formed by runoff of water during submerging of the model and do not have any effects at depth.

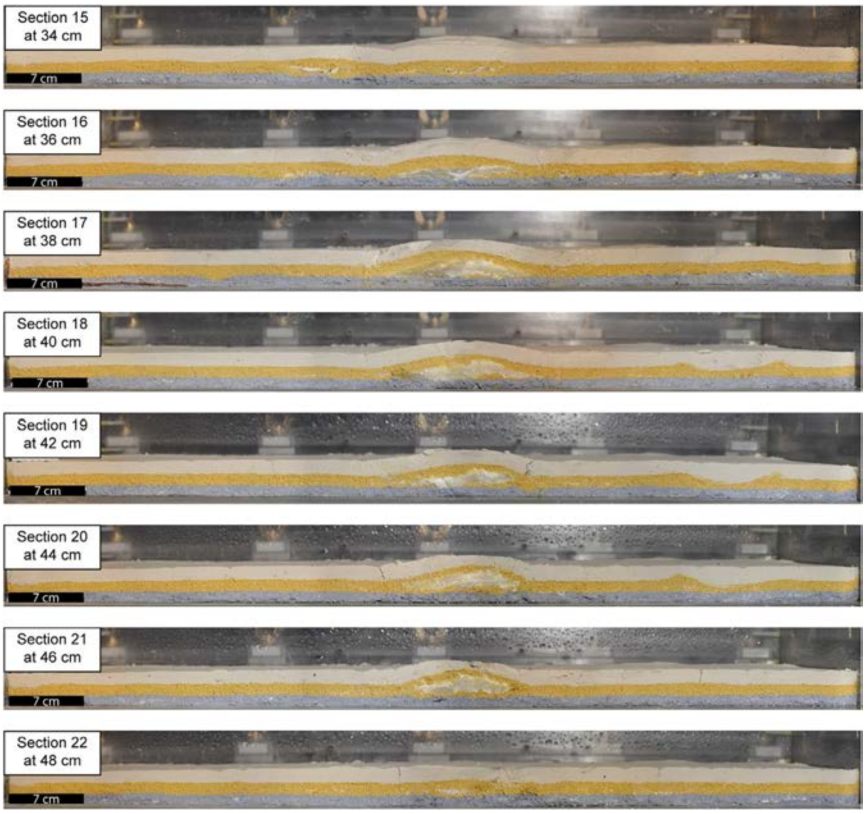

Figure 4. Selection of 8 full-length serial cross-sections, Experiment 4 – Series II (no applied horizontal deformation). For number and position of each section, see key (top left). Wax has migrated upward (and laterally) through pore space, from basal blue source layer and into open horizontal hydraulic fractures, forming sills (white) upon solidifying. At centre of model, sills are most numerous and thick within yellow layer; whereas, near edges of model, some sills are visible in blue basal source layer. Large bulges at top of model are above thick sills within source layers. Scale bar is 7 cm long. (For interpretation of the references to colour in this figure legend, the reader is referred to the web version of this article.)

Please cite this article in press as: Zanella, A., et al., Physical modelling of chemical compaction, overpressure development, hydraulic fracturing and thrust detachments in organic-rich source rock, Marine and Petroleum Geology (2014), http://dx.doi.org/10.1016/j.marpetgeo.2013.12.017

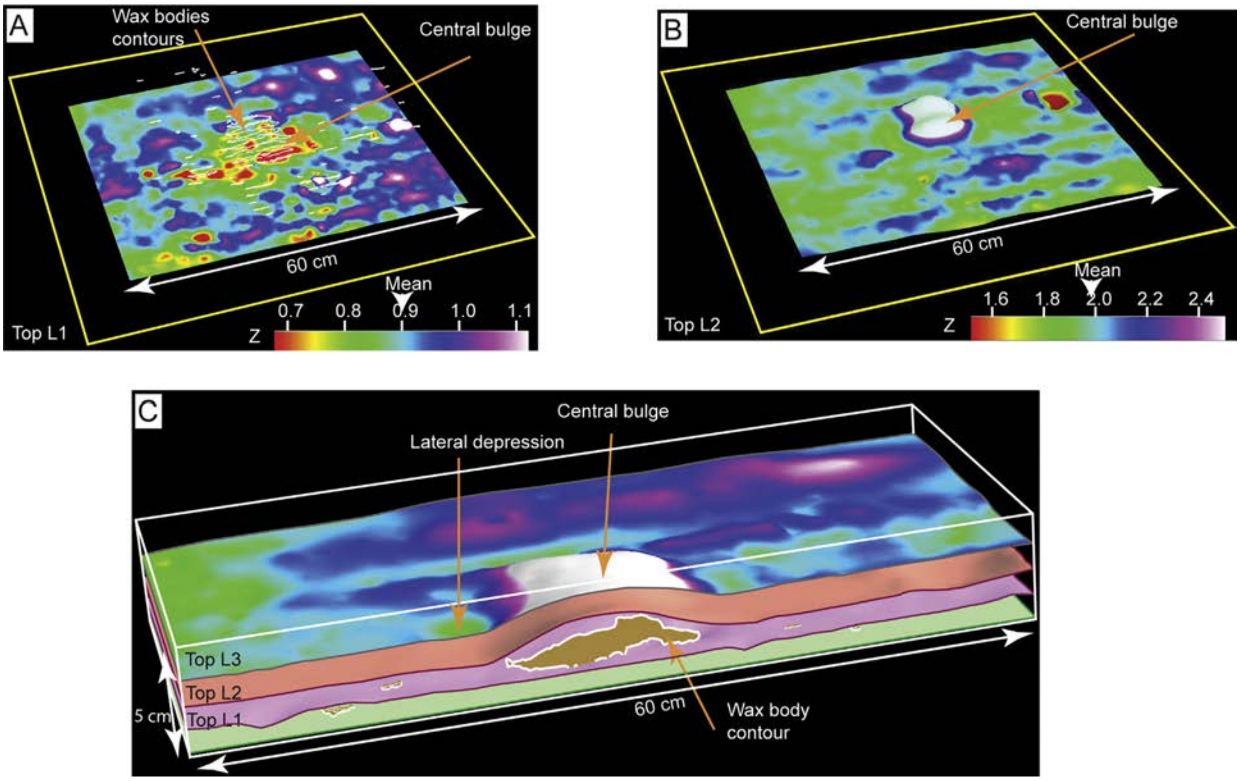

Figure 5. Three views of 3-D model, Experiment 4 – Series II. A. Oblique view of upper surface of layer L1. Colours and contours indicate altitudes (see key at bottom right). Notice central depression (red or green colours) and surrounding bulges (blue, pink or white). B. Similar view of upper surface, layer L2, showing central bulge (white). C. Cross-section of centre of model and adjacent views of three upper surfaces (layers L1 to L3). Large wax body (tan, with white contour) is immediately beneath bulges (at top L2 and top L3) and at centre of annular lateral depression (at top L3). (For interpretation of the references to colour in this figure legend, the reader is referred to the web version of this article.)

200 min from the beginning of heating, a central bulge appeared at the surface. The visibility was even greater after drying the model, because this avoided the optical distortions due to the water, which initially covered the model. Surrounding the central bulge was a local depression of the top surface (Fig. 3B). Other bulges, similar in shape but smaller, formed a circular pattern around the centre of the model, at about 20 cm from its edges. These structures were discernable, in part at the surface, but more so on cross-sections and in the 3D model (Figs. 6 and 7). Also visible at the surface were some shallow runnels, which formed during the progressive wetting of the model (Fig. 3). However, these did not have any effects at depth.

The temperature data revealed a horizontal thermal gradient within the model, which stabilized at about 0.6 °C/cm during much of the experiment. We attribute this gradient to loss of heat by conduction through the sidewalls of the box and/or radiation from their outer surfaces. After melting of the wax, the hydrostatic heads in the glass tubes increased (to 2 mm), but then they appeared to stop. We suspect that this may have been due to wax, which penetrated the tubes when molten and then solidified.

At the end of the experiment, serial cross-sections of the entire model (every 2 cm) revealed many sills of wax (white, Fig. 4). The thickest and widest formed in the yellow source layer, in the central part of the model, but thinner and smaller sills formed in both the blue and yellow layers.

Another change was in the thickness of the basal blue layer. A wide depression formed at the centre of the model, beneath the main wax sill. Local irregularities in the thickness of the yellow layer also developed, but mainly during submerging of the model, when water penetrated the mixture of silica powder and beeswax microspheres.

4.2.1.1. 3D reconstruction of model, experiment 4. The cross-sections yielded only sparse information on the three-dimensional shapes of layers and wax bodies. Unfortunately, on trying to cut sections at a closer spacing, we found that the intervening slabs tended to deform. Thus, for Experiment 4 (which involved no overall horizontal shortening), we decided instead to use a numerical method (gOcad 3D geomodeller; Mallet, 2002), to reconstruct the shapes of the layer interfaces and to calculate the volumes of wax bodies and layers (see Appendix for method).

According to the results of this gOcad modelling, the layers developed topographic bulges and depressions, which formed a broadly axisymmetric pattern about the centre of the model. We attribute this pattern to the thermal gradient, acting horizontally across the model. The upper surface of layer L1 (5A) had a central depression (20 cm wide, 2 mm deep) and a surrounding ring of minor bulges (2 mm high); whereas the upper surfaces of layers L2 (Fig. 5B) and L3 (Fig. 5C) had central bulges (13 cm wide, 9 mm high), as well as surrounding inner rings of depressions (2 mm deep) and outer rings of bulges (2 mm high).

Sectioning and 3D modelling also revealed a large number of wax bodies in the model. About 750 of these bodies were small (only a few mm wide), whereas about 65 of them were larger (more than 10 mm wide) and had shapes like magmatic sills. The latter formed only in layers L1 and L2. In L1, a few sills were at the base,

Please cite this article in press as: Zanella, A., et al., Physical modelling of chemical compaction, overpressure development, hydraulic fracturing and thrust detachments in organic-rich source rock, Marine and Petroleum Geology (2014), http://dx.doi.org/10.1016/j.marpetgeo.2013.12.017

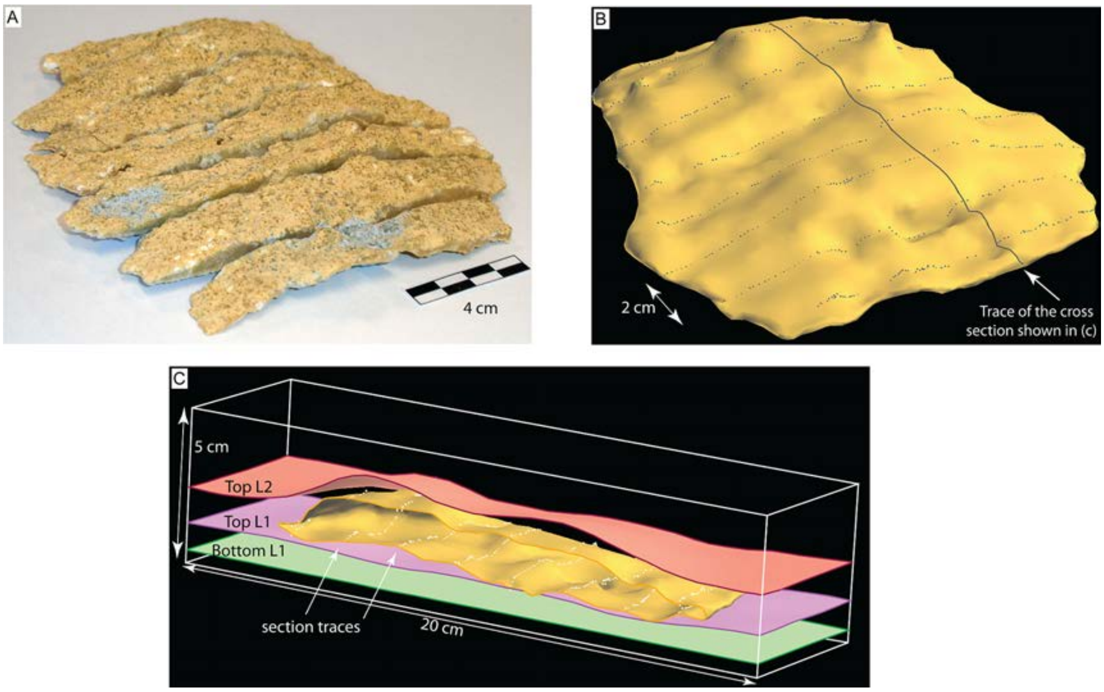

Figure 6. Three views of main wax body, Experiment 4 – Series II. A. Oblique photograph of upper surface and cross sections, after removal of surrounding silica powder. In its original position, base of body was gently dipping (see Fig. 6C). B. Oblique view (3D model) after gOcad reconstruction (model 1, small parts disconnected, see Appendix). By comparison with A, notice that many second-order deflections are missing. C. New cross-section of entire model (including layer boundaries). For line of section, see B. Main wax body appears to root locally into top of layer L1 (centre right) and to spread elsewhere within layer L2 (as in true sections, Fig. 4).

reflecting local melting, but most of them were close to the top. Some of them developed within L1, inducing bulges at the top of that layer. Other sills were larger and developed, partly at the top of L1, but more so within L2. Beneath them depressions formed (at the top of L1), whereas above them bulges formed (at the tops of both L2 and L3). This was particularly true in the centre of the model, where a large wax body (130 × 150 × 20 mm; Fig. 6) developed.

4.2.1.2. Calculation of volumes. The layers in the model underwent changes in volume (Table 2A), as a result of two main processes: (1) vertical compaction, during submersion under water, and (2) migration and intrusion of wax and consequent deformation.

For layer L3, which contained no original wax microspheres and was not subject to intrusion by wax, the volume change (ca. 20%, Table 2A) was due to compaction during wetting. In contrast, for each of layers L1 and L2, volume changes were due to compaction, intrusion, or both. However, on considering both layers (L1 and L2) together, the wax remained within the system. Thus the overall volume change was due to compaction only. However its value (1.4%, Table 2A) was significantly smaller than for layer L3. A possible explanation is that the density of the wax (ca. 0.95 g/cm^3) was smaller than that of water, so that its buoyancy impeded compaction.

On removing the effects of compaction from layers L1 and L2 (assuming an even distribution within each layer), it is possible to estimate the volume changes, due to migration and intrusion of wax. According to the results, layer L1 lost about 500 cm^3 of wax, whereas L2 gained the same amount (Table 2B). Alternatively, 3D modelling, using the gOcad 3D modeller, yields the total volumes of wax bodies in each layer (Table 2C). We have investigated two such 3D models, which assume different degrees of connectivity between cross-sections (see Appendix). The first model, which assumes no connectivity, yields a total volume of 500 cm^3 (215 cm^3 in L1 and 285 cm^3 in L2); whereas the second model, which assumes connectivity, yields a larger total volume of 810 cm^3 (380 cm^3 in L1 and 430 cm^3 in L2). The difference in results between the two models reflects the difficulty of reconstructing complex objects from cross-sections alone. Taking into account the uncertainties in calculating volumes (ca. 150 cm^3, see Appendix), the volumes of wax bodies for both models (Table 2C) are comparable to the volume changes estimated from the gOcad modelling for layers L1 and L2 (Table 2B).

Finally, amongst the wax bodies, we may distinguish those that we consider as "intrusive" from those that were not. Most of the small wax bodies developed within L1 resulted from in-situ melting of one or more microspheres and were therefore not intrusive. In contrast, larger bodies resulted from migration of molten wax. Conservatively, we consider as intrusive those wax bodies that traversed the interface between the two layers, L1 and L2, or those in L1 that led to bulging at the top of the layer. We have chosen not to list or illustrate these intrusive bodies, because they number as many as 100. However, on taking them into account, Model 2, which assumes connectivity between the wax bodies visible in the sections and thereby predicts a total intrusive volume of 550 ± 50 cm^3 (Table 2C), would appear to be more realistic than Model 1.

4.2.1.3. Interpretation. Wax bodies within layer L1 produced overlying bulges, which were visible at the end of the experiment. In contrast, bodies that developed within both layers (L1 and L2) produced depressions at the top of L1 and bulges at the top of L2, these structures resulting from intrusion. For L2, the similarity (within the range of uncertainty), between (1) the volume change of the entire layer and (2) the volumes of wax bodies, supports the idea that those bodies were mainly intrusive and that they derived from the melting of wax in layer L1 (where the temperature was

Please cite this article in press as: Zanella, A., et al., Physical modelling of chemical compaction, overpressure development, hydraulic fracturing and thrust detachments in organic-rich source rock, Marine and Petroleum Geology (2014), http://dx.doi.org/10.1016/j.marpetgeo.2013.12.017

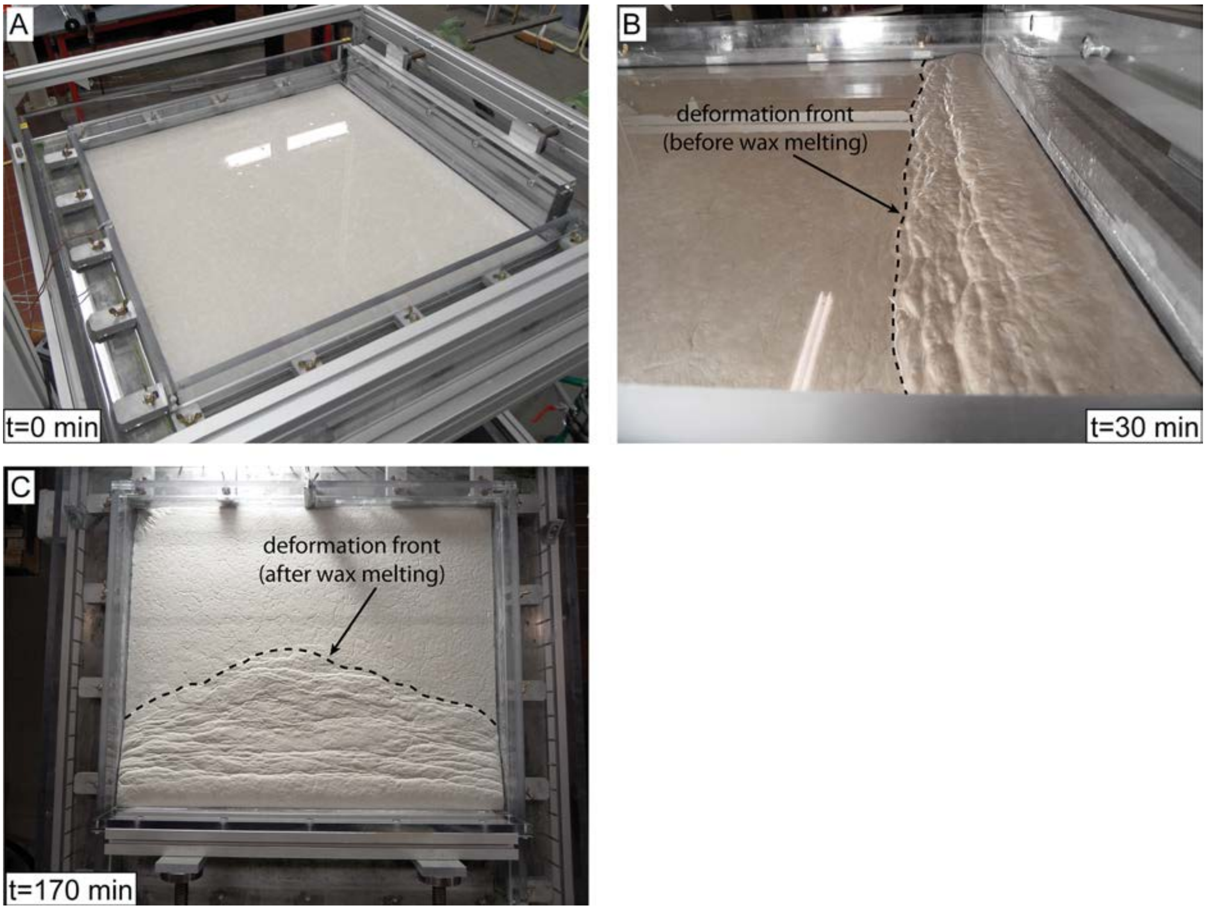

Figure 7. Photographs of top surface, Experiment 5 – Series II (compressional deformation), before deformation (A, $t = 0$) and at two later stages (B, $t = 30$ min; C, $t = 170$ min). Before melting of wax and consequent generation of fluid overpressure (until $t = 30$ min, B), compressional deformation resulted in formation of a high-angle prism, next to piston and deformation front was straight. Subsequently the deformation front migrated more rapidly away from piston and began to curve, migrating fastest in centre of model, where temperature was highest (see text for details).

hotter) and its subsequent migration. This happened especially, but not only, in the centre of the model. Local intrusion resulted in deflation of layer L1 (and a resulting depression at its top), together with inflation of layer L2 (and a bulge at its top), as previously mentioned.

Finally, from the results it is possible to derive the fraction of melt. Assuming (1) a volume of intrusion of 550 ± 50 cm^3, (2) that this originated mainly in layer L1, (3) an initial porosity of 30% for layer L1 (neglecting compaction), and (4) an initial wax content of 50% for layer L1, we calculate that the melt fraction was between 25 and 30%. However, because it is likely that some of the intrusive wax originated also in layer L2, a melt fraction of 25% would appear to be more realistic.

4.2.2. Compressional deformation

In Experiment 5 (Series II), a piston caused horizontal shortening of the model. This was the first experiment of the kind that we performed in the large box. So as not to disturb the model, we avoided using vertical wells to measure the pore fluid pressure. The aim of the experiment was to observe the effects of the generation of overpressure in a source material on the development of folds and thrusts. Thus we activated the piston at the beginning of heating. During the first hour of the experiment, the temperature at the base of the model did not exceed the melting point of wax (~62–64 °C) and shortening resulted in the formation of a high-angle wedge (next to the piston), which contained a series of fore thrusts and a single back thrust (Fig. 7B). At this stage, the structures had relatively straight traces. However, after one hour of experiment, once melting had occurred, the style of deformation began to change. In the central part of the model, the deformation front migrated very quickly, away from the piston, and it also began to curve. By the end of the experiment (after 170 min), the curvature was greater than one might expect as a result of boundary friction alone (Fig. 7C).

After deformation, serial cross-sections of the model revealed that the high-angle wedge, which had formed near the piston during the earliest stages of the experiment, was thick-skinned, in the sense that it involved all the layers in the model, including the basal layer of black sand (Fig. 8). The wedge contained a major back thrust and several steep fore thrusts. Toward the centre of the model, thrusts were less steep. They were also thin-skinned, in that they affected, not so much the basal black layer, as the source layers (yellow and blue) or the overburden (white). The gently dipping thrusts detached at the base of the yellow source layer (Fig. 8). Within that same layer, some small gently dipping wax lenses appeared (Figs 8 and 9B). We infer that they formed by hydraulic

Please cite this article in press as: Zanella, A., et al., Physical modelling of chemical compaction, overpressure development, hydraulic fracturing and thrust detachments in organic-rich source rock, Marine and Petroleum Geology (2014), http://dx.doi.org/10.1016/j.marpetgeo.2013.12.017

Figure 8. Selection of 8 full-length serial cross-sections (13–22), Experiment 5 – Series II (compressional deformation). Piston (at left) has moved inward (to right). From bottom to top, black layer is of sand, yellow and blue layers are source layers (equal initial volumes of wax microspheres and of silica powder); and white layer is of pure silica powder. Near piston (left) fore thrusts and back thrusts (thick-skinned deformation) were responsible for formation of a high-angle wedge, affecting all layers; whereas further away (right), deformation was thin-skinned, above detachment at base of yellow layer, producing low-angle wedge in uppermost three layers. Thrust offsets decreased away from piston. Some imbricate zones formed in source layers. Small wax bodies (white) also formed, especially in yellow layer. Scale bar (bottom right) is 7 cm long. (For interpretation of the references to colour in this figure legend, the reader is referred to the web version of this article.)

fracturing during thrust development (top to right, Fig. 9B). These results were reproducible.

4.3. Conclusions for experiments in the large apparatus (Series II)

In the larger apparatus, edge effects were less widespread than they were in the smaller apparatus. Furthermore, the deformation was easier to study. However, wax bodies formed widely throughout the models. As for the experiments in the smaller apparatus, we infer that the melting of wax (and so the generation of more liquid) led to load transfer from the solid framework to the pore fluid. Under the resulting overpressure gradient, the wax migrated through pore space. Some of it filled the horizontal hydraulic fractures, as they opened. Then the wax solidified, upon cooling. In Experiment 4 (no applied horizontal deformation), the horizontal hydraulic fractures clearly opened in tensile mode, locally uplifting parts of the blue source layer (Fig. 9A).

The gOcad 3-D geomodeller allowed us to define shapes and to estimate volumes, on the basis of sections alone. It therefore helped us to understand (1) the migration of fluid from areas of generation to 'reservoirs' and (2) the distribution of compaction. In our experiments, wax appeared to have migrated from the basal warmest area, at the centre of the model, to colder areas above and at the sides. Thus the 3D model has revealed both vertical and lateral migration of wax.

In experiments where a piston caused horizontal shortening (compressional deformation) of a model, the deformation was thick-skinned before the melting of wax, but changed to thin-skinned during the melting of wax and the development of fluid overpressure. Thrusts propagated into the model by detaching at the base of the source layers and the deformation front became strongly curved (Fig. 9B). We infer that detachment was easier in the centre of the model, because there the temperatures were higher and so was the overpressure.

5. Discussion

Most previous physical modelling of the structural effects of overpressure in sedimentary basins made use of external fluid injectors (Cobbold et al., 2001; Mourgues and Cobbold, 2003; Cobbold and Rodrigues, 2007). In contrast, in our experiments, an overpressured fluid arose by transformation from a solid to a liquid phase (in fact, by melting). For this purpose, following Lemrabott and Cobbold (2010), we used microspheres of beeswax.

In all experiments where source layers were present, we observed the development of fluid overpressure and hydraulic fracturing within them. In contrast, when no source layers were present, no fluid overpressure or hydraulic fractures developed. In other words, it was the production of liquid wax (from solid wax), which led to the generation of fluid overpressure and hydraulic

Please cite this article in press as: Zanella, A., et al., Physical modelling of chemical compaction, overpressure development, hydraulic fracturing and thrust detachments in organic-rich source rock, Marine and Petroleum Geology (2014), http://dx.doi.org/10.1016/j.marpetgeo.2013.12.017

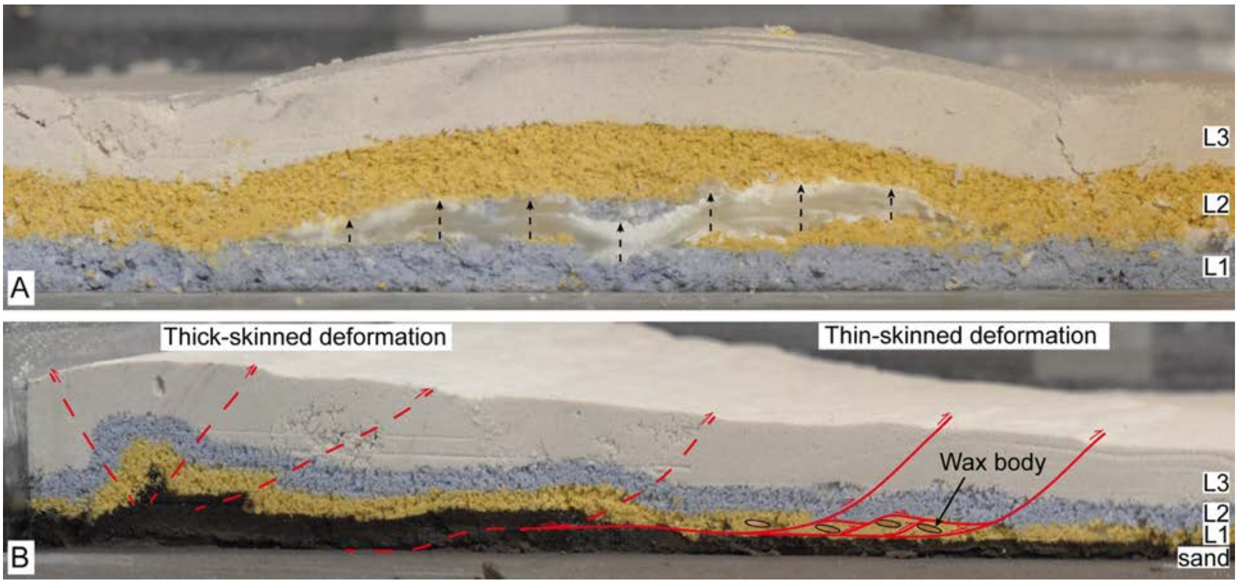

Figure 9. Close-up views of two models, illustrating structural details. A. Central part of cross-section number 16, Experiment 4 — Series II (no applied horizontal deformation). Main wax sill (white) is clearly visible (centre) and attests to tensile opening (arrows) of horizontal hydraulic fracture. Upward bulging of white and yellow layers corresponds to opening of fracture. Basal blue layer has compacted, due to collapse of solid framework, as wax melted and migrated upwards. However, area of compaction is wider than length of main wax body. B. Part of model near piston, after horizontal shortening (Experiment 5 — Series II). Deformation is thick-skinned, near piston (left) and thin-skinned, away from piston (right). Flat-lying detachment is visible at base of yellow source layer. This layer also contains an imbricate thrust zone and several gently dipping wax bodies, which we interpret as having formed during horizontal simple shear (top to right). (For interpretation of the references to colour in this figure legend, the reader is referred to the web version of this article.)

fracturing in our models. During melting, the volume change did not exceed 15% and this was not enough to explain the supra-lithostatic overpressure. However, the melting led to collapse of the solid load-supporting framework and therefore, inevitably, to load transfer from the overburden to the fluid, this process being mechanically analogous to chemical compaction (Swarbrick et al., 2002). Finally, the overpressure gradient was enough to initiate hydraulic fractures, which filled with liquid wax.

In those experiments, for which we also imposed a compressional deformation, some hydraulic fractures formed and filled with molten wax. However, the main features were faults. Before any overpressure developed, the deformation was thick-skinned and produced a high-angle wedge, containing fore thrusts and back thrusts; whereas, when melting started, the deformation became thin-skinned, above detachments in the source layers (and not the underlying black layer), leading to the formation of a low-angle wedge. Analogous features are visible in the Magallanes–Austral Basin, where Zanella et al. (2013) have found bedding-parallel veins of fibrous calcite (beef), due to hydraulic fracturing, as well as thrust detachments, all within mature source rock of Early Cretaceous age, lying upon Jurassic volcanic rocks or Palaeozoic basement.

In the future, we anticipate that it will useful to model what happens in other tectonic contexts (such as strike-slip). It will also be important to study in more detail the mechanical properties of the various materials used in the experiments, especially when the amount of pore fluid increases and intrusion becomes significant.

Table 2
Data for Experiment 4 — Series II (according to gOcad 3D modeller). A. Compaction data. B. Volume changes. C. Volumes of wax bodies.

A. Compaction data for Experiment 4 — Series II					
Layer	Initial wax	Intrusion or melting	Initial volume, cm^3	Final volume, cm^3	Compaction, %
L3	No	No	8662	6944	19.8
L1 + L2	Yes	Yes	11550	11394	1.4

B. Volume changes in Experiment 4 — Series II				
Layer	Initial volume, cm^3	Volume after compaction, cm^3	Final volume, cm^3	Volume change, cm^3
L2	5775	5697	6201	+504 (gain)
L1	5775	5697	5193	−504 (loss)

C. Volumes of wax bodies in Experiment 4 — Series II			
	Total volume, cm^3	Volume in L1, cm^3	Volume in L2, cm^3
Model 1	500	215	285
Model 2	810	380	430

6. Conclusions

In sedimentary basins worldwide, abnormally high values of pore fluid pressure are common within mature source rock. This phenomenon is probably the result of chemical compaction and increases in volume during hydrocarbon generation. To investigate processes of chemical compaction, overpressure development and hydraulic fracturing, we have used physical models, which are able to generate a fluid from solid particles (beeswax microspheres) within a closed system. In our experiments, it was the transformation, from solid wax to liquid wax, which led to internal compaction, overpressure development and hydraulic fracturing, all within a physical model of a source rock. In experiments where the piston was static, rapid melting led to vertical compaction of the source layer, under the weight of overburden, and to high fluid overpressure (lithostatic or greater). Cross-sections of the models, after cooling, revealed that molten wax had migrated through pore space and into open hydraulic fractures (sills). Under conditions of horizontal shortening and compressional deformation, sills also formed. However, these were thicker than in static models and

Please cite this article in press as: Zanella, A., et al., Physical modelling of chemical compaction, overpressure development, hydraulic fracturing and thrust detachments in organic-rich source rock, Marine and Petroleum Geology (2014), http://dx.doi.org/10.1016/j.marpetgeo.2013.12.017

some of them were subject to folding or faulting. For experiments, in which horizontal shortening started, before the wax had melted, overpressure development had a large effect on the style and speed of propagation of thrusting, which changed from thick-skinned to thin-skinned, above detachments within the source layers. According to our measurements of overpressure, load transfer was the main mechanism of overpressure development, but volume changes also contributed, producing supra-lithostatic overpressure and therefore tensile failure of the mixture.

Acknowledgements

We are grateful to Statoil for funding the PhD project of Alain Zanella. Jean-Jacques Kermarrec, Ingénieur d'études au CNRS, and Pascal Roland, technician at the University of Rennes 1, helped to build the first apparatus. Alain Zanella thanks the engineers and technicians of the Centre Commun de Mécanique, Institut National des Sciences Appliquées (INSA) de Rennes, especially Patrick Weber, for their professional and technical help in designing and building the new apparatus.

Appendix. gOcad 3D modelling

The gOcad 3D modeller and the available data

We used the gOcad 3D numerical modeller (Mallet, 2002) to reconstruct the shapes of layer boundaries and to estimate the volumes of intrusive bodies and layers. GOcad modelling is a purely geometrical form of computer-assisted design, which provides a discrete representation of geological objects in terms of regular meshes (grids) or irregular meshes (polygonal curves, triangulated surfaces, or tetrahedralized solids; Mallet, 2002). Triangulated surfaces appeared to be particularly relevant for representing closed surfaces, such as those of the wax bodies. The 3D reconstruction of geological structures from the data is by Discrete Smooth Interpolation (DSI; Mallet, 1992, 2002).

For our purposes, we digitized the contours of objects on the 29 cross sections of Experiment 4, imported the data into gOcad and removed the optical distortions that were due to photography. Cross-sections lie in the *X-Z* plane, so that the *Y* axis is normal to them. The modelling yielded two kinds of polygonal lines, (1) open lines, representing the interfaces between the main layers, and (2) closed lines, representing molten wax bodies.

3D modelling process

Reconstructing a surface from cross-sections alone is a common need, for example in geological or bio-medical imaging (Boissonnat and Memari, 2007; Liu et al., 2008). When building 3D objects from 2D sections, two potential problems arise. First, the sections imply data anisotropy, more information being available along the sections than transversely. To reduce this problem, we smoothed the data and this implied a choice of smoothing parameters. Second, the reconstruction of 3D shapes from cross-sections requires correlation from one section to another. This is more difficult for bodies that are small, in comparison with the spacing of sections (the "cut section effects" of Higgins, 2000). The dimensions of the bodies, as visible on sections, may not be representative of their true sizes in three dimensions and the sections are more likely to intersect small bodies than large ones, because the latter are more numerous. Therefore, we adopted the following procedure.

1. To reconstruct the layer boundaries, we used Discrete Smooth Interpolation, so obtaining continuous triangulated surfaces from the sections.
2. For the wax bodies, we used an implicit method (Frank et al., 2007), which is robust and able to handle arbitrary shapes (e.g. holes or bifurcations). An implicit method reconstructs a surface from an equipotential of a 3D implicit scalar function. In general, this function is obtained from the data by interpolation on a 3D grid (see review by Frank et al., 2007). In our application of this method, we interpolated the implicit function on a 3-D grid with corner-point hexahedral cells, using the DSI method. Then, we extracted triangulated surfaces, corresponding to wax bodies, as isovalues of the 3D grid. Because hexahedral grids have limited adaptativity, we improved the fit of the obtained surfaces to the wax contours, using the DSI method.
3. In order to estimate the degree of connection of the wax bodies, we tried 2 end-member models, using implicit methods. The first model reconstructs only the largest wax bodies, for which connections are clear. For small bodies the model estimates volumes, assuming that they are separate ellipsoids. This first model clearly underestimates the total volume of wax bodies. Thus we tried a second model, which includes contours for all wax bodies. This model tends to result in more connections between small bodies and therefore yields a larger estimate for the total volume of wax bodies.

References

Abraham, H., 1960. Asphalt and Allied Substances, sixth ed., vol. 1. D. Van Nostrand Company, New York, U.S.A., p. 325
Benn, K., Odonne, F., Saint Blanquat, M. de, 1998. Pluton emplacement during transpression in brittle crust: new views from analogue experiments. Geology 26, 1079–1082.
Boissonnat, J.D., Memari, P., 2007. Shape reconstruction from unorganized cross-sections. In: SGP '07: Proceedings of the Fifth Eurographics Symposium on Geometry Processing, pp. 89–98.
Borrello, A.V., 1956. Recursos minerales de la República Argentina. III. Combustibles sólidos minerales. Rev. Del Inst. Nac. Investig. Las Cienc. Nat. Cienc. Geol. 5, 665.
Cobbold, P.R., 2005. Hydrocarbon Generation, Fluid Overpressure and Source Rock Detachments in Thrust Belts, vol. 99. Thrust Tectonics, Egham, pp. 7–9. Extended Abstracts.
Cobbold, P.R., Castro, L., 1999. Fluid pressure and effective stress in sandbox models. Tectonophysics 301, 1–19.
Cobbold, P.R., Durand, S., Mourgues, R., 2001. Sandbox modelling of thrust wedges with fluid-assisted detachments. Tectonophysics 334, 245–258.
Cobbold, P.R., Rodrigues, N., 2007. Seepage forces, important factors in the formation of horizontal hydraulic fractures and bedding-parallel fibrous veins ("beef" and "cone-in-cone"). Geofluids 7, 313–332. http://dx.doi.org/10.1111/j.1468-8123.2007.00183.x.
Cobbold, P.R., Zanella, A., Rodrigues, N., Løseth, H., 2013. Bedding-parallel fibrous veins (beef and cone-in-cone): worldwide occurrence and possible significance in terms of fluid overpressure, hydrocarbon generation and mineralization. Mar. Pet. Geol. 43, 1–20. http://dx.doi.org/10.1016/j.marpetgeo.2013.01.010.
Diraison, M., Cobbold, P.R., Gapais, D., Rossello, E.A., Gutiérrez Pleimling, A., 1997. Neogene tectonics within the Magellan basin (Patagonia). In: VI Simposio Bolivariano, Petroleum exploration in the Subandean basins, Cartagena de Indias, Colombia, Memorias, Tomo. 1, pp. 1–14.
Frank, T., Tertois, A.-L., Mallet, J.-L., July 2007. 3D-reconstruction of complex geological interfaces from irregularly distributed and noisy point data. Comput. Geosci. 33 (7), 932–943.
Galland, O., de Bremond d'Ars, J., Cobbold, P.R., Hallot, E., 2003. Physical models of magmatic intrusion during thrusting. Terra Nova 15, 405–409.
Galland, O., Cobbold, P.R., Hallot, E., de Bremond d'Ars, J., Delavaud, G., 2006. Use of vegetable oil and silica powder for scale modelling of magmatic intrusion in a deforming brittle crust. Earth Planet. Sci. Lett. 243, 786–804.
Galland, O., Cobbold, P.R., de Bremond d'Ars, J., Hallot, E., 2007. Rise and emplacement of magma during horizontal shortening of the brittle crust: insights from experimental modeling. J. Geophys. Res. 112, B06402.
Graveleau, F., Hurtrez, J.E., Dominguez, S., Malavieille, J., 2011. A new experimental material for modeling relief dynamics and interactions between tectonics and surface processes. Tectonophysics 513, 68–87.
Gressier, J.B., Mourgues, R., Bodet, L., Matthieu, J.Y., Galland, O., Cobbold, P., 2010. Control of pore fluid pressure on depth of emplacement of magmatic sills: an experimental approach. Tectonophysics 489, 1–13.
Higgins, M., 2000. Measurement of crystal size distributions. Am. Mineral. 85, 1105–1116.
Lemrabott, A., Cobbold, P.R., 2010. Physical modeling of fluid overpressure and compaction during hydrocarbon generation in source rock of low permeability. American Association of Petroleum Geologists, International Conference and

Please cite this article in press as: Zanella, A., et al., Physical modelling of chemical compaction, overpressure development, hydraulic fracturing and thrust detachments in organic-rich source rock, Marine and Petroleum Geology (2014), http://dx.doi.org/10.1016/j.marpetgeo.2013.12.017

Exhibition, Rio de Janeiro, Brazil, 15–18 November. Search Discov. Article #40518 http://www.searchanddiscovery.com.

Liu, L., Bajaj, C., Deasy, J.O., Low, D.A., Ju, T., 2008. Surface Reconstruction from Non-parallel Curve Networks. In: EUROGRAPHICS, vol. 27. The eurographics association and Blackwell Publishing Co Ltd., p. 2. Available at: http://diglib.eg.org/EG/Publications/bookstore/Proc

Mallet, J.-L., 1992. Discrete smooth interpolation in geometric modeling. Comput. Aided Des. 24 (4), 178–191.

Mallet, J.L., 2002. Geomodeling. Oxford University Press, p. 613.

Mourgues, R., Cobbold, P.R., 2003. Some tectonic consequences of fluid overpressures and seepage forces as demonstrated by sandbox modelling. Tectonophysics 376, 75–97.

Osborne, M.J., Swarbrick, R.E., 1997. Mechanisms for generating overpressure in sedimentary basins: a reevaluation. Am. Assoc. Pet. Geol. Bull. 81, 1023–1041.

Parnell, J., Carey, P.F., 1995. Emplacement of bitumen (asphaltite) veins in the Neuquén Basin, Argentina. Am. Assoc. Pet. Geol. Bull. 79, 1798–1816.

Parnell, J., Honghan, C., Middleton, D., Haggan, T., Carey, P., 2000. Significance of fibrous mineral veins in hydrocarbon migration: fluid inclusion studies. J. Geochem. Explor. 69–70, 623–627.

Rodrigues, N., Cobbold, P.R., Løseth, H., 2009. Physical modelling of sand injectites. Tectonophysics 474, 610–632.

Rojas, L., Mpodozis, C., 2006. Geología estructural de la Faja Plegada y Corrida de Tierra del Fuego, Andes Patagónicos Chilenos. In: 11 Congreso Geológico Chileno, Actas, vol. 1, pp. 325–328.

Román-Berdiel, T., 1999. Geometry of granite emplacement in the upper crust: contribution of analogue modelling. In: Castro, A., Fernández, C., Vigneresse, J.L. (Eds.), Understanding Granites: Integrating New and Classical Techniques, Geological Society, London, Special Publication, vol. 174, pp. 77–94.

Swarbrick, R.E., Osborne, M.J., Yardley, G.S., 2002. Comparison of overpressure magnitude resulting from the main generating mechanisms. In: Huffman, A.R., Bowers, G.L. (Eds.), Pressure Regimes in Sedimentary Basins and Their Prediction, vol. 76. American Association of Petroleum Geologists Memoir, pp. 1–12.

Zanella, A., Cobbold, P.R., Ruffet, G., Rojas, L., 2013. Beef veins and thrust detachments in Early Cretaceous source rocks, foothills of the Magallanes–Austral Basin, southern Chile and Argentina: structural evidence for fluid overpressure during hydrocarbon maturation (in press). Mar. Pet. Geol. http://dx.doi.org/10.1016/j.marpetgeo.2013.10.006.

Please cite this article in press as: Zanella, A., et al., Physical modelling of chemical compaction, overpressure development, hydraulic fracturing and thrust detachments in organic-rich source rock, Marine and Petroleum Geology (2014), http://dx.doi.org/10.1016/j.marpetgeo.2013.12.017

Conclusions générales

Dans ce travail de thèse, nous avons démontré l'importance des surpressions de fluides et de la fracturation hydraulique dans les bassins sédimentaires, en particulier dans les roches mères d'hydrocarbures, au moyen d'études de terrain et de la modélisation analogique. Pour ceci, nous avons étudié des veines fibreuses parallèles à la stratification de la roche (beef) et des veines de bitume. Ces deux objets géologiques matérialisent en effet les fractures hydrauliques d'une roche qui se sont développées en contexte de surpression de fluides.

Par une étude de grande échelle, menée essentiellement sur les évidences de veines fibreuses parallèles à la stratification de la roche (beef), nous avons illustré la grande étendue des processus de surpression de fluides et de fracturation hydraulique dans les bassins sédimentaires. Ainsi, nous montrons que les composants majeurs de ces veines minéralisées sont le gypse, la calcite ou le quartz. Cependant, quelques minéraux plus accessoires peuvent se retrouver dans ces veines comme l'or, l'émeraude ou l'uranium par exemple. La composition des beef est essentiellement due à la disponibilité des éléments chimiques disséminés à proximité ou au sein même de la roche encaissante. Ainsi, dans les roches carbonatées les beef sont constitués essentiellement de calcite. Mais ceci ne semble pas être le seul facteur. La température du fluide qui circule dans les roches est également un paramètre important. En effet, les températures de formation des trois différents constituants majeurs du beef sont différentes : jusqu'à 60°C pour le gypse ; de 70°C à 120°C pour la calcite ; et de 200°C à 350°C pour le quartz.

Afin de mieux comprendre la formation des fractures hydrauliques, nous avons également étudié trois bassins sédimentaires différents. Dans le cas du bassin du Wessex, en Angleterre du sud, nous avons pu mettre en évidence que le beef était beaucoup plus répandu que ce qui était déjà documenté dans la littérature. En effet, nous avons observé qu'il était présent dans de nombreuses formations argileuses de la série sédimentaire mésozoïque, et plus particulièrement dans, ou aux alentours, des trois roches mères potentielles du bassin. La présence d'hydrocarbures dans le beef montre qu'il existe une synchronicité entre la migration des hydrocarbures et la formation du beef. Concernant le timing de formation de ce dernier, nous proposons que ces deux phénomènes aient lieu en même temps durant la réactivation en inversion du bassin. En effet, nous avons constaté que les filons de beef étaient structuralement synchrones de la déformation compressive. Plus précisément, et en nous appuyant sur les données déjà publiées, nous envisageons que ces phénomènes soient d'âge Tertiaire.

L'étude du nord du bassin de Neuquén, dans la Province de Mendoza en Argentine, nous a permis d'appréhender le développement des surpressions de fluides et de la fracturation hydraulique dans le contexte d'un bassin sédimentaire d'avant-pays. Dans cette partie du bassin, les veines de bitume et de beef constituent deux évidences de surpression de fluides et de fracturation hydraulique. Bien que d'échelles complètement différentes, ces objets géologiques sont régis par les mêmes processus de mise en place. En effet même si les veines de bitume dérivent de la maturation de la matière organique et le beef de la cristallisation d'un fluide aqueux, tous deux se sont mis en place dans un contexte de surpression de fluides. A partir des fragments de bitume se retrouvant dans le beef, nous avons pu déterminer que les deux évènements de génération étaient synchrones. Beef et bitume se sont formés pendant la tectonique compressive du bassin. Nous avons également pu mettre en avant une particularité dans le nord du bassin de Neuquén : le volcanisme. En effet, cette région est très affectée par ce dernier et nous montrons qu'il semble exister une corrélation entre les emplacements des veines de bitume et la position des roches volcaniques. Dans cette région, la maturation de la matière est probablement favorisée par la chaleur apportée lors des évènements volcaniques. Nous avons daté le volcanisme par la méthode $^{40}Ar/^{39}Ar$ et obtenu des âges Miocène moyen (de 14 à 9,5 Ma). D'après les arguments structuraux, nous envisageons une mise en place des veines de bitume et de beef au Miocène.

Dans le dernier cas d'étude, nous nous sommes intéressés au bassin de Magellan, se situant entre l'Argentine et le Chili. Dans ce bassin, la composition de beef est fonction du degré de maturité de la roche mère. Les filons de beef sont principalement constitués de calcite et contiennent des hydrocarbures. Cependant, dans les zones où la roche mère est surmature, les filons sont constitués de quartz et sont dépourvus d'hydrocarbures. Nous montrons aussi que le style de déformation dans le bassin est contrôlé par la génération des hydrocarbures. En effet, les décollements sont nombreux dans ce bassin et apparaissent à la base de la roche mère. Les décollements se propagent en chevauchement, ce qui amène la roche mère à la surface. C'est en particulier dans ces zones déformées que le beef est présent. Au regard de cette étude, nous pensons donc que la génération d'hydrocarbures a conduit à la génération de surpression de fluides, ce qui a favorisé la mise en place des décollements à la base de la roche mère.

Lors de ce travail nous avons également développé la modélisation analogique, afin de mieux comprendre les mécanismes de génération des surpressions de fluides et de la fracturation hydraulique. Nous avons donc construit un appareillage permettant d'étudier les surpressions de fluides et la fracturation hydraulique sans aucun système d'injection de fluide. Dans ce nouveau dispositif c'est la transformation d'un solide en liquide qui génère notre fluide, le tout ce faisant sous eau. Pour ceci, nous avons utilisé les mêmes matériaux que Lemrabott et Cobbold 2010, à savoir de la poudre de silice (matériau faiblement perméable) et des microbilles de cire d'abeille. Dans nos modèles, la transformation de solide à liquide de la cire d'abeille permet d'obtenir des pressions de fluide équivalentes au moins à la pression lithostatique. En l'absence de contraintes horizontales externes, des fractures hydrauliques horizontales remplies de cire se sont formées au cours des expériences. Ainsi par un processus analogue à la compaction chimique, nous montrons qu'il est possible d'obtenir de très fortes surpressions de fluides (équivalentes à la valeur lithostatique) au sein même du matériau qui génère le fluide. Dans les expériences où nous avons ajouté une déformation compressive, nous montrons que des décollements se forment à la base de la couche source, seulement dans les parties où la cire d'abeille est en fusion. Nous avons donc constaté que lors de la génération des surpressions de fluides, la déformation passe du type thick-skin au type thin-skin grâce aux décollements à la base des couches sources. Ces résultats de modélisation corroborent les observations de terrain que nous avons faites précédemment.

Ce travail de thèse a permis de mettre en évidence le développement de surpression de fluides durant la génération d'hydrocarbures au sein des roches mères. Ces surpressions s'expriment notamment par l'apparition de fractures hydrauliques, matérialisées par le beef et/ou les veines de bitume dans notre étude. Pour expliquer ces phénomènes, nous pensons donc que la transformation de solide à liquide de la matière organique lors la maturation, ainsi que l'augmentation de volume associé, conduit par un mécanisme de transfert de charge à la fracturation hydraulique de la roche.

Ce travail a soulevé beaucoup de questions également. L'une d'entre elles attire particulièrement notre attention. Nous avons pu voir qu'à l'intérieur même des filons de beef des structures de type cone-in-cone pouvaient être générées. Ces structures restent sans réponses aujourd'hui face aux mécanismes qui en sont à leur origine. Nous savons actuellement que ces structures sont délimitées par des fines couches d'argiles, qui semblent avoir été déformées lors de la croissance des fibres de calcite et donc au cours de l'ouverture de la veine. Mais celles-ci ne sont pas toujours présentes dans le beef. Dans une étude future, il serait intéressant de déterminer la cause de la formation des cone-in-cone. En effet, nous pensons que ces derniers peuvent nous renseigner d'avantage sur la propagation des surpressions de fluides au sein des roches mères.

Références Bibliographiques

A

Abalos, B., Elorza, J., 2011. Latest Cretaceous cone-in-cone structures and softsediment deformation (Basque-Cantabrian Basin, North Spain): a record of deep marine paleoseismicity? Geological Society of America Bulletin 123, 427e438.

Abraham, H., 1960. Asphalt and allied substances. Volume 1, Sixth Edition, D. Van Nostrand Company, New York, U.S.A., 325 pages.

Aguirre Urreta, M.B., Ramos, V.A., 1981. Estratigrafía y paleontología de la alta cuenca del Río Roble, provincia de Santa Cruz. 8° Congreso Geológico Argentino, Actas, 3, 101-138.

Al-Aasm, I.S., Muir, I., Morad, S., 1993. Diagenetic conditions of fibrous calcite vein formation in black shales: petrographic, chemical and isotopic evidence. Bulletin of Canadian Petroleum Geology 41, 46e56.

Al-Aasm, I.S., Morad, S., Durocher, S., Muir, I., 1996. Sedimentology, CeSeFe relationships and stable isotopic compositions in Devonian black mudrocks, Mackenzie Mountains, Northwest Territories, Canada. Sedimentary Geology l06, 279e298.

Alvarez-Marrón, J., McClay, K.R., Harambour, S., Rojas, L., Skarmeta, J. 1993. Geometry and evolution of the frontal part of the Magallanes Foreland Thrust and Fold Belt (Vicuña area), Tierra del Fuego, southern Chile. American Association of Petroleum Geologists Bulletin, 77, 1904-1921.

Andrews, W.R., 1881. Note on the Purbeck Beds at Teffont. Quarterly Journal of the Geological Society, London 37, 251e253.

Andrews, W.R., Jukes-Brown, A.J., 1894. The Purbeck Beds of the Vale of Wardour. Quarterly Journal of the Geological Society, London 50, 44e71.

Annels, A.E., Roberts, D.E., 1989. Turbidite-hosted gold mineralization at the Dolaucothi Gold Mines, Dyfed, Wales. Economic Geology 84, 1293e1314.

B

Barbeau, D.L., Olivero, E.B., Swanson-Hysell, N.L., Zahid, K.M., Murray, K.E., Gehrels, G.E., 2009. Detrital-zircon geochronology of the eastern Magallanes foreland basin: Implications for Eocene kinematics of the northern Scotia Arc and Drake Passage: Earth and Planetary Science Letters, 284, 489-503.

Barker, 1970. Plate tectonics of the Scotia Sea region. Nature, 228, 1293-1296.

Barker, S.L.L., Cox, S.F., Eggins, S.M., Gagan, M.K., 2006. Microchemical evidences for episodoic growth of antitaxial veins during fracture-controlled fluid flow. Earth and Planetary Science Letters 250, 331e344.

Beadnell, J.L.B., 1905. The relations of the Eocene and Cretaceous systems in the Esna-Aswan reach of the Nile Valley. Quarterly Journal of the Geological Society, London 244, 667e678.

Becq-Giraudon, J.F., 1990. La structure cone-in-cone en milieu de dépôt siliclastique; observations nouvelles sur les cone in cone de l'Ordovicien Inférieur de la Montagne Noire, sud du Massif Central Français.Géologiede la France1990 (2),11e20.

Begbie, M.J., Falconer, D., Craw, D., 2005. Characteristics of gold bearing quartz veins at the historic Morning Star mine, Preservation Inlet, SW Fiordland, New Zealand. 2005 NZ Minerals Conference: Realising New Zealand's mineral potential, 13e16 November, Auckland, pp. 320e327.

Benali, S., Schreiber, B.C., Helman, M.L., Philp, R.P., 1995. Characterization of organic matter from a restricted/evaporative sedimentary environment, southeastern Spain. American Association of Petroleum Geologists Bulletin 79, 816e830.

Benn, K., Odonne, F., Saint Blanquat, M. de, 1998. Pluton emplacement during transpression in brittle crust: new views from analogue experiments. Geology 26, 1079**e**1082.

Biddle, K. T., Uliana, M. A., Mitchum, R. M., Fitzgerald, M. G., Wright, R.C. 1986. The stratigraphic and structural evolution of the central and eastern Magallanes Basin, southern South America. In: Foreland basins (ed. Allen, P.A., Homewood, P.). International Association of Sedimentologists, Special Publication, 8, 41-66.

Biondi, J.L. 1942a. Informe preliminar de la zona de Mina Mercedes, Provincia de Mendoza. Yacimientos Carboníferos Fiscales, Informe, 97, 1-6.

Biondi, J.L., 1942b. Informe de la Comisión Carbón Mineral N° 52, correspondiente al mes de abril de 1942. Yacimientos Carboníferos Fiscales, Informe (unpublished report).

Boissonnat, J.D., Memari, P., 2007. Shape reconstruction from unorganized crosssections. In: SGP '07: Proceedings of the Fifth Eurographics Symposium on Geometry Processing, pp. 89**e**98.

Bonney, T.G., 1897. A note on cone-in-cone structure. The Mineralogical Magazine and Journal of the Mineralogical Society, London 11, 24e27.

Bons, P.D., Jessell, M.W.,1997. Experimental simulation of the formation of fibrous veins by localised dissolution-precipitation creep. Mineralogical Magazine 61, 53e63.

Bonte, A., 1942. Sur l'origine sédimentaire de la structure cone-in-cone. Comptes Rendus de l'Académie des Sciences de Paris 214, 498e500.

Bonte, A., 1945a. Sur les gradins concentriques de la structure cone-in-cone. Comptes Rendus de l'Académie des Sciences de Paris 221, 507.

Bonte, A., 1945b. Observations sur les nodules à structure cone-in-cone de l'Arenig de la Montagne Noire. Bulletin de la Société Géologique de France, séries V 15, 453e478.

Bonte, A., 1952. Réflexions se le «beef», à propos d'une note de M.L. David. Comptes Rendus Sommaires de la Société Géologique de France 7, 110e112.

Bonte, A., Denaeyer, M.-E., Goguel, J., 1947. Les facteurs mécaniques dans la genèse de la structure "cone-in-cone". Comptes Rendus sommaires de la Société Géologique de France 9, 182e184.

Borrello, A.V., 1942a. El yacimiento de asfaltita “El Toki”, Mendoza. Yacimientos Carboníferos Fiscales, Informe, 65, 1-4 (unpublished report).

Borrello, A.V. 1942b. Informe sobre la mina “Eloisa” (San Rafael) Provincia de Mendoza. Yacimientos Carboníferos Fiscales, Informe, 91, 1-7.

Borrello, A.V., 1956. Recursos minerales de la República Argentina. III. Combustibles sólidos minerales. Revista del Instituto Nacional de Investigación de las Ciencias Naturales, Ciencias Geológicas 5, 665.

Bray, R.J., Duddy, I.R. & Green, P.F. 1998. Multiple heating episodes in the Wessex Basin: implications for geological evolution and hydrocarbon generation. *Geological Society, London, Special Publications*, 133, 199-213.

Brigaud, B., Durlet, C., Deconinck, JF., Vincent, B., Thierry, J. & Trouiller A. 2009. The origin and timing of multiphase cementation in carbonates: Impact of regional scale geodynamic events on the Middle Jurassic Limestones diagenesis (Paris Basin, France). *Sedimentary Geology*, 222, 161–180

Broadhead, G.C., 1907. Cone in cone. Science 26 (670), 597.

Broadhead, R.F., Kepferle, R.C., Potter, P.E., 1982. Stratigraphic and sedimentologic controls of gas in shale e example from Upper Devonian of Northern Ohio. American Association of Petroleum Geologists Bulletin 66, 10e27.

Brodie, P.B., 1854. On the insect beds of the Purbeck Formation in Wiltshire and Dorsetshire. Quarterly Journal of the Geological Society, London 10, 475e482.

Brown, R.W., 1954. How does cone-in-cone material become emplaced? American Journal of Science 252, 372e376.

Brown, M.C., Oliver, N.H.S., Dickens, G.R., 2004. Veins and hydrothermal fluid flow in the Mt. Whaleback Iron Ore District, eastern Hamersley province, Western Australia. Precambrian Research 128, 441e474.

Buchanan, J.G. 1998. The exploration history and controls on hydrocarbon prospectivity in the Wessex basins, southern England, UK. *Geological Society, London, Special Publications*, 133, 19-37.

Buckland, W., De la Beche, H.T., 1835. On the Geology of the Neighbourhood of Weymouth and the Adjacent Parts of the Coast of Dorset. Transactions of the Geological Society, London, s2e4, pp.1e46.

Butterlin, J. 1972. Comparaison des caractères structuraux de la cordillère Caraïbe (Vénézuela) et de la cordillère Magellanienne (Chili-Argentine). 6th Caribbean Geological Conference, Transactions, 6, 265-273.

C

Cagnolatti, M., Covellone, G., Erlicher, J., Fantin, F. 1987. Fallamiento y plegamiento de cobertura al suroeste del Rio Grande, Cuenca Austral, Tierra del Fuego, Argentina: Decimo Congreso Geológico Argentino, San Miguel de Tucumán, Actas, 1, 149-152.

Cameron, A.C.G., 1892. On the continuity of the Kellaway Beds over extended areas near Bedford and on the extension of the Fuller's Earth works at Woburn Sands. Geological Magazine 9, 66e71.

Caminos, R., Haller, M., Lapido, O., Lizuain, A., Page, R., Ramos, V.A. 1981. Reconocimiento geológico de los Andes Fueguinos, Territorio Nacional de Tierra del Fuego. 8º Congreso Geológico Argentino (San Luis), Actas, 3, 759- traps.

Catuneanu, O., Wopfner, H., Eriksson, P.G., Cairncross, B., Rubidge, B.S., Smith, R.M.H., Hancox, P.J., 2005. The Karoo basins of south-central Africa. Journal of African Earth Sciences 43, 211e253.

Cayeux, L., 1935. Les roches sédimentaires de France. Roches Carbonates (calcaires et dolomies). Masson, Paris, 447 pp.

Cecioni, G.O., 1957. Cretaceous flysch and molasse in Departamento Ultima Esperanza, Magallanes Province, Chile. American Association of Petroleum Geologists Bulletin 41, 538e564.

Chadwick, R.A., Kenoulty, N. & Whittaker, A. 1983. Crustal structure beneath southern England from deep seismic reflection profiles. Journal of the Geological Society, London, 140, 893-912.

Cobbold, P.R., 1999. Hydrocarbon generation, fluid overpressure and source rock detachments in thrust belts. Thrust Tectonics 99, Egham, Extended Abstracts, p. 7-9.

Cobbold, P.R., 2005. Hydrocarbon Generation, Fluid Overpressure and Source Rock Detachments in Thrust Belts, vol. 99. Thrust Tectonics, Egham, pp. 7**e**9. Extended Abstracts.

Cobbold, P.R. and Castro, L., 1999. Fluid pressure and effective stress in sandbox models. Tectonophysics, 301: 1-19.

Cobbold, P.R., Durand, S., Mourgues, R., 2001. Sandbox modelling of thrust wedges with fluid-assisted detachments. Tectonophysics 334, 245–258.

Cobbold, P.R., Rossello, E.A., 2003. Aptian to recent compressional deformation, foothills of the Neuquén Basin, Argentina. Marine and Petroleum Geology, 20, 429–443.

Cobbold, P.R., Mourgues, R., Boyd, K., 2004. Mechanism of thin-skinned detachment in the Amazon Fan: assessing the importance of fluid overpressure and hydrocarbon generation. Marine and Petroleum Geology 21, 1013–1025.

Cobbold, P.R., Rodrigues, N., 2007. Seepage forces, important factors in the formation of horizontal hydraulic fractures and bedding-parallel fibrous veins ("beef" and "cone-in-cone"). Geofluids 7, 313e332.

Cobbold, P.R., Watkinson, A.J., Cosgrove, J.W., 2008. Faults of the Pharaohs. Geoscientist 18 (6), 18e22. http://www.geolsoc.org.uk/gsl/geoscientist/ features/page3994.html.

Cobbold, P.R., Ruffet, G., Leith, L., Løseth, H., Rodrigues, N., Galland, O., Leanza, H.A., 2011. Combustibles sólidos (asfaltita). XVIII Congreso Geológico Argentino, Neuquén, Relatorio, Capítulo 58, pp. 689e695.

Cobbold, P.R., Zanella, A., Ruffet, G., Rodrigues, N., Loseth, H., 2012. Beef (Bedding-parallel Fibrous Veins): Worldwide Occurrence and Significance in Terms of Fluid Overpressure, Hydrocarbon Generation and Mineralization (Including Sulfides, Emerald, Uranium or Gold). American Association of Petroleum Geologists Annual Convention, Long Beach, California. 22-25 April.

Cobbold, P.R., Zanella, A., Rodrigues, N., Løseth, H. 2013. Bedding-parallel fibrous veins (beef and cone-in-cone): worldwide occurrence and possible significance in terms of fluid overpressure, hydrocarbon generation and mineralization. Marine and Petroleum Geology 43, 1-20, doi: 10.1016/j.marpetgeo.2013.01.010.

Cole, G.A.J., 1893. On some examples of cone-in-cone structure. Mineralogical Magazine 10, 136e141.

Collins, E.W., 1984. Styles of deformation in Permian strata, Texas Panhandle. Bureau of Economic Geology, Geological Circular 84-4, 32.

Cosgrove, J.W., 1995. The expression of hydraulic fracturing in rocks and sediments. In: Ameen, M.S. (Ed.), Fractography: Fracture Tomography as a Tool in Fracture Mechanics and Stress Analysis. Geological Society, London, Special Publications, vol. 92, pp. 187e196.

Cosgrove, J.W., 2001. Hydraulic fracturing during the formation and deformation of a basin: a factor in the dewatering of low-permeability sediments. American Association of Petroleum Geologists Bulletin 85, 737e748.

Cossey, P.J., Buckman, J.O., Steward, D.I., 1995. The geology and conservation of Brown End Quarry, Waterhouses, Staffordshire. Proceedings of the Geologists' Association 106, 11e25.

Coutand, I., Diraison, M., Cobbold, P.R., Gapais, D., Rossello, E.A., Miller, M. 1999. Structure and kinematics of a foothills transect, Lago Viedma, southern Andes (49°30'S). Journal of South American Earth Sciences, 12, 1-15.

Crame, J.A., Pirrie, D., Crampton, J.S., Duane, A.M., 1993. Stratigraphy and regional significance of the Upper Jurassic e Lower Cretaceous Byers Group, Livingston Island, Antarctica. Journal of the Geological Society, London 150, 1075e1087.

Cunningham, W. D. 1993. Strike-slip faults in the southernmost Andes and the development of the Patagonian Orocline. Tectonics, 12, 169-186.

D

Daintree, R., 1872. Notes on the geology of the colony of Queensland. Quarterly Journal of the Geological Society 28, 271e317.

Dalziel, I.W.D., 1981. Back-arc extension in the southern Andes, a review and critical reappraisal. Phil. Trans. R. Soc. Lond. A 300, 319**e**335.

Dalziel, I.W.D. 1985. Collision and cordilleran orogenesis: an Andean prespective. In: M.P. Coward, A.C. Ries (Eds.), Collision tectonics. Geological Society, London, Special Publications, 19, 389-404.

Dalziel, I.W.D., Brown, R.L., 1989. Tectonic denudation of the Cordillera Darwin metamorphic core complex in the Andes of Tierra del Fuego, southernmost Chile:

implications for Cordilleran Orogenesis. Geology 17, 699**e**703.

Dalziel, I.W.D., Palmer, F.K. 1979. Progressive deformation and orogenic uplift at the southern extremity of the Andes. Geological Society of America Bulletin, 90, 259-280.

Dalziel, I. W. D., de Wit, M. J., Palmer, F. K. 1974. Fossil marginal basin in the southern Andes. Nature, 250, 291-294.

Darwin, C., 1846. Geological Observations on South America: Being the Third Part of the Geology of the Voyage of the Beagle. Smith, Elder and Co, London, p. 279.

David, L., 1952. Présence de la structure «beef» et «cone-in-cone» dans le Crétacé de l'Est-Constantinois (Algérie). Comptes Rendus sommaires de la Société Géologique de France 3, 51e52.

Davies, G.M., 1915. Curious forms of ice. Nature 94 (2360), 563. Dawson, J.W., 1862. On the flora of the Devonian period in north-eastern America. Proceedings of the Geological Society, London 18, 296e330.

Dawson, J.W., 1862. On the flora of the Devonian period in north-eastern America. Proceedings of the Geological Society, London 18, 296–330.

Denaeyer, M.-E., 1938. Présentation d'un échantillon de phyllade noir à structure «cone-in-cone» provenant des carrières du Péry à Morhet (Ardennes belges). Bulletin de la Société belge de Géologie, de Paléontologie et d'Hydrologie 48, 408–410.

Denaeyer, M.-E., 1939a. A propos des gradins concentriques propres à la structure cone-in-cone. Comptes Rendus Sommaires de la Société Géologique de France 11, 154e155.

Denaeyer, M.-E., 1939b. La reproduction expérimentale de la structure cone-incone. Ses conséquences au point de vue de la tectonique. Comptes Rendus de l'Académie des Sciences de Paris 208, 2004–2006.

Denaeyer, M.-E., 1939c. Les «Cone-in-Cone» de la Lufubu (Maniéma, Congo Belge). Annales de la Société géologique de Belgique, Bulletin 62 (10e11), 493e512.

Denaeyer, M.-E., 1940a. Sur la microstructure et la composition des «cone-in-cone» du Siegenien métamorphique de Morhet (Ardennes belges). Bulletin de la Société belge de Géologie, de Paléontologie et d'Hydrologie 49, 119e125.

Denaeyer, M.-E., 1940b. Résultats d'expériences relative à la genèse de la structure «cone-in-cone». Bulletin de la Société belge de Géologie, de Paléontologie et d'Hydrologie 49 (3), 313e318.

Denaeyer, M.-E., 1940c. Les schistes arénigiens à structure «cone-in-cone» de la tranchée de Sart-Bernard (province de Namur). Bulletin de la Société belge de Géologie, de Paléontologie et d'Hydrologie 49 (3), 318e326.

Denaeyer, M.-E., 1940d. Genèse des gradins concentriques propres à la structure cone-in-cone. Comptes Rendus Sommaires de la Société Géologique de France 7, 77e79.

Denaeyer, M.-E., 1942. Les miches à structure cone-in-cone du Silurien de la tranchée de Statte (Province de Namur). Bulletin de la Société belge de Géologie, de Paléontologie et d'Hydrologie 50, 74e77.

Denaeyer, M.-E., 1943a. Les cone-in-cone du Toarcien de Saint-Mard (Province de Luxembourg). Bulletin de la Société belge de Géologie, de Paléontologie et d'Hydrologie 52, 229e241.

Denaeyer, M.-E., 1943b. Les cone-in-cone de la France métropolitaine et d'outremer. Bulletin de la Société française de Minéralogie 66 (1e6), 173e221.

Denaeyer, M.-E., 1944a. Les marnes à structure cone-in-cone ("nagelkalk")dela Lorraine. Comptes Rendus Sommaires de la Société Géologique de France 8, 79e81.

Denaeyer, M.-E., 1944b. Observations sur les structures cone-in-cone du Trias et du Jurassique de la Lorraine. Bulletin de la Société belge de Géologie, de Paléontologie et d'Hydrologie 53 (1 et 2), 26e43.

Denaeyer, M.-E., 1945. Essai d'une théorie mécanique de la structure cone-in-cone. Bulletin de la Société Géologique de France 15, 141e160.

Denaeyer, M.-E., 1946. Sur les cone-in-cone et les septaria. Comptes Rendus de l'Académie des Sciences de Paris 223, 953e954.

Denaeyer, M.-E., 1947a. Les gisements de cone-in-cone de France et de Grande-Bretagne. Première Partie. Bulletin de la Société belge de Géologie, de Paléontologie et d'Hydrologie 56 (1e2), 21e46.

Denaeyer, M.-E., 1947b. Sur l'existence de structures cone-in-cone dans le Siegenien inférieur, à Bastogne. Bulletin de la Société belge de Géologie, de Paléontologie et d'Hydrologie 56 (3), 272e279.

Denaeyer, M.-E., 1947c. Les gisements de cone-in-cone de France et de Grande-Bretagne. Deuxième Partie. Gisements britanniques. Bulletin de la Société belge de Géologie, de Paléontologie et d'Hydrologie 56 (3), 382e411.

Denaeyer, M., 1952. Sur la signification des «filons» transversaux à structure «beef» et «cone-in-cone». Comptes Rendus Sommaires de la Société Géologique de France 8, 138e141.

Diraison, M., Cobbold, P. R., Gapais, D., Rossello, E. A. 1996. Tertiary kinematics of the southern Andes and the development of the Magellan foreland basin (Patagonia): in Andean Geodynamics, O.R.S.T.O.M. éditions, Paris, 347-350.

Diraison, M., Cobbold, P.R., Gapais, D., Rossello, E.A. 1997a. Magellan Strait: Part of a Neogene rift system. Geology, 25, 703-706.

Diraison, M., Cobbold, P.R., Gapais, D., Rossello, E.A., Gutiérrez Pleimling, A. 1997b. Neogene tectonics within the Magellan basin (Patagonia). VI Simposio Bolivariano, Petroleum exploration in the Subandean basins, Cartagena de Indias, Colombia, Memorias, Tomo I, 1-14.

Diraison, M., Cobbold, P.R., Gapais, D., Rossello, E.A., Le Corre, C. 2000. Cenozoic crustal thickening, wrenching and rifting in the foothills of the southernmost Andes. Tectonophysics, 316, 91-119.

Distler, V.V., Yudovskaya, M.A., Mitrofanov, G.L., Prokof'ev, V.Y., Lioshnevskii, E.N., 2004. Geology, composition and genesis of the Sukhoi Log noble metals deposit, Russia. Ore Geology Reviews 24, 7e44.

Dobes, P., Suchy, V., Stejskal, M., 1999. Diagenetic fluid circulation through fractures: a case study from the Barrandian Basin (Lower Paleozoic), Czech Republic. Geolines (Praha) 8, 18.

Donovan, D.T., 1957. The Jurassic and Cretaceous systems in East Greenland. Meddelelser on Grœnland 155. 9e214.

Doumani, G.A., Tasch, P.A., 1965. Leaiid Conchostrachan zone (Permian) in the Ohio Range, Horlick Mountains, Antarctica. Antarctic Research Series, Geology and Paleontology of the Antarctic 6, 229e239.

Durand-Delga, M., 1952. Observations complémentaires sur le «beef». Comptes Rendus sommaires de la Société Géologique de France 7, 112e114.

Durney, D.W., Ramsay, J.G., 1973. Incremental strains measured by syntectonic crystal growths. In: De Jong, K.A., Scholten, R. (Eds.), Gravity and Tectonics. Wiley, New York, pp. 67e96.

Dypvik, H., Hvoslef, S., Bjaerke, T., Finnerud, E., 1985. The Wilhelmoya Formation (Upper Triassic e Lower Jurassic) at Bohemanflyja, Spitsbergen. Polar Research 3, 155e165.

E

Ebukanson, E.J. & Kinghorn, R.R.F. 1985. Kerogen Facies in the Major Mudrock Formations of Southern England and the Implication on the Depositional Environments of their Precursors. Journal of the Petroleum Geology, 8, 435-462.

Ebukanson, E.J. & Kinghorn, R.R.F. 1986. Maturity of organic matter in Jurassic of Southern England and its relation to the burial history of the sediments. Journal of the Petroleum Geology 9, 259-280.

Egenhoff, S., Fishman, N., Jackson, A., Ketki, K., Mackie, J., Newby, W., Petrowski, M.J., Ahlberg, P., 2012. High Life on the Seafloor During an Ocean Anoxic Event e the Sedimentology of Spice, Middle to Late Cambrian Alum Shale, Sweden. American Association of Petroleum Geologists Annual Convention, Long Beach. Poster 1236903.

El Albani, A., Cloutier, R., Candilier, A.-M., 2002. Early diagenesis of the Upper Devonian Escuminac Formation in the Gaspé Peninsula, Québec: sedimentological and geochemical evidence. Sedimentary Geology 146, 209e223.

Elburg, M.A., Bons, P.D., Foden, J., Passchier, C.W., 2002. The origin of fibrous veins: constraints from geochemistry. In: de Meer, S., Drury, M.R., de Bresser, J.H.P., Pennock, G.M. (Eds.), Deformation Mechanisms, Rheology and Tectonics. Current Status and Future Perspectives. Geological Society, London, Special Publications, vol. 200, pp. 103e118.

El-Tabakh, M.,Schreiber,B.C.,Warren,J.K.,1998.Originof fibrous gypsum in the Newark Rift Basin, eastern North America. Journal of Sedimentary Research 68, 88e89.

ENAP, 1978, Mapa geologico de la XII Region, Magallanes y Antarctica Chilena, Chile. Santiago, Empresa Nacional del Petroleo Depto. de Exploraciones, scale 1:500,000.

England, G.L., Rasmussen, B., Krapez, B., Groves, D.I., 2002. Archaean oil migration in the Witwatersrand Basin of South Africa. Journal of the Geological Society, London 159, 189e201.

Enos, J.S., Kyle, J.R., 2002. Diagenesis of the Carrizo Sandstone at Butler Salt Dome, East Texas Basin, U.S.A.: evidence for fluid-sediment interaction near halokinetic structures.

Journal of Sedimentary Research 72, 68e81.

Evans, M.A., 2011. Deformation and Fluid History of the Marcellus Shale in the Pennsylvania Valley and Ridge: Evidence From Fluid Inclusion Microthermometry of Vein Minerals. Geological Society of America, Northeastern (46th Annual) and North-Central (45th Annual) Joint Meeting (20e22 March 2011), Paper No. 56-4 (abstract).

Evans, R., Hendry, J.P., Parnell, J., Kalin, R.M., 1998. Origin and Significance of Fracture-related Dolomite in Porous Sandstones: an Example from the Carboniferous of County Antrim, Northern Ireland. In: International Association of Sedimentologists, Special Publications, vol. 26, pp. 409e435.

F

Fary, R.W., 1980. A Review of the Petroleum Geology of Venezuela. U.S. Geological Survey Open File Report, 80e782, 37 pp.

Feruglio, E., 1949. Descripción geológica de la Patagonia. In: Dirección General Y.P.F., 1, pp. 1**e**334.

Fester, G.A. y Cruellas, J. 1941. Yacimientos de asfaltitas de carácter especial. Revista de Minería y Geología Minera, 12 (1,2), 31-37.

Fildani, A., Cope, T.D., Graham, S.A., Wooden, J.L. 2003, Initiation of the Magallanes foreland basin: Timing of the southernmost Patagonian Andes orogeny revised by detrital zircon provenance analysis. Geology, 31, 1081-1084.

Fischer, M.P., Lefticariu, L., Romanek, C., Perry, E.C., 2005. Kinematics of fibrous vein growth: insights from stable isotope analyses. Eos Transactions American Geophysical Union 86 (52). Abstract T53C-1456.

Fischer, M.P., Higuera-Diaz, I.C., Evans, M.A., Perry, E.C., Lefticariu, L., 2009. Fracture-controlled paleohydrology in a map-scale detachment fold: insights from the analysis of fluid inclusions in calcite and quartz veins. Journal of Structural Geology 31, 1490e1510.

Fitches, B., 1987. Aspects of veining from the Welsh Lower Palaeozoic Basin. In: Jones, M.E., Preston, R.M.F. (Eds.), Deformation of Sediments and Sedimentary Rocks. Geological Society, London, Special Publications, vol. 29, pp. 325e342.

Fitz-Diaz, E., Hudleston, P., Siebenaller, L., Kirschner, D., Camprubí, A., Tolson, G., Puig, T.P., 2011. Insights into fluid flow and water-rock interaction during deformation of carbonate sequences in the Mexican fold-thrust belt. Journal of Structural Geology 33, 1237e1253.

Fornari, M., Herail, G., 1991. Lower Paleozoic gold occurrences in the 'Eastern Cordillera' of southern Peru and northern Bolivia. In: Ladeira, E.A. (Ed.), Brazil Gold'91: the Economics, Geology, Geochemistry and Genesis of Gold Deposits. A.A. Balkema, Rotterdam, pp. 135e142.

Fosdick, J.C., Romans, B.W., Fildani, A., Bernhardt, A., Calderón, M., Graham, S.A., 2011. Kinematic evolution of the Patagonian retroarc fold-and-thrust belt and Magallanes foreland basin, Chile and Argentina, 51_300'S. Geol. Soc. Am. Bull. 123, 1679**e**1698. http://dx.doi.org/10.1130/B30242.1.

Fosdick, J.C., Grove, M., Hourigan, J.K., Calderón, M. 2013. Retroarc deformation and exhumation near the end of the Andes, southern Patagonia. Earth and Planetary Science Letters, 361, 504-517.

Foster, S.J., 1987. Geological Report, Punchbowl Property, Golden Mining Division. B.C. Geological Branch Assessment Report N° 16,242, Edmonton, Alberta, Canada.

Fournier, R.O., Rowe, J.J., 1977. The solubility of amorphous silica in water at high temperatures and high pressures. American Mineralogist 62, 1052e1056.

Fowler, T.J., 1996. Flexural-slip generated bedding-parallel veins from central Victoria, Australia. Journal of Structural Geology 18, 1399e1415.

Fox-Strangways, C., Barrow, G., 1882. The Geology of the Country Between Whitby and Scarborough. Memoirs of the Geological Survey, Great Britain, pp. 1e60.

Frandsen, N., Surlyk, F., 2003. An offshore transgressiveeregressive mudstonedominated succession from the Sinemurian of Skåne, Sweden. Geological Survey of Denmark and Greenland Bulletin 1, 543e554.

Frank, T., Tertois, A.-L., Mallet, J.-L., July 2007. 3D-reconstruction of complex geological interfaces from irregularly distributed and noisy point data. Comput. Geosci. 33 (7), 932**e**943.

Franks, P.C., 1969. Nature, origin and significance of cone-in-cone structures in the Kiowa Formation (Early Cretaceous), North-Central Kansas. Journal of Sedimentary Petrology 39, 1438e1454.

Frizon de Lamotte, D., Leikine, M., 1985. Métamorphisme miocène du Rif Oriental et individualisation de la nappe d'Aknoul. Revue de Géologie Dynamique et de Géographie Physique 26, 29e42.

Fuchs, F.C., 1898. Estudio sobre la región aurífera de Santo Domingo en la provincia de Carabaya. Boletín de Minas, Industria y Construcciones, Lima 14.

G

Gale, J.F.W., Holder, J., 2010. Natural fractures in some US shales and their importance for gas production. In: Vining, B.A., Pickering, S.C. (Eds.), Petroleum Geology: From Mature Basins to New Frontiers e Proceedings of the 7th Petroleum Geology Conference. Petroleum Geology Conference Series, vol. 7, pp. 1131e1140.

Galland, O., de Bremond d'Ars, J., Cobbold, P.R., Hallot, E., 2003. Physical models of magmatic intrusion during thrusting. Terra Nova 15, 405**e**409.

Galland, O., Cobbold, P.R., Hallot, E., de Bremond d'Ars, J., Delavaud, G., 2006. Use of vegetable oil and silica powder for scale modelling of magmatic intrusion in a deforming brittle crust. Earth Planet. Sci. Lett. 243, 786**e**804.

Galland, O., Cobbold, P.R., de Bremond d'Ars, J., Hallot, E., 2007. Rise and emplacement of magma during horizontal shortening of the brittle crust: insights from experimental modeling. J. Geophys. Res. 112, B06402.

Gallois, R.W., 2001. The lithostratigraphy of the Mercia Mudstone Group (mid to late Triassic) of the South Devon coast. Geoscience in south-west England. Proceedings of the Ussher Society, 195e204.

Gallois, R.W., 2008. The lithostratigraphy of the shales-with-beef member of the Charmouth Mudstone Formation, Lower Jurassic. Geoscience in South-west England 12, 32e40.

Gallois, R.W., 2009. The lithostratigraphy of the Penarth Group (late Triassic) of the Severn Estuary area. Geoscience in South-west England 12, 71e84.

Garwood, E.J., 1892. Cone-in-cone structure. Geological Magazine 9, 334e335.

Gay, R., 1942. Théorie de la formation de la structure cone-in-cone. Comptes Rendus de l'Académie des Sciences de Paris 214, 500e502.

Geel, T., 1976. Messinian gypsiferous deposits of the Lorca basin (province of Murcia, SE Spain). Memorie della Societa Geologica Italiana 16, 369e385.

Geikie, A., 1902. Text Book of Geology. Book 6. Stratigraphical Geology. American Home Library Company, New York, pp. 1419e1861.

George, T.N., 1954. Pre-seminulan main limestone of the Avonian series in Breconshire. Quaterly Journal of the Geological Society, London 110, 283e322.

Ghiglione, M.C. 2002. Diques clásticos asociados a deformación transcurrente en depósitos sinorogénicos del Mioceneo inferior de la cuenca Austral. Asociación Geológica Argentina Revista, 57, 103-118.

Ghiglione, M.C., Cristallini, E.O. 2007. Have the southernmost Andes been curved since Late Cretaceous time? An analog test for the Patagonian orocline. Geology, 35, 13-16.

Ghiglione, M.C., Ramos, V.A. 2005. Progression of deformation and sedimentation in the southernmost Andes. Tectonophysics, 405, 25-46.

Ghiglione, M.C., Navarrete-Rodríguez, A.T., González-Guillot, M., Bujalesky, G. 2012. The opening of the Magellan Strait and its geodynamic implications. Terra Nova, 25, 13-20.

Ghiglione, M.C., Ramos, V.A., Cristallini, E.O. 2002. Fuegian Andes foreland fold and thrust belt: structure and growth strata. Revista Geológica de Chile, 29, 17-41.

Ghiglione, M.C., Suárez, F., Ambrosio, A., Da Poian, G., Cristallini, E.O., Pizzio, M.F., Reinoso, R.M. 2009. Structure and evolution of the Austral Basin fold-thrust belt, southern Patagonian Andes. Asociación Geológica Argentina Revista, 65, 215-226.

Giacosa, R., Fracchia, D., Heredia, N. 2012. Structure of the Southern Patagonian Andes at 49ºS, Argentina. Geologica Acta, 10, 265-282.

Giambiagi, L., Bechis, F., García, V., Clark, A.H., 2008. Temporal and spatial relationships of thick- and thin-skinned deformation: A case study from the Malargue fold-and-thrust belt, southern Central Andes. Tectonophysics, 459, 123–139, doi:10.1016/j.tecto.2007.11.069.

Giambiagi, L., Ghiglione, M., Cristallini, E., Botesi, G., 2009. Kinematic models of basement-cover interaction: Insights from the Malargue fold and thrust belt, Mendoza, Argentina. Journal of Structural Geology, 31, 1443–1457, doi:10.1016/j.jsg.2009.10.006

Gill, J.R., Cobban, W.A., Schultz, L.G., 1972. Stratigraphy and composition of the Sharon Springs member of the Pierre shale in western Kansas. U.S. Geological Survey Professional Paper 728, 1e50.

Gilman, R.A., Metzger, W.J., 1967. Cone-in-cone concretions from western New York. Journal of Sedimentary Petrology 37, 87e95.

Glennie, K.W. & Underhill, J.R. 1998. Origin, development and evolution of structural styles. In: Glennie, K.W. (ed.) Petroleum Geology of the North Sea. Blackwell Scientific Publications, Oxford.

Gratier, J.-P., Frery, E., Deschamps, P., Røyne, A., Renard, F., Dysthe, D., Ellouz-Zimmerman, N., Hamelin, B., 2012. How travertine veins grow from top to bottom and lift the rocks above them: the effect of crystallization force. Geology, http://dx.doi.org/10.1130/G33286.1 (published online).

Graveleau, F., Hurtrez, J.E., Dominguez, S., Malavieille, J., 2011. A new experimental material for modeling relief dynamics and interactions between tectonics and surface processes. Tectonophysics 513, 68**e**87.

Gresley, W.S., 1887. Notes on “cone-in-cone structure”. Geological Magazine, Decade III IV (1), 17e22.

Gresley, W.S., 1892. Cone-in-cone structure. Geological Magazine 9, 432.

Gresley, W.S., 1894. Cone-in-Cone: how it occurs in the ‘Devonian’ series in Pennsylvania, U.S.A. Quarterly Journal of the Geological Society, London 50, 731e739.

Gresley, W.S., 1898. Cone-in-Cone: additional facts from various countries. Quarterly Journal of the Geological Society, London 50, 196.

Gressier, J.B., Mourgues, R., Bodet, L., Matthieu, J.Y., Galland, O., Cobbold, P., 2010. Control of pore fluid pressure on depth of emplacement of magmatic sills: an experimental approach. Tectonophysics 489, 1**e**13.

Groeber, P., 1923. Origen del petróleo de Barrancas. Deducciones que sugiere su estudio. Boletín de la Dirección General de Minas, Geología e Hidrología, Serie F (Informes Preliminares y Communicaciones), 6 (1), 3-14.

Gross, M.R., Becker, A., Gutiérrez-Alonso, G., 1997. Transfer of displacement from multiple slip zones to a major detachment in an extensional regime: example from the Dead Sea rift, Israel. Geological Society of America Bulletin 109, 1021e1035.

Gross, W.G., 1950. Examen geológico-minero de mina Aída, Llano Blanco - Mendoza. Yacimientos Carboníferos Fiscales, Informe, 714, 1-6 (unpublished).

Grové, D., Harris, C., 2010. O-and H-isotope study of the Carbon Leader reef at the Tau Tona and Savuka mines (western deep levels), South Africa: Implications for the origin and evolution of Witwatersrand Basin fluids. South African Journal of Geology 113, 1e14.

Guibal, C.-F., 1841. Mémoire sur le terrain jurassique du département de la Meurthe. Mémoires de la Société Royale des Sciences, Lettres et Arts de Nancy, pp. 9e56.

Guillaume, B., Martinod, J., Husson, L., Roddaz, M., Riquielme, R. 2009. Neogene uplift of central eastern Patagonia: Dynamic response to active spreading ridge subduction? Tectonics, 28, doi: 10.1029/2002008TC002324.

Gustavson, T.C., Hovorka, S.D., Dutton, A.R., 1994. Origin of satin spar veins in evaporite basins. Journal of Sedimentary Research A64, 88e94.

H

Hammes, U., Frébourg, G., 2012. Haynesville and Bossier mudrocks: a facies and sequence stratigraphic investigation, East Texas and Louisiana, USA. Marine and Petroleum Geology 31, 8e26.

Hammes, U., Hamlin, H.S., Ewing, T.E., 2011. Geologic analysis of the Upper Jurassic Haynesville Shale in east Texas and west Louisiana. American Association of Petroleum Geologists Bulletin 95, 1643e1666.

Harambour, S.M., 2002, Deep-seated thrusts in the frontal part of the Magallanes fold and thrust belt, Ultima Esperanza, Chile. 15th Congreso Geológico Argentino, Actas, 3, 232.

Harrington, H.J., Leanza, A.F., 1957. Ordovician Trilobites of Argentina. In: University of Kansas, Department of Geology, Special Publications, vol. 1, 276 pp.

Harker, A., 1892. Cone-in-cone structure. Geological Magazine 9, 240.

Harker, A., 1908. The geology of the small isles of Inverness-shire. (Rum, Canna, Eigg, Muck, etc.). (Sheet 60, Scotland). Memoirs of the Geological Society of Great Britain, 210.

Harley, M., Charlesworth, E.G., 1996. The role of fluid pressure in the formation of bedding-parallel, thrust-hosted gold deposits, Sabie e Pilgrim's Rest goldfield, eastern Transvaal. Precambrian Research 79, 125e140.

Harnly, H.J., 1898. "Cone-in-cone" (an impure calcite). Kansas Academy of Sciences Transactions 15, 22. Haselhurst, S.R., 1915. Some observations on cone-in-cone structure and their relation to its origin. Proceedings of the Geological Society, London 71, 7.

Haselhurst, S.R., 1915. Some observations on cone-in-cone structure and their relation to its origin. Proceedings of the Geological Society, London 71, 7.

Hatcher, J.B. 1897. On the geology of Southern Patagonia. American Journal of Science, 4, 321-354.

Hausmann, J.F.L., 1812. Ueber den sogenannten Tutenmergel von Görarp in Schonen. Annalen der Wetterauischen Gesellschaft für die gesammte Naturkunde, Hanau 3, 25e28.

Hawkes, P. W., Fraser, A. J., & Einchcomb, C. C. G. 1998. The tectono-stratigraphic development and exploration history of the Weald and Wessex basins, Southern England, UK. Geological Society, London, Special Publications, 133(1), 39-65.

Hector, J., 1861. On the geology of the country between Lake Superior and the Pacific Ocean (between the 48th and 54th parallels of latitude), visited by the Government Exploring Expedition under the command of Captain J. Palliser (1857e60). Proceedings of the Geological Society, London 17, 388e445.

Hedberg, H.D., Sass, L.C., Funkhouser, H.J., 1947. Oil fields of Greater Oficina Area, Central Anzoategui, Venezuela. American Association of Petroleum Geologists Bulletin 81, 2089e2169.

Henderson, M.N., Henderson, J.R., 1986. Constraints on the origin of gold in the Meguma Zone, Ecum Secum area, Nova Scotia. Maritime Sediments and Atlantic Geology 22, 1e13.

Hendry, J.P., 2002. Geochemical trends and palaeohydrological significance of shallow burial calcite and ankerite cements in Middle Jurassic strata on the East Midlands Shelf (onshore UK). Sedimentary Geology 151, 149e176.

Herdendorff, C.E., 1977. Cone-in-cone Structure in the Ohio Shale of Erie County. Ohio State University, Center for Lake Erie Area Research, Ohio, 7 pp.

Higgins, M., 2000. Measurement of crystal size distributions. Am. Mineral. 85, 1105**e**1116.

Hilgers, C., Urai, J.L., 2005. On the arrangement of solid inclusions in fibrous veins and the role of the crack-seal mechanism. Journal of Structural Geology 27, 481e494.

Hilgers, C., Koehn, D., Bons, P.D., Urai, J.L., 2001. Development of crystal morphology during antitaxial growth in a progressively widening vein: II. Numerical simulations of the evolution of antitaxial fibrous veins. Journal of Structural Geology 23, 873e885.

Hillier, R.D., Cosgrove, J.W., 2002. Core and seismic observations of overpressurerelated deformation within Eocene sediments of the Outer Moray Firth, UKCS. Petroleum Geoscience 8, 141e149.

Hoover, K.V., 1960. Devonian-Mississippian Shale Sequence in Ohio. State of Ohio Geological Survey, Information Circular N° 27, 154 pp.

Howitt, F., 1964. Stratigraphy and structure of the Purbeck inliers of Sussex (England). Quarterly Journal of the Geological Society, London 120, 77e113.

Hubbert, M.K., Willis, D.G., 1957. Mechanics of hydraulic fracturing. AIME 210, 153–166.

Hudson, J.D., Clements, R.G., 2007. The Middle Jurassic succession at Ketton, Rutland. Proceedings of the Geologists' Association 118, 239e264.

Hubbard, S.M., Romans, B.W., Graham, S.A. 2008. Deep-water foreland basin deposits of the Cerro Toro Formation, Magallanes Basin, Chile: Architectural elements of a sinuous basin axial channel belt. Sedimentology, 55, 1333-1359.

Hughes, R.A., 2003. Permian and Triassic Rocks of the Appleby District (Part of Sheet 30, England and Wales). British Geological Survey. Research Report RR/02/01, 15 pp.

Hulka, C., Gräfe, K.-U., Sames, B., Uba, C.E., Heubeck, C., 2006. Depositional setting of the Middle to Late Miocene Yecua Formation of the Chaco Foreland Basin, southern Bolivia. Journal of South American Earth Sciences 21, 135e150.

Hurst, A., Scott, A., Vigorito, M., 2011. Physical characteristics of sand injectites. Earth-Science Reviews 106, 215e246.

I

Iddings, A., Olsson, A., 1928. Geology of northwest Peru. American Association of

Petroleum Geologists Bulletin 12, 1e39.

Ingram, J.A., 1972. Donors Hill, Queensland. Geological Survey of Queensland, 1:250 000 Series e Explanatory Notes, 16 pp.

Israelson, C., Halliday, A.N., Buchardt, B., 1996. UePb dating of calcite concretions from Cambrian black shales and the Phanerozoic time scale. Earth and Planetary Science Letters 141, 153e159.

J

Jacob, H., 1989. Classification, structure, genesis and practical importance of natural solid oil bitumen (“migrabitumen”). International Journal of Coal Geology, 11, 65-79

Jessell, M.W., Willman, C.E., Gray, D.R., 1994. Bedding parallel veins and their relationship to folding. Journal of Structural Geology 16, 753e767.

Jiao, Y.Q., Wu, L.Q., He, M.C., Mason, R., Wang, M.F., Xu, Z.C., 2007. Occurrence, thermal evolution and primary migration processes derived from studies of organic matter in the Lucaogou source rock at the southern margin of the Junggar Basin, NW China. Science in China, Series D e Earth Sciences 50, 114e123.

Jochum, J., Friedrich, G., Leythaeuser, D., Littke, R., Ropertz, B., 1995. Hydrocarbonbearing fluid inclusions in calcite-filled horizontal fractures from mature Posidonia Shale (Hils Syncline, NW Germany). Ore Geology Reviews 9, 363e370.

Jowett, D.M.S., Schröder-Adams, C.J., 2005. Paleoenvironments and regional stratigraphic framework of the Middle-Upper Albian Lepin Formation in the Liard Basin, northern Canada. Bulletin of Canadian Petroleum Geology 53, 25e50.

Jowett, E.C., 1987. Formation of sulfide-calcite veinlets in the Kupferschiefer CueAg deposits in Poland by natural hydrofracturing during basin subsidence. Journal of Geology 95, 513e526.

Jowett, E.C., Cathles, L.M., Davis, B.W., 1993. Predicting depths of gypsum dehydration in evaporitic sedimentary basins. American Association of Petroleum Geologists Bulletin 77, 402e413.

Judd, J.W., 1871. On the Punfield Formation. Quarterly Journal of the Geological Society, London 27, 207e227.

Judd, J.W., 1878. On the Secondary rocks of Scotland. Third paper. The strata of the Western Coast and Islands. Quarterly Journal of the Geological Society, London 34, 660e739.

K

Katz, H.R. 1962. Fracture patterns and structural history in the sub-Andean belt of southernmost Chile. Journal of Geology, 70, 593-603.

Katz, H.R. 1963. Revision of Cretaceous stratigraphy in Patagonian Cordillera of Ultima Esperanza, Magallanes Province, Chile. American Association of Petroleum Geologists Bulletin, 47, 506-524.

Kay, S. M., Burns, W. M ., Copeland, P., Mancilla, O. 2006. Upper Cretaceous to Holocene magmatism and evidence for transient Miocene shallowing of the Andean subduction zone under the northern Neuquen Basin. In: Kay, S.M., Ramos, V.A. (eds), Evolution of an Andean Margin: A tectonic and magmatic view from the Andes to the Neuquén Basin (35° - 39°S lat), Geological Society of America, Special Paper, 407, 19-60.

Kelling, G., Moshrif, M.A., 1977. The orientation of fossil bivalves in a pene-littoral sequence (the Rhaetian of South Wales). Journal of Sedimentary Petrology 47, 1342e1346.

Kendall, A.C., 1975. Anhydrite replacements of gypsum (satin-spar) veins in the Mississippian caprocks of southeastern Saskatchewan. Canadian Journal of Earth Sciences 12, 1190e1195.

Keulen, N. T., den Brok, S.W.J., Spiers, C.J., 2001. Force of crystallisation of gypsum during hydration of synthetic anhydrite rock. 13th DRT conference, Deformation Mechanisms, Rheology, and Tectonics, Noordwijkerhout, The Netherlands.

Keyes, C.R., 1896. Note on the nature of cone-in-cone. Iowa Academy of Science, Proceedings 3, 75e76.

Klepeis, K. A. 1994a. Relationship between uplift of the metamorphic core of the southernmost Andes and shortening in the Magallanes foreland fold and thrust belt, Tierra del Fuego, Chile. Tectonics, 13, 882-904.

Klepeis, K. A. 1994b. The Magallanes and Deseado fault zones: Major segments of the South American-Scotia transform plate boundary in southernmost South America, Tierra del Fuego. Journal of Geophysical Research, 99, 22001-22014.

Klepeis, K.A., Austin, J.A. 1997. Contrasting styles of superposed deformation in the southernmost Andes. Tectonics, 16, 755-776.

Kolokol'tsev, V.G., 2002. The cone-in-cone structure and its origin. Lithology and Mineral Resources 37 (6), 523e535.

Kowal-Linka, M., 2010. Origin of cone-in-cone calcite veins during calcitization of dolomites and their subsequent diagenesis: a case study from the Gogolin Formation (Middle Triassic), SW Poland. Sedimentary Geology 224, 54e64.

Kozlowski, E.E., Manceda R., Ramos, V.A., 1993. Estructura: XII Congreso Geológico Argentino, Geología y Recursos Naturales de Mendoza, Relatorio 1, 235–256.

Kraemer, P.E. 1993. Perfil estructural de la Cordillera Patagónica Austral a los 50° L.S., Santa Cruz. XII Congreso Geológico Argentino y II Congreso de Exploración de Hidrocarburos, Buenos Aires, Actas, 3, 119-125.

Kraemer, P.E. 1998. Structure of the Patagonian Andes: Regional balanced cross section at 50°S, Argentina. International Geology Review, 40, 896-915.

Kraemer, P.E. 2003. Orogenic shortening and the origin of the Patagonian orocline (56°S.Lat). Journal of South American Earth Sciences, 15, 731-748.

Kraemer, P.E., Riccardi, A.C. 1997. Estratigrafía de la región comprendida entre los lagos Argentino y Viedma (49° 40' - 50° 10' lat. S), Provincia de Santa Cruz. Asociación Geológica Argentina Revista, 52, 333-360.

Kraemer, P.E., Ploskiewicz, Ramos, V.A. 2002. Estructura de la Cordillera Patagónica Austral entre los 46° y 52° S. In: Geología y Recursos Naturales de Santa Cruz, (Ed. Haller, M.J.), XV Congreso Geológico Argentino (El Calafate), Relatorio, 353-364.

Kranck, E.H. 1932. Geological investigations in the Cordillera of Tierra del Fuego. Acta Geog. Soc. Geogr. Fenn., 4, 1-231.

L

Lacroix, A., 1923. Minéralogie de Madagascar, Tome 3. Augustin Chalamel, Paris.

Laffitte, G.A., Arias, W.E., Marinelli, R.V. 1986. Caracterización térmica de la F. Springhill, Cuenca Austral. Relación con el entrampamiento de hidrocarburos. LX Reunión Anual a Nivel de Expertos, Lima, Perú, Exploración, Actas, 70-78.

Lamplugh, G.W., Kitchin, F.L., 1911. On the Mesozoic rocks in some of the coal explorations in Kent. Memoirs of the Geological Survey, Great Britain. 1e212.

Lang, W.D., 1914. The geology of the Charmouth Cliffs, Beach and Foreshore. Proceedings of the Geological Association 25, 293e360.

Lang, W.D., Spath, L.F., Richardson, W.A., 1923. Shales-With-'Beef', a sequence in the Lower Lias of the Dorset Coast. Quarterly Journal of the Geological Society, London 79, 47e99.

Large, R.R., Bull, S.W., Maslennikov, V.V., 2011. A carbonaceous sedimentary source-rock model for Carlin-type and orogenic gold deposits. Economic Geology 106, 331e356.

Lash, G.G., Engelder, T., 2005. An analysis of horizontal microcracking during catagenesis: example from the Catskill delta complex. American Association of Petroleum Geologists Bulletin 89, 1433e1449.

Law, B.E., Spencer, C.W., 1998. Abnormal pressures in hydrocarbon environments. In: Law, B.E., Ulmishek, G.F., Slavin, V.I. (Eds.), Abnormal Pressures in Hydrocarbon Environments, American Association of PetroleumGeologists, Memoir, 70, pp.1**e**11.

Leanza, A.F. 1972. Andes Patagónicos Australes. In: Geología Regional Argentina, Academia Nacional de Ciencias, Córdoba, 689-706.

Lee, G.W., 1920. The Mesozoic Rocks of Applecross, Raasay and North-east Skye. H.M. Geological Survey, Scotland, 93 pp.

Lees, G.M. & Cox, P.T. 1937. The geological basis of the present search for oil in Great Britain by the D'Arcy Exploration Compagny. Limited, Quarternary Journal of The Geological Society, London, XCIII, 156-194.

Lefticariu, L., 2005. Kinematics of Fibrous Vein Growth: Insights from Stable Isotopes and Trace Elemental Data (Abstract). American Geophysical Union. Fall Meeting, Section T26.

Legarreta, L., Gulisano, C.A., 1989. Análisis estratigráfico de la cuenca Neuquina (Triásico superior–Terciario inferior). In: Chebli, G.A. & Spalletti, L.A. (eds) Cuencas Sedimentarias Argentinas. Universidad Nacional de Tucumán, Serie de Correlación Geológica, 6, 221–244.

Legarreta, L., Villar, H.J. 2011. Geological and geochemical keys of the potential shale resources, Argentina basins. American Association of Petroleum Geologists, Geoscience Technology Workshop, "Unconventional Resources: Basics, Challenges, and Opportunities for New Frontier Plays," Buenos Aires, Argentina, June 26-28, 2011, Search and Discovery Article, 80196.

Lemrabott, A., Cobbold, P.R., 2009. Physical Modeling of Fluid Overpressure and Compaction during Hydrocarbon Generation in Source Rock of Low Permeability. American Association of Petroleum Geologists, International Conference and Exhibition, Rio de Janeiro, Brazil, 15**e**18 November. Search and Discovery Article #40518 (2010) http://www.searchanddiscovery.com.

Leonhard, K.C. von, 1823. Charakteristik der felsarten, 418 pp.

LePain, D.L., Decker, P.L., Wartes, M.A., 2008. Measured sections and preliminary interpretations of the Nanushuk Formation exposed along the Colville River near the confluences with the Awuna and Killik rivers. In: Wartes, M.A., Decker, P.L. (Eds.), Preliminary Results of Recent Geologic Field Investigations in the Brooks Range Foothills and North Slope, Alaska. Alaska Division of Geological & Geophysical Surveys Preliminary Interpretive Report, 2008-1, pp. 41e45.

Lesta, P.J., Digregorio, J., Mozetic, M.E. 1985. Presente y futuro de la exploración de petróleo en las cuencas subandinas, Argentina. II Simposio Bolivariano, Exploración Petrolera en las Cuencas Subandinas, Asociación Colombiana de Geólogos y Geofísicos del Petróleo (ACGGP), Bogotá, Publicaciones, 3, 1-35.

Leythaeuser, D., Littke, R., Radke, M., Schaefer, R.G., 1988. Geochemical effects of petroleum migration and expulsion from Toarcian source rocks in the Hils Syncline area, NW-Germany. In: Mattavelli, L., Novelli, L. (Eds.), Advances in Organic Geochemistry 1987. Organic Geochemistry, vol. 13, pp. 489e502.

Linck, G., 1931. Tutenmergel und Nagelkalk. Chemie der Erde 6, 227e238.

Linck, G., Noll, W., 1928. Uber Tutenmergel. Chemie der Erde 3, 699e721.

Liu, L., Bajaj, C., Deasy, J.O., Low, D.A., Ju, T., 2008. Surface Reconstruction from Nonparallel Curve Networks. In: EUROGRAPHICS, vol. 27. The eurographics association and Blackwell Publishing Co Ltd., p. 2. Available at: http://diglib.eg.org/EG/Publications/bookstore/Proc

Ljungner, E. 1931. El carbón asfáltico de Las Romanas (Mina La Valenciana) en el Distrito de Malargüe (Departamento de San Rafael). Dirección General de Minas, Geología e Hidrología, Informe, 1-11 (unpublished report).

Lodolo, E., Menichetti, M., Bartole, R., Ben-Avraham, Z., Tassone, A., Lippai, H. 2003. Magallanes–Fagnano continental transform fault (Tierra del Fuego, southernmost South America). Tectonics, 22, 1076.

Lonsdale, W., 1832. Series 2. On the Oolitic District of Bath, vol. 3. Transactions of the Geological Society, London, pp. 241e276.

Lott, G.K., 1985. Late Triassic, Jurassic and Early Cretaceous geology of the southern North Sea Basin. PhD thesis, University of Leicester, U.K., 239 pp.

Lozej, G.P., Beales, F., 1997. Stratigraphy and structure of La Encantada mine area, Coahuila, Mexico. Geological Society of America Bulletin 88, 1793e1807.

Lugli, S., Reimold, W.U., Koeberl, C., 2005. Silicified cone-in-cone structures from Erfoud (Morocco): a comparison with impact-generated shatter cones. In: Koeberl, C., Henkel, H. (Eds.), Impact Tectonics. Impact Studies Series, vol. 6, pp. 81e110.

M

Machel, H.-G., 1985. Fibrous gypsum and fibrous anhydrite in veins. Sedimentology 32, 443e454.

MacKenzie, W.S., 1972. Fibrous calcite, a Middle Devonian geologic marker, with statigraphic significance, District of Mackenzie, Northwest Territories. Canadian Journal of Earth Sciences 9, 1431e1440.

Macsotay, O., Erlich, R.N., Peraza, T., 2003. Sedimentary structures of the La Luna, Navay and Quercual Formations, Upper Cretaceous of Venezuela. Palaios 18, 334e348.

Mahboubi, A., Moussavi-Harami, R., Collins, R.B., Muhling, J.R., 2010. Petrography and geochemical signatures in cracks filling calcite sequences in septarian concretions, Sanganeh Formation, Kopet-Dagh Basin, NE Iran. Journal of Applied Sciences 10, 526e534.

Mallet, J.-L., 1992. Discrete smooth interpolation in geometric modeling. Comput. Aided Des. 24 (4), 178**e**191.

Mallet, J.L., 2002. Geomodeling. Oxford University Press, p. 613.

Maillot, H., Bonte, A., 1983. Cone-in-cone texture from Deep Sea Drilling Project Leg 71, Site 511, Falkland Plateau, south Atlantic Ocean. Initial Reports of the Deep Sea Drilling Project 71 (1), 345e349.

Mantell, G.A., 1850. Notice of the remains of the Dinornis and other birds, and of fossils and rock-specimens recently collected by Mr Walter Mantel in the Middle Island of New Zealand, etc. Quarterly Journal of the Geological Society, London 6, 319e342.

Markello, J.R., Koepnick, R.B., Waite, L.E., Collins, J.F., 2007. The carbonate analogs through time (CATT) hypothesis and the global atlas of carbonate fields e a systematic and predictive look at Phanerozoic carbonate systems. In: Controls on Carbonate Platform and Reef Development, vol. 89. Society for Sedimentary Geology (SEPM), pp. 1e31. Special Publications.

Marshall, J.D., 1982. Isotopic composition of displacive fibrous calcite veins; reversals in pore-water composition trends during burial diagenesis. Journal of Sedimentary Petrology 52, 615e630.

Marshall, P., 1926. The Upper Cretaceous ammonites of New Zealand. Philosophical Transactions of the Royal Society of New Zealand 56, 129e210.

Martill, D.M., 1987. A taphonomic and diagenetic case study of a partially articulated ichthyosaur. Palaeontology 30, 543e555.

Martinius, A.W., Hegner, J., Kaas, I., Bejarano, C., Mathieu, X., Mjús, R., 2012. Sedimentology and depositional model for the Early Miocene Oficina Formation in the Petrocedeño Field (Orinoco heavy-oil belt, Venezuela). Marine and Petroleum Geology 35, 354e380, http://dx.doi.org/10.1016/j.marpetgeo.2012.02.013.

Maubeuge, P.L., 1945. Sur quelques niveaux marneux de Lorraine à structure cône in cône. Comptes Rendus de la Société Géologique de France 9, 114e116.

Maubeuge, P.L., 1991. Le forage de Rosiéres aux Salines (M & M), un carottage continu dans le Trias moyen. Bulletin des Académie et Société Lorraines des Sciences 30, 25e33.

McCaig, A.M., Wayne, D.M., Marshall, J.D., Banks, D., Henderson, I., 1995. Isotopic and fluid inclusion studies of fluid movement along the Gavarnie Thrust, Central Pyrenees: reaction fronts in carbonate mylonites. American Journal of Science 295, 309e343.

Means, W.D., Li, T., 2001. A laboratory simulation of fibrous veins: some first observations. Journal of Structural Geology 23, 857e863.

Meyerhoff, H.A., 1948. The occurrence and mining of solid bitumens in western Argentina. Transactions of the American Institute of Mining Engineers, 181, 403-412.

Michel, J., Baumgartner, L., Putlitz, B., Schaltegger, U., Ovtcharova, M. 2008. Incremental growth of the Patagonian Torres del Paine laccolith over 90 k.y. Geology, 36, 459-462.

Milliken, K.L., Day-Stirrat, R.J., 2012. Cementation in Mudrocks: Brief Review with Examples from Cratonic Basin Mudrocks.

Milliken, K.L., Esch, W.L., Reid, R.M., Zhang, T., 2012. Grain assemblages and strong diagenetic overprinting in siliceous mudrocks, Barnett Shale (Mississippian), Fort Worth Basin, Texas. American Association of Petroleum Geologists Bulletin 96, 1553e1578.

Milnes, A.G. 1987. Tectonic evolution of the southern Andes, Tierra del Fuego: a summary. In: J.P. Schaer, J. Rodgers (Eds.), The anatomy of mountain ranges, Princeton University Press, 173-177.

Mingramm, A.R.G., 1982. Evolution scheme of Fueguian Andes along Los Cerros - Pla Hardy Section, Shell Compañía Argentina de Petróleo (unpublished report).

Molyneux, A.J.C., 1909. On the Karroo system in Northern Rhodesia, and its relation to the general geology. Quarterly Journal of the Geological Society, London 65, 408e439.

Morgans-Bell, H.S., Coe, A.L., Hesselbo, S.P., Jenkyns, H.C., Weedon, G.P., Marshall, J.E.A., Tyson, R.V., Williams, C.J., 2001. Integrated stratigraphy of the Kimmeridge Clay Formation (Upper Jurassic) based on exposures and boreholes in south Dorset, U.K. Geological Magazine 138, 511e539.

Mourgues, R., Cobbold, P.R., 2003. Some tectonic consequences of fluid overpressures and seepage forces as demonstrated by sandbox modeling. Tectonophysics 376, 75–97.

Mpodozis, C., Rojas, L. 2006. Orogénesis en los Andes Patagónicos Australes de Tierra del Fuego: cierre de una “cuenca marginal” o collision intracontinental? 11 Congreso Geológico Chileno, Actas, 1, 329-332.

Mügge, O., 1928. Über die Entstehung faseriger Minerale und ihrer Aggregationsformen. Neues Jahrbuch für Mineralogie, Geologie und Paläontologie 58A, 303e348.

N

Natland, M.L., González, E., Cañón, A., Ernst, M. 1974. A system of stages for correlation of Magallanes Basin sediments. Geological Society of America Memoir, 139, 1-126.

Nelson, E.P., Dalziel, I.W.D., Milnes, A.G., 1980. Structural geology of the Cordillera Darwin e collision style orogenesis in the southernmost Andes. Eclo. Geol. Helvet. 73, 727e751.

Neubauer, F., Liu, Y., Genser, J., Rieser, A.B., Friedl, G., Ge, X., Thöni, M., 2010. Quaternary celestine and gypsum extensional veins in a folded hypersaline lake infill: the Qaidam Basin, Western China. Austrian Journal of Earth Sciences 103, 81e91.

Newberry, J.S., 1885. On cone-in-cone. Geological Magazine, Decade III II, 559.

Newton, E.T., Teall, J.J.H., 1897. Notes on a collection of rocks and fossils from Franz Josef Land, made by the Jackson-Harmworth Experidtion during 1894e1896. Quarterly Journal of the Geological Society, London 53, 477e512.

Nicholas, C.J., Pearson, P.N., Bown, P.R., Jones, T.D., Huber, B.T., Karega, A., Lees, J.A., McMillan, I.K., O'Halloran, A., Singano, J.M., Wade, B.S., 2006. Stratigraphy and sedimentology of the Upper Cretaceous to Paleogene Kilwa Group, southern coastal Tanzania. Journal of African Earth Sciences 45, 431e466.

Nullo, F.E., Stephens, G., Combina, A., Dimieri, L., Baldauf, P., Bouza, P., 2005. Hoja geológica 3569-III/3572-IV, Malargüe, Provincia de Mendoza. Programa Nacional de Cartas Geológicas de la República Argentina, 1:250.000, Servicio Geológico Minero Argentino, Instituto de Geología y Recursos Minerales, Boletín, 346, 1-85.

Nyambe, I.A., Dixon, O., 2000. Sedimentology of the Madumabisa Mudstone Formation (Late Permian), Lower Karoo Group, mid-Zambezi Valley Basin, southern Zambia. Journal of African Earth Sciences 30, 535e553.

O

ODP Shipboard Scientific Party, 2003. Demerara Rise: Equatorial Cretaceous and Paleogene Plaeoceanographic Transect. Leg 207 Preliminary Report. Ocean Drilling Program, Texas A&M University, 63 pp.

Oliver, N.H.S., Bons, P.D., 2001. Mechanisms of fluid flow and fluid-rock interaction in fossil metamorphic-hydrothermal systems inferred from vein-wallrock patterns, geometry, and microstructure. Geofluids 1, 137e163.

Olivero, E.B., Malumián, N. 1999. Eocene stratigraphy of southeastern Tierra del Fuego island, Argenrtina. American Association of Petroleum Geologists Bulletin, 83, 295-313.

Olivero, E.B., Malumián, N., 2008. Mesozoic–Cenozoic stratigraphy of the Fuegian Andes, Argentina. Geologica Acta, 6, 5-18.

Olivero, E.B., Martinioni, D.R. 2001. A review of the geology of the Argentinian Fueguian Andes. Journal of South American Earth Sciences, 14, 175-188.

Olivero, E.B., Martinioni, D.R., Malumián, N., Palamarczuk, S. 1999. Bosquejo geológico de la Isla Grande de Tierra del Fuego, Argentina. XIV Congreso Geológico Argentino, Salta, Actas, 1, 291-294.

Orchard, M.J., McRoberts, C.A., Tozer, E.T., Johns, M.J., Sandy, M.R., Shaner, J.S., 2001. An intercalibrated biostratigraphy of the Upper Triassic of Black Bear Ridge, Williston Lake, northeast British Columbia. Geological Survey of Canada, Current Research 2001eA6, 21.

Ortí, F., Alonso, R.N., 2000. Gypsum-hydroboracite association in the Sijes Formation (Miocene, NW Argentina): Implications for the genesis of Mg-bearing borates. Journal of Sedimentary Research 70, 664e681.

Osborne, M.J. and Swarbrick, R.E., 1997. Mechanisms for generating overpressure in sedimentary basins: A reevaluation. AAPG Bulletin, 81(6): 1023-1041.

P

Parnell, J., 1999. Petrographic evidence for emplacement of carbon into Witwatersrand conglomerates under high fluid pressure. Journal of Sedimentary Research 69, 164e170.

Parnell, J., Ansong, G., Veale, C., 1994. Petrology of the bitumen (manjak) deposits of Barbados: hydrocarbon migration in an accretionary prism. Marine and Petroleum Geology 11, 743e755.

Parnell, J., Carey, P.F., 1995. Emplacement of bitumen (asphaltite) veins in the Neuquén Basin, Argentina. American Association of Petroleum Geologist Bulletin 79, 1798-1816.

Parnell, J., Honghan, C., Middleton, D., Haggan, T., Carey, P., 2000. Significance of fibrous mineral veins in hydrocarbon migration: fluid inclusion studies. Journal of Geochemical Exploration 69-70, 623e627.

Pashin, J.C., 2011. Geological Foundation for Production of Natural Gas from Diverse Shale Formations. Research Partnership to Secure Energy for America, Final Report 07122.17.01. Geological Survey of Alabama, Tuscaloosa, 156 pp.

Pearson, P.N., Nicholas, C.J., Singano, J.M., Bown, P.R., Coxall, H.K., van Dongen, B.E., Huber, B.T., Karega, A., Lees, J.A., MacLeod, K., McMillan, I.K., Pancost, R.D., Pearson, M., Msaky, E., 2006. Further Paleogene and Cretaceous sediment cores from the Kilwa area of coastal Tanzania: Tanzania Drilling Project Sites 6e10. Journal of African Earth Sciences 45, 279e317, http://dx.doi.org/10.1016/ j.jafrearsci.2006.02.005.

Pedersen, G.K., 1989. The sedimentology of Lower Palaeozoic black shales from the shallow wells Skelbro 1 and Billegrav 1, Bornholm, Denmark. Bulletin of the Geological Society of Denmark 37, 151e173.

Penn, I.E., Cox, B.M., Gallois, R.W., 1986. Towards precision in stratigraphy: geophysical log correlation of Upper Jurassic (including Callovian) strata of the Eastern England

Shelf. Journal of the Geological Society, London 143, 381e410.

Peroni, G., Cagnolatti, M., Pedrazzini, M., 2002. Cuenca Austral: Marco geológico y reserva histórica de la actividad petrolera. In: Schiuma, M., Hinterwimmer, G., Vergani, G. (Eds.), Rocas reservorio de las cuencas productivas de la Argentina, 5_ Congreso de Exploración y Desarrollo de Hidrocarburos, Mar del Plata, pp. 11**e**26.

Perrone, V., Capoa, P., de Cesarini, F., 1998. Remise en question, à propos de la Nappe du Val Varecchia, d'attributions paléogéographiques et structurales de l'Appenin nord-oriental (Italie). Comptes Rendus de l'Académie des Sciences de Paris. Sciences de la Terre et des Planètes 326, 347e353.

Philipp, S.L., 2008. Geometry and Formation of Gypsum Veins in Mudstones at Watchet, vol. 145. Geological Magazine, Somerset, SW England, pp. 831e844.

Pittion, J.-L., Arbe, H.A. 1999. Sistemas petroleros de la Cuenca Austral. IV Congr. Exploración y desarrollo de hidrocarburos, Mar del Plata, Actas, I, 239-262.

Pittion, J.L., Gouadain, J. 1992. Source-rocks and oil generation in the Austral Basin. Thirteenth World Petroleum Congress, Buenos Aires, Proceedings, John Wiley & Sons, New York, 2, 113-120.

Piscione, C.A.S., 1947. Asfaltitas y pirobitumen asfáltico. Revista de la Sociedad Geológica Argentina, 2, 65-87.

Pompeckj, J.F., 1900. The Jurassic fauna of Cape Flora, Franz Josef Land, with a geological sketch of Cape Flora and its neighbourhood by Fridtjof Nansen. In: Nansen, F. (Ed.), The Norwegian North Polar Expedition, 1893e1896, Scientific Results, vol. 1, pp. 1e147.

Pratt, L., Mompart, L., Murat, B., 1993. Hydrocarbon Generation Potential of the Cretaceous Section from Well ALP-6, Perija Region. American Association of Petroleum Geologists, Search and Discovery, Venezuela. Article 90988.

Provo, L.J., Kepferle, R.C., Potter, P.E., 1978. Division of Black Ohio Shale in eastern Kentucky. American Association of Petroleum Geologists Bulletin 62, 1703e 1713.

R

Radelli, L., 1975. Geology and oil of Sakamena Basin, Malagasy Republic (Madagascar). American Association of Petroleum Geologists Bulletin 59, 97e114.

Raisossadat, S.N., 2004. The ammonite family Deshayesitidae in the Kopet Dagh Basin, north-east Iran. Cretaceous Research 25, 115e136.

Ramos, V.A. 1982. Geología de la region del Lago Cardiel, Provincia de Santa Cruz. Asociación Geológica Argentina Revista, 37, 23-49.

Ramos, V. A. 1989. Andean foothills structures in the northern Magallanes Basin, Argentina. American Association of Petroleum Geologists Bulletin, 73, 887-903.

Ramos, V.A. 2005. Seismic ridge subduction and topography: Foreland deformation in the Patagonian Andes. Tectonophysics, 399, 73-86.

Ramsay, J.G., 1980. The crack-seal mechanism of rock deformation. Nature 284, 135e139.

Rassmuss, J., 1923. Breves apuntes geológicos sobre la parte del territorio del Neuquén entre Auca Mahuida y El Tromen. Dirección General de Minas, Geológia e Hidrogeología, Serie F (Informes Preliminares y Communicaciones), 6 (1), 15-20.

Reid, C., 1903. The geology of the country around Salisbury (Explanation of Sheet 298). Memoirs of the Geological Survey, England and Wales 298, 1e77.

Renne, P.R., Swisher, C.C., Deino, A.L., Karner, D.B., Owens, T.L., DePaolo, D.J., 1998. Intercalibration of standards, absolute ages and uncertainties in $^{40}Ar/^{39}Ar$ dating. Chemical Geology, 145, 117-152.

Renz, H.H., 1957. Stratigraphy and geological history of Eastern Venezuela. Geologisches Rundschau 45, 728e759.

Reynolds, S.H., Vaughan, A., 1904. The Rhaetic Beds of the South Wales direct line. Quaterly Journal of the Geological Society, London 60, 194e214.

Riccardi, A.C. 1971. Estratigrafía en el oriente de Bahía La Lancha, Lago San Martín, Santa Cruz, Argentina. Revista del Museo de La Plata, 7, 245-318.

Riccardi, A.C., Rolleri, E.O. 1980. Cordillera Patagónica Austral. Segundo Simposio de Geología Regional Argentina, Actas, 2, 1173-1306.

Riccardi, A.C., Aguirre Urreta, M.B., Medina, F.A., 1987. Aconeceratidae (Ammonitina) from the Hauterivian-Albian of southern Patagonia. Palaeontographica, Abt. A 196, 105e185.

Richardson, L., 1905. The Rhaetic and contiguous deposits of Glamorgan. Quarterly Journal of the Geological Society, London 61, 385e424.

Richardson, L., 1911. The Rhaetic and contiguous deposits of West, Mid, and part of East Somerset. Quarterly Journal of the Geological Society, London 67, 1e74.

Richardson, W.A., 1920. The fibrous gypsum of Nottinghamshire. Mineralogical Society Journal 19, 77e95.

Richardson, W.A., 1923. Petrology of the Shales-with-“Beef”. Quarterly Journal of the Geological Society, London 79, 88e99.

Richiano, S., 2012. Sedimentología e icnología de la formación Rio Mayer, cuenca Austral, provincia de Santa Cruz, Argentina. Tesis de doctorado. Facultad de Ciencias Naturales y Museo, Universidad Nacional de La Plata, Argentina, p. 278.

Richiano, S., Varela, A.N., Cereceda, A., Poiré, D.G., 2012. Evolución paleoambiental de la Formación Rio Mayer, Cretácico Inferior, Cuenca Austral, Provincia de Santa Cruz, Argentina. Latin Am. J. Sedimentol. Basin Anal. 19, 3**e**26.

Riediger, C.L., Coniglio, M., 1992. Early diagenetic calcites and associated bitumens in the “Nordegg Member”; implications for Jurassic paleogeography of the Western Canada sedimentary basin. Bulletin of Canadian Petroleum Geology 40, 381e394.

Rodrigues, N.T., 2008. Fracturation hydraulique et forces de courant: modélisation analogique et données de terrain. Mémoire de Doctorat, Université de Rennes 1, 164 pp.

Rodrigues, N., Cobbold, P.R., Løseth, H., Ruffet, G., 2009. Widespread beddingparallel veins of fibrous calcite (“beef”) in a mature source rock (Vaca Muerta Fm, Neuquén Basin, Argentina): evidence for overpressure and horizontal compression. Journal of the Geological Society, London 166, 695e709, http:// dx.doi.org/10.1144/0016-76492008-111.

Rodriguez, F., Villar, J. H., Baudino, R. 2007. Hydrocarbon generation, migration, and accumulation related to igneous intrusions: An atypical petroleum system from the Neuquén Basin of Argentina. SPE Paper 107926-PP, 4 p.

Rodriguez Monreal, F., Villar, H.J., Baudino, R., Delpino, D., Zencich, S. 2009. Modeling an atypical petroleum system: A case study of hydrocarbon generation, migration and accumulation related to igneous intrusions in the Neuquen Basin, Argentina. Marine and Petroleum Geology, 26, 590-605.

Rodriguez, J.F., Cagnolatti, M.J. 2008. Source Rocks and Paleogeography, Austral Basin, Argentina. American Association of Petroleum Geologists Convention, San Antonio, Texas, April 20-23, 2008, Search and Discovery Article, 10173, 1-24.

Rodríguez, J.F., Miller, M., Cagnolatti, M.J. 2008. Sistemas petroleros de Cuenca Austral, Argentina y Chile. In: Sistemas Petroleros de las Cuencas Andinas (ed: Cruz, C.E., Rodríguez, J.F., Hechem, J.J., Villar, H.J.), Instituto Argentino del Petróleo y del Gas. 1-31.

Rodríguez, J., Miller, M., 2005. Cuenca Austral. In: Frontera Exploratoria de la Argentina. VI Congreso de Exploración y Desarrollo de Hidrocarburos, pp. 307[e] 324.

Rojas, L., Mpodozis, C. 2006. Geología estructural de la Faja Plegada y Corrida de Tierra del Fuego, Andes Patagónicos Chilenos. 11 Congreso Geológico Chileno, Actas, 1, 325-328.

Román-Berdiel, T., 1999. Geometry of granite emplacement in the upper crust: contribution of analogue modelling. In: Castro, A., Fernández, C., Vigneresse, J.L. (Eds.), Understanding Granites: Integrating New and Classical Techniques, Geological Society, London, Special Publication, vol. 174, pp. 77**e**94.

Romans, B.W., Fildani, A., Hubbard, S.M., Covault, J.A., Fosdick, J.C., Graham, S.A. 2011. Evolution of deep-water stratigraphic architecture, Magallanes Basin, Chile. Marine and Petroleum Geology, 28, 612-628.

Rossello, E.A., Haring, C.E., Cardinali, G., Suárez, F., Laffitte, G.A., Nevistic, A.V. 2008. Hydrocarbons and petroleum geology of Tierra del Fuego, Argentina. Geologica Acta, 6, 69-83, doi: 10.1344/105.000000242.

Rubinstein, C., Melo, J.H.G., Steemans, P., 2005. Lochkovian (earliest Devonian) miospores from the Solimões Basin, northwestern Brazil. Review of Palaeobotany and Palynology 133, 91e113.

Ruffet, G., Féraud, G., Ballèvre, M., Kiénast, J-R., 1995. Plateau ages and excess argon in phengites: an ^{40}Ar-^{39}Ar laser probe study of Alpine micas ‘Sesia Zone, Western Alps, northern Italy). Chemical Geology (Isotopic Geosciences Section), 121, 327-343.

Ruffet, G., Gruau, G., Ballèvre, M., Féraud, G., Philippot, P., 1997. Rb-Sr and ^{40}Ar-^{39}Ar laser probe dating og high-pressure phengites from the Sesia zone (western Alps): underscoring of excess argon and new age constraints on the high-pressure metamorphism. Chemical Geology, 141, 1-18.

S

Sach, A.J., 1892. On a sample of cone-in-cone structure found at Picton, New South Wales. Geological Magazine 9, 505e507.

Sælen, G., Tyson, R.V., Telnæs, N., Talbot M.R., 2000. Contrasting watermass conditions during deposition of the Whitby Mudstone (Lower Jurassic) and Kimmeridge Clay (Upper Jurassic) formations, UK. Palaeogeography, Palaeoclimatology, Palaeoecology 163, 163–196

Salas, J., 1892. Noticias y documentos sobre el carbón de piedra de San Rafael (Mendoza). Revista del Museo de La Plata, 4, 138-.

Sánchez, A., Pavlishina, P., Godoy, E., Hervé F., Fanning, C.M. 2010. On the presence of Upper Paleocene rocks in the foreland succession at Cabo Nariz, Tierra del Fuego, Chile: geology and new palynological and U-Pb data. Andean Geology, 37, 413-432.

Sanderson, D.J., Roberts, S., Gumiel, P., 1994. A fractal relationship between vein thickness and gold grade in drill core from La Codosera, Spain. Economic Geology 89, 168e173.

Sangster, A.L., Smith, P.K., 2007. Metallogenic summary of the Meguma gold deposits, Nova Scotia. In: Goodfellow, W.D. (Ed.), Mineral Deposits of Canada: a Synthesis of Major Deposit-types, District Metallogeny, the Evolution of Geological Provinces, and Exploration Methods. Geological Association of Canada, Mineral Deposits Division, Special Publication, vol. 5, pp. 723e732.

Schwarz, J.-O., Koehn, D., 2011. Geometry of and fluid flow in bedding parallel crackseal veins. EGU General Assembly. Geophysical Research Abstracts 13, 5699.

Scott, K.M. 1966. Sedimentology and dispersal patterns of a Cretaceous flysch sequence, Patagonian Andes, southern Chile. American Association of Petroleum Geologists Bulletin, 50, 72-107.

Secretaría de Energía, Ministerio de Planificación Federal, Inversión Pública y Servicios. 2012. Cuenca Austral. http://www.energia.gov.ar/contenidos/verpagina.php?idpagina=814.

Séjourné, S., Malo, M., Savard, M.M., Kirkwood, D., 2005. Multiple origin and regional significance of bedding parallel veins in a fold and thrust belt: the example of a carbonate slice along the Appalachian structural front. Tectonophysics 407, 189e209, http://dx.doi.org/10.1016/j.tecto.2005.07.009.

Selles-Martinez, J., 1994. New insights in the origin of cone-in-cone structures. Carbonates and Evaporites 9, 172e186.

Shao, L., Zhang, P., Hilton, J., Gayer, R., Wang, Y., Zhao, C., Luo, Z., 2003. Paleo-environments and paleogeography of the Lower and lower Middle Jurassic coal measures in the Turpan-Hami oil-prone coal basin, northwestern China. American Association of Petroleum Geologists Bulletin 87, 335e355.

Shaub, B.M., 1937. The origin of cone-in-cone and its bearing on the origin of concretions and septaria. American Journal of Science 203, 331e334.

Shaw, R.P., Morton, R.D., 1990. A fluid inclusion study of quartzite-hosted lode gold mineralization at Athabasca Pass, Central Rocky Mountains, Canada. Economic Geology

85, 1881e1893.

Shearman, D.J., Mossop, G., Dunsmore, H., Martin, M., 1972. Origin of gypsum veins by hydraulic fracture. Institute of Mining and Metallurgy, Transactions B181, 149e155.

Shelton, R., 1997. Tectonic evolution of the Larne Basin. In: Meadows, N.S., Trueblood, S.P., Hardman, M., Cowan, G. (Eds.), Petroleum Geology of the Irish Sea and Adjacent Areas. Geological Society, London, Special Publications, vol. 124, pp. 113e133.

Short, A.R., 1904. A description of some Rhaetic sections in the Bristol District, with considerations on the mode of deposition of the Rhaetic Series. Quarterly Journal of the Geological Society, London 60, 170e193.

Sibson, R.H., 2003. Brittle-failure controls on maximum sustainable overpressure in different tectonic regimes. American Association of Petroleum Geologists Bulletin 87, 901e908.

Silva, A.L. da, 2003. Estratigrafia física e deformação do sistema lacustre carbonático (Aptiano-Albiano) da Bacia do Araripe em afloramentos selecionados. Dissertação de Mestrado, Universidade Federal de Pernambuco, Pós-graduação em Geociências, 118 pp.

Silvestro, J., Kraemer, P., 2005. Evolución tecto-sedimentaria de la Cordillera Principal en el sector surmendocino a los 35° 30′ S, Faja plegada de Malargüe, Republica Argentina. 6° Congreso de Exploración y Desarrollo de Hidrocarburos, Artículo 25, Mar del Plata, CD-ROM.

Soffia, C., José, M., Harambour, P., Salvador, S. 1988. Estructuras en el cinturon plegado y fallado de Ultima Esperanza, Magallanes, Chile. Departamento de Geologia, Facultad de Ciencias Fisicas y Matematicas, Universidad de Chile, Comunicaciones, Serie 22, 39-36.

Sorby, H.C., 1860. On the origin of “cone-in-cone”. British Association for the Advancement of Science, Report of the 29th Meeting, 1859, Transactions of Sections, Geology, 124 pp.

Spain, D.R., Anderson, G.A., 2010. Controls on reservoir quality and productivity in the Haynesville Shale, northwestern Gulf of Mexico Basin. Gulf Coast Association of Geological Studies Transactions 60, 657e668.

Speed, R., 1990. Volume loss and defluidization history of Barbados. Journal of Geophysical Research 95 (B6), 8983e8996.

Stauffer, C.R., 1911. A review of literature on the geology of South America. The Ohio Naturalist 11, 273e285.

Stewart, A.J., 1979. A barred-basin marine evaporite in the Upper Proterozoic of the Amadeus Basin, central Australia. Sedimentology 26, 33e62.

Stoneley, R. 1982. The structural development of the Wessex Basin. Journal of the Geological Society, London, 139, 543-554.

Stoneley, R., 1983. Fibrous calcite veins, overpressures, and primary oil migration. American Association of Petroleum Geologists Bulletin 67, 1427e1428.

Stow, G.W., 1874. Geological notes upon Griqualand west. Quarterly Journal of the Geological Society, London 30, 581e680.

Suárez, D., M. 1980. Mapa geológíco de Chile. Servicio Nacional de Geología y Minería, scale 1:1 000 000, 6 sheets.

Suárez, M., de la Cruz, R., Bell, C.M. 2000. Timing and origin of deformation along the Patagonian fold and thrust belt. Geological Magazine, 137, 345-353.

Suchy, V., Dobes, P., Filip, J., Stejskal, M., Zeman, A., 2002. Conditions for veining in the Barrandian Basin (Lower Palaeozoic), Czech Republic: evidence from fluid inclusion and apatite fission track analysis. Tectonophysics 348, 25e50.

Swarbrick, R.E., Osborne, M.J., Yardley, G.S., 2002. Comparison of overpressure magnitude resulting from the main generating mechanisms. In: Huffman, A.R., Bowers, G.L. (Eds.), Pressure Regimes in Sedimentary Basins and Their Prediction. American Association of Petroleum Geologists Memoir, vol. 76, pp. 1e12.

T

Taber, S., 1916. The growth of crystals under external pressure. American Journal of Science 41 (246), 532e556. Series 4.

Taber, S., 1918. The origin of veinlets in the Silurian and Devonian strata of New York. Journal of Geology 26, 56e63.

Taber, S., 1930. The mechanics of frost heaving. Journal of Geology 38, 303e317.

Talukdar, S., Gallango, O., Vallejos, C., Ruggiero, A., 1988. Observations on the primary migration of oil in the La Luna source rocks of the Maracaibo Basin, Venezuela. Oil & Gas Science and Technology (Revue de l'Institut Français du Pétrole) 43, 357e370.

Tanner, P.W.G., 1989. The flexural-slip mechanism. Journal of Structural Geology 11, 635e655.

Tarney, J., Schreiber, B.C., 1976. Cone-in-cone and beef-in-shale textures from DSDP site 330, Falkland Plateau, South Atlantic. In: Barker, P.F., Dalziel, I.W.D., et al. (Eds.), Initial Reports of the Deep Sea Drilling Project, vol. 36. U.S. Government Printing Office, Washington, D.C, pp. 865e870.

Tarr, W.A., 1922. Cone-in-Cone. American Journal of Science 4, 199e213.

Testa, G., Lugli, S., 2000. Gypsum-anhydrite transformations in Messinian evaporites of central Tuscany (Italy). Sedimentary Geology 130, 249e268.

Thickpenny, A., 1984. The Sedimentology of the Swedish Alum Shales. In: Geological Society, London, Special Publications, vol. 15, pp. 511e525.

Tassone, A., Lippai, H., Lodolo, E., Menichetti, M., Comba, A., Hormaechea, J.L., Vilas, J.F. 2005. A geological and geophysical crustal section across the Magallanes-Fagnano fault in Tierra del Fuego. Journal of South American Earth Sciences, 19, 99-109.

Thomas, C.R. 1949. Geology and petroleum exploration in Magallanes Province, Chile. American Association of Petroleum Geologists Bulletin, 33, 1553-1578.

Thompson, B., 1902. Geology. In: Adkins, W.R.D., Serjeantson, R.M. (Eds.), A History of the County of Northampton, vol. 1. University of London, Institute for Historical Research, pp. 1e40.

Thoral, M., 1942. A propos de la structure “cone-in-cone”. Comptes Rendus de la Société Géologique de France 13, 144e146.

Tobin, K.J., Walker, K.R., Steinhauff, D.M., Mora, C.I., 1996. Fibrous calcite from the Ordovician of Tennessee: preservation of marine oxygen isotopic composition and its implications. Sedimentology 43, 235e251.

Torres Carbonell, P.J., Dimieri, L.V., Olivero, E.B. 2011. Progressive deformation of a Coulomb thrust wedge: the eastern Fuegian Andes Thrust-Fold Belt. In: Kinematic Evolution and Structural Styles of Fold-and-Thrust Belts (ed. Poblet, J., Lisle, R.J.), Geological Society, London, Special Publications, 349, 123-147, doi:10.1144/SP349.7.

Torres, T., Barale, G., Méon, H., Philippe, M., Thévenard, F., 1997. Cretaceous floras from Snow Island (South Shetland Islands, Antarctica) and their biostratigraphic significance. In: Ricci, C.A. (Ed.), The Antarctic Region: Geological Evolution and Processes. Terra Antarctica Publication, Siena, pp. 1023e1028.

Trabucho-Alexandre, J., Dirkx, J., Veld, H., Klaver, G., De Boer, P.L., 2012. Toarcian black shales in the Dutch Central Graben: record of energetic, variable depositional conditions during an oceanic anoxic event. Journal of Sedimentary Research 82, 104e120.

Turner, E.C., Kamber, B.S., 2012. Arctic Bay Formation, Borden Basin, Nunavut (Canada): basin evolution, black shale, and dissolved metal systematics in the Mesoproterozoic ocean. Precambrian Research 208-211, 1e18.

Twenhofel, W.H., Tester, A.C., 1926. New data on the Comanchean strata of central Kansas. American Association of Petroleum Geologists Bulletin 10, 553e561.

U

Uliana, M.A., Arteaga, M.E., Legarreta, L., Cerdán, J.J., Peroni, G.O. 1995. Inversion structures and hydrocarbon occurrences in Argentina. In: J.G. Buchanan, P.G. Buchanan (Eds.), Basin inversion. Geological Society, London, Special Publication, 88, 211-233.

Underhill, J.R. & Paterson, S. 1998. Genesis of tectonic inversion structures: seismic evidence for the development of key structures along the Purbeck-Isle of Wight Disturbance. Journal of the Geological Society, London, 155 (6), 975-992.

Underhill, J. R. & Stoneley, R. 1998. Introduction to the development, evolution and petroleum geology of the Wessex Basin. *Geological Society, London, Special Publications*, *133*(1), 1-18.

Urai, J.L., Williams, P.F., van Roermund, H.L.M., 1991. Kinematics of crystal growth in syntectonic fibrous veins. Journal of Structural Geology 13, 823e836.

Ure, D., 1793. History of Rutherglen and East Kilbride. David Niven, Glasgow, 334 pp.

Urien, C.M., Zambrano, J.J., 1994. Petroleum systems in the Neuquén Basin, Argentina. In: Magoon, L.B. & Dow, W.G. (eds) The Petroleum System — from Source to Trap. American Association of Petroleum Geologists, Memoirs, 60, 513–534.

Urien, C.M., Zambrano, J.J., Yrigoyen, M.R. 1995. Petroleum basins of southern South America: An overview. In: A.J. Tankard, R. Suárez Soruco, H.J. Welsink (Eds.), Petroleum basins of South America, American Association of Petroleum Geologists Memoir, 62, 63-77.

V

Van Noten, K., Muchez, P., Sintubin, M., 2011. Stress-state evolution of the brittle upper crust during compressional tectonic inversion as defined by successive quartz vein types (High-Ardenne slate belt, Germany). Journal of the Geological Society, London 168, 1e16, http://dx.doi.org/10.1144/0016-76492010-112.

Vergani, G.D., Tankard, A.J., Belotti, H.J., Welsink, H.J., 1995. Tectonic evolution and paleogeography of the Neuquén basin, Argentina. In: Tankard, A.J., Suarez, R., Welsink, H.J. (eds), Petroleum Basins of South America. American Association of Petroleum Geologists, Memoirs, 62, 383–402.

Videla Leaniz, J.R., 1945. Informe mensual sobre los trabajos efectuados en abril 1945 (Comisión Carbón Mineral n° 55). Yaciminetos Carboníferos Fiscales (unpublished report).

Villar, H.J., Legarreta, L., Cruz, C.E., Laffitte, G., Vergani, G., 2006. Los cinco sistemas petroleros coexistentes en el sector sudeste de la Cuenca Neuquina: definición geoquímica y comparación a lo largo de una transecta de 150 km. Boletín de Informaciones Petroleras, Cuarta época, 3, 50–66.

Vincent, B., Emmanuel, L., Houel, P., Loreau, JP., 2007. Geodynamic control on carbonate diagenesis: Petrographic and isotopic investigation of the Upper Jurassic formations of the Paris Basin (France). Sedimentary Geology 197, 267–289

Vincent, S.J., Allen, M.B., 2001. Sedimentary record of Mesozoic intracontinental deformation in the eastern Junggar Basin, northwest China: response to orogeny at the Asian margin. Geological Society of America Memoir 194, 341e360.

Volk, H., Horsfield, B., Mann, U., Suchy, V., 2002. Variability of petroleum inclusions in vein, fossil and vug cements e a geochemical study in the Barrandian Basin (Lower Palaeozoic, Czech Republic). Organic Geochemistry 33, 1319e1341.

Von Terzaghi, K., 1923. Die Berechnung der Durchlâssigkeitsziffer des Tones aus dem Verlauf der hydrodynamischen Spannungerscheinungen. Sitzungsberichte der Akademie der Wissenschaften in Wien, mathematischnaturwissenschaftliche Klasse, Abteilung IIa 132, 125e138.

W

Warrington, G., Whittaker, A., Scrivener, R.C., 1986. The late Triassic succession in central and eastern Somerset. Proceedings of the Ussher Society 6, 368e374.

Watt, J.A., 1898. Saddle reefs at Hargraves. New South Wales Geological Survey Records 5, 153e160.

Watts, N.L., 1978. Displacive calcite: evidence from recent and ancient calcretes. Geology 6, 699e703.

Webster, T., 1826. Observations on the Purbeck and Portland Beds. In: Transactions of the Geological Society, London, Series 2, vol. 2, pp. 37e44.

West, I.M., 2013. Geology of the Wessex Coast of Southern England e the World Heritage Jurassic Coast e and More. Internet page. http://www.southampton.ac.uk/wimw/index.htm.

Wignall, P.B., Pickering, K.T., 1993. Palaeoecology and sedimentology across a Jurassic fault scarp, NE Scotland. Journal of the Geological Society, London 150, 323e340.

Willman, C.E., 2007. Regional structural controls on gold mineralisation, Bendigo and Castlemaine goldfields, Central Victoria, Australia. Mineralium Deposita 42, 449e464.

Wilson, T.J. 1991. Transition from back-arc to foreland basin development in the southernmost Andes: Stratigraphic record from the Ultima Esperanza District, Chile. Geological Society of America Bulletin, 103, 98-111.

Wilson, T.J., Dalziel, I.W.D., 1983. Geology of the Ultima Esperanza fold-thrust belt, southernmost Andes. U.S. Antarc. J., Annu. Rev. 18, 75**e**76.

Windh, J., 1995. Saddle reef and related gold mineralization, Hill End Gold Field, Australia: evolution of an auriferous vein system during progressive deformation. Economic Geology 90, 1764e1775.

Windhausen, A., 1931. Geología Argentina. Segunda Parte. Geología histórica y regional del territorio argentino. Buenos Aires, Jacobo Peuser, p. 645.

Winslow, M. A. 1981. Mechanisms for basement shortening in the Andean foreland fold belt of southern South America. In: Thrust and nappe tectonics (ed. McClay, K. R., Price, N. J.), Geological Society, London, Special Publications, 9, 513-528.

Winslow, M.A. 1982. The structural evolution of the Magallanes Basin and neotectonics in the southernmost Andes. In: C. Craddock (Ed.), Antarctic Geoscience, University of Wisconsin Press, Madison, 143-154.

Winslow, M.A. 1983. Clastic dike swarms and the structural evolution of the foreland fold and thrust belt of the southern Andes. Geological Society of America Bulletin, 94, 1073-1080.

Witte, J., Bonora, M., Carbone, C., Oncken, O., 2012. Fracture evolution in oil-producing sills of the Rio Grande Valley, northern Neuquén Basin, Argentina. American Association of Petroleum Geologists Bulletin, 96 (7), 1253-1277.

Woodland, B.G., 1964. The nature and origin of cone-in-cone structure. Fieldiana: Geology 13 (4). 187e305.

Woodland, B.G., 1975. Pyritic cone-in-cone concretions. Fieldiana Geology 33, 125e 139.

Woodward, H.B., 1893. The Jurassic Rocks of Britain. In: The Lias of England and Wales (Yorkshire Excepted), vol. 3. Memoir of the Geological Survey of the United Kingdom, 399 pp.

Y

Yates, J., 1821. Account of a variety of argillaceous limestone, found in connexion with the iron-stone of Staffordshire. Transactions of the Geological Society of London 5, 375e378. Series 1.

Young, J., 1885. Notes on “cone-in-cone” Structure, vol. 8. Transactions of the Geological Society, Glasgow, Part 1, pp. 1e27.

Young, J., 1886. Cone-in-cone. Geological Magazine 2, 139e140. Decade 3.

Young, J., 1892a. Cone-in-cone structure. Geological Magazine 9, 138e139. Decade 3.

Young, J., 1892b. Cone-in-cone structure. Geological Magazine 9, 278e279. Decade 3.

Young, J., 1892c. Cone-in-cone structure. Geological Magazine 9, 480. Decade 3.

Z

Zanella, A., Cobbold, P.R., Lemrabott, A., 2010 27**e**29 September. Physical Models of Chemical Compaction, Overpressure Development and Hydraulic Fracturing in Various Tectonic Contexts. GeoMod2010, Lisbon, Portugal.

Zanella, A., Cobbold, P.R., 2011. Influence of Fluid Overpressure, Maturation of Organic Matter, and Tectonic Context during the Development of ‘beef ’: Physical Modelling and Comparison With the Wessex Basin, SW England, vol. 13. EGU General Assembly, Vienna, Austria. Geophysical Research Abstracts.

Zanella, A., Cobbold, P.R., 2012. ‘Beef’: Evidence for Fluid Overpressure and Hydraulic Fracturing in Source Rocks During Hydrocarbon Generation and Tectonic Events: Field Studies and Physical Modelling. Geofluids VII International Conference, Rueil-Malmaison, May 2012.

Zanella, A., Cobbold, P.R., 2013, 19**e**22 May. Physical Modeling of Fluid Overpressure and Hydraulic Fracturing in Source Rocks in Various Tectonic Contexts. American Association of Petroleum Geologists Annual Convention, Pittsburgh, Tennessee.

Zanella, A., Cobbold, P.R., Le Carlier de Veslud, C., 2014. Physical modelling of chemical compaction, overpressure development, hydraulic fracturing and thrust detachments in organic-rich source rock. Mar. Pet. Geol.

Zanella, A., Cobbold, P.R., Ruffet, G., Rojas, L., 2013. Beef veins and thrust detachments in Early Cretaceous source rocks, foothills of the Magallanes**e**Austral Basin, southern Chile and Argentina: structural evidence for fluid overpressure during hydrocarbon maturation (in press). Mar. Pet. Geol. http://dx.doi.org/10.1016/j.marpetgeo.2013.10.006.

Zilli, N., Pedrazzini, M., Peroni, G. 2002. La Cuenca Austral. In: Geología y Recursos Naturales de Santa Cruz, (Ed. Haller, M.J.), XV Congreso Geológico Argentino (El Calafate), Relatorio, 607-662.